Flutter Analysis of a Two-Dimensional Airfoil Containing Structural Hysteresis Nonlinearities

by

Brett M. Brooking, B.Eng. (Aerospace)

A thesis submitted to the
Faculty of Graduate Studies and Research
in partial fulfilment of
the requirements for the degree of

Master of Engineering (Aerospace)

Ottawa-Carleton Institute for
Mechanical & Aerospace Engineering
Carleton University
Ottawa, Ontario
Canada

The undersigned hereby recommend to the

Faculty of Graduate Studies and Research

acceptance of the thesis,

Flutter Analysis of a Two-Dimensional Airfoil

Containing Structural Hysteresis Nonlinearities

submitted by

Brett M. Brooking, B.Eng. (Aerospace)

in partial fulfilment of the requirements

for the degree of Master of Engineering (Aerospace)

Chair, Department of Mechanical & Aerospace Engineering

Thesis Supervisor

Thesis Supervisors

Carleton University

May 1998

ABSTRACT

Aeroelastic flutter is a dangerous phenomenon where aerodynamics interact with the structure of an aeronautical component to produce potentially damaging oscillations. Small concentrated structural nonlinearities can have significant effects on the flutter behaviour and can, in particular, cause large-amplitude oscillations at lower airspeeds than for linear systems.

This thesis documents an investigation of one particular type of nonlinearity, hysteresis. The effects of introducing hysteresis into an otherwise linear aeroelastic system are determined. This work was a continuation of previous work that examined the effects of bilinear and cubic type nonlinearities in a dynamic system consisting of a two-dimensional airfoil having two degrees of freedom. This thesis first outlines a method of characterizing the response of the system through the use of a finite difference formulation to produce a time marching simulation that traces the response of the system through time. A second solution method outlined is a semi-analytical method using a Describing Function technique to approximate the amplitude of the response of the system based on the nonlinearity present.

Results are presented in the form of "maps" that indicate configurations where Limit Cycle Oscillations (LCO) are induced, and in the form of amplitude versus airspeed plots for the LCO cases. The simulation and describing function methods were found to compare with reasonably good accuracy. It was found that the Describing Function solution tends to become less accurate as the assumptions of sinusoidal motion break down.

ACKNOWLEDGEMENTS

I would like to thank Peter Barrington, of Carleton University, my Master's thesis supervisor, who has provided me with guidance and assistance through this project. I would also like to thank my co-supervisor Ben Lee of the Institute for Aerospace Research, National Research Council for his help and insight into this topic, and for the use of the NRC facilities. I would also like to thank my third co-supervisor Dick Kind, of Carleton University, for going to great lengths ensure this project drew to completion and not forgetting me. Thanks also to the people at Davis Engineering for giving me time, facilities and support to complete the project. The support of all these people is greatly appreciated.

This thesis is dedicated to Nicole. She is my light whenever it is dark.

TABLE OF CONTENTS

LIST OF FIGURES

NOMENCLATURE

A	amplitude of input signal to Describing Function $\alpha(t) = B + A\sin(\omega t+\theta)$
a_h	position of elastic axis relative to midchord position
B	bias of input signal to Describing Function $x(t) = B + A\sin(\omega t+\theta)$
b	semi-chord
C_{L_α}	coefficient of lift
C_h	linear heave structural damping coefficient per unit span, see Equation 3.2
C_α	linear pitch structural damping coefficient per unit span, see Equation 3.2
$F(\alpha)$	nonlinear function returning the restoring moment in pitch
$f(\alpha)$	function to show nonlinearity is small, $F(\alpha) = \nu f(\alpha)$
h	heave position
I_α	mass moment of inertia about elastic axis per unit span
K_α	linear pitch spring stiffness
K_h	linear heave spring stiffness
L	lift per unit span
m	airfoil mass per unit span
m	slope of hysteresis nonlinearity
M	moment per unit span

N_A	Describing Function complex gain, $n_p + j\, n_q$
n_p	real component of Describing Function gain N_A
n_q	imaginary component of Describing Function gain N_A
p	Laplace Transform variable
$\bar{p}$	nondimensional Laplace Transform variable, pV/b
q	dynamic air pressure, $\frac{1}{2}\rho V^2$
r_α	radius of gyration about elastic axis
S	static offset per unit span, $m(x_\alpha b - a_h b)$
s	plan form area per unit span, $2b$
V	air stream velocity
ξ	nondimensional heave position, h/b
x	variable representing input signal $x(t)$ to a Sinusoidal Describing Function
x_α	position of centre of mass from elastic axis relative to semi-chord
y_a	variable representing output $y_a(t)$ from Sinusoidal Describing Function
α	pitch angle
ζ	damping term
ζ_α	nondimensional pitch damping coefficient, $C_a/(2(I_\alpha K_\alpha)^{1/2}$
ζ_ξ	nondimensional heave damping coefficient, $C_h/(2(mK_h)^{1/2}$
θ	phase angle
μ	nondimensional airfoil mass ratio, $m/\pi\rho b^2$
ν	small parameter indicating nonlinearity $F(\alpha)$ is small
ξ	nondimensional heave position, h/b

ρ	air density
ψ	$\omega t + \theta$
ω_a	natural frequency of uncoupled pitch motion when S=0
ω_h	natural frequency of uncoupled heave motion when S=0
$\bar{\omega}$	ratio of heave to pitch frequency, ω_h/ω_α

1.0 INTRODUCTION

The work described in this thesis was performed for the purpose of investigating the effects of hysteretic nonlinearities on the dynamic response of an aeroelastic system, and to compare results between computer simulations and a semi-analytic solution. The goal was to evaluate the effectiveness of using the described semi-analytical solution method to predict the flutter behaviour of this nonlinear system and determine where the method's accuracy breaks down for the hysteresis nonlinearity and why.

1.1 Problem Definition

The studied system represented a generic airfoil section that had been simplified to a two-dimensional dynamic system in two degrees of freedom – pitch and heave. When subjected to large aerodynamic forces, i.e. airspeed, and an initial pitch angle the dynamic system can be shown to enter into a state of oscillation that after the removal of transient effects results in a system that is either stable and decays to zero, or is unstable and diverges for a linear system. A condition of oscillation of an airfoil that continues to grow out of control is known as *flutter* and is a dangerous condition that can cause violent

damage to aircraft structures. The airspeed at which flutter is induced in a linear aeroelastic system is known as the *linear flutter speed.*

By introducing structural nonlinearities into the elastic response of the airfoil, the dynamics can be reevaluated with respect to the stability of the system and may subsequently include steady state oscillations that are sustainable and neither decay nor grow beyond the bounds of the system. Typical nonlinearities that have been analysed in theoretical work include the *freeplay* nonlinearity where a dead band of zero change in restoring force occurs over a range of displacement, cubic nonlinearity where the reaction force *versus* displacement curve is represented by a cubic function, and the *hysteresis* nonlinearity where the reaction force response curve is dependent upon the current state of the system. It is this hysteresis type nonlinearity which was studied in the work being presented in this thesis.

Aeroelasticity, as a topic of study, describes the interactions between aerodynamic forces and the reaction forces of an elastic structure. Aerodynamic forces deform an elastic structure and the deformation of the structure in turn changes the nature of the aerodynamic forces acting on it. In a dynamic system these forces can feedback onto each other causing reactions that are sometimes complex and difficult to predict. The feedback nature of the dynamic system can, under certain conditions, lead to instabilities resulting in physical damage to the structure.

In aeronautics, aeroelastic reactions become very important for components that combine large aerodynamic forces with low structural stiffness. Specifically wing sections and tail sections are susceptible to damage from aeroelastic instabilities. The

aerodynamic lifting forces can cause these relatively low stiffness components to dynamically oscillate under loading. If the airspeed is great enough and certain stability conditions are met the oscillations can increase to the point where failure of the part occurs. For the purposes of design, it is important to be able to predict when these unstable conditions are met such that the structure can be designed to fly within the safe operating envelope.

Traditionally most aeroelastic computer based evaluations of aircraft structures are performed through the use of finite element type numerical problems that use linear models to simulate the response of the structure to the aerodynamic loading. The finite element model is typically based either upon a simplified construction of simulation elements or on experimentally obtained vibration responses. The assumption of a linear behaviour for the model generally models the response of the structure well but even small nonlinearities, that are present in any real world structure, can have a large influence on the response of an aeroelastic structure.

1.2 Scope of Present Work

Computer code was developed to perform a finite difference method simulation solution for the behaviour of the defined dynamic system. Simulations were performed for a large matrix of airfoil configurations and initial conditions and the results were amassed to characterize the response of each airfoil configuration. The semi-analytical describing function method was also utilized to characterize the same airfoil

configurations and initial conditions.

This thesis will present the results of the comparisons between the two methods for the hysteresis nonlinearity present in the pitch degree of freedom of the airfoil. Their similarities are discussed and reasons for the differences and relative shortcomings are explained. The areas where the accuracy of the semi-analytical method breaks down are examined and methods are proposed for predicting these conditions. Real-world applications for the methods are discussed as well as topics for future work.

2.0 BACKGROUND

The importance of aeroelastic analysis has been realized since the early days of aviation. This chapter presents an overview of the work that preceded the work described in this thesis. Previous work that lead up to the presented thesis material included experimental and analytical work with both linear aerosystems and structural nonlinearities.

2.1 Previous Work

The foundations of experimental and theoretical study of aeroelasticity and flutter were laid by Theodorsen and Fung who developed methods for characterizing flutter through experiment and theory. Theodorsen and Garrick (1940) performed numerous experiments using scale model wing sections in the high speed wind tunnels of NACA. His experiments clearly showed the dangers involved with uncontrolled flutter. Both Theodorsen and Garrick and Fung (1955) used linearizing assumptions for simplifying the dynamic systems they studied. While these assumptions provided a basis for solution of the systems it was evident that nonlinearities were still quite important for the resulting behaviour of the airfoil. Woolston et. al. (1957) performed analyses using an analog computer for a number of structural nonlinearities including a free play spring, hysteresis,

and cubic nonlinear restoring forces. They were able to correlate their results with wind tunnel experiments. They made note of how the stability of the system was highly dependent upon the initial displacement from equilibrium. Subsequently work was presented by Shen and Hsu (1957) showing a comparison and explanation of Woolston's results using an equivalent linear stiffness comparison.

Analyses of nonlinear effects in aeroelasticity have typically taken the form of analysing either nonlinear aerodynamic forces or nonlinearities in the structural response of aircraft components. Nonlinear aerodynamics usually refer to transonic flows and are not considered within this thesis. The importance of nonlinearities in the performance of aircraft structures was broadly outlined by Breitbach (1977) who gives an overview of the types of nonlinear behaviours exhibited by aircraft structures. His analysis was derived partly from theory and partly from observations and experiments. He classified the nonlinear effects as either being *distributed nonlinearities*, the nonlinear response of the aircraft structure due to the many small nonlinearities dispersed throughout the aircraft, or *concentrated nonlinearities*, which are locally acting on one particular degree of freedom of the structure. It is the behaviour of these concentrated nonlinearities that analytic and numerical methods such as those presented in this thesis attempt to model. Concentrated nonlinearities in aircraft come in the form of nonlinear restoring forces on aircraft components such as control surfaces. The nonlinear response of the component to displacement can be in such forms as a dead band of response in the centre of the displacement range (freeplay) such as might be due to a loose control cable or a preload condition on a flap. Hysteresis effects can be produced by the deformation of some

materials as well as by solid friction in control cables and hinge bearings. A dynamic system with one of these nonlinearities in the restoring force or moment has the characteristic of a *stiffness* that varies with displacement. This stiffness, the rate of change of the restoring force with displacement, would normally be a constant for a linear system. The resulting system can, given a certain set of initial conditions, reach a state of oscillation where the system response neither decays to rest nor grows beyond the bounds of the system. These *limit cycle oscillations* (LCO) can occur at speeds significantly below the flutter speed predicted by the linear approximation, and the amplitude can be such as to affect the flight dynamics of the aircraft or cause damage. Breitbach stressed the need for nonlinear analysis methods in aeroelastic investigations as he found the nonlinearities to have serious detrimental effects on component response.

Dowell and Ilgamov (1988) provided another overview of nonlinearities present in both aircraft structures and aerodynamics as well as an overview of methods of solving these problems and nonlinear systems in general. Dowell paid particular attention to the aeroelastic analysis of helicopter rotor blades and for solution methods for nonlinear vibrations.

Laurensen and Trn (1979) performed a nonlinear analysis of missile control surfaces with structural nonlinearities. They found that the effective stiffness of the resulting system was less than that for the corresponding linear system. This result leads to the conclusion that nonlinearities are likely to induce flutter at a lower speed than is indicated by a classical linear analysis.

The describing function method is a *semi-analytical* solution method for nonlinear systems where the output of the system is first assumed to be harmonic, then an *effective stiffness* for the system is determined. The resulting linear system approximates the nonlinear system such that the resulting magnitude of linear system harmonic response for a prescribed set of conditions approaches that of the nonlinear system being modelled. Gelb and Vander Velde (1968) gave a good description of the method and outlined how it can be applied to nonlinear systems. The method effectively linearizes the nonlinear portion of the system to allow for an iterative analytical solution.

Many uses for the describing function technique for the purposes of modelling nonlinear systems for linear analysis have been developed. C. L. Lee (1985) described an iterative procedure for making use of the describing function and how it was compared to experiments and simulations for flutter analysis of large dynamic systems. He provided a good validation of the method for a range of nonlinearities of increasing complexity and showed good agreement with the experimental and simulation data. Murty (1995) used a describing function method to solve systems with nonlinearity in the torsional degree of freedom. Mast and Pierce (1995) made use of the technique for the analysis of nonlinear vibrations in the field of acoustics.

Lee and Tron (1989) gave an analysis of a practical nonlinearity in a modern fighter aircraft. They used a describing function method to predict the flutter characteristics of a CF-18 wing fold hinge. They showed that the nonlinearities in the hinge could be modelled using springs with bilinear stiffnesses and freeplay zones. They

used the describing function method to predict the speed at which flutter would ensue and the magnitude to which the oscillations would grow at various speeds.

An alternative to searching for analytical solutions to nonlinear problems is to solve the equations of motion using numerical time marching methods. Modern computing advances have made feasible the use of algorithms utilising millions of iterative computer steps to simulate the response of a system to hundreds of conditions and configurations. Jones and Lee (1985) showed how a single degree of freedom dynamic system known as Duffing's equation could be solved using a time marching backward difference approach as outlined by Houbolt (1950). Houbolt outlined a method of a step by step solution for the aircraft structural response. He utilised a *recurrence matrix solution* to solve for the stepwise time based simulation of the aircraft response. Jones and Lee were able to show that solving the Duffing's equation system through a similar numerical means was both feasible and in some areas more accurate than previous analytical work. A similar numerical technique was later used by Lee and Leblanc (1986) to perform flutter analyses of two-dimensional airfoils with cubic structural nonlinearities. They used Houbolt's scheme to investigate the flutter response of the airfoil to varying initial conditions. They found that different initial pitch angles could cause the airfoil to achieve limit cycle flutter at speeds below the linear flutter speed. Lee and Desrochers (1987) used the same numerical method to investigate airfoils with restoring forces that contained bilinear and freeplay nonlinearities. They numerically determined the speed at which different airfoil configurations would achieve either limit cycle or divergent flutter for differing initial pitch angles of the airfoil. The analysis was

performed by simulating the motion of the system for each configuration and set of initial conditions through a sufficient number of steps to ensure the system had reached steady state. From observing the final state of the system for each set of parameters they characterized the response of the airfoil. Lee and Desrochers also investigated the relationships between the amplitude of the limit cycle flutter and the simulated airspeed for various configurations of the airfoil and found the amplitude to be independent of the initial conditions.

Hauenstein et. al. (1992) performed both experimental and analytical investigations of various types of nonlinearities in the structural response of aerosurfaces. They found that the response of the system depended greatly upon the initial conditions and could range from damped decay to unstable oscillations (flutter) to limit cycle response or chaotic motion. They drew a conclusion that the system would not experience a chaotic response for a single structural nonlinearity.

Price, Alighanbari, and Lee (1994) performed work extending the results of Lee and Desrochers on two-dimensional airfoil systems with bilinear and cubic restoring forces. They solved the systems using both the numerical time marching method and a semi-analytical describing function method. They found the describing function method was able to predict reasonably well both the speed of the onset of flutter and the magnitude to which a limit cycle flutter condition would grow. Price et. al. were also able to show that, contrary to the results of Hauenstein et. al., small regions of chaotic motion could be obtained using single cubic or bilinear nonlinearities in the aerosurface root (i.e. the mounting point for the two-dimensional airfoil)..

The problem of aeroelastic flutter, as pointed out by Dowell (1988), contains a great number of possibilities to observe some of the more intriguing aspects of nonlinear motion such as chaos. Stockard et. al. (1967) showed, using a nonlinear oscillator, how discontinuous changes in amplitude of the response of the system (amplitude jumps) could be observed. Yang and Zhao (1988) used a harmonic balance method compared to experimental techniques to observe the response of the two-dimensional airfoil system. They found that with a freeplay nonlinearity, different limit cycle oscillation amplitudes could be observed for the same airfoil configuration subjected to the same airspeed condition. Subsequent work by Zhao and Yang (1990) detailed their observations of chaotic responses in airfoil systems with cubic nonlinearities in the pitch degree of freedom.

The analysis and characterization of chaotic responses within the context of the problem being examined herein is beyond the scope of the present thesis. It does however present an area for the extension of the current work

3.0 THEORY

The studied system involves the combination of a two degree of freedom vibrating system with an aerodynamic forcing term that is dependent upon the value of the pitch degree of freedom. The two degrees of motion as shown in Figure 3.1 are rotation about the elastic axis (pitch, α) and vertical motion (heave, h). The system is elastically constrained about each of the degrees of freedom where the restoring force for the pitch degree of freedom is torsion and the restoring force for the heave degree of freedom represents what would be the bending of a wing in a three dimensional aircraft. The "motion induced" forcing terms result from aerodynamics forces evaluated according to simple unsteady thin airfoil theory using the assumptions of incompressible inviscid airflow. The aerodynamic forces on the system are in turn dependent upon the value of the pitch angle α, the heave rate $\partial h/\partial \tau$, and the prescribed airspeed. Classical solution methods exist for both a coupled two degree of freedom linear system and for the aerodynamic forces on a two-dimensional airfoil. Aeroelastic analysis techniques will be presented in this thesis to outline how the structural and aerodynamic portions of the problem are solved simultaneously.

The two degrees of freedom in the system are effectively *coupled* both due to the structure of the airfoil system and the aerodynamics. The aerodynamic response to the

pitch of the airfoil is lift. The change in lift causes both a change in heave and a subsequent change in pitch due to inertial effects. The changes in pitch and heave feed back to a change in lift and the resulting system effectively couples the displacements, forces and moments. The result is a two degree of freedom dynamic system where the forcing term is dependent upon the value of the pitch degree of freedom.

This chapter will present the equations of motion that govern the described dynamic system and develop them into a form that is suitable for solution both by analytical methods and finite difference numerical methods. Aerodynamics are implemented into the system first with an assumption of *quasi-steady aerodynamics* to demonstrate the method of analytic solution. A description of changes made to implement unsteady aerodynamics is then presented.

3.1 Equations of Motion

To derive the equations of motion that govern the two degree of freedom system we begin with the equations of motion for a 2 degrees of freedom dynamic system which moves in the pitch and heave degrees of freedom [Fung, 1955]:

$$m\,h + S\,\ddot{\alpha} + C_h\,\dot{h} + K_h\,h = -L(t) \tag{3.1a}$$

$$S\,h + I_\alpha\,\alpha + C_\alpha\,\dot{\alpha} + F(\alpha) = M(t) \tag{3.1b}$$

where α represents the airfoil pitch angle and h is the heave displacement at the elastic axis. Note that the negative sign on the lift term arises because h has been defined as positive for downward motion. The structural properties of the airfoil are depicted in Figure 3.1 showing the relative locations of the *centre of mass*, *elastic axis*, and *aerodynamic centre* of the airfoil. The single and double dots over the variables indicate the first and second derivative respectively with respect to time. S represents the static offset per unit span where:

$$S = m * (x_\alpha b - a_h b) \tag{3.1c}$$

and m is the airfoil mass per unit span. C_h and C_α are the structural damping coefficients per unit span for heave and pitch, I_α is the mass moment of inertia per unit span about the elastic axis, and K_h is the heave spring stiffness per unit span. Variables b, a_h, and x_α are depicted in Figure 3.1 and represent the position of the midchord, and positions of the elastic axis and centre of mass of the airfoil measured from the midchord respectively. $F(\alpha)$ represents the nonlinear function by which the pitch degree of freedom restoring force is determined. This function acts as a nonlinear pitch degree of freedom stiffness determining the restoring torque according to the value of the airfoil pitch. L(t) and M(t) are the motion induced lifting force and moment arising from the aerodynamic forces where L(t) is negative due to the positive in the downward definition of h.

Expressed in matrix form, the expressions are represented by:

$$\begin{bmatrix} m & S \\ S & I_\alpha \end{bmatrix} \begin{Bmatrix} \ddot{h} \\ \ddot{\alpha} \end{Bmatrix} + \begin{bmatrix} C_h & 0 \\ 0 & C_\alpha \end{bmatrix} \begin{Bmatrix} \dot{h} \\ \dot{\alpha} \end{Bmatrix} + \begin{bmatrix} K_h & 0 \\ 0 & \overline{F}(\alpha) \end{bmatrix} \begin{Bmatrix} h \\ \alpha \end{Bmatrix} = \begin{Bmatrix} -L \\ M \end{Bmatrix} \tag{3.2}$$

where $F(\alpha) = \overline{F}(\alpha)\cdot\alpha$. Assuming for the moment that there is a linear restoring moment in the pitch degree of freedom represented by the spring constant K_α and zero initial conditions, taking the Laplace Transform yields:

$$\begin{bmatrix} mp^2 + C_h p + K_h & Sp^2 \\ Sp^2 & I_\alpha p^2 + C_\alpha p + K_\alpha \end{bmatrix} \begin{Bmatrix} h(p) \\ \alpha(p) \end{Bmatrix} = \begin{Bmatrix} -\overline{L}(p) \\ \overline{M}(p) \end{Bmatrix} \tag{3.3}$$

Substituting the non-dimensional Laplace transform variable $\overline{p} = bp/V$, this equation becomes:

$$\begin{bmatrix} \frac{mV^2}{b^2} b\overline{p^2} + C_h bp + K_h b & \frac{SV^2}{b^2}\overline{p^2} \\ \frac{SV^2}{b^2} b\overline{p^2} & \frac{I_\alpha V^2}{b^2}\overline{p^2} + C_\alpha p + K_\alpha \end{bmatrix} \begin{Bmatrix} h(\overline{p})/b \\ \alpha(\overline{p}) \end{Bmatrix} = \begin{Bmatrix} -\overline{L}(\overline{p}) \\ \overline{M}(\overline{p}) \end{Bmatrix} \tag{3.4}$$

In order to non-dimensionalize the terms, the following definitions were used:

$$\omega_\alpha^2 = \frac{K_\alpha}{I_\alpha} \tag{3.5a}$$

$$\omega_\xi^2 = \frac{K_h}{m} \tag{3.5b}$$

where ω_α and ω_ξ represent the natural frequencies of the pitch and heave degrees of freedom when the static offset S from Equation 3.1c is 0. Additional definitions for the purposes of non-dimensionalizing the parameters include:

$$\xi = \frac{h}{b} \tag{3.6a}$$

$$r_\alpha = \left(\frac{I_\alpha}{mb^2}\right)^{\frac{1}{2}} \tag{3.6c}$$

$$\zeta_\xi = \frac{C_h}{2(mK_h)^{\frac{1}{2}}} \tag{3.6d}$$

$$\zeta_\alpha = \frac{C_\alpha}{2(I_\alpha K_\alpha)^{\frac{1}{2}}} \tag{3.6e}$$

where ξ is therefore the non-dimensional heave variable and ζ_ξ and ζ_α are the non-

$$x_\alpha = \frac{S}{bm} \tag{3.6b}$$

dimensional damping coefficients. It is also necessary to define a non-dimensional flow velocity:

$$U^* = \frac{V}{b\omega_\alpha} \tag{3.7}$$

where V is the reference velocity and ω_α is the natural frequency of the system in the pitch degree of freedom. A non-dimensional natural frequency $\bar{\omega}$ is defined from the ratio of the natural frequencies of the two degrees of freedom according to:

$$\bar{\omega} = \frac{\omega_\xi}{\omega_\alpha} \tag{3.8}$$

Equation 3.4 thus becomes:

$$\begin{bmatrix} \overline{p^2} + 2\frac{\overline{\omega}}{U^*}\zeta_\xi \bar{p} + (\frac{\overline{\omega}}{U^*})^2 K_h & x_\alpha \overline{p^2} \\ \frac{x_\alpha}{r_\alpha^2}\overline{p^2} & \overline{p^2} + 2\frac{\zeta}{U^*}\bar{p} + \frac{K_\alpha}{U^{*2}} \end{bmatrix} \begin{Bmatrix} \xi(\bar{p}) \\ \alpha(\bar{p}) \end{Bmatrix} = \begin{Bmatrix} -\bar{L}(\bar{p}) \\ \bar{M}(\bar{p}) \end{Bmatrix} \tag{3.9}$$

or, in the time domain:

$$\begin{bmatrix} 1 & x_\alpha \\ \dfrac{x_\alpha}{r_\alpha^2} & 1 \end{bmatrix} \begin{Bmatrix} \ddot{\xi}(\tau) \\ \ddot{\alpha}(\tau) \end{Bmatrix} + \begin{bmatrix} 2\dfrac{\overline{\omega}}{U^*}\zeta_\xi & 0 \\ 2\dfrac{\zeta_\alpha}{U^*} & 0 \end{bmatrix} \begin{Bmatrix} \dot{\xi}(\tau) \\ \dot{\alpha}(\tau) \end{Bmatrix} + \begin{bmatrix} (\dfrac{\overline{\omega}}{U^*})^2 K_h & 0 \\ 0 & \dfrac{K_\alpha}{U^{*2}} \end{bmatrix} \begin{Bmatrix} \xi(\tau) \\ \alpha(\tau) \end{Bmatrix} = \begin{Bmatrix} -L(\tau) \\ M(\tau) \end{Bmatrix} \quad (3.10)$$

where τ is the non-dimensional time variable:

$$\tau = \frac{Vt}{b} \quad (3.11)$$

Using this system of equations as the basis, solution methods can now be utilised that approach the problem either in the time domain or in the frequency domain. The aerodynamic side of the system also requires more refinement as it is not only dependent upon time τ but also upon the pitch angle α. The aerodynamics for the system can be approached in one of two ways. For the purposes of this thesis, an assumption of quasi-steady aerodynamics was initially used to develop the solution method in a manner that was easier to implement. Because of the time based nature of the simulations, a solution incorporating unsteady aerodynamics was then later implemented to provide for a more accurate solution.

3.1.1 Quasi-Steady Aerodynamics

For the purposes of illustration only, the above systems (Equations 3.9 and 3.10) can be solved more easily if an assumption of quasi-steady aerodynamics is applied. Because the mathematics involved in using this simplified definition of the aerodynamics are more basic, the solution method will be outlined in this section using the quasi-steady

aerodynamics assumption. Details on defining the system using more accurate unsteady aerodynamics terms will be outlined in the next section and can then be substituted into the solution method outlined for the quasi-steady aerodynamics.

A quasi-steady aerodynamics assumption for the response of the airfoil implies that the aerodynamic forces acting upon the aerosurface change instantaneously with changes in airfoil pitch. For the purposes of illustrating the development of the model of the system, the quasi-steady assumption is crude but valid. For the purposes of numerical accuracy for subsequent simulations and analytical solutions the unsteady aerodynamics terms will be reintroduced.

Let the aerodynamic relationship of lift (L) force and moment (M) torque to the pitch and heave positions of the airfoil be represented by the aerodynamic transfer matrix:

$$\begin{Bmatrix} -bL(\bar{p}) \\ M(\bar{p}) \end{Bmatrix} = qSb \begin{bmatrix} -A_{11}(\bar{p}) & -A_{12}(\bar{p}) \\ A_{21}(\bar{p}) & A_{22}(\bar{p}) \end{bmatrix} \begin{Bmatrix} h(\bar{p})/b \\ \alpha(\bar{p}) \end{Bmatrix} \tag{3.12}$$

Thin airfoil theory shows that for an inviscid incompressible steady flow, the lift and moment terms can be determined according to:

$$L(t) = 2\pi q s \alpha(t) \tag{3.13}$$

$$M(t) = 2\pi q (\frac{1}{2} + a) b s \alpha(t) \tag{3.14}$$

where q is the dynamic pressure term and s is the planform area of the airfoil per unit span and is equal to 2b. It should be noted that equations 3.13 and 3.14 assume that the pitch angle makes the only contributions to lift and moment of the airfoil. In reality, the heave rate term $\dot{h}$ and pitch rate term $\dot{\alpha}$ would alter the effective angle of attack and contribute to lift and moment. Since the steady assumptions for this method are for illustrative purposes, the loss of accuracy by neglecting the heave contribution is not important. Thus for quasi-steady aerodynamics, the terms of the [A] matrix in equation 3.12 become:

$$A_{11} = A_{21} = 0 \quad ; \quad A_{12} = -2\pi b \quad ; \quad A_{22} = 2\pi(\frac{1}{2} + a) \tag{3.15}$$

and equation 3.12 becomes:

$$\begin{Bmatrix} -\bar{L}(\bar{p}) \\ \bar{M}(\bar{p}) \end{Bmatrix} = qsb \begin{bmatrix} 0 & 2\pi \\ 0 & 2\pi\left(\frac{1}{2} + a\right) \end{bmatrix} \begin{Bmatrix} \xi(\bar{p}) \\ \alpha(\bar{p}) \end{Bmatrix} \tag{3.16}$$

assuming that the lift curve slope for the airfoil is $C_{L_\alpha}=2\pi$. If the structural damping terms are neglected, when this equation is substituted back into equation 3.4 we then obtain:

$$\begin{bmatrix} \frac{mV^2}{b}\overline{p^2} + bK_h & \frac{V^2 S}{b^2}\overline{p^2} - 2\pi\rho V^2 b^2 \\ \frac{SV^2}{b}\overline{p^2} & I_\alpha \frac{V^2}{B^2}\overline{p^2} + K_\alpha - 2\pi(\frac{1}{2} + a)\rho V^2 b^2 \end{bmatrix} \begin{Bmatrix} \xi(\bar{p}) \\ \alpha(\bar{p}) \end{Bmatrix} = \begin{Bmatrix} 0 \\ 0 \end{Bmatrix} \tag{3.17}$$

Non-dimensionalizing this matrix as before, it simplifies to:

$$\begin{bmatrix} \overline{p^2} + \left(\frac{\overline{\omega}}{U^*}\right)^2 K_h & x_\alpha \overline{p^2} - \frac{2b}{\mu} \\ \frac{x_\alpha}{r_\alpha^2}\overline{p^2} & \overline{p^2} + \frac{K_\alpha}{U^{*2}} - \frac{2(\frac{1}{2}+a)}{\mu r_\alpha^2} \end{bmatrix} \begin{Bmatrix} \xi(\overline{p}) \\ \alpha(\overline{p}) \end{Bmatrix} = \begin{Bmatrix} 0 \\ 0 \end{Bmatrix} \tag{3.18}$$

where μ is defined as the non-dimensional airfoil mass ratio $\mu = m/\pi\rho b^2$. This expression is of the general form:

$$\left[B(\overline{p})\right] \begin{Bmatrix} \xi(\overline{p}) \\ \alpha(\overline{p}) \end{Bmatrix} = \begin{Bmatrix} 0 \\ 0 \end{Bmatrix} \tag{3.19}$$

According to the well known theory of dynamic systems (Steidel 1971, Thomson 1993), the roots of the *characteristic equation*, det $[B(\overline{p})] = 0$, are the eigenvalues of the system and they reveal whether the system is stable or unstable. Instability in this case indicates that the system would achieve flutter for the given configuration and initial conditions. If det $[B(\overline{p})] = 0$ is written out as a polynomial in $\overline{p}$ and the real parts of all roots (eigenvalues) of the equation are negative, then the system is considered stable and all vibrations will eventually damp out to zero. A solution with positive real roots and no imaginary roots indicates a divergent solution, while roots that are complex with a positive real component indicate an oscillatory instability, that is flutter in this case.

Using this method, the stability of a system with linear spring constants for both degrees of freedom can be determined analytically for the case of quasi-steady aerodynamics. This solution allows one to determine the linear flutter speed for various configurations of the airfoil as well as to examine the relationship between the stiffness of the pitch spring and the flutter speed.

3.1.2 Unsteady Aerodynamics

To accurately model the effects of realistic unsteady aerodynamics on the response of the airfoil, the assumptions of quasi-steady aerodynamics in the solution method of the previous section were replaced by unsteady aerodynamics terms. A more accurate determination of the unsteady aerodynamic forces resulting from the unsteady motions of the airfoil requires the use of *Wagner's function*:

$$\varphi(\tau) = f - ae^{-b\tau} - ce^{-d\tau} \tag{3.20}$$

where from Fung (1955), f=1, a=0.165, b=0.0455, c=0.335, d=0.300 for inviscid incompressible flow. Wagner showed that the Laplace Transform of the expressions for lift and moment are:

$$\begin{Bmatrix} b\overline{L}(\overline{p}) \\ \overline{M}(\overline{p}) \end{Bmatrix} = qsb \begin{bmatrix} [\pi + 2\pi\overline{\varphi}(\overline{p})]\overline{p}^2 & [-\pi a + 2\pi(\frac{1}{2} - a)\overline{\varphi}(\overline{p})]\overline{p}^2 + [\pi + 2\pi\overline{\varphi}(\overline{p})]\overline{p} \\ [\pi a + 2\pi(\frac{1}{2} + a)\overline{\varphi}(\overline{p})]\overline{p}^2 & [-\pi(\frac{1}{8} + a^2) + 2\pi(\frac{1}{4} - a^2)\overline{\varphi}(\overline{p})]\overline{p}^2 + [-\pi(\frac{1}{2} - a) + 2\pi(\frac{1}{2} + a)\overline{\varphi}(\overline{p})]\overline{p} \end{bmatrix} \begin{Bmatrix} \overline{\xi}(\overline{p}) \\ \overline{\alpha}(\overline{p}) \end{Bmatrix}$$

(3.21)

where $\bar{\phi}$ is the Laplace transform of Wagner's function:

$$\bar{\varphi}(\bar{p}) = \frac{0.5\overline{p^2} + 0.281\bar{p} + 0.01365}{\bar{p}\,(\bar{p} + 0.3)\,(\bar{p} + 0.0455)} \tag{3.22}$$

Equation 3.21 is therefore once again in the form of equation 3.12 and can be substituted into equation 3.9 in order to solve directly for the stability conditions for a given airfoil configuration. Note that the only term left that can prevent a direct solution for the problem is the nonlinear term, $F(\alpha)$ in equation 3.2 representing the pitch degree of freedom restoring moment.

Fung (1955) also gives the following expressions for lift and moment in the time domain:

$$L(\tau) = -\frac{1}{\mu}\left[\ddot{\xi}(\tau) - a_h\,\ddot{\alpha}(\tau) + \dot{\alpha}(\tau)\right] - \frac{2}{\mu}\left[\left\{\alpha(0) + \dot{\xi}(0) + (\tfrac{1}{2} - a_h)\dot{\alpha}(0)\right\}\varphi(\tau)\right.$$

$$\left. + \int_o^{\tau}\varphi(\tau-\sigma)\left[\dot{\alpha}(\sigma) + \ddot{\xi}(\sigma) + (\tfrac{1}{2} - a_h)\ddot{\alpha}(\sigma)\right]d\sigma\right] \tag{3.23}$$

$$M(\tau) = \frac{2}{\mu r_\alpha^2}(\tfrac{1}{2} + a_h)\left\{\left[\alpha(0) + \dot{\xi}(0) + (\tfrac{1}{2} - a_h)\dot{\alpha}(0)\right]\varphi(\tau)\right.$$

$$\left. + \int_o^{\tau}\varphi(\tau-\sigma)\left[\dot{\alpha}(\sigma) + \ddot{\xi}(\sigma) + (\tfrac{1}{2} - a_h)\ddot{\alpha}(\sigma)\right]d\sigma\right\}$$

$$+ \frac{1}{\mu r_\alpha^2}\left\{a_h\left[\ddot{\xi}(\tau) - a_h\,\ddot{\alpha}(\tau)\right] - (\tfrac{1}{2} - a_h)\dot{\alpha}(\tau) - \tfrac{1}{8}\ddot{\alpha}(\tau)\right\} \tag{3.24}$$

These expressions can be combined with equation 3.9 to obtain the equations of motion for a two-dimensional airfoil in two degrees of freedom in an inviscid incompressible airflow. In the studied case of a nonlinear stiffness in the pitch degree of freedom, the pitch stiffness K_α in equations 3.9 and 3.10 was replaced with a function $F(\alpha)$ relating the pitch angle to the restoring moment. Solutions for solving the system with this nonlinear operator are described below.

Note that the aeroelastic system has now been described in a non-dimensional form in both the time domain (equations 3.9, 3.23, 3.24) and the Laplace domain

(equations 3.10, 3.21, 3.22). Two different approaches, numerical and analytical for solving the equations will now be outlined.

The time domain equations will be solved using the Houbolt finite difference method [Houbolt, 1950] to give a time stepping simulation solution for the response of the system to initial stimuli. The Laplace domain approach will be used to provide an analytical solution to the system. The only factor preventing solution of both systems is the nonlinear restoring moment $F(\alpha)$ which now replaces the linear pitch stiffness K_α. Within the Houbolt method simulation, the parameter $F(\alpha)$ can be evaluated at each time step according to the instantaneous value of α as outlined in section 3.2.1. For the Laplace domain equations the nonlinear term must first be linearized through the use of a describing function approach as outlined in section 3.2.3

3.2 Solution Methods

With the aeroelastic system characterized in both the time and Laplace domains, the nonlinear restoring moment $F(\alpha)$ in the pitch degree of freedom is substituted into equations 3.9 and 3.10 in place of the assumed linear pitch stiffness K_α. Because of the non-constant nature of the nonlinear restoring moment $F(\alpha)$, directly solving for the stability of the system as shown above, using the Laplace domain, is not feasible. Two approaches were used to evaluate the response of the airfoil with a structural nonlinearity and determine the stability of the system. The Houbolt finite difference scheme solves for the state of the dynamic system at successive time steps. By simulating the system for a sufficient number of time steps to reach a steady state condition where all transient

effects in the system have disappeared, the stability of the system may be explicitly determined. Conversely, the describing function method outlined later provides an analytical method by which the flutter speed and amplitude of the limit cycle may be approximated through a linearization of the nonlinear spring represented by $F(\alpha)$.

3.2.1 Houbolt Finite Difference Method

The use of a *backward looking finite difference* solution allows the user to solve the nonlinear differential equation that results from equation 3.10. The Houbolt finite difference method uses a fourth order explicit finite difference method to evaluate the pitch and heave parameters of the system using a time marching scheme that effectively tracks through time the response of the airfoil to a given stimulus. As in previous work (Lee and Desrochers 1987, Price et. al. 1993) a fourth order Houbolt scheme was utilized. While this is a relatively low order method of solution, it has been shown that higher order methods such as eighth order Houbolt or Runge Kutta schemes provide a greater degree of accuracy but can be more complex to use as well as being more computationally intensive [Lee and Leblanc, 1985]. Using the fourth order scheme, the time derivatives are approximated in finite difference form as:

$$\dot{\alpha}_{n-1} = \frac{1}{\Delta\tau^2}\,[2\alpha_{n-1} - 5\alpha_n + 4\alpha_{n-1} - \alpha_{n-2}] \tag{3.25}$$

$$\ddot{\alpha}_{n-1} = \frac{1}{6\Delta\tau}\,[11\alpha_{n-1} - 18\alpha_n + 9\alpha_{n-1} - 2\alpha_{n-2}] \tag{3.26}$$

where n represents the current time step for which all conditions are known. Thus n+1 represents the subsequent time step for which the system is being solved, and n-1 and n-2 represent solutions at the two previous steps. The $\Delta\tau$ represents the size of the time step. The finite difference expressions for $\dot{\xi}_{n-1}$ and $\ddot{\xi}_{n-1}$ are similar. Substituting these equations into equation 3.10 gives a complicated expression which can be represented by:

$$\begin{bmatrix} \overline{P_{11}} & \overline{P_{12}} \\ \left[\overline{P_{21}} + \dfrac{F_p}{U^{*2}}\right] & \overline{P_{22}} \end{bmatrix} \begin{Bmatrix} \overline{\alpha_{n-1}} \\ \overline{\xi_{n-1}} \end{Bmatrix} = \begin{Bmatrix} \overline{X_1} \\ \overline{X_2} - \dfrac{F_\alpha}{U^{*2}} \end{Bmatrix} \tag{3.27}$$

where expressions for $\overline{P}$ and $\overline{X}$ can be found in Appendix A. The $\overline{P}$ matrix represents the time domain differential equation terms in equation 3.10 and $\overline{X}$ represents the time domain unsteady aerodynamics terms from equations 3.23 and 3.24. This equation has been modified such that $F[\alpha(\tau)]$ has been replaced by $F_p(\alpha;\overline{\alpha}) + F_\alpha(\overline{\alpha})$, where $\overline{\alpha}$ is an estimate of α at $\tau + \Delta\tau$ determined by linear extrapolation. The system can therefore be represented as:

$$\left[\, \overline{P} \,\right] \begin{Bmatrix} \overline{\alpha_{n-1}} \\ \overline{\xi_{n-1}} \end{Bmatrix} = \left\{ \overline{X} \right\} \tag{3.28}$$

Solving for the unknowns by inverting the $\overline{P}$ matrix gives the solution for the system at

$$\begin{Bmatrix} \overline{\alpha_{n-1}} \\ \overline{\xi_{n-1}} \end{Bmatrix} = \left[\overline{P} \right]^{-1} \left\{ \overline{X} \right\} \tag{3.29}$$

the next (n+1) time step.

3.2.1.1 Houbolt Method Starting Procedure

Because Houbolt's method is a time marching backward difference scheme, it requires that values at time $\tau = 0$ and two time steps previous be known before the system can be started. Since the initial conditions for the system ($\ddot{\alpha}(0)$, $\dot{\alpha}(0)$, $\alpha(0)$, $\dot{\xi}(0)$, $\ddot{\xi}(0)$, $\xi(0)$) are required to be known in order to define the problem, only the two previous time steps need to be determined to begin the simulation. By using a Taylor series around the τ=0 point, values for n-1 and n+1 for both the first and second derivatives can be estimated and substituted into the [X] matrix (See Appendix A for details). Conditions for three consecutive time steps are then known and Houbolt's scheme can be used to determine the next time step in the series.

3.2.1.2 Houbolt's Recurrence Formula

In order to integrate within the [X] matrix terms, a recurrence formula is used. The integral $I_1(\tau+\Delta\tau)$ can be written as:

$$I_1(\tau+\Delta\tau) = e^{-b\Delta\tau} I_1(\tau) + \frac{\Delta\tau}{24}\{9\lambda(\tau+\Delta\tau) + 19\lambda(\tau)e^{-b\Delta\tau} - 5\lambda(\tau-\Delta\tau)e^{-2b\Delta\tau} + \lambda(\tau-\Delta\tau)e^{-3b\Delta\tau}\} \tag{3.30}$$

See Appendix A for details. $I_2(\Delta\tau)$ is similarly expressed by substituting d in the place of b in equation (3.30).

3.2.2 Describing Function Approach

The describing function approach is a semi-analytical method of solving nonlinear systems by replacing the nonlinear portion of the system with a linear replacement where the gain, or stiffness in the case of a spring, of the linearized spring is dependent upon the amplitude of the harmonic motion. As it is implemented here, the nonlinear pitch spring function $F(\alpha)$ is replaced by a linear spring whose stiffness is determined such that a sinusoidal input to either the nonlinear or the linearized spring will produce the same output response.

The describing function method requires the assumption that the resulting motion of the system will be harmonic with an amplitude that may vary only slowly. The linearized spring is also sometimes known as an *equivalent stiffness* and allows for a solution that in the described case approximates the amplitude *versus* airspeed

relationship of the nonlinear system, as well as the airspeed at which limit cycle flutter will ensue. In the system described in Section 3.1 the nonlinear operator is the pitch restoring moment function $F(\alpha)$ which replaced the linear pitch stiffness K_α.

The describing function method seeks to replace the nonlinear spring in the system with the linearized one by first assuming a harmonic input to the spring in terms of the pitch angle of the airfoil of the form:

$$\alpha(t) = B + A \sin(\omega t + \theta) \tag{3.31}$$

and an output restoring moment of:

$$F(t) = N_B B + n_p A \sin(\omega t + \theta) + n_q A \cos(\omega t + \theta) \tag{3.32}$$

where N_B is the relationship between the mean input B, and the mean output and $N_A = n_p + jn_q$, where j denotes the imaginary component of the complex variable, is the relationship between the sinusoidal input and the fundamental harmonic output. In the well known harmonic equation 3.31, parameter A represents the amplitude of the input signal and B represents the DC offset or bias of the signal. In the case of the symmetric hysteresis loops studied here, there is no bias of the signal and both N_B and B can be neglected. The resulting formulation is a sinusoidal input describing function. These relations form the describing function portion of the system depicted in Figure 3.3.

For the system studied here, the describing function seeks to linearize the nonlinearity in the restoring moment of the pitch degree of freedom. The input to the

nonlinearity is the pitch angle of the airfoil. The output of the describing function represents the restoring moment F(t) of the structure.

The formulation for the describing function N_A can be derived from a method of slowly varying amplitude and phase as outlined by Gelb and Vander Velde (1968). They describe the *extensively developed theory of linear systems* studying a system characterized by:

$$\ddot{\alpha} + \omega_0^2\alpha + \nu f(\alpha,\dot{\alpha}) = 0 \tag{3.33}$$

where ν is a small parameter from $F(\alpha) = \nu f(\alpha,\dot{\alpha})$ and the limit of the system as $\nu \to 0$ is a linear oscillator. A solution to the system is proposed of the form:

$$\alpha(t) = A(t) \sin\,[\omega_0 t + \theta(t)] \tag{3.34}$$

where A is the amplitude of the oscillating pitch and θ is the random phase angle uniformly distributed over a complete cycle. The *method of slowly varying amplitude and phase* specifies that for small ν the system is oscillatory and $\dot{A}$ and $\dot{\theta}$ are small such that A and θ are slowly varying with time. Approximations can be made to determine A and θ by averaging $\dot{A}$ and $\dot{\theta}$ over one complete cycle:

$$\dot{A} \approx \frac{1}{2\pi\omega_0} \int_0^{2\pi} \mu f(A\sin\psi,\ A\omega_0\cos\psi)\ \cos\psi\ d\psi \tag{3.35a}$$

$$\dot{\theta} \approx \frac{1}{2\pi\omega_0} \int_0^{2\pi} \frac{1}{A}\ \mu f(A\sin\psi,\ A\omega_0\cos\psi)\ \sin\psi\ d\psi \tag{3.35b}$$

where $\psi = \omega_0 t + \theta$.

Applying these results for the purposes of illustration to the well known, simpler one degree of freedom linear second-order damped oscillator, the equation of motion is given by:

$$\ddot{\alpha} + 2\zeta\omega_{\alpha}\dot{\alpha} + \omega_n^2\alpha = 0 \tag{3.36}$$

The solution can be expressed [Gelb and Vander Velde, 1967] in the form:

$$\ddot{\alpha} - 2\left(\frac{\dot{A}}{A}\right)\dot{\alpha} + \left[\omega^2 + \left(\frac{\dot{A}}{A}\right)^2\right]\alpha = 0 \tag{3.37}$$

Substituting from Equation 3.35, Equation 3.37 can be expressed as:

$$\ddot{\alpha} - \frac{n_q(A,\omega_0)}{\omega_0}\dot{\alpha} + [\omega_0^2 + n_p(A,\omega_0)]\,\alpha = 0 \tag{3.38}$$

where $\omega = \omega_0 + \theta$ and the describing function terms n_p and n_q have been defined by:

$$n_p(A,\omega_0) = \frac{1}{\pi A}\int_0^{2\pi} y\,(A\sin\psi,\ A\omega_0\cos\psi)\ \sin\psi\ d\psi \tag{3.39a}$$

$$n_q(A,\omega_0) = \frac{1}{\pi A}\int_0^{2\pi} y\,(A\sin\psi,\ A\omega_0\cos\psi)\ \cos\psi\ d\psi \tag{3.39b}$$

Thus the nonlinearity has in effect been replaced by a *linear proportional plus derivative network* whose coefficients are functions of the amplitude and frequency of the system.

The linearization is essentially derived from an averaging of the of the amplitude over one complete cycle of the oscillation. From Equation 3.38 it can be seen that for this type of dynamic system the parameter n_p acts in place of the spring stiffness coefficient and the n_q term comprises a damping term. The complex linear gain N_A determined from the describing function therefore incorporates both stiffness and damping terms n_p and n_q respectively.

For a hysteresis nonlinearity, Gelb and Vander Velde (1968) list the parameters for the describing function according to:

$$n_p = \frac{m}{2}\left[2 - f\left(\frac{\frac{D}{m} + \delta}{A}\right) + f\left(\frac{\frac{D}{m} - \delta}{A}\right)\right] \tag{3.40}$$

$$n_q = -\frac{4\,D\,\delta}{\pi\,A^2} \tag{3.41}$$

which is valid only where $A > \delta + D/m$, meaning that the describing function approximation can only be used where the amplitude of the pitch oscillations lies outside the bounds of the hysteresis loop. The parameter m represents the slope of the linear portion of the hysteresis loop from the relation between pitch angle α and the restoring moment $F(\alpha)$ as illustrated in Figure 3.2. In all cases presented here the slope was assumed to be unity, or 1 non-dimensional moment unit per radian of pitch angle. The

parameter δ is equal to $\Delta H/2$ and D is equal to V_1 as illustrated in Figure 3.2. The functions f() is the saturation function that describes the deadband area where:

$$
\begin{aligned}
f(\gamma) &= -1 && \gamma < -1 \\
&= (2/\pi)(\sin^{-1}\gamma + \gamma\sqrt{1-\gamma^2}) && |\gamma| \le 1 \\
&= 1 && \gamma > 1
\end{aligned}
\tag{3.41}
$$

where γ is a dummy variable. For illustration, the values for the describing function parameters N_A, n_p, and n_q for the airfoil configuration used in Run 14 (μ=100, $\bar{\omega}$=0.8, ΔV=1.0, ΔH=0.2) are plotted against oscillation amplitude A.

The feedback nature of the system is illustrated in Figure 3.3 where the describing function is the linear operator N that replaces the nonlinear operator of the hysteresis spring $F(\alpha)$ in the otherwise linear dynamic airfoil system represented in Figure 3.3 as L(S). The method determines what sinusoidal *input* is required for the linearized operator to emulate the nonlinear *output*. Thus the properties of the operator are dependent upon the amplitude of the input signal. An iterative approach to solving the system of equations is therefore required that first guesses at the amplitude of the pitch oscillation of $\alpha(t)$, then compares the output of the system to the guess. How this method was specifically implemented in the studied case is outlined in Chapter 4.

A similar solution method was also applied to the bilinear type nonlinearity illustrated in Figure 3.4 for comparison with results by Lee and Desrochers (1986) and Price et. al. (1994).

It can be shown [Gelb and Vander Velde, 1968] that if there is no steady state component to the moment about the two-dimensional airfoil and N_B represents the bias of

the input signal to linear spring (see equation 3.32), then N_B must equal zero. In the case of the hysteresis loops that are symmetric about the origin of the restoring moment *versus* pitch angle space B is also equal to zero and the Sinusoidal Input Describing Function (SIDF) formulation may be used. The system can therefore be solved in an iterative manner by first assuming a value for pitch amplitude A and solving the equations 3.40 and 3.41 for n_p and n_q as a function of A. A value for $N_A = n_p + jn_q$, which represents the equivalent stiffness of the nonlinear spring, can then be substituted into the equations of motion for the airfoil in place of $F(\alpha)$ and a linear solution determined. The resulting pitch amplitude of the system is then compared to the initial estimate, A, and revised. The iterations are repeated until the solution resolves to a single amplitude solution.

4.0 ANALYSIS

The analysis of the studied systems consisted of comparisons between the numerical solution method involving time marching simulations, and the semi-analytical approximation using the describing function approach. This section describes how the theory described in Chapter 3 was implemented and the system configurations to which the solution methods were applied. The parameters which were examined and the respective results are also presented here.

4.1 System Definition

The aeroelastic system that was modelled consisted of a two-dimensional airfoil in a free stream of air with restoring forces in both the pitch and heave degrees of freedom. This system is represented schematically in Figure 3.1. Aerodynamically, the lifting forces were determined from thin airfoil theory where the unsteady aerodynamic forces follow the relationship described by Wagner's function (Equation 3.20). Structurally, the restoring force in the heave direction is modelled as a linear spring and the restoring force in the pitch degree of freedom is the restoring spring with the structural nonlinearity. The nonlinearities studied included a bilinear type nonlinearity, for validation with previous work as illustrated in Figure 3.4, and a hysteresis type

nonlinearity as depicted in Figure 3.2. Both types of nonlinearities represent structural restoring forces with discontinuities in the force *versus* pitch slope.

The airfoil used for the analysis was configured such that the elastic axis was placed at the ¼ chord position and the centre of mass placed at the 3/8 chord position downstream of the elastic axis. The resulting parameters used for the airfoil structure as defined in Figure 3.1 were:

$$a_h = -0.5$$

$$r_\alpha = 0.5$$

$$x_\alpha = 0.25$$

where r_α represents the radius of gyration of the airfoil about the elastic axis. These values were kept constant throughout the analysis and are consistent with those used in previous works. Thin airfoil theory specifies that the aerodynamic centre is located at the ¼ chord position. For the sake of clarity and comparison it was decided to keep these characteristics of the airfoil consistent. The damping coefficients for the system were neglected throughout the analysis and only the frequency ratio ω, the mass ratio μ and non-dimensional airspeed U were varied. For each airfoil configuration the airspeed was expressed as a fraction of the linear flutter speed U*, the airspeed at which divergence of the system occurs if the pitch spring is linear, and was denoted as U/U*.

4.2 Time Marching Simulation Solutions

Both the simulation method and the describing function method were first used to reproduce the results of Lee and Desrochers (1986) by implementing the model with a

bilinear spring in the pitch degree of freedom. The Houbolt finite difference method was used to produce a time based "recording" of the airfoil response in pitch and heave in a time marching manner. The solution method was subsequently used for Hysteresis spring configurations to produce time based response solutions as illustrated in Figure 4.1.

The response of the system was simulated subject to a set of given initial conditions, in this case mainly the initial pitch angle and airspeed were varied, to produce a response of the system with time in each of the degrees of freedom. The simulation was computed until the system response either damped out to zero, diverged beyond acceptable bounds, or had completed enough time steps to be certain transient effects had disappeared and steady state had been achieved.

The simulations were completed for the Hysteresis airfoil configurations on a parametric basis for each airfoil configuration listed in Table 4.1, by varying the airspeed (U/U*) and initial pitch angle (α_o)as the set of initial conditions. The results of each simulation were then evaluated to determine which of the three conditions resulted:

1. Damped oscillations (stable)
2. Divergent oscillations (unstable)
3. Limit cycle oscillations (LCO)

For cases where LCO's resulted, the amplitude of the steady state oscillation was recorded. From these results, diagrams showing the flutter boundaries, regions of stability and LCO's within the airspeed U/U* versus initial pitch angle α_o parameter

space, as well as the airspeed U/U* *versus* LCO amplitude relationship were evaluated.

For the bilinear spring simulations, close comparison of results with those from the previous work confirmed the correct implementation of the model. All results agreed well with the results of Lee and Desrochers with some small differences explicable by slight differences in compiler implementation and computer platform as discussed in Chapter 5.

The hysteresis spring was subsequently implemented into the model using the nomenclature outlined in Figure 3.2 where the spring's parameters have been characterized by the ΔV, ΔH, V_{offset} and H_{offset} variables. The hysteresis spring was essentially a bilinear type spring with a memory such that the parameters of the model varied depending upon the direction of change of the pitch ($\partial\alpha / \partial\tau$). The spring was modelled to maintain a constant pitch vs restoring moment slope of 1 non-dimensional moment unit per radian as shown in the diagram except when on the deadband portions of the hysteresis at the top and bottom of the figure. Exception handling was also implemented into the behaviour of the spring to maintain a piecewise continuous response. The code was implemented such that a reversal in direction of pitch between H^- and H^- maintains the pitch-moment slope of 1 between the V_1 and V_2 marks. The response of the spring was finally modelled according to the relationship:

$$\text{For } \partial\alpha / \partial\tau > 0 \quad (\alpha \text{ increasing}) \qquad F(\alpha) = \begin{cases} \alpha + \Delta H/2 - H_{off} & : \alpha \le H_1^- \\ V1 & : H_1^- < \alpha < H_1^- \\ \alpha - \Delta H/2 - H_{off} & : \alpha \ge H_1^- \end{cases} \tag{4.1}$$

$$\text{For } \partial\alpha / \partial\tau < 0 \quad (\alpha \text{ decreasing}) \qquad F(\alpha) = \begin{cases} \alpha - \Delta H/2 - H_{off} & : \alpha \ge H_2^- \\ V2 & : H_2^- < \alpha < H_2^- \\ \alpha + \Delta H/2 - H_{off} & : \alpha \le H_2^- \end{cases} \tag{4.2}$$

where the H and V terms were defined as outlined in Figure 3.2

Simulations were performed using hysteresis spring configurations varying the parameters ΔV and ΔH from 1.0 to 0.1 and with vertical and horizontal offsets up to 0.5 with various combinations of all four parameters. The parameters for the simulated systems are listed in Table 4.1. Results consisted of time based traces of the airfoil motions in both the pitch and heave degrees of freedom which were then interpreted to provide flutter boundary maps indicating the regions of stability as well as the limit cycle amplitude α vs flutter speed U/U^*.

The finite difference method was used for each parameter set to simulate the response of the system to an initial perturbation, the initial pitch angle α_o, to the point in time where the transient effects were no longer affecting the system. The three stability conditions were evaluated according to the following criteria:

1. Damped (stable) - the oscillations of the system died out over time such that the amplitude of the system reached approximately zero and no

further motion was present. The criterion implemented was pitch amplitude $\alpha < 0.001$.

2. Divergent (unstable) - the oscillations of the system grew beyond the bounds of the simulation and the system was deemed to have become unstable. The criterion implemented was pitch amplitude $\alpha > 100$.

3. Limit Cycle Oscillations - the oscillations tended neither to damp out to zero nor to grow to infinity but rather became self sustaining at an amplitude of some intermediate value. This result was determined to be a limit cycle response. The criterion implemented was "time steps" > 50000.

The results of particular interest are those where the oscillations either enter a steady state in the form of a limit cycle or diverge entirely to instability. It is this behaviour that is of concern to aerospace applications as the deflection beyond anticipated amplitudes could cause damage or failure. This flutter type behaviour can not be predicted by linear analysis techniques and can only be present in systems containing nonlinearities. Developing techniques to predict the effects of these nonlinearities becomes important.

For each airfoil configuration of interest, simulations were performed for a range of non-dimensional airspeed ratios of 0.1 to 1.0. For each simulation run the steady state response of the system was recorded with respect to the stability of the system as specified above. Also recorded was the amplitude of the limit cycle response if the limit cycle existed.

4.3 Describing Function Solutions

As outlined in Chapter 3, the describing function semi-analytical method provides a means of emulating the effect of the nonlinear element by relating a linearized spring stiffness to the output amplitude. In effect, the nonlinear spring modelled in the pitch degree of freedom can be replaced by an appropriately linearized spring that approximates the same amplitude of oscillations as the nonlinear spring it replaces. The method allows for the development of a relationship between the airspeed and the resulting effective stiffness of the linearized spring.

The Describing Function (DF) analysis technique was implemented in this project for three purposes:

- To provide for a means by which to compare the results of the simulation and confirm the validity of the data.
- To evaluate the Describing Function approximation with respect to its accuracy and efficiency as a substitute for the nonlinear simulation.
- To attempt to show where semi-analytical methods break down and why.

To this end, the describing function was first implemented as the bilinear spring with freeplay, illustrated in Figure 3.4, as evaluated numerically by Lee and Desrochers (1986) and both numerically and using DF's by Price, et. al. (1994). After successful comparison with the simulations for the bilinear spring and the DF work by Price, et. al.

(1994) the method was modified to use the describing function parameters corresponding to the hysteresis spring used in the finite difference simulations.

As described in Section 3.1.2 the system describing the two-dimensional airfoil with unsteady aerodynamics represented in Equation 3.21 can be solved directly for stability if the structural elements are linear. The describing function method was implemented by first choosing the value of the limit cycle amplitude A. A value for $N=n_p + jn_q$ from equations 3.33 and 3.34 was found and represented the linear pitch stiffness K_α replacing nonlinear spring $F(\alpha)$, in equation 3.17. When the system is simplified and represented in the form of Equation 3.19, the system is in the form of a free vibration response problem. As described in Chapter 3, the roots of the system are the solutions to the *characteristic equation* $\det(B) = 0$.

The expression for [B] was determined from the equations for unsteady aerodynamics by substituting Equation 3.22 into Equation 3.21 and then substituting the expressions for lift and moment into equation 3.9. The polynomial was explicitly determined using the symbolic math processing software Maple. The resulting expression was solved using the software analysis tool Matlab. Using Matlab the explicit roots for the characteristic equation were found for the system using the linearized pitch stiffness N.

The roots of the [B] matrix could then plotted in a root locus plane and the speed at which the first real root crossed the real=0 line revealed the flutter speed for that pitch stiffness. Figure 4.10 is an example of a root locus result plotting the values of the roots

of the characteristic equation for the given aeroelastic system as the airspeed U* is varied. In the case of Figure 4.10 the roots for the linear system where $\bar{\omega} = 0.2$ are plotted with a pitch stiffness term of 1.0 substituted for the nonlinear $F(\alpha)$ function. The result shows that the system will become unstable for a non-dimensional airspeed of $U^* = 6.285$. This value represents the linear flutter speed for this airfoil configuration. This solution method allows for a relationship to be established between the pitch stiffness and the flutter speed. Figure 4.11 is a plot of how the flutter speed varies with pitch stiffness for a variety of airfoil configurations. 4

The describing function approach essentially provides a means for relating the pitch amplitude to the pitch stiffness, calculating linearized pitch stiffness N from A, while the flutter analysis essentially provides for a relation between the pitch stiffness and the flutter speed. By assuming a harmonic output for the dynamic system the nonlinear pitch relation $F(\alpha)$ was replaced by the describing function equivalent stiffness effectively creating a solution method that relates the pitch amplitude to the flutter speed.

The flutter speed is solved in an iterative manner, varying the speed U for which the dynamic system is analysed until the speed for which the system goes unstable is found. The result is an approximate solution for the limit cycle amplitude A for the speed U that was found.

5.0 DISCUSSION AND COMPARISON OF RESULTS

The results described in the previous section were compiled for the various airfoil configurations and initial conditions. This section presents an analysis of those results as well as comparisons between the two solution methods. Strengths and weaknesses of the methods are discussed and improvements to the analysis suggested. The results are put into context and their applicability to real world situations is reviewed.

The results of the parametric study of various airfoil configurations are plotted in Figures 5.5 through 5.31. The 'a' figures (Figure 5.5a, 5.6a, 5.7a, ... ,5.31a) plot the flutter map results from the finite difference method numerical simulations. The plots show the parameter space of airspeed ratio, U/U^*, *versus* initial pitch angle, α_0. Regions within the parameter space are indicated where for the specific airfoil configuration damped oscillations occurred, limit cycle oscillations (LCO) were observed, or where unstable oscillations were induced. The x's represent a change in stability from damped to LCO or vice versa. The 'b' figures (Figure 5.5b, 5.6b, 5.7b, ... , 5.25b) plot the pitch restoring moment $F(\alpha)$ against the pitch angle $\alpha(\tau)$ indicating the geometry of the hysteresis loop for each of the indicated cases. The 'c' figures (Figure 5.5c, 5.6c, 5.7c, ..., 5.31c) indicated the amplitude of limit cycle oscillations, where they were observed, as

induced by the varying airspeeds U/U*. Where the describing function was used, the solution from this method was also included in the figure.

5.1 Finite Difference Simulations

5.1.1 Validation

As stated previously, the results of the numerical simulations were in the form of time based histories of the pitch and heave motions of the airfoil system as illustrated for example in Figure 4.1. Results were first obtained for airfoil configurations using a bilinear spring with freeplay and preload as explored by Lee and Desrochers (1987). A large number of simulation plots were accessible for comparison with their work and present the results compared very well with theirs, with only a very few minor discrepancies. For individual cases compared, i.e. the same airfoil configuration, initial conditions and bilinear nonlinear spring, in all cases the same stability condition was met for a given simulation. Similarly, comparisons of boundaries of limit cycle and divergent flutter for given airfoil properties matched exactly. It was found that for a few configurations for which the system was just barely stable the simulations did not reach stability after the exact same amount of time. This discrepancy was easily explainable by the sensitivity of the nonlinearities to very small changes in initial conditions. A slightly different implementation of the code, small hardware based differences, and possible differences in the numerical accuracy of the methods all contributed to small differences that were amplified by the nonlinearity into larger differences in the results of the simulation run. It was not found that these differences caused discrepancies in the overall

characterization of the airfoil system. It was rather found that there were noticeable differences in the time at which the system achieved stability.

These small discrepancies aside, the two methods appeared to agree as closely as could be determined. By utilizing a bilinear spring and comparing with previous work, the implementation of the Houbolt scheme was validated. Subsequently validating the behaviour of the hysteresis spring and substituting it into the simulation code allowed the simulation to be utilised with a high degree of confidence.

Validation of the hysteresis spring took the form of performing simulations of the motions of the spring and its response to various stimuli. The response of the spring was analysed graphically to ensure that the pitch angle *versus* restoring moment response of the operator followed the specified curve. Figure 3.2 shows the general structure of the curve and the difference in the path of the curve depending upon the direction of the change in pitch. Exceptions in the path of the curve were noted during certain portions of the simulation. Attention was paid to how the spring model responded to reversals in the direction of pitch change within the "loop" portion of the hysteresis curve. It was determined that the loop was best described by allowing the restoring moment to return along the sloped path of the curve when reversal occurred as depicted in Figure 4.8. When reversal occurred on the flat portion of the curve the response was modelled such that the slope of m=1 was maintained as depicted in Figure 4.9. The spring response was therefore maintained piecewise continuous.

Figures 5.5b to 5.9b and Figures 5.18b to 5.25b trace the path of the hysteresis loop restoring moment for an example of each of the corresponding runs. A small

amount of under-run can be observed in some of the plots. This result is in fact just a "cutting of the corner" by path of the restoring moment. This particularly occurs for cases where the amplitude of the pitch response is large and the pitch angle is therefore changing very rapidly as it moves through the area of the hysteresis loop. The finite difference source code includes a small algorithm to look ahead and test each step for overrun and ensure that the moment follows the curve explicitly.

5.1.2 Flutter Boundaries

Simulation results for the airfoil system were subsequently obtained for a hysteresis spring with a variety of spring parameters as outlined in Chapter 4. The results were first analysed in the form of plots of the stability characteristics of the system for varying airspeeds as shown for example in Figure 5.5a. This data allowed for a "mapping" of the flutter boundaries indicating at what airspeeds the system achieved stability, limit cycle oscillations, or instability. Results were also plotted for the amplitudes of limit cycle oscillations for the various hysteretic spring parameter values.

The flutter maps in Figures 5.5a to 5.31a show that, as predicted, there lies a zone of limit cycle flutter at airspeeds lower than the linear flutter speeds. The linear flutter speed for the airfoil configuration was determined using both the simulation and the analytical solution methods. The linear flutter speed was determined using the classical analytical solution method by determining the speed U* at which the system became unstable. As described in the previous chapter, this was performed by assuming a linear spring in the pitch degree of freedom then solving the equations of motion from the

Laplace domain for the eigenvalues of the system. The linear flutter speed was found by varying the airspeed to find the speed at which the system just goes unstable, indicated by negative real portions of the roots. The numerical simulation method was later used to confirm the linear flutter speed by setting the spring to be a linear spring and performing iterative simulations to find the speed at which the system became unstable. The results were found to be nearly identical.

The flutter boundaries show the extreme sensitivity of the nonlinear system to the initial conditions. For example, Figures 4.2 to 4.7 show how the same initial conditions will result in different stability conditions for the system depending upon the airspeed. The pitch angle time traces from Run 14, depicted in Figures 4.2 to 4.7, demonstrate how for the same initial conditions the stability of the system varies depending on the airspeed. The corresponding flutter map for this configuration, Figure 5.7a also shows the speeds and initial pitch angles for which there is LCO motion. For the same initial pitch angle of $\alpha = 6°$ the system would achieve a limit cycle condition if the non-dimensional flutter speed was between 0.864 and 0.910 and between 0.942 and 1.0. The system was stable below a speed of 0.864, but a zone of stability also existed between 0.910 and 0.942. From these results it can be seen that it becomes very difficult to predict the stability of a system from a given set of initial conditions without preforming an actual time based simulation. This behaviour is characteristic of nonlinear systems.

It was also observed that the flutter boundaries were a continuous line for most of the $\bar{\omega} = 0.8$ runs with a clear boundary showing the stable and LCO regions of the parameter space. Most of the $\bar{\omega} = 0.2$ runs however showed the boundary of flutter as a

large area of conditions were the airfoil exhibited stability or LCO depending upon small differences in speed U/U*, as shown for example in Figure 5.12a. This figure shows the flutter map for the given airfoil configuration and conditions where the x's mark each airspeed U/U* where for the same initial pitch angle the stability condition has switched from stable to LCO motion or vice versa compared to the next lowest airspeed simulated.

In all cases the runs diverged to instability at the point U/U*=1.0 regardless of configuration or initial conditions. This result is as expected since the nonlinearity tends to reduce the stiffness of the degree of freedom in the region of the hysteresis loop. Therefore there is no tendency for the system to diverge when the pitch amplitude is much larger than the size of the hysteresis loop unless the linear flutter speed has been achieved.

5.1.3 Airspeed vs Limit Cycle Amplitude

In addition to compiling results with respect to the stability of the dynamic system at various speeds, for speeds at which a limit cycle stability existed the amplitude of the limit cycle was recorded. These results were then plotted to show the relationship between the limit cycle amplitude and the flutter speed for various airfoil configurations and initial conditions, as shown for example in Figure 5.5c. The first characteristic for these relationships that was noted was that for all the airfoil configurations tested in this work, the limit cycle amplitudes were for the most part invariant with initial conditions. This result is consistent with the results published by Lee and Desrochers (1987) and Price et. al. (1994) for many bilinear and cubic springs. The exceptions to this case are

the bifurcation diagrams in the Price et. al. (1994) report where specific configurations of the nonlinear spring lead to different LCO amplitudes, i.e. different limit cycle amplitudes could be achieved depending upon the initial conditions. From the results it can be seen that these kinds of amplitude jumps were present mainly in the results of the $\bar{\omega} = 0.2$ family of results. This result would seem to indicate that the results for the $\bar{\omega} = 0.8$ group were the more nearly sinusoidal cases without the harmonic structures observed in the $\bar{\omega} = 0.2$ cases.

Observations were also made of the type of response achieved depending upon the shape of the hysteresis curve. As would be expected, the response of the system becomes the same as for a linear system as ΔH approaches zero, and the same as for a system with a bilinear type nonlinearity as ΔV approaches zero. It can be seen from Figures 5.5c to 5.17c that as the ratio $\Delta H/\Delta V$ approaches infinity from zero the difference between the two solution methods for the speeds at which LCO may be induced and the linear flutter speed becomes greater. Table 5.1 shows that for the $\bar{\omega} = 0.8$ cases the speeds at which LCO motion is initiated varies from $U/U^* = 0.816$ for the $\Delta H/\Delta V = 10$ case to $U/U^* = 0.954$ for the $\Delta H/\Delta V = 0.1$ case. For the $\bar{\omega} = 0.2$ cases the configuration for which the speed at which LCO motion was initiated was the case of $\Delta V = 0$, a bilinear type operator similar to that shown in Figure 3.4, for which LCO was initiated at $U/U^* = 0.136$. From the table it can be seen that there is a distinct correlation between the speeds of initiation of the LCO motion and the $\Delta H/\Delta V$ shape of the hysteresis curve.

5.1.4 Numerical Error

The finite difference approximation to differential equations can serve to introduce certain errors into the solution because of the nature of their numerical approximation. One example of this type of error is the introduction of what is termed in Computational Fluid Dynamics (CFD) work as *artificial viscosity* [Strikwerda, 1989] or would in this case be termed an *artificial damping* component. This error is introduced because the finite measure of time, $\Delta\tau$ can not *exactly* describe the motion of the airfoil when changes occur very rapidly. This approximation to the airfoil behaviour has the effect of appearing to dampen the response of the system.

From the validation runs performed to determine the linear flutter speed for the airfoil configurations, the known solution of a direct analytical analysis of the linear flutter speed was compared to the finite difference solution for the same parameter. For the airfoil configuration where $\mu = 100$ and $\bar{\omega} = 0.8$, the analytical solution to the flutter speed is $U^* = 4.1144$ while the finite difference method produced a solution of $U^* = 4.1128$. The error of the finite difference solution was therefore -0.04% and was therefore not determined to be important for the purposes of the present analysis.

It should however be noted that the finite difference method is *not* an exact solution to the problem and should not be considered absolutely correct when compared to the describing function method. It becomes quite difficult to evaluate the error inherent in the finite difference solution, especially for cases such as the studied nonlinear spring where no exact solution for comparison exists. The two studied solution methods

were essentially being compared to each other and a determination of one or the other being considered *exact* was not made.

5.2 Describing Functions

As with the numerical simulations, the describing function method was first applied to systems with the bilinear spring with freeplay nonlinearities as reported by Price et. al (1994). Sample systems were solved as described in the theory section and the results were compared with both the results of the bilinear spring simulations and the results published by Price et. al (1994). The solutions were found to agree quite well between the describing function method and the finite difference simulation method.

Subsequent to the application of the describing function method to the bilinear spring this solution method was used to model the systems with hysteresis nonlinearities. The systems with hysteresis springs that were modelled were symmetric springs with ΔV and ΔH varying from 0.1 to 1.0 and cases completed for both $\bar{\omega} = 0.8$ and $\bar{\omega} = 0.2$. Figures 5.5c to 5.31c plot the values of pitch angle α vs flutter speed U/U^* and where applicable compare the describing function approximation to the numerical simulation solution. It can be seen from these plots that the agreement between the two methods is quite good considering the approximations and assumptions that have been made in order to provide for the semi-analytical solution.

Similar to the observations in the previous section, a correlation was also observed between the shape of the hysteresis curve, described by the $\Delta H/\Delta V$ ratio, and the accuracy of the describing function method compared to the finite difference results.

From Table 5.1 , the largest discrepancies between prediction of the speed at which LCO motion is initiated were found in the cases where the shape ratio $\Delta H/\Delta V$ was highest. The largest percent error between the two solution methods was found for the case where $\Delta V = 0$, which is essentially a bilinear type nonlinearity. The largest absolute difference in the prediction of the initiation of LCO motion was for the case where $\Delta H/\Delta V = 10$. There would appear to therefore also be a correlation between the accuracy of the describing function method and the shape of the hysteresis loop as described by the ratio $\Delta H/\Delta V$.

The predictions for the airspeeds at which LCO oscillations initiate were found to be in good agreement with the finite difference method and the semi-analytical method. The agreement from Table 5.1 ranges from 0.2 % to 37.5 % with the cases where $\bar{\omega} = 0.8$ agreeing somewhat better than the cases where $\bar{\omega} = 0.2$. It was noted earlier that the simulation results for the $\bar{\omega} = 0.8$ cases appeared to be more sinusoidal, without the harmonics observed in the $\bar{\omega} = 0.2$ cases so that better agreement is to be expected for $\bar{\omega} = 0.8$.

Quantifying the accuracy of the describing function for predicting the amplitude *versus* airspeed relation, as predicted by the finite difference solution method, was difficult due to the multiple values of LCO amplitude for many of the finite difference results. Observations of results in Figures 5.5c to 5.15c showed that the describing function method results generally followed the finite difference results quite closely. The $\bar{\omega} = 0.8$ run that appeared to have the largest error between the two methods is shown in Figure 5.5c corresponding to run 6. From Table 5.1 it was also seen that this

configuration also had the largest error in predicting the speed at which LCO motion initiated. In the $\bar{\omega} = 0.2$ family of results, the figures displaying the largest discrepancies between the two solution results were in Figures 5.10c, 5.12c, and 5.16c corresponding to runs 100, 102 and 110 respectively. Of the three configurations Figure 5.16c appeared to have the largest error, although difficult to quantify due to the multiple amplitude solutions. Table 5.1 indicates that these are the same hysteresis configurations that had the larger errors between the describing function method and finite difference method predictions of the airspeed of onset of limit cycle motion.

Similarly, the differences between the describing function prediction of the LCO amplitude and the finite difference method appeared greater for the $\bar{\omega} = 0.2$ data. It was noted that the accuracy of the describing function method solution was greatly improved as the amplitude of the limit cycle increased greatly. This relation is expected since, as before, the accuracy of the describing function method will increase as the response becomes more sinusoidal. As the amplitude of the limit cycle becomes large with respect to the size of the hysteresis loop, the effects of the nonlinearity become less significant and the response becomes sinusoidal.

Because of the complications of implementing a *dual input* type describing function it was decided to restrict the describing function solutions to those hysteresis loop configurations that were symmetric, i.e. no offsets. From the numerical simulation results for the offset hysteresis configurations as shown in Figures 5.18 to 5.31, there appeared to be little effect in terms of the general behaviour of the system. The same

relationships with respect to the frequency ratio and the shape of hysteresis loops were observed in the offset results as were described above for the symmetric results.

5.3 Comparisons

The amplitude vs speed relationships determined by the describing function method followed quite closely the results of the finite difference method in the majority of the cases. In particular the describing function agreed better for the cases where $\overline{\omega}$ = 0.8. This result is not surprising, considering that the time-based results from the simulations indicated a purely harmonic result. Since the describing function method has an assumption of harmonic results, the harmonic results of the simulations could be expected to compare quite closely with the analytical approximation. From Figures 5.5c and 5.8c it was seen that as the hysteresis spring approached a condition of $\Delta V=0$ the describing function method was less accurate than those where ΔH approached zero (linear spring). This result confirms the conclusion that the describing function merely loses accuracy as the nonlinearity has a greater impact on the response of the system.

The presence of harmonic structure in the response of the system is shown in Figures 5.1 to 5.4. The sample run shown in Figure 5.1, from run 105, shows little or no difference from an ordinary sinusoid and the power spectrum of the sample, as shown in Figure 5.2 shows integer harmonics of the fundamental but of little power and no additional structure. Figure 5.3 however, from run 102, obviously has additional frequencies in response. The power spectrum in Figure 5.4 shows that the sample was

definitely not sinusoidal in nature. Comparing the flutter maps and describing function method solutions for those two runs shows that of the two, run 102 has the "bifurcation" type multiple amplitudes in the LCO amplitude plots as well as a very cluttered flutter map. We can infer from the comparison of these two sets of results that the higher $\Delta H/\Delta V$ shaped hysteresis nonlinearities are introducing harmonics into the response of the system that the describing function is fundamentally unable to account for.

Because of the tendency of the hysteresis nonlinearities to provide "more interesting" results for those cases where ΔV approaches zero, i.e. the bilinear case, it could be observed that the bilinear case represents a good configuration for examining the behaviour of the nonlinear system. Previous works has mostly utilized bilinear and cubic functions for nonlinearities because they are more easily implemented. The question arises whether by simplifying the analysis process they were limiting their potential to find unusual behaviour such as chaotic motion. It would appear that the hysteresis loop provides what amounts to a continuum from the simple sinusoidal response of a linear system where ΔH approaches zero, to the much more unpredictable behaviour of the system as ΔV approaches zero. The bilinear type nonlinearity therefore proves to be a good candidate for observing unusual behaviour in nonlinear systems, at least when compared to the hysteresis type nonlinearities studied here.

The question of why the describing function breaks down as the system response becomes less sinusoidal is known because of the underlying assumptions of sinusoidal behaviour in the solution method. Why the system response becomes less sinusoidal should also be examined. For the cases where the shape of the hysteresis nonlinearity

affect the harmonics of the system, it can be seen that as the spring becomes less like the linear case where $\Delta V = 0$, the "path" of the restoring moment with pitch angle is deflected further and further from the linear. It can be surmised that it is this deflection that introduces the harmonic structure into the system response. Thus the bilinear spring is again shown to be a good choice for observing nonlinear systems as ΔH is essentially fixed at zero and only ΔV is acting upon the system. For the cases where the difference in the frequency ratio $\bar{\omega}$ affected the response of the system, it can be assumed that since as discussed previously the two degrees of freedom are coupled, reducing the ratio of their frequencies could make the system more sensitive to the effects of the nonlinearity.

5.4 Applications to Aircraft Design

While the accuracy of the simulations has been shown to be quite good in a mathematical sense, caution must be exercised in the application of these types of analysis methods to "real world" situations. In most cases a real aircraft wing section is subject to more than simply two degrees of freedom and three dimensional effects are going to keep the flutter motion of the wing from being exactly as assumed in the present model. However there are some cases whereby components such as control surfaces do behave in a very two-dimensional manner. For example a flap might pivot about its hinge and be far enough outboard for the bending of the wing to be treated as pure heave. The pure heaving motion of the wing as a whole is actually more of a bending motion in a three-dimensional situation and the pitching of the wing occurs as a twist that varies the

angle of the wing section depending on its outboard position. Despite these limitations there are still some good generalities that can be inferred from the model results. From the simulations it is quite apparent that limit cycle flutter due to nonlinearities in the response of the wing is achievable at speeds substantially lower than the linear flutter speed calculated using classical aeroelastic methods. Work by people such as Woolston et. al. (1957) and Breitbach (1977) have recognized this phenomenon for some time now but adequate tools for predicting the results of these nonlinearities are still being developed. Breitbach mentions the hysteresis nonlinearity as being a particularly prevalent type of concentrated nonlinearity.

While this reduction in the actual flutter speed of the aircraft component is of concern, both the simulation results and the describing function results point to the fact that the amplitude of the limit cycle oscillation slowly increases with speed, building up to the instability condition. This result can actually be considered a benefit in terms of the operation of the aircraft. As the wing flutter amplitude increases with speed, either sensors installed in the wing or the feedback through the flight controls can be used to warn the pilot of impending flutter danger similar to the manner in which aircraft buffeting and sensors warn the pilot of stall conditions.

It has been shown that these types of limit cycle oscillations can occur at airspeeds well below the linear flutter speed and care must therefore be taken when analysing the aeroelastic properties of a component to ensure that the flight speeds do not encroach upon the speeds at which the small aeroelastic vibrations are induced. While the

amplitude of the oscillations may not be large enough to affect the flight dynamics it is possible that they could contribute to fatigue loading on the structure.

There are some cases where the nonlinearities present in the response of an aircraft structure do closely resemble the motion simulated by the two-dimensional airfoil. Lee and Tron (1989) were successfully able to model the flutter characteristics on a CF-18 control surface using a describing function type solution method. They showed how the solution method could be used to correctly predict LCO behaviour at speeds well below the linear flutter speed.

The system studied in this thesis makes the assumption of inviscid incompressible air flow. There are nonlinearities associated with compressible flows and shocks that are beyond the scope of this analysis. When incompressible-flow aeroelastic analysis techniques are applied to a structure, including analyses dealing with nonlinearities, it should therefore be determined that compressible effects can safely be neglected.

The value of a describing function method for application to real-world problems is quite good so long as the limitations of the solution method are taken into account and caution is exercised to ensure the underlying assumptions are still valid. Validation with a simulation type solution method could be valuable for the purposes of checking the semi-analytical solution. As shown, as the effects of the nonlinearity on the system become more pronounced and the response less sinusoidal, the describing function becomes less accurate. Thus applying it to solve problems where nonlinearities are prevalent becomes difficult to justify. It's greater value is perhaps for those cases where the nonlinearities are known to be small and their effects subtle.

5.4 Future Work

Several aspects of the results of this work appear appropriate for further study. The first area for continuation of this work lies with the analysis of the time based pitch angle results from the Houbolt finite difference method. Many of the studies performed in recent years on these types of two-dimensional aeroelastic systems have focussed on analysing the results for evidence of chaotic behaviour. The analysis tools for studying the chaotic nature of this kind of time based response include power spectral densities (PSDs), phase-plane plots and Poincaré sections. For example Price et. al. (1994) analysed the responses of bilinear and cubic systems and detected chaotic behaviour in the responses of particular configurations of each type. It is therefore suggested that a natural extension of the analysis of the results already presented in this thesis is to continue and apply chaotic analysis tools to these results to determine if regions of chaotic motion are also present. A comparison of the chaotic motion for the hysteresis type nonlinearities, if found, to those previously studied would enable further comparison and contrast with the response of the bilinear and cubic nonlinearities. By studying and characterizing the chaotic response of this type of nonlinear system, researchers hope to be able to in turn characterise the system itself and find new analytical methods of predicting the response of the system without the need for time consuming simulations.

Another area of possibilities for continued work includes the application of the describing function method to systems whose responses are not purely sinusoidal. It has been shown here and in other works that it is the nature of the describing function to

break down when predicting higher order system responses. While this is a fundamental limitation of this solution method, a technique could be determined to evaluate the system *before* the describing function solution method is applied. Tools such as PSDs and Bode Plots could be used to determine the sensitivity of the system to higher frequencies. The system could then be evaluated with respect to its suitability for solution by describing function method.

All of the configurations presented here used zero structural damping. An investigation of the effects of adding structural damping to the system might be studied to approach the problem from a more realistic perspective. Since it is the goal of this type of work to provide some useful real-world application of these theories, adding some structural damping to the system might indicate what some of the differences might be when applied to a real situation. That is to say, all real-world systems have a certain amount of damping and in the case of aircraft components the amount of damping may not be negligible. Price et. al. (1994) investigated several cases where they added structural damping to the system and they found that the damping tended to eliminate the chaotic nature of the system response. It might then be inferred that a real-world component that is known to be sensitive to concentrated nonlinearities would become less sensitive to those nonlinearities with the addition of damping components.

6.0 CONCLUSIONS

From the work summarized and presented in this thesis, several conclusions may be drawn.

The describing function solution method provided good agreement with the numerical simulation solutions, except in those cases where the response of the system strayed significantly away from a sinusoidal type motion.

There were two parameters that appeared to most affect the accuracy of the describing function prediction of system behaviour. The describing function compared least favourably to the Houbolt finite difference method when:

- the hysteresis spring configuration had a high $\Delta H/\Delta V$ ratio, and/or
- the frequency ratio $\bar{\omega} = 0.2$ rather than $\bar{\omega} = 0.8$

Of the two configuration parameters the $\Delta H/\Delta V$ ratio appeared to have the greater effect on the response of the system.

The $\bar{\omega} = 0.2$ family of runs exhibited LCO behaviour had much lower airspeeds, compared to the linear flutter ratio, then did the $\bar{\omega} = 0.8$ set of runs. Additionally the flutter maps for the $\bar{\omega} = 0.2$ runs were much less "ordered" than those of the $\bar{\omega} = 0.8$

results, showing a much greater sensitivity to the U/U* flow speed and changing back and forth between stability and LCO motion.

Because of the noted effects of the shape of the hysteresis nonlinearity on the response of the system, it was concluded that the bilinear nonlinearity that has been used for many investigations of this type into nonlinear system provides good opportunities, at least equal to that of the hysteresis nonlinearity, for observing unusual behaviour.

REFERENCES

Barrington, P., 1994, 87.462 Introduction to Aeroelasticity course notes, Dept. of Mechanical and Aerospace Engineering, Carleton University.

Brietbach, E., 1978, "Effect of Structural Nonlinearities on Aircraft Vibration and Flutter", AGARD Report 665, January.

Dowell, E. H., Ilgamov, M., 1988, *Studies in Nonlinear Aeroelasticity*, Springer-Verlag: New York.

Fung, Y.C., 1955, *An Introduction to the Theory of Aeroelasticity*, John Wiley & Sons, Inc., New York.

Gelb, A., Vander Velde, W. A., 1968, *Multiple-Input Describing Functions and Nonlinear Systems Design*, McGraw-Hill: New York.

Hauenstein, A. J., Zara, J. A., Eversman, W., Qumei, I. K., 1992, "Chaotic and Nonlinear Dynamic Response of Aerosurfaces with Structural Nonlinearities", AIAA-92-2547-CP, AIAA/ASME/ASCE/AHS/ASC, 33rd Structures, Structural Dynamics and Materials Conference

Houbolt, J. C., 1950, "A Recurrence Matrix Solution for the Dynamic Response of Elastic Aircraft", *Journal of Aeronautical Sciences*, Vol. 17, pp. 540-550.

Jones, D. J., Lee, B. H. K., 1985, "Time Marching Numerical Solution of the Dynamic Response of Nonlinear Systems, *National Research Council of Canada*, Aeronautical Note NAE-AN-25.

Katz, J., Plotkin, A., 1991, *Low-Speed Aerodynamics*, McGraw-Hill Inc., Toronto.

Laurenson, R. M., Trn, R. M., 1980, "Flutter Analysis of Missile Control Surfaces Containing Structural Nonlinearities", *AIAA Journal*, Vol. 18, October, pp. 1245-1251.

Lee, B. H. K., Desrochers, J., 1987, "Flutter Analysis of a Two-Dimensional Airfoil Containing Structural Nonlinearities", *National Research Council of Canada*, Aeronautical Report LR-618.

Lee, B. H. K., Gong, L., Wong, Y., 1996, "Analysis and Computation of Nonlinear Dynamic Response of a Two-Degree-of-Freedom System and its Application in Aeroelasticity", AIAA Paper-96-1248.

Lee, B. H. K., Leblanc, P., 1986, "Flutter Analysis of a Two-Dimensional Airfoil with Cubic Non-Linear Restoring Force", *National Research Council of Canada*, NAE-AN-36, NRC No. 25438.

Lee, B. H. K., Tron, A., 1989, "Effects of Structural Nonlinearities on Flutter Characteristics of the CF-18 Aircraft", *Journal of Aircraft*, Vol. 26, No. 8., pp. 781-786.

Lee, C. L., 1985, "An Iterative Procedure for Nonlinear Flutter Analysis", *Proceedings of the 26th AIAA-85-0688, AIAA/ASM/ASCE/AHS Structures, Structural Dynamics and Materials Conference*, April 15-17.

McIntosh, S. C. Jr., Reed, R. E., Rodden, W. P., 1981, "Experimental and Theoretical Study of Nonlinear Flutter", *Journal of Aircraft*, Vol. 18, No. 12, pp. 1057-1063.

Moon, F. C., 1987, *Chaotic Vibration: An Introduction for Applied Scientists and Engineers*, John Wiley: New York.

Murty, H. S., 1995, "Aeroelastic Stability Analysis of an Airfoil with Structural Nonlinearities Using a State Space Unsteady Aerodynamics Model", AIAA-95-1293-CP, *Proceedings of the 36th AIAA/ASME/ASCE/AHS/ASC Structures, Structural Dynamics and Materials Conference*, New Orleans, LA, Apr. 10-13.

O'Neil, T., Strganac, T. W., 1995, "An Experimental Investigation of Nonlinear Aeroelastic Response", *Proceedings of the 36th AIAA/ASME/ASCE/AHS/ASC Structures, Structural Dynamics, and Materials Conference*.

Price, S., Lee, B. H. K., Alighanbari, H., 1994, "Post-Instability Behaviour of a Two-Dimensional Airfoil with a Structural Nonlinearity", *Journal of Aircraft*, Vol. 31, pp. 1395-1401.

Price, S., Alighanbari, H., Lee, B. H. K., 1994, "The Aeroelastic Response of a Two-Dimensional Airfoil with Bilinear and Cubic Structural Nonlinearities", *Proceedings of the 35th AIAA/ASME/ASCE/AHS/ASC Structures, Structural Dynamics, and Materials Conference*, pp 1771-1780.

Shen, S. F., Hsu, C. C., 1957, "Analytical Results of Certain Nonlinear Flutter Problems", *Journal of the Aeronautical Sciences*, Vol. 25, Feb., pp. 136-137.

Stockard, D. P., Johnson, T. L., Sears, F. W., 1967, "Study of Amplitude Jumps", *American Journal of Physics*, Vol. 35, pp. 961-963.

Strikwerda, J., C., 1989, *Finite Difference Schemes and Partial Differential Equations*, Wadsworth and Brooks: Pacific Grove, California.

Theodorsen, Theodore, Garrick, I. E., 1940, "Mechanism of Flutter: A Theoretical and Experimental Investigation of the Flutter Problem", *National Advisory Committee for Aeronautics*, NACA-TR-685.

Thomson, J. M. T., Stewart, H. B., 1986, *Nonlinear Dynamics and Chaos*, John Wiley: Chichester.

Thomson, W. T., 1993, *Theory of Vibration with Applications*, 4th ed., Prentice Hall, New Jersey.

White, F. M., 1986, *Fluid Mechanics*, 2nd ed., McGraw Hill.

Woolston, D. S., Runyan, H. W., Andrews, R. E., 1957, "An Investigation of Effects of Certain Types of Structural Nonlinearities on Wing and Control Surface Flutter", *Journal of the Aeronautical Sciences*, Vol. 24, Jan., pp. 57-63.

Yang, Z. C., Zhao, L. C., 1988, "Analysis of Limit Cycle Flutter of an Airfoil in Incompressible Flow", *Journal of Sound and Vibration*, No. 123, pp. 1-13.

Zhao, L. C., Yang, Z. C., 1990, "Chaotic Motions of an Airfoil with Non-linear Stiffness in Incompressible Flow", *Journal of Sound and Vibration*, No. 138, pp. 245-254.

TABLES

Run #	Refer to Figure	Frequency Ratio $\bar{\omega}$	Mass Ratio μ	Hysteresis Vertical Size ΔV	Hysteresis Horizontal Size ΔH	Vertical Offset V_{off}	Horizontal Offset H_{off}
6	5.5	0.8	100	0.2	1	0	0
10	5.6	0.8	100	1	1	0	0
14	5.7	0.8	100	1	0.2	0	0
15	5.8	0.8	100	1	0.1	0	0
16	5.9	0.8	100	0.1	1	0	0
100	5.10	0.8	100	1	1	0.5	0
101	5.11	0.8	100	0.2	1	0.5	0
102	5.12	0.8	100	0.2	1	0	0.5
103	5.13	0.8	100	1	0.2	0.5	0
104	5.14	0.8	100	1	0.2	0	0.5
105	5.15	0.8	100	1	1	0.5	0.5
110	5.16	0.8	100	0.2	1	0.5	0.5
111	5.17	0.8	100	1	0.2	0.5	0.5
25	5.18	0.2	100	0	0.5	0	0
27	5.19	0.2	100	0.1	0.5	0	0
28	5.20	0.2	100	0.2	0.5	0	0
29	5.21	0.2	100	0.5	0.5	0	0
30	5.22	0.2	100	0.5	0.2	0	0
31	5.23	0.2	100	0.5	0.1	0	0
32	5.24	0.2	100	0.05	0.5	0	0
33	5.25	0.2	100	0.5	0.05	0	0
120	5.26	0.2	100	0.2	1	0	0
121	5.27	0.2	100	1	0.2	0	0
130	5.28	0.2	100	0	0.5	0.25	0.5
131	5.29	0.2	100	0.5	0.5	0	0.25
132	5.30	0.2	100	1	0.5	-0.25	0
133	5.31	0.2	100	1.5	0.5	-0.5	-0.25

TABLE 4.1 Simulation Runs Performed for Hysteresis Nonlinearities

(refer to Figure 3.2 for notation)

Flutter Speed Ratio (U/U*) for Initial LCO							
Run #	Refer to Figure	Frequency Ratio - $\bar{\omega}$	Shape Ratio $\Delta H/\Delta V$	Describing Function Result - U/U*	Finite Difference Result - U/U*	Difference	Difference %
6	5.5c	0.8	5	0.942	0.83	0.112	13.5
10	5.6c	0.8	1	0.824	0.852	-0.028	-3.3
14	5.7c	0.8	0.2	0.942	0.922	0.02	2.2
15	5.8c	0.8	0.1	0.969	0.954	0.015	1.6
16	5.9c	0.8	10	0.801	0.816	-0.015	-1.8
100	5.18c	0.2	undefined	0.187	0.136	0.051	37.5
101	5.19c	0.2	5	0.366	0.4	-0.034	-8.5
102	5.20c	0.2	2.5	0.528	0.532	-0.004	-0.8
103	5.21c	0.2	1	0.726	0.73	-0.004	-0.5
104	5.22c	0.2	0.4	0.366	0.4	-0.034	-8.5
105	5.23c	0.2	0.2	0.93	0.928	0.002	0.2
110	5.26c	0.2	5	0.366	0.424	-0.058	-13.7
111	5.27c	0.2	0.2	0.93	0.9	0.03	3.3

TABLE 5.1 - FLUTTER RATIO SPEEDS AT WHICH LCO MOTION WAS INITIATED

FIGURES

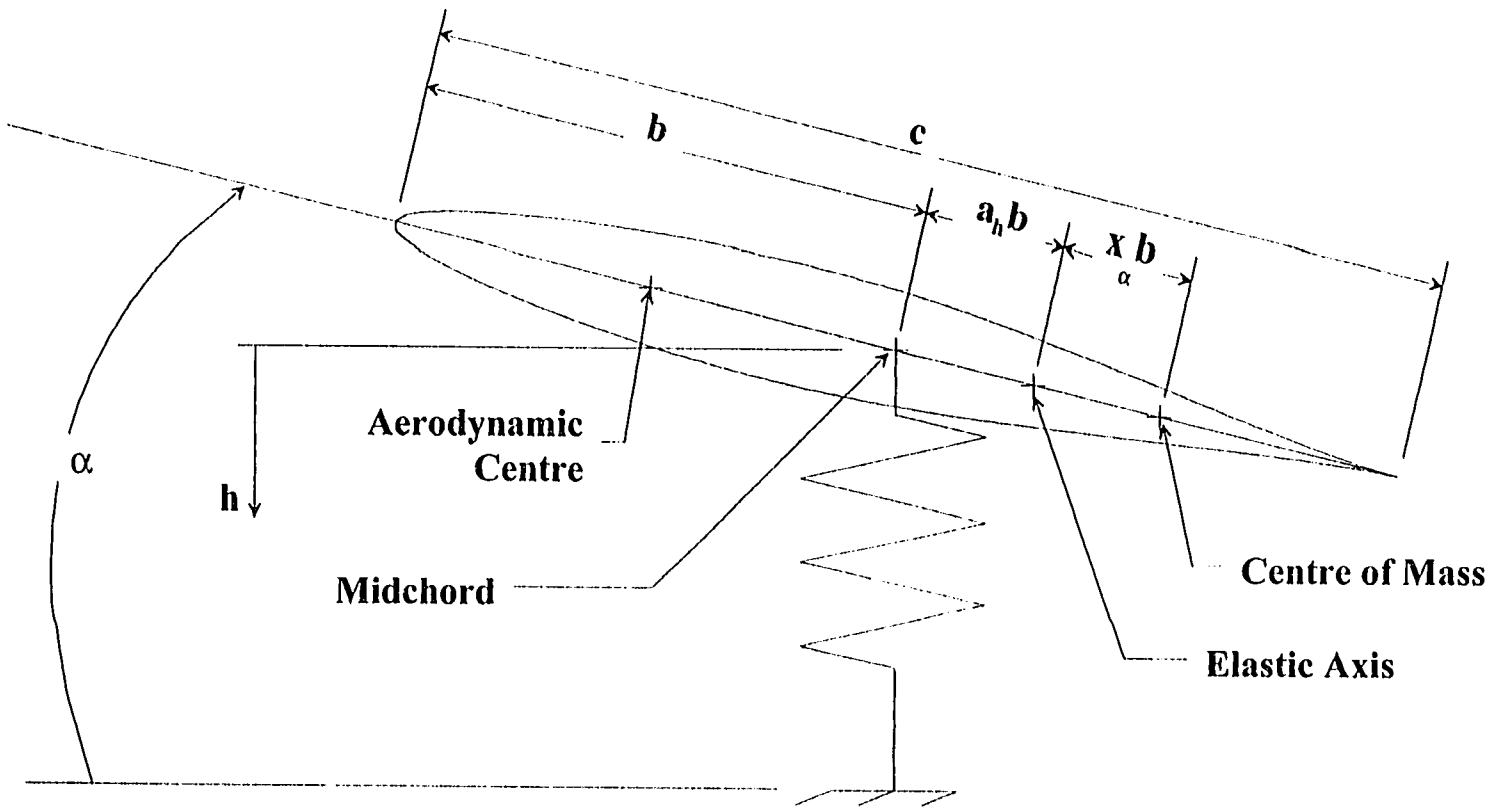

Figure 3.1 - Schematic Diagram of Two-Dimensional Airfoil with Two Degrees of Freedom

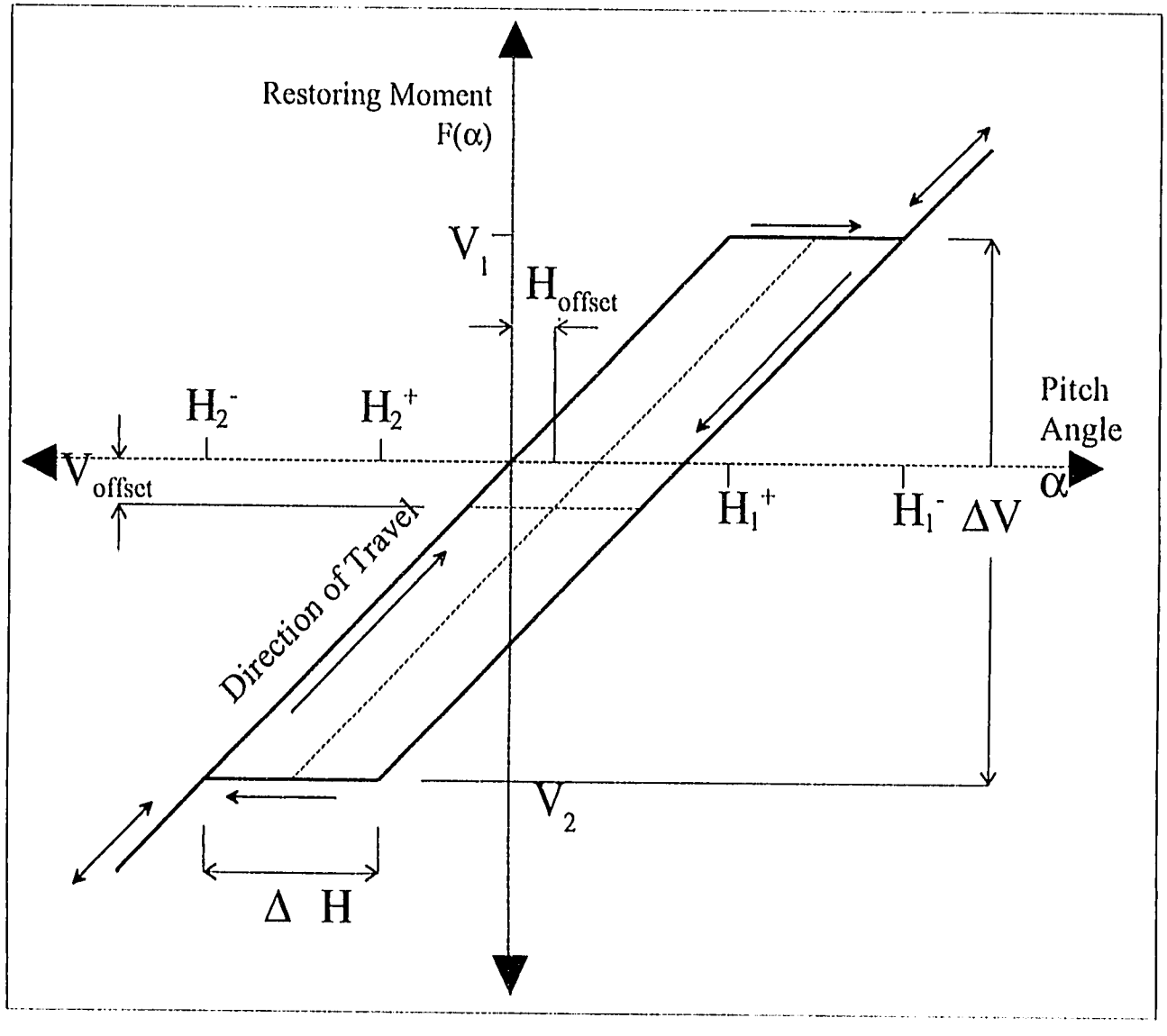

Figure 3.2 - Diagram of Restoring Moment vs Pitch Angle for Hysteresis Spring

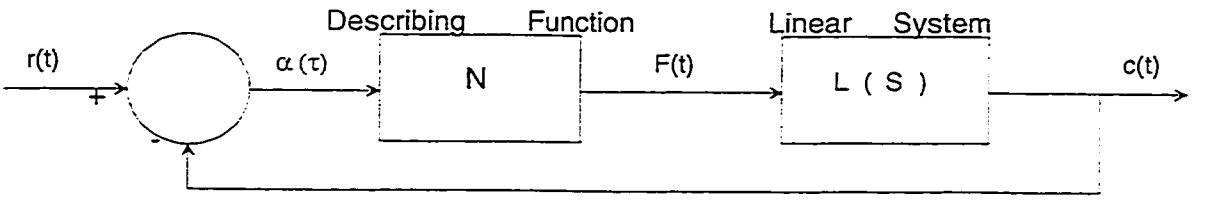

FIGURE 3.3 Block Diagram of Describing Function Method in Limit Cycle System

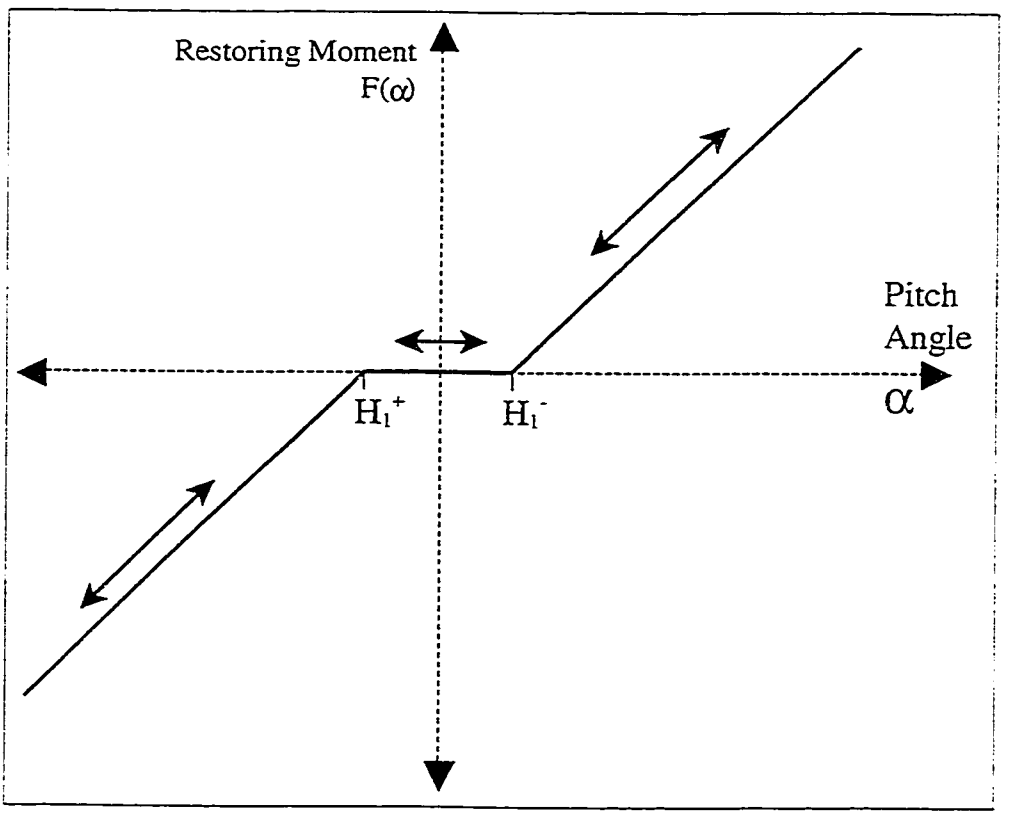

FIGURE 3.4 Diagram of Restoring Moment vs Pitch Angle for Bilinear Spring with Freeplay

Figure 4.1 - Pitch and Heave Response for Hysteresis Nonlinearity

$\mu = 100,\ \overline{\omega} = 0.80,\ \Delta H = 0.20,\ \Delta V = 1.0,\ \alpha_o = 6.0^o,\ U^*_{linear} = 4.1144,\ U/U^* = 0.80$

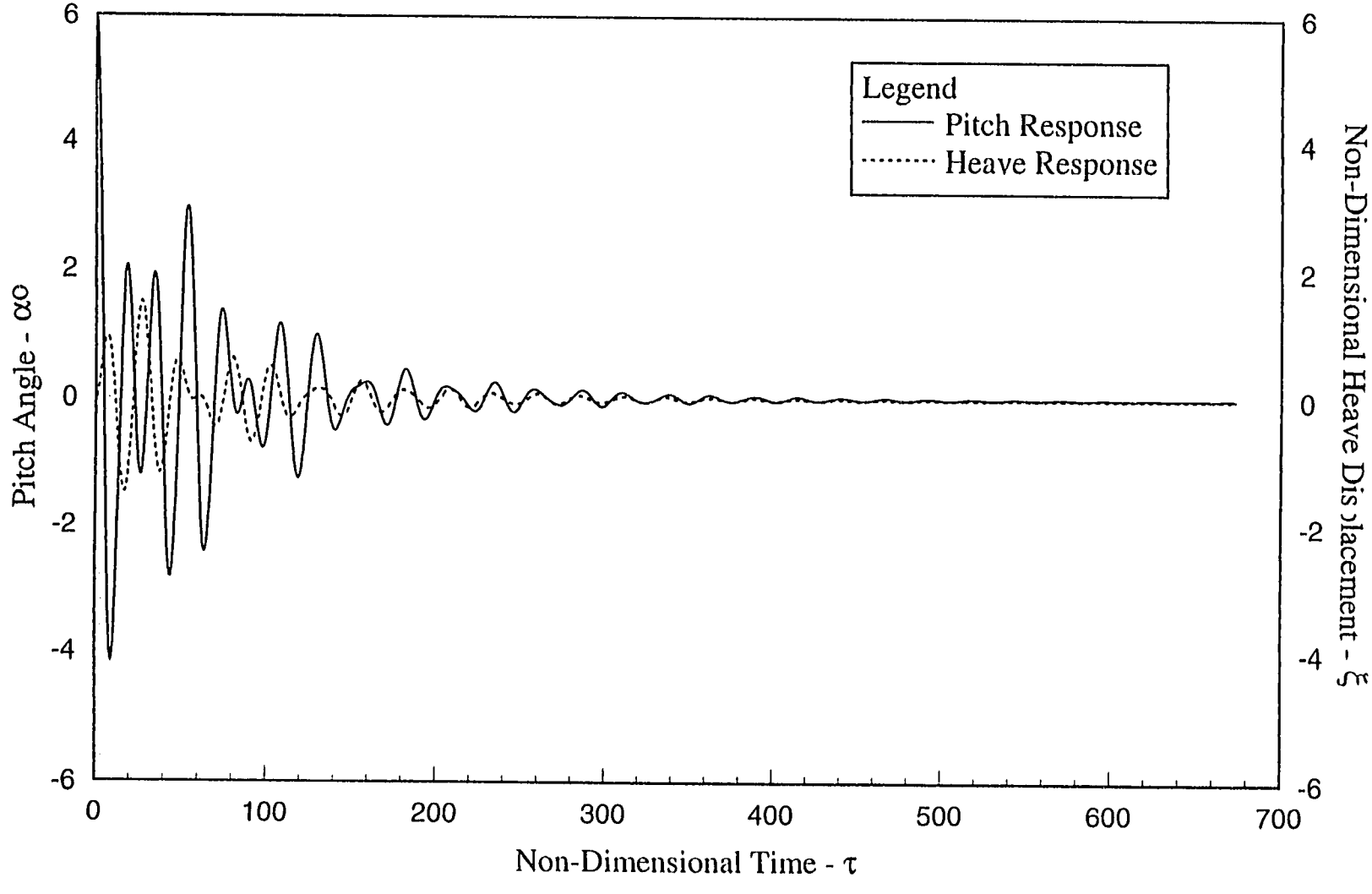

Figure 4.2 - Damped Pitch Response for Hysteresis Nonlinearity

$\mu = 100,\ \overline{\omega} = 0.80,\ \Delta H = 0.20,\ \Delta V = 1.0,\ \alpha_o = 6.0^o,\ U^*_{linear} = 4.1144,\ U/U^* = 0.92$

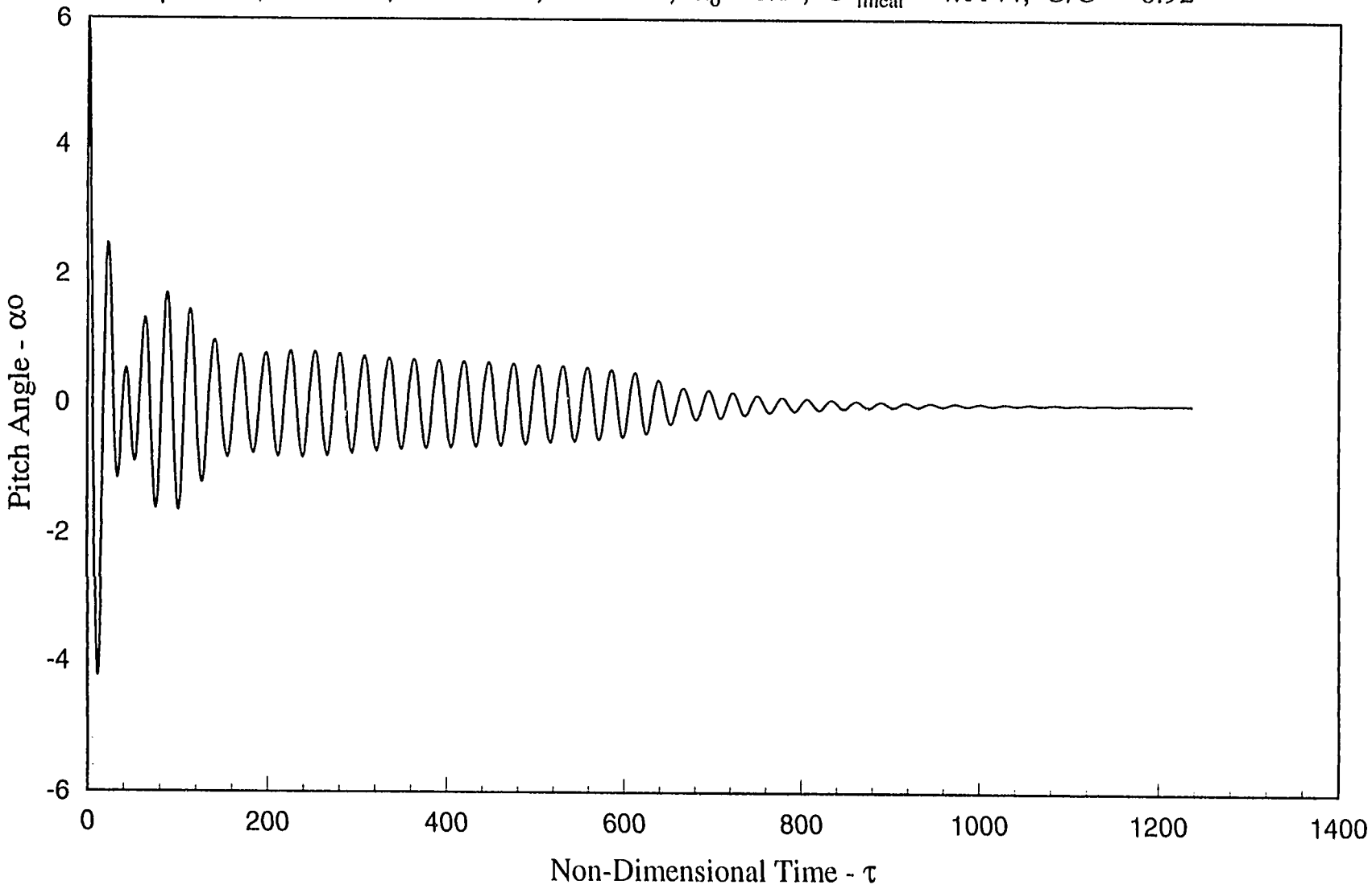

Figure 4.3 - LCO Pitch Response for Hysteresis Nonlinearity

$\mu = 100,\ \bar{\omega} = 0.80,\ \Delta H = 0.20,\ \Delta V = 1.0,\ \alpha_o = 6.0^o,\ U^*_{linear} = 4.1144,\ U/U^* = 0.94$

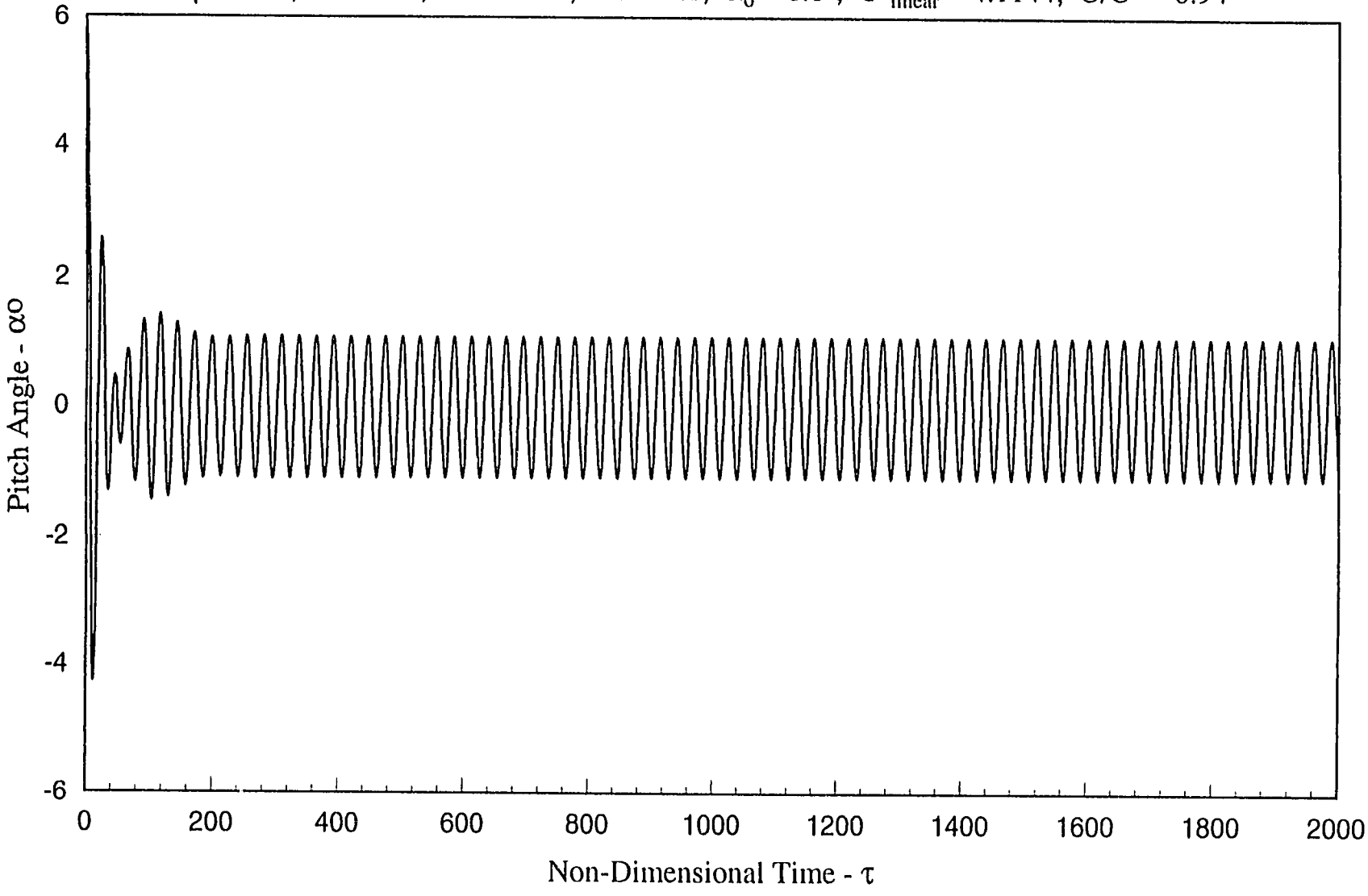

Figure 4.4 - Damped Pitch Response for Hysteresis Nonlinearity

$\mu = 100,\ \bar{\omega} = 0.80,\ \Delta H = 0.20,\ \Delta V = 1.0,\ \alpha_o = 6.0^o,\ U^*_{linear} = 4.1144,\ U/U^* = 0.983$

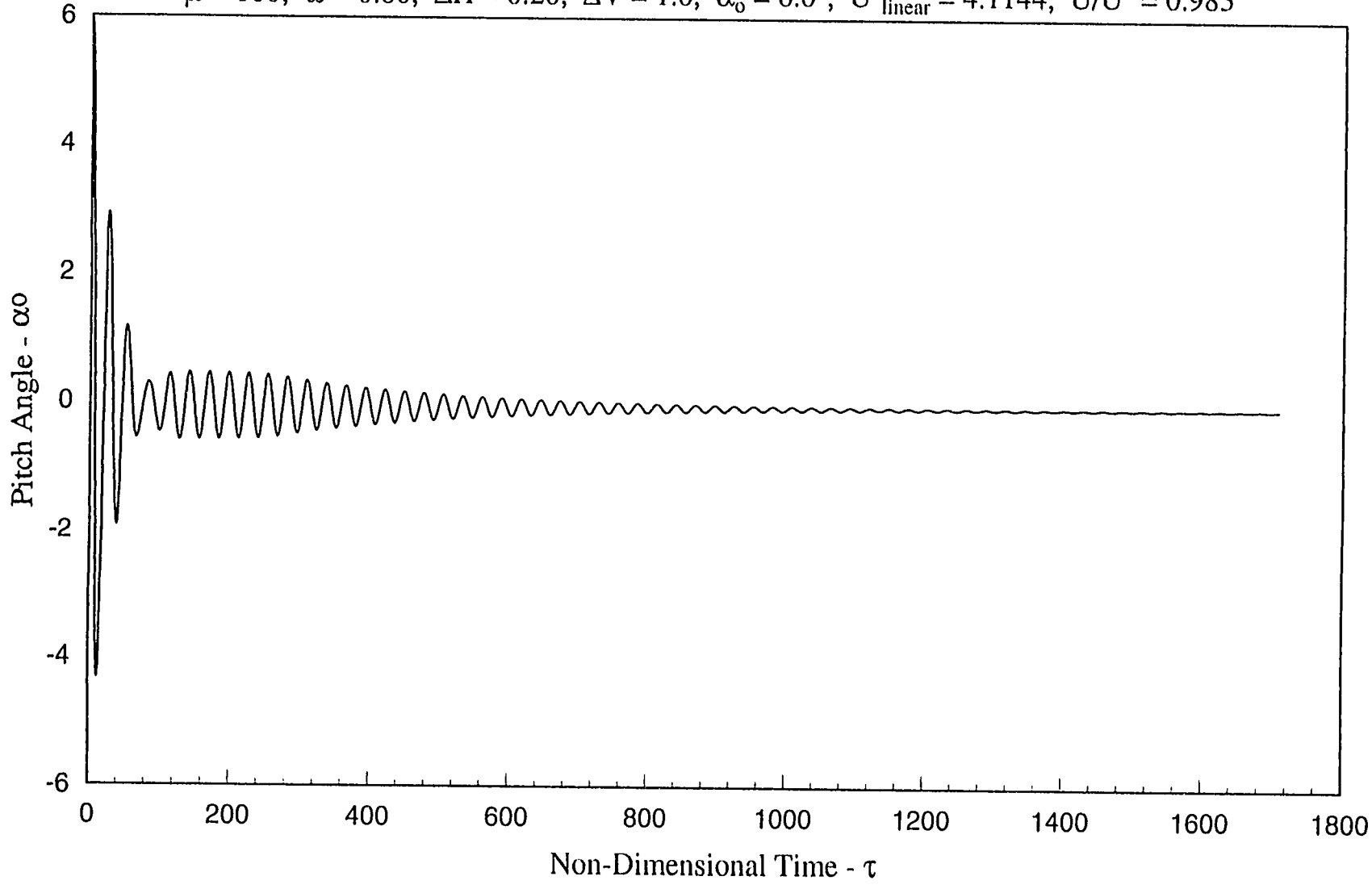

Figure 4.5 - LCO Pitch Response for Hysteresis Nonlinearity

$\mu = 100,\ \bar{\omega} = 0.80,\ \Delta H = 0.20,\ \Delta V = 1.0,\ \alpha_o = 6.0^o,\ U^*_{linear} = 4.1144,\ U/U^* = 0.984$

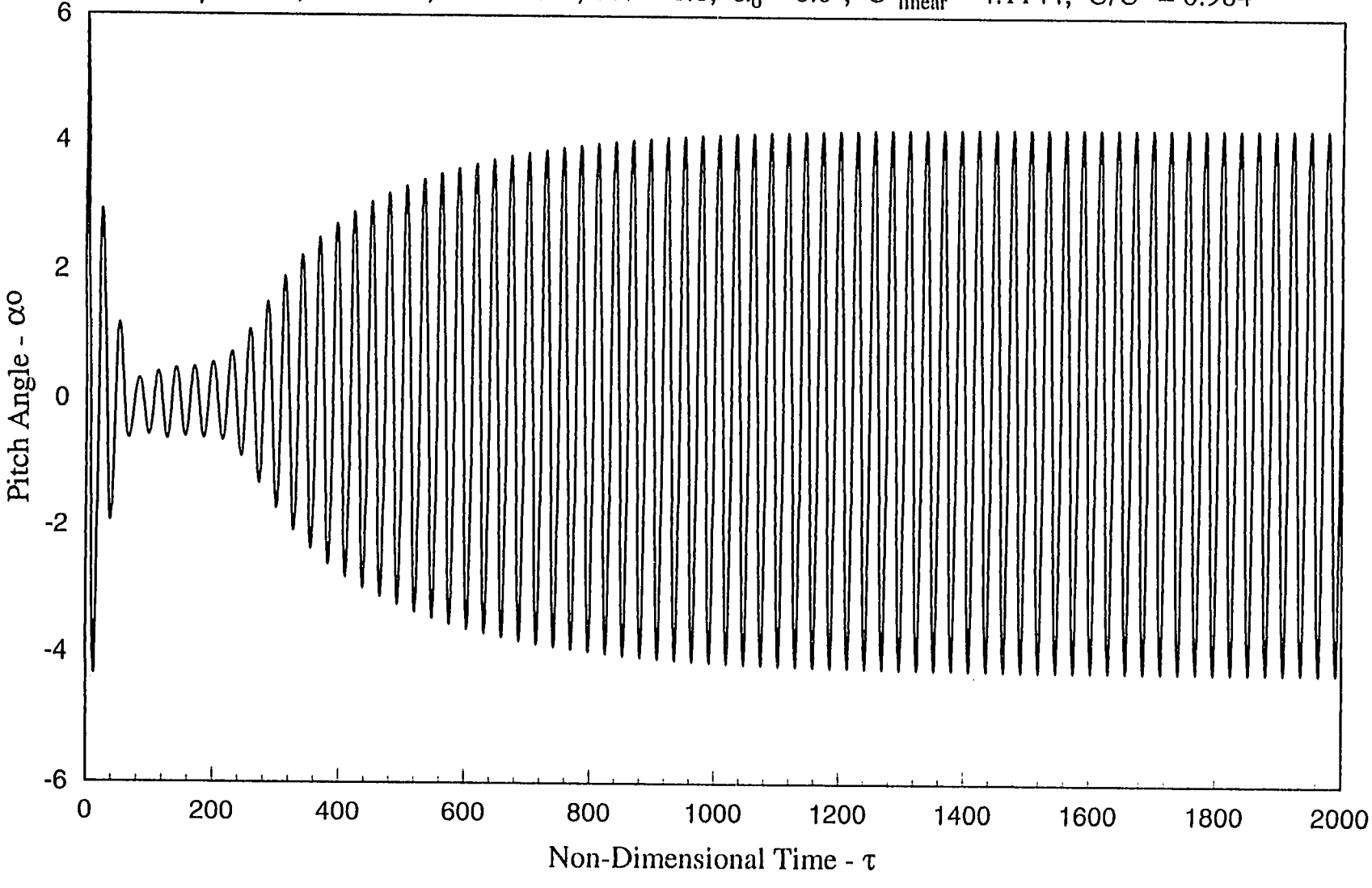

Figure 4.6 - LCO Pitch Response for Hysteresis Nonlinearity

$\mu = 100,\ \varpi = 0.80,\ \Delta H = 0.20,\ \Delta V = 1.0,\ \alpha_o = 6.0^o,\ U^*_{linear} = 4.1144,\ U/U^* = 0.99$

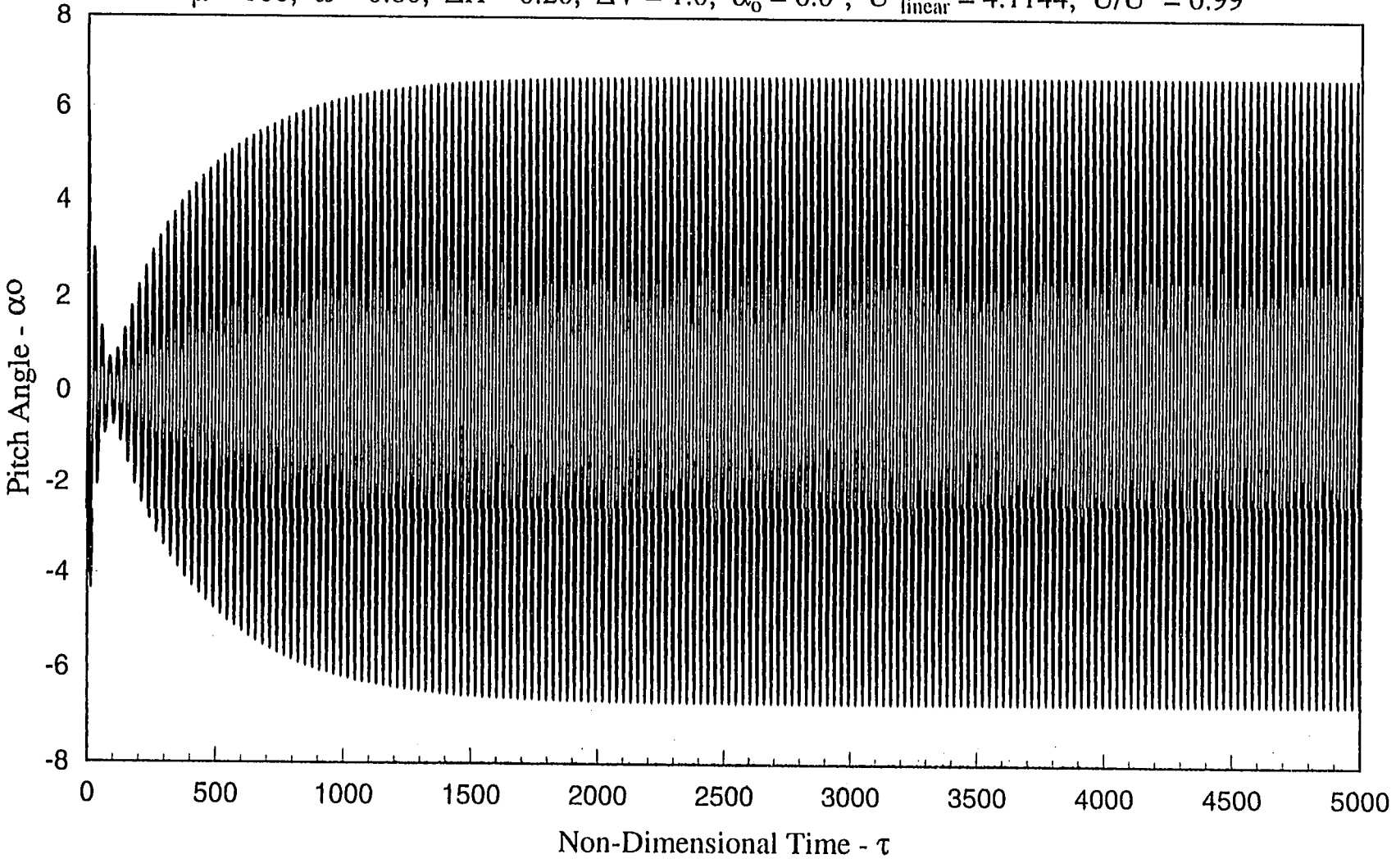

Figure 4.7 - Unstable Pitch Response for Hysteresis Nonlinearity

$\mu = 100,\ \overline{\omega} = 0.80,\ \Delta H = 0.20,\ \Delta V = 1.0,\ \alpha_o = 6.0^o,\ U^*_{linear} = 4.1144,\ U/U^* = 1.00$

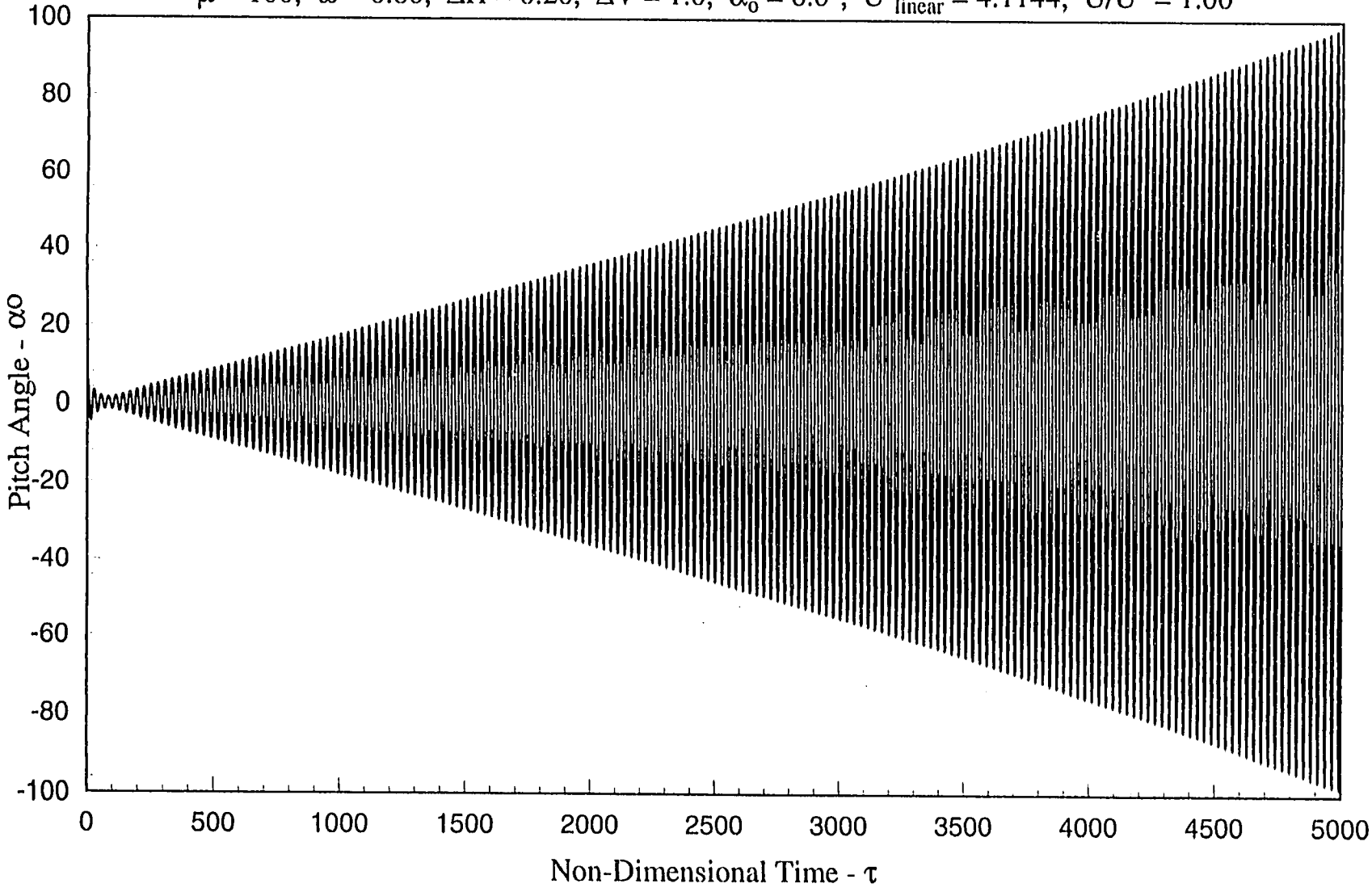

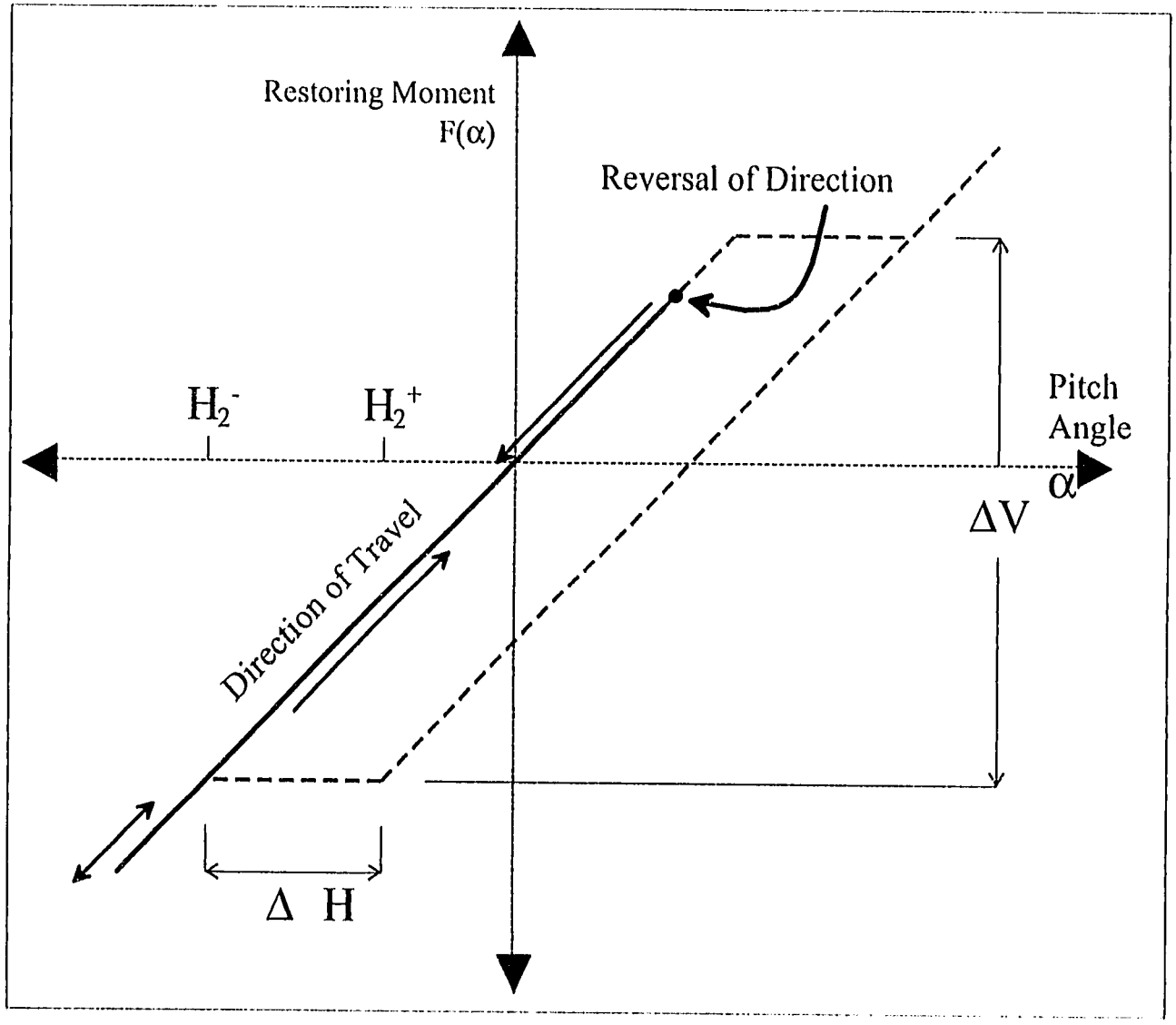

Figure 4.8 - Hysteresis Spring: Reversal of Pitch Direction on Slope

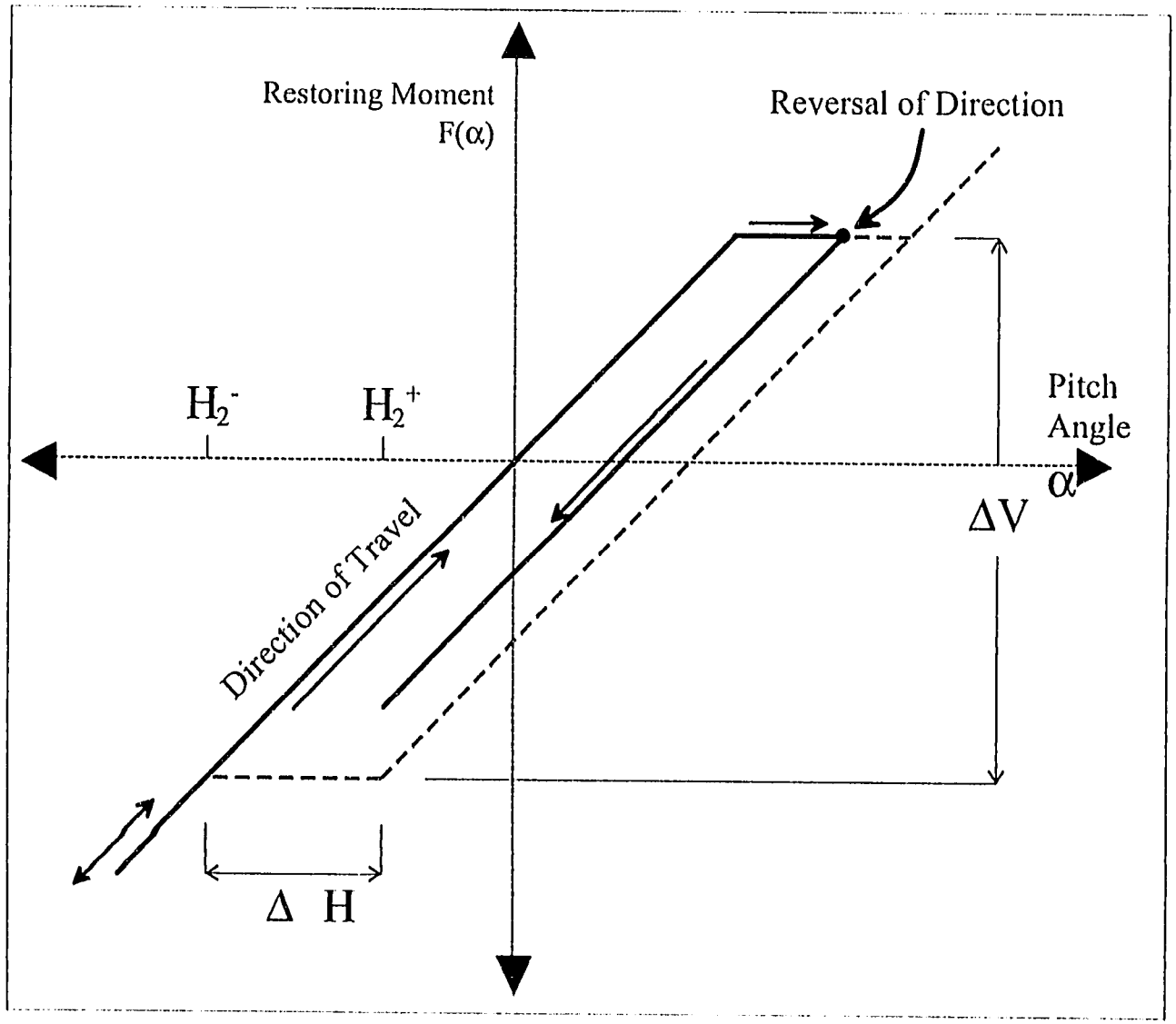

Figure 4.9 - Hysteresis Spring: Reversal of Pitch Direction on Flat

Figure 4.10 - Root Locus Plot for Two Degree of Freedom Airfoil: $\bar{\omega} = 0.2$

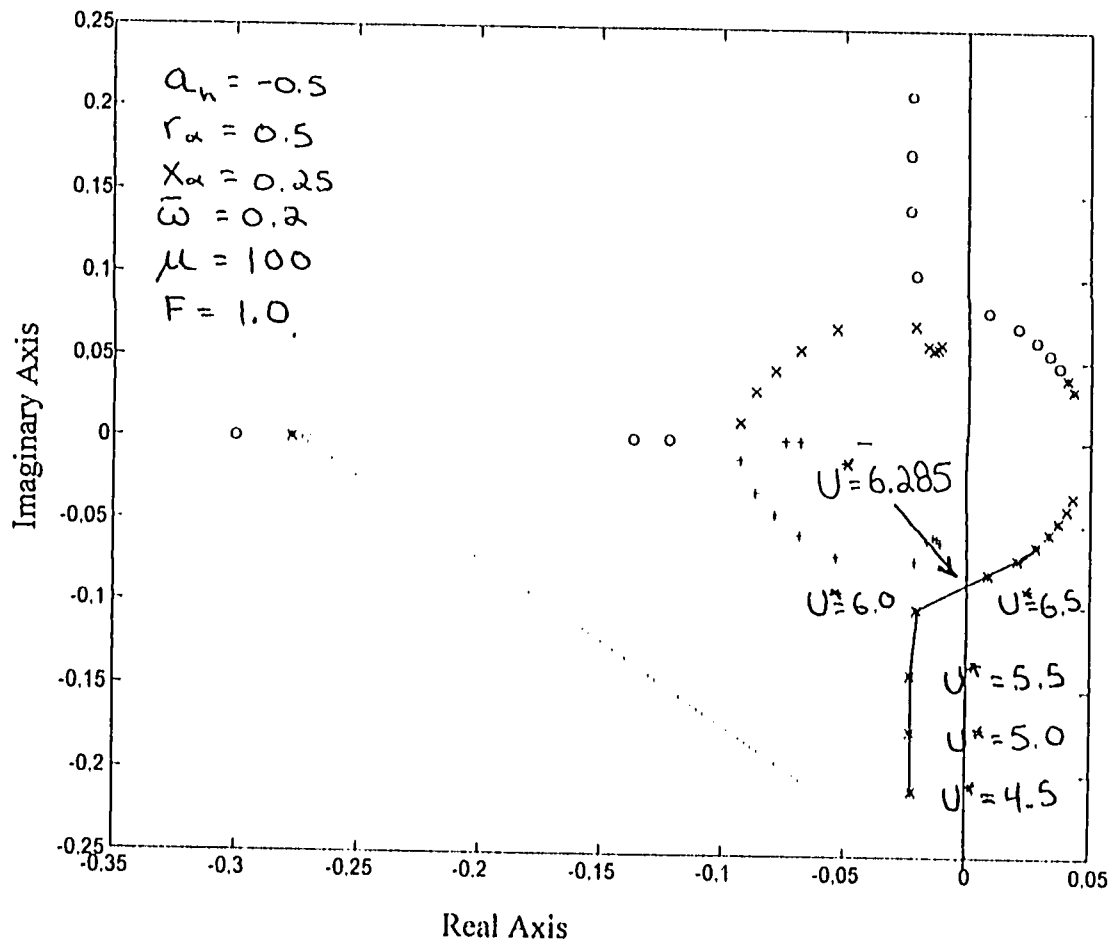

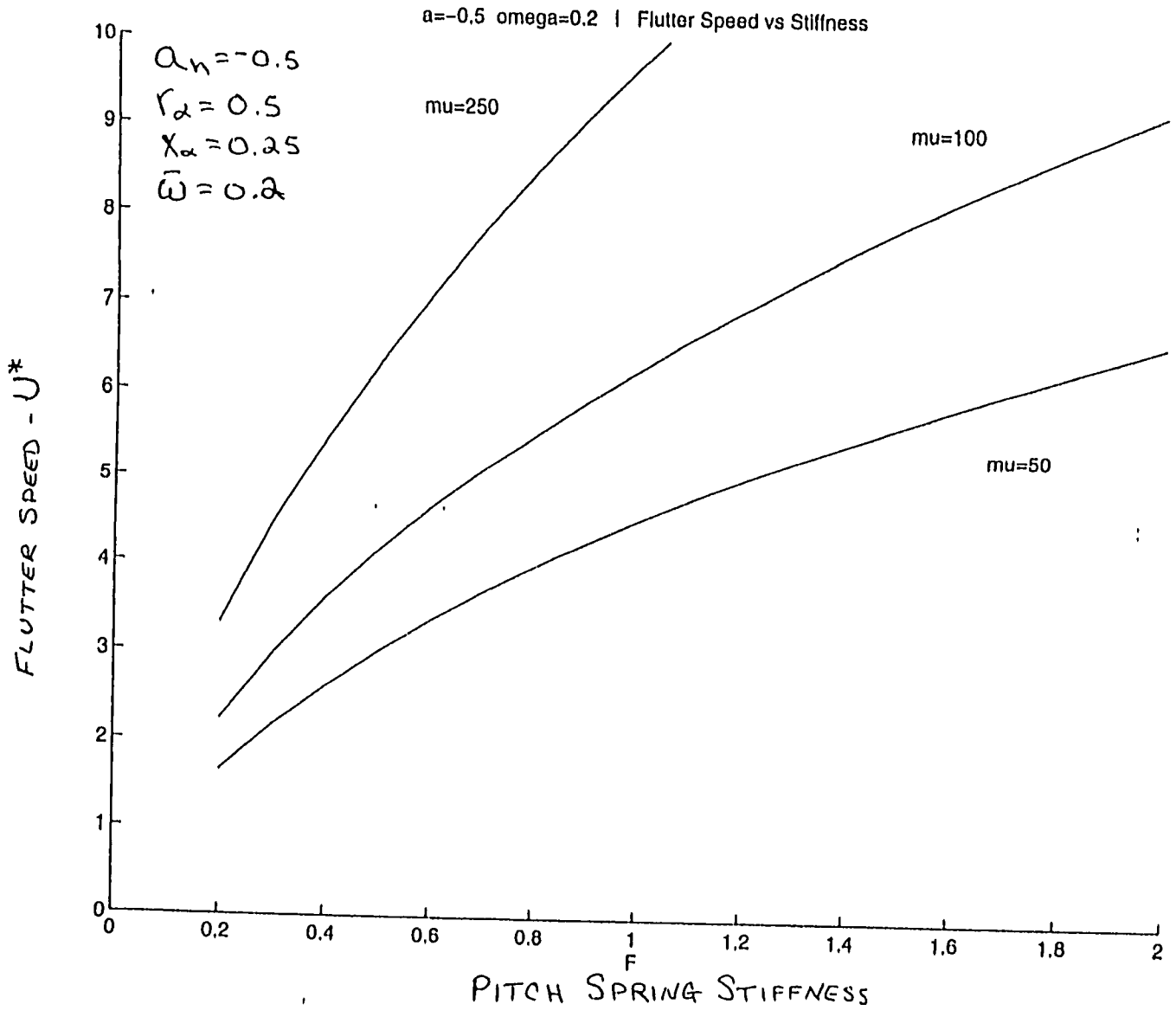

FIGURE 4.11 - PITCH SPRING STIFFNESS VS. FLUTTER SPEED

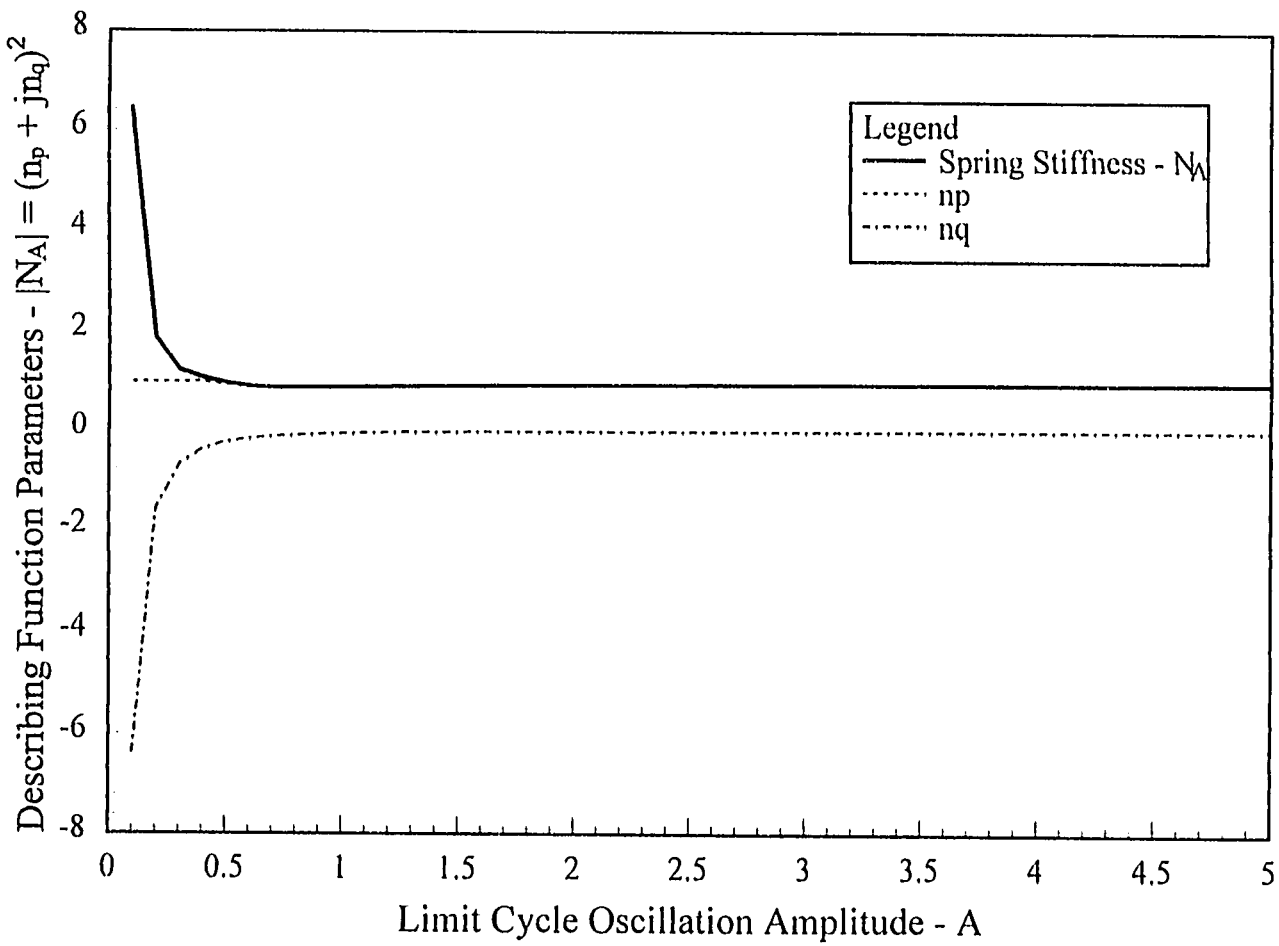

Figure 4.12 - Plot of Describing Function Variables with respect to LCO Amplitude A for Run 14 ($\bar{\omega}$=0.2, μ=100, ΔV=1.0, ΔH=0.2)

Figure 5.1 - Sinusoidal Type Pitch Response for Hysteresis Nonlinearity

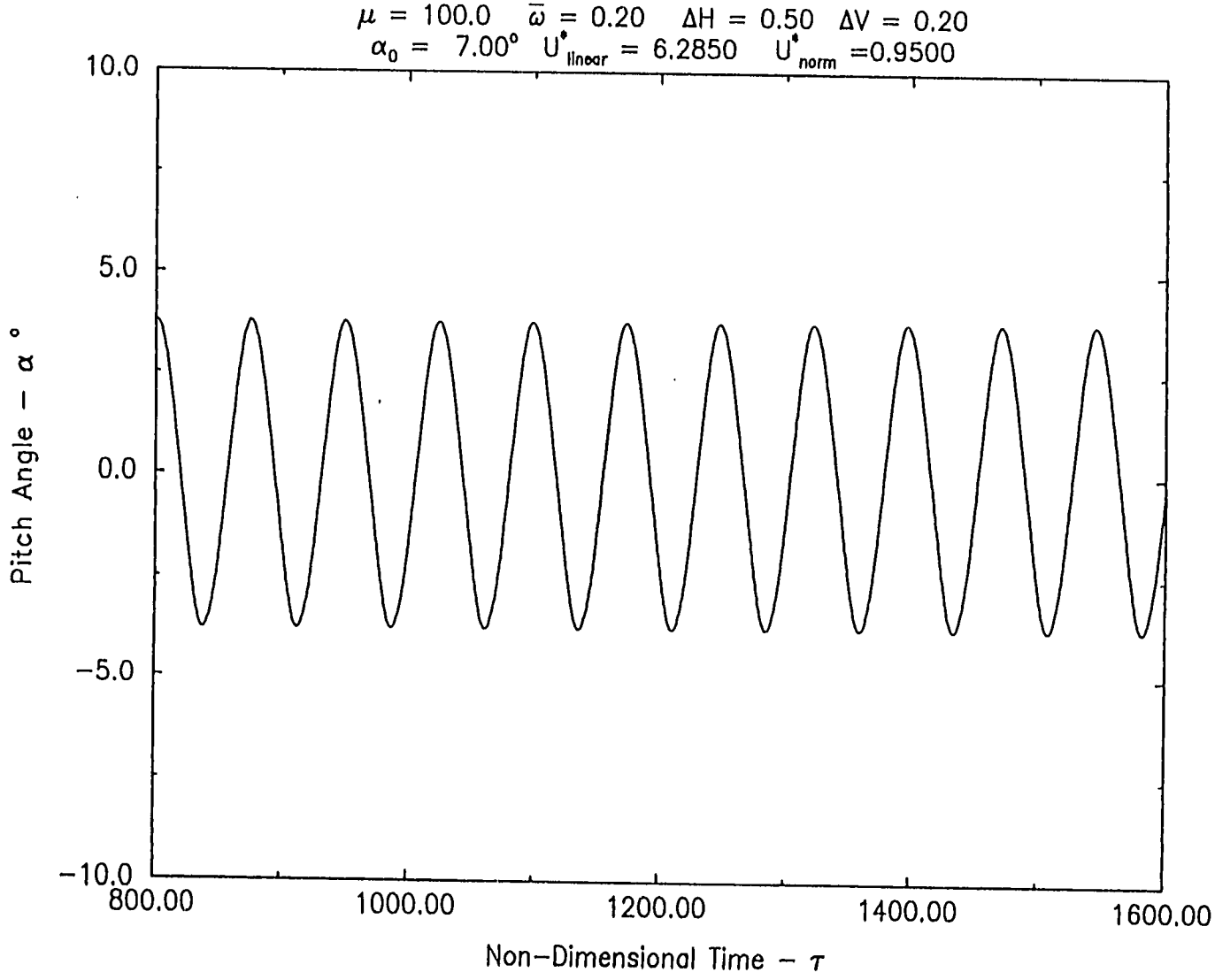

Figure 5.2 - Power Spectral Density of Pitch Response for Hysteresis Nonlinearity

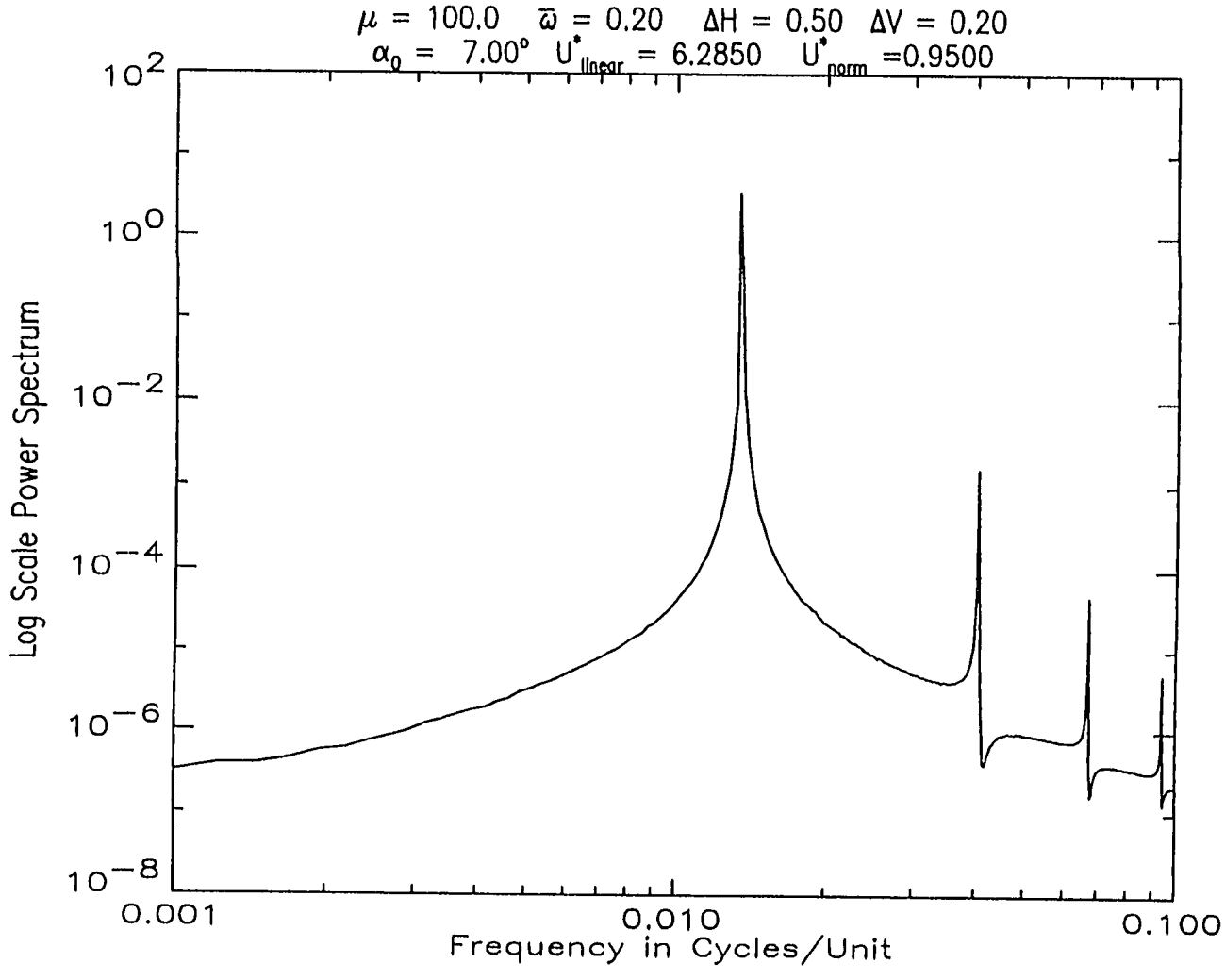

Figure 5.3 - Pitch Response with Harmonic Structure for Hysteresis Nonlinearity

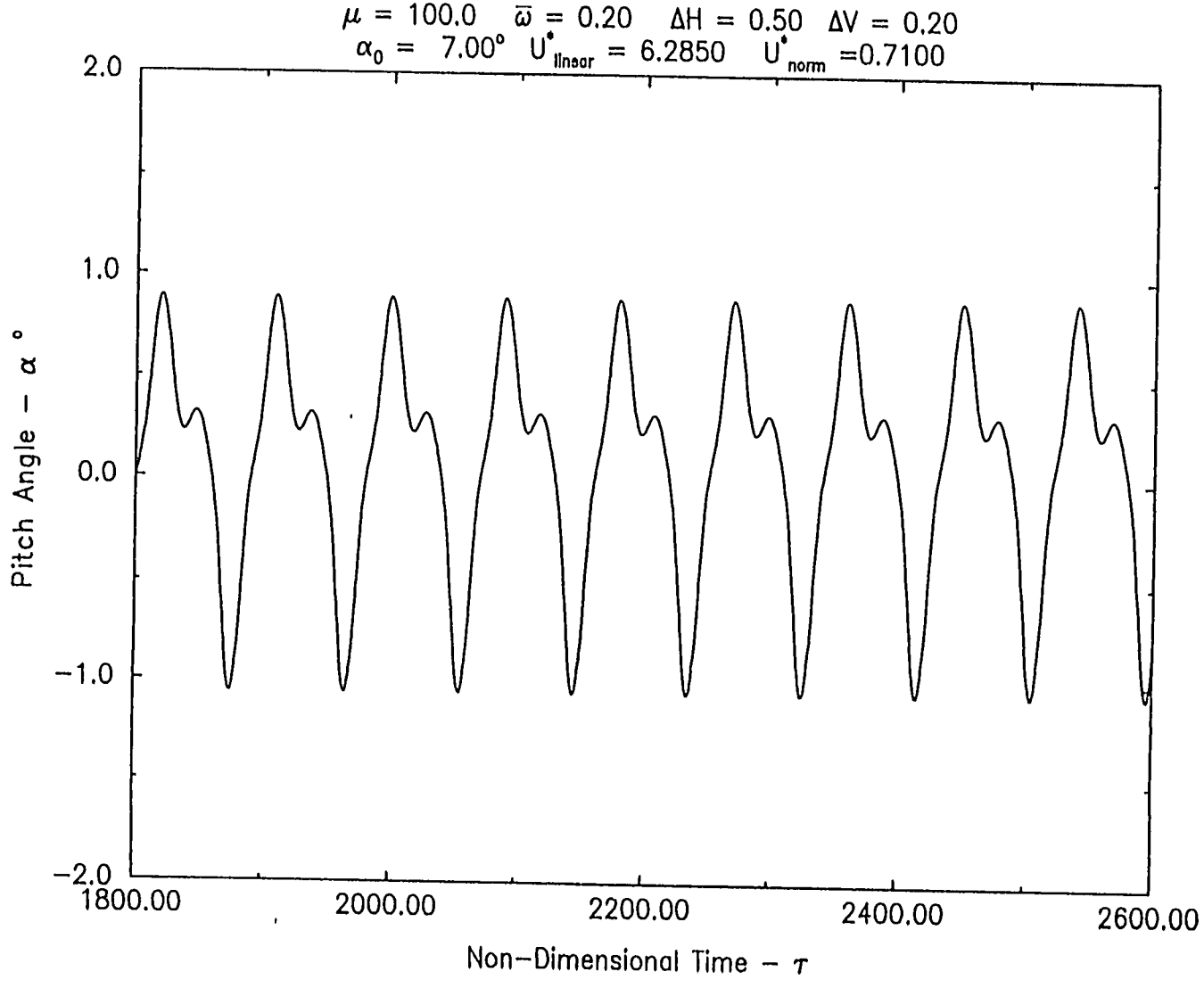

Figure 5.4 - Power Spectral Density of Pitch Response for Hysteresis Nonlinearity

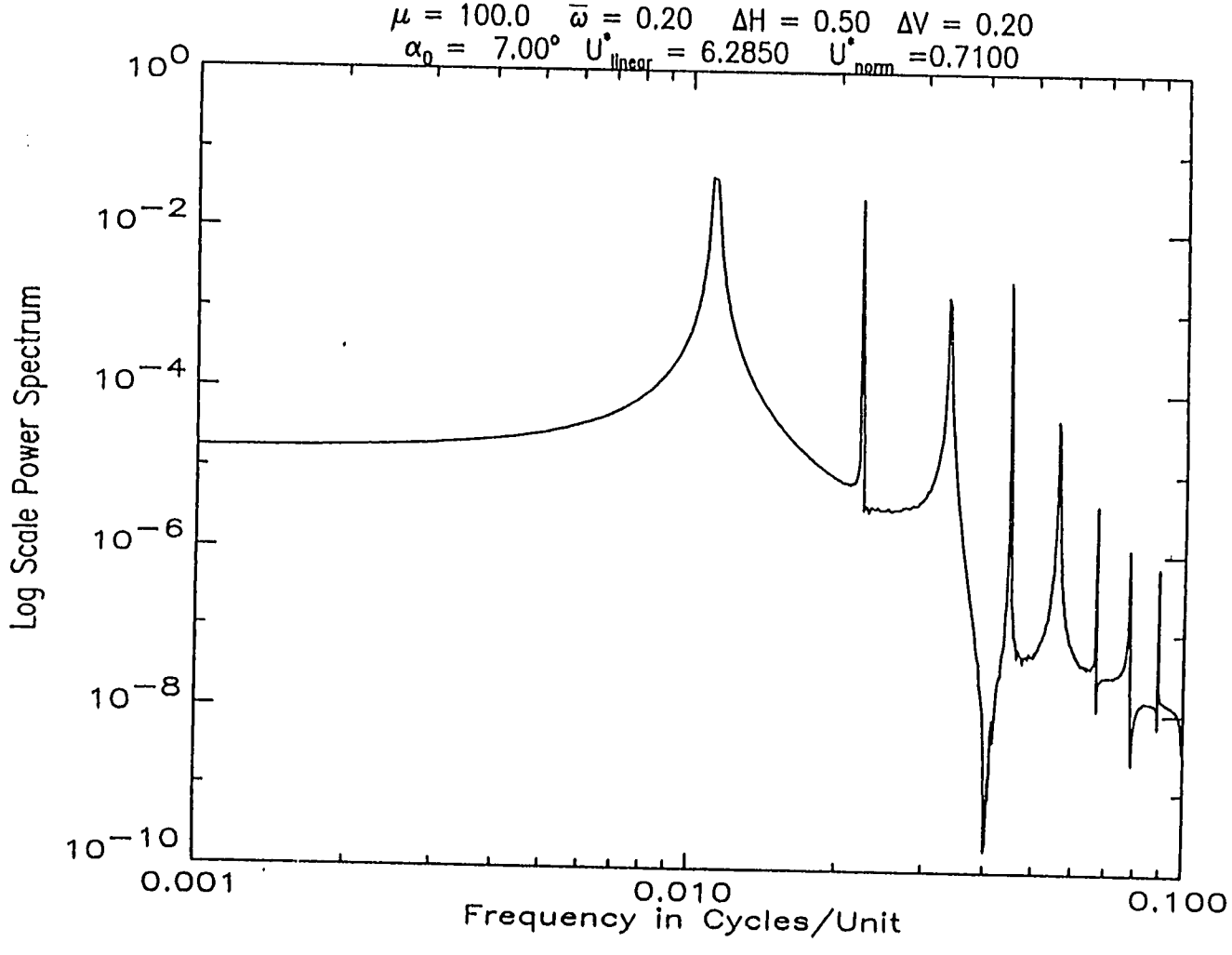

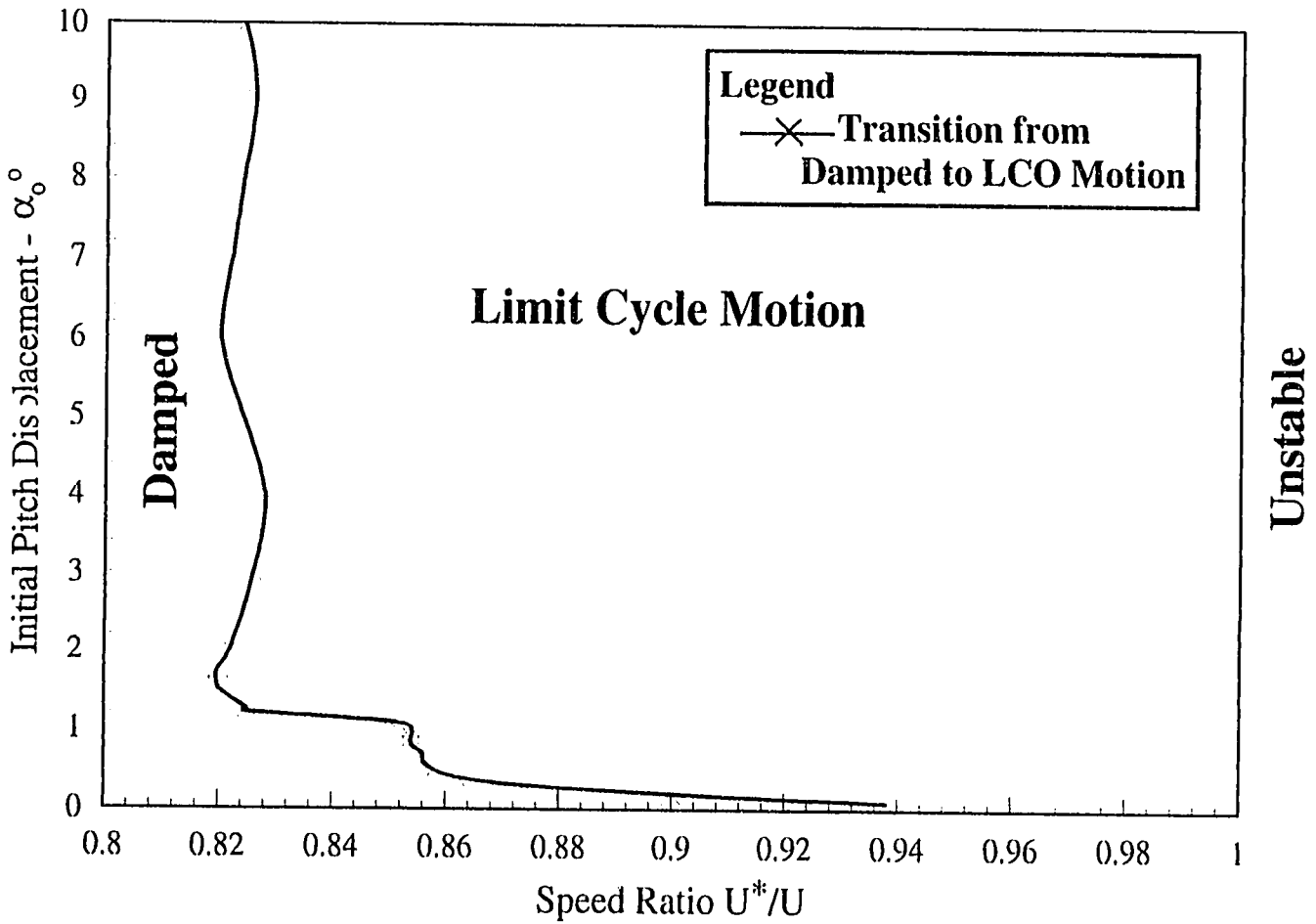

Figure 5.5a - Flutter Boundary for Hysteresis Nonlinearity:
μ=100, $\overline{\omega}$=0.8, ΔV=0.2°, ΔH=1.0°, Symmetric

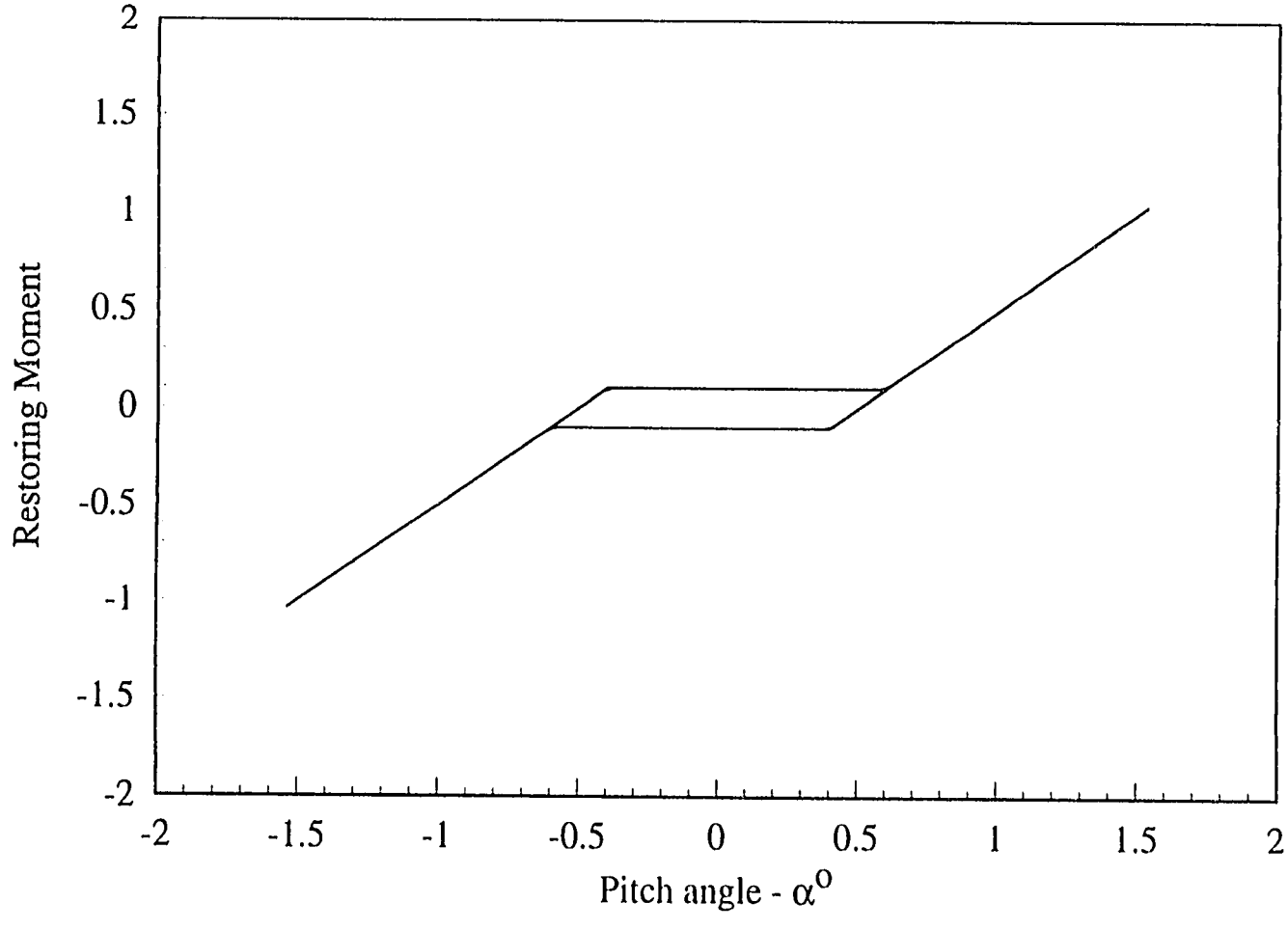

Figure 5.5b - Hysteretic Spring Response
α_o=1.5, U*/U=0.83, ΔV=0.2, ΔH=1.0, $\bar{\omega}$=0.8, μ=100.0

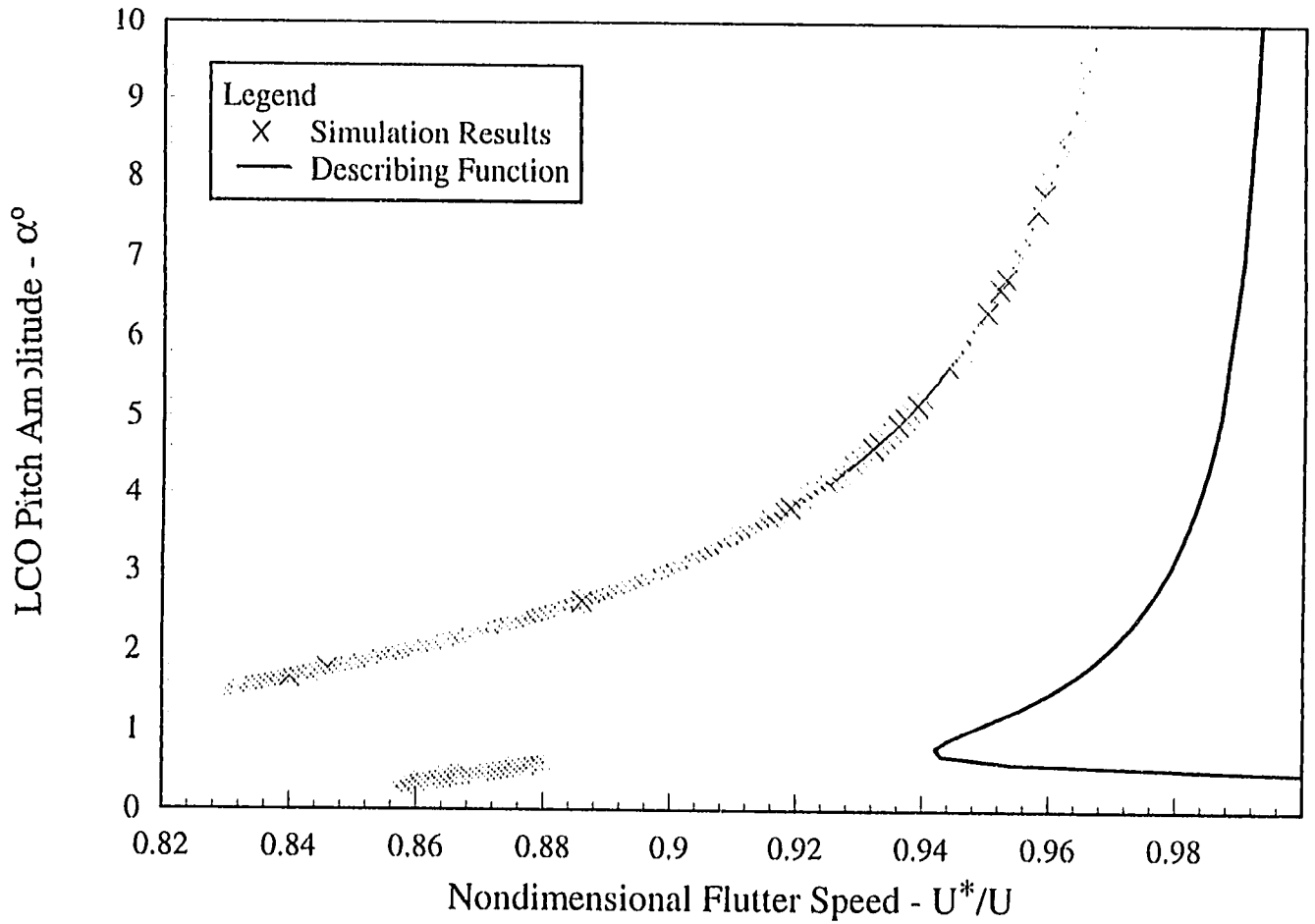

Figure 5.5c - Variation of LCO Amplitude with Speed:
μ=100, $\overline{\omega}$=0.8, ΔV=0.2°, ΔH=1.0°, symmetric

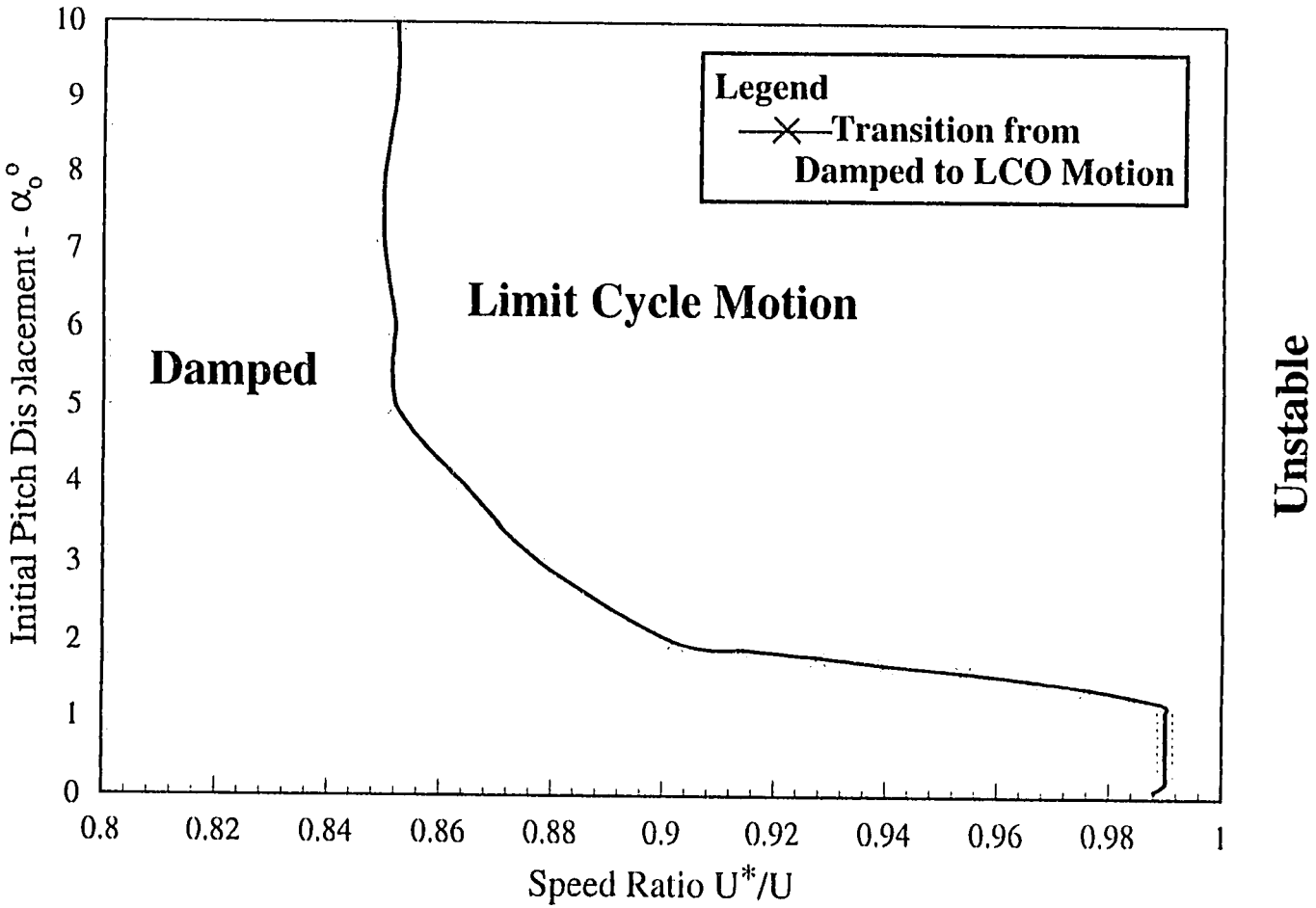

Figure 5.6a - Flutter Boundary for Hysteresis Nonlinearity:
μ=100, $\overline{\omega}$=0.8, $\Delta V=1.0^o$, $\Delta H=1.0^o$, Symmetric

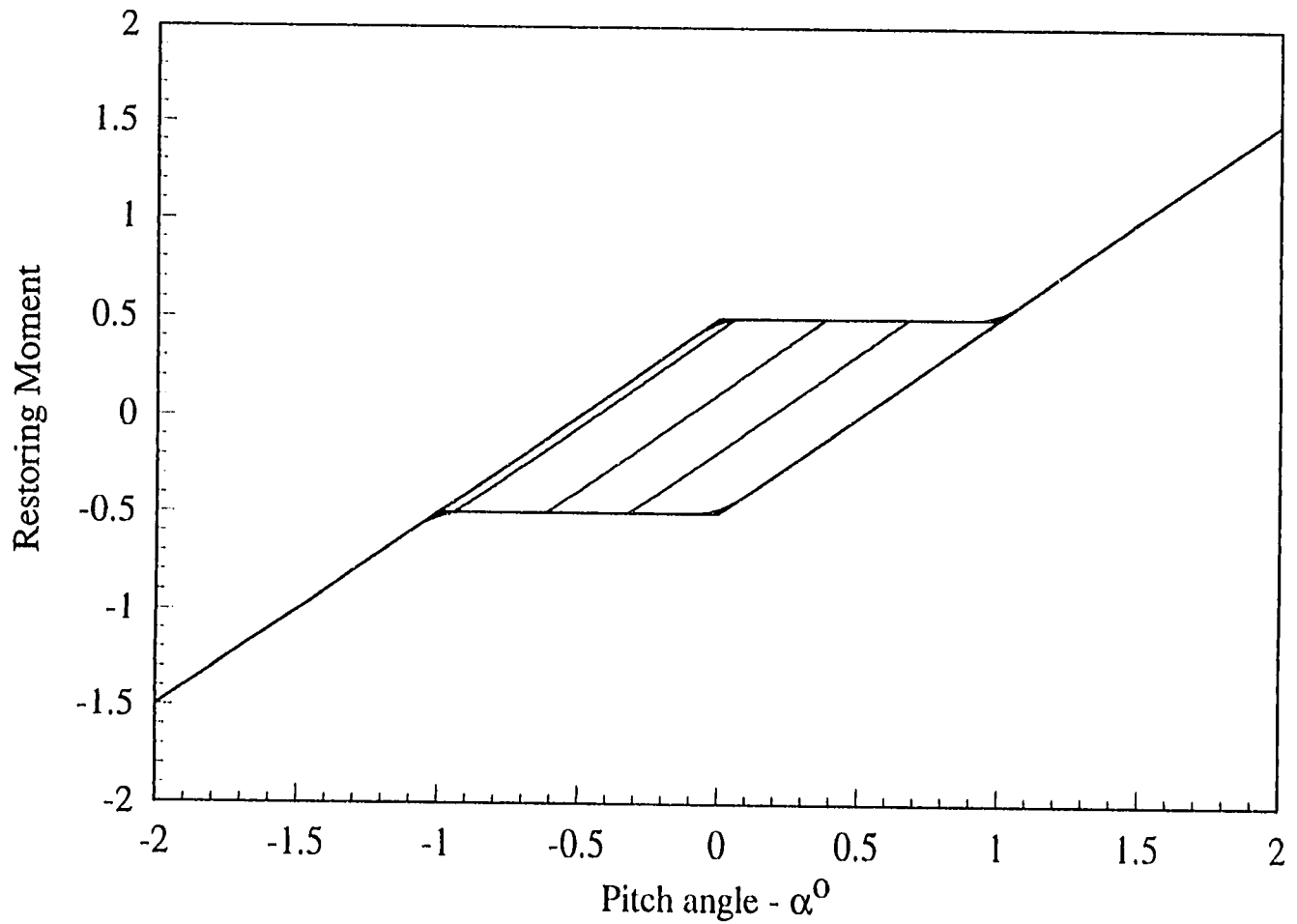

Figure 5.6b - Hysteretic Spring Response
α_o=2.0, U*/U=0.92 ΔV=1.0, ΔH=1.0, $\overline{\omega}$=0.8, μ=100.0

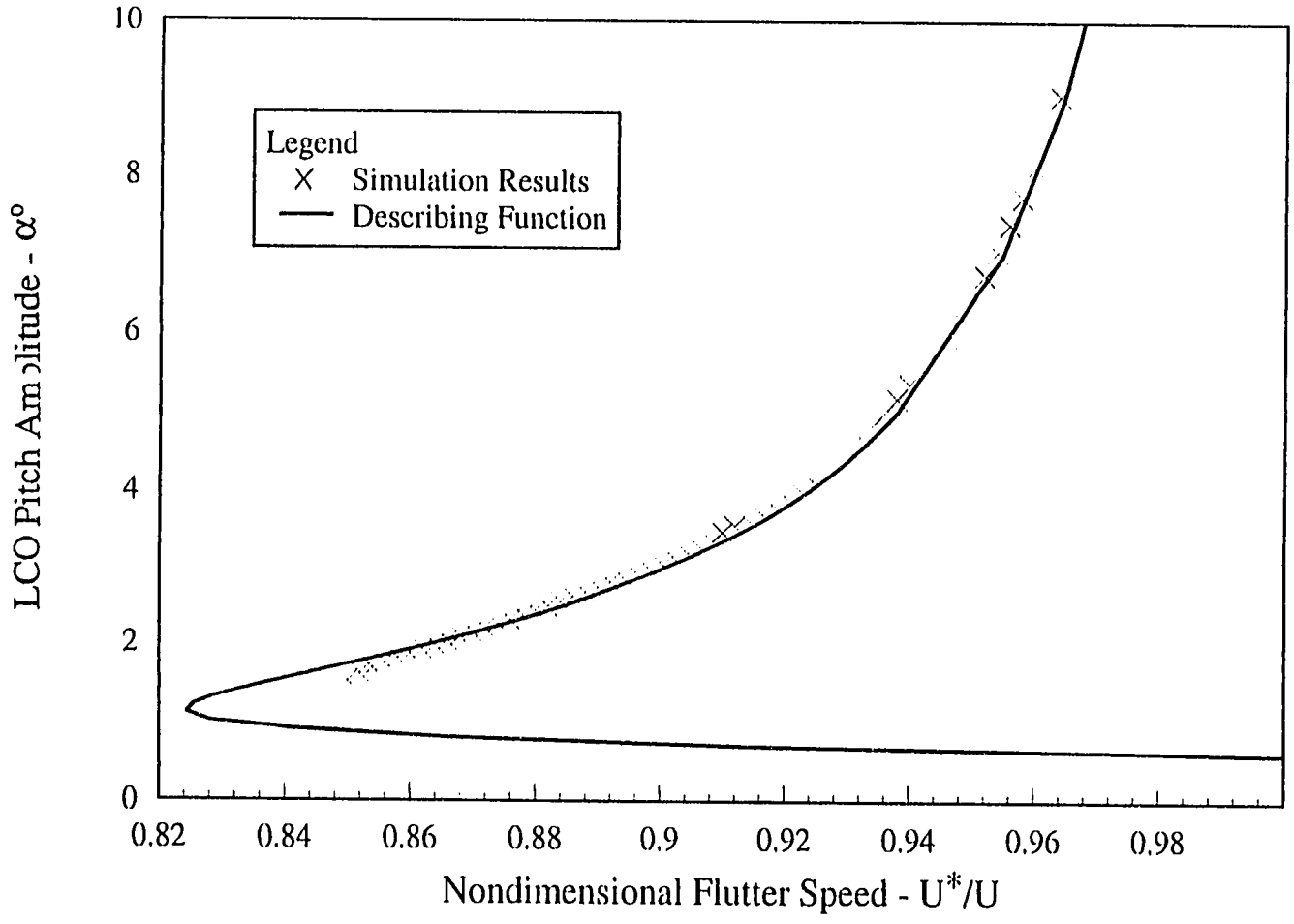

Figure 5.6c - Variation of LCO Amplitude with Speed:
μ=100, $\bar{\omega}$=0.8, ΔV=1.0°, ΔH=1.0°, symmetric

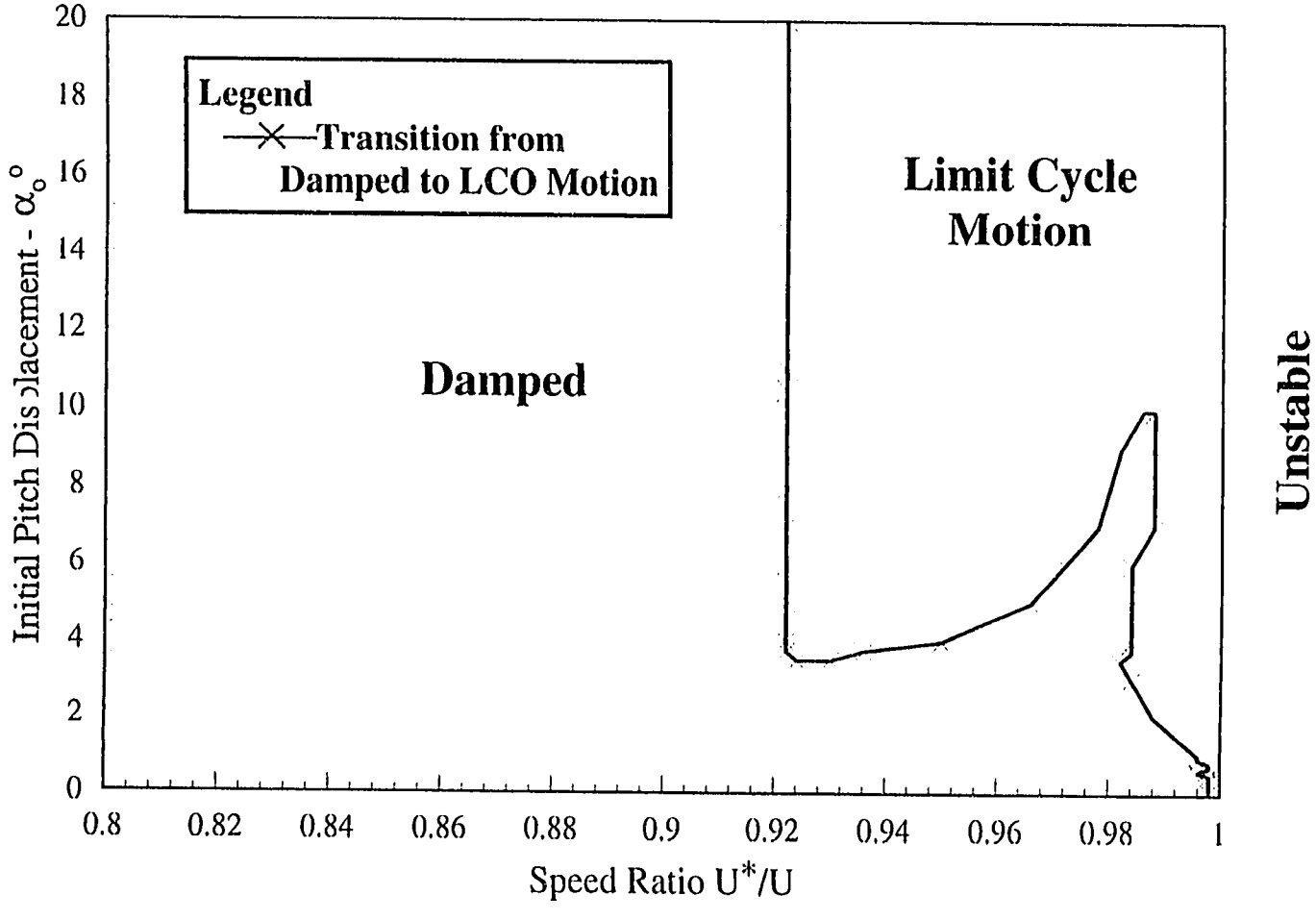

Figure 5.7a - Flutter Boundary for Hysteresis Nonlinearity:
μ=100, $\bar{\omega}$=0.8, ΔV=1.0^o, ΔH=0.2^o, Symmetric

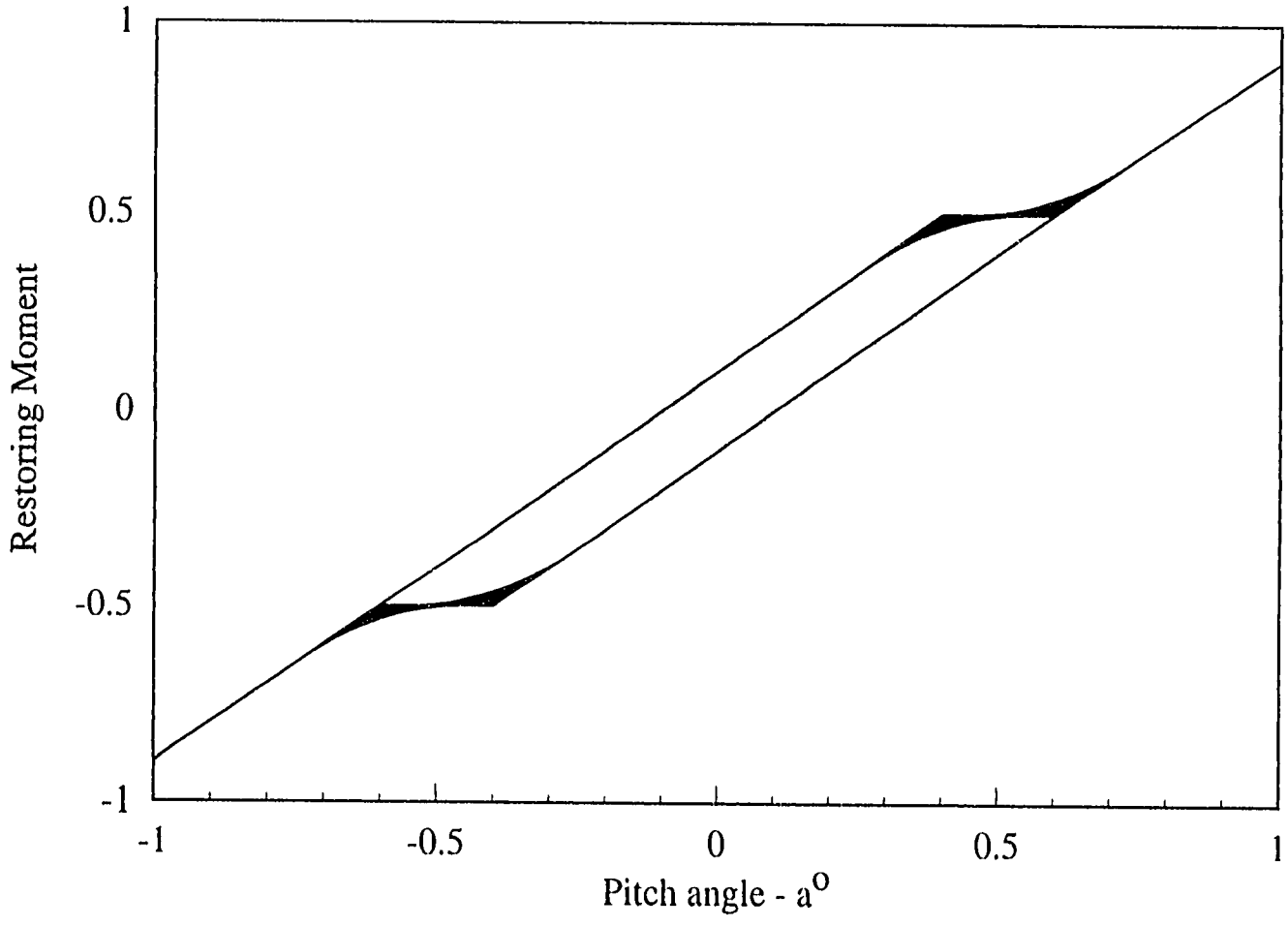

Figure 5.7b - Hysteretic Spring Response
α_o=6.0, ΔV=1.0, ΔH=0.2, $\overline{\omega}$=0.8, μ=100.0

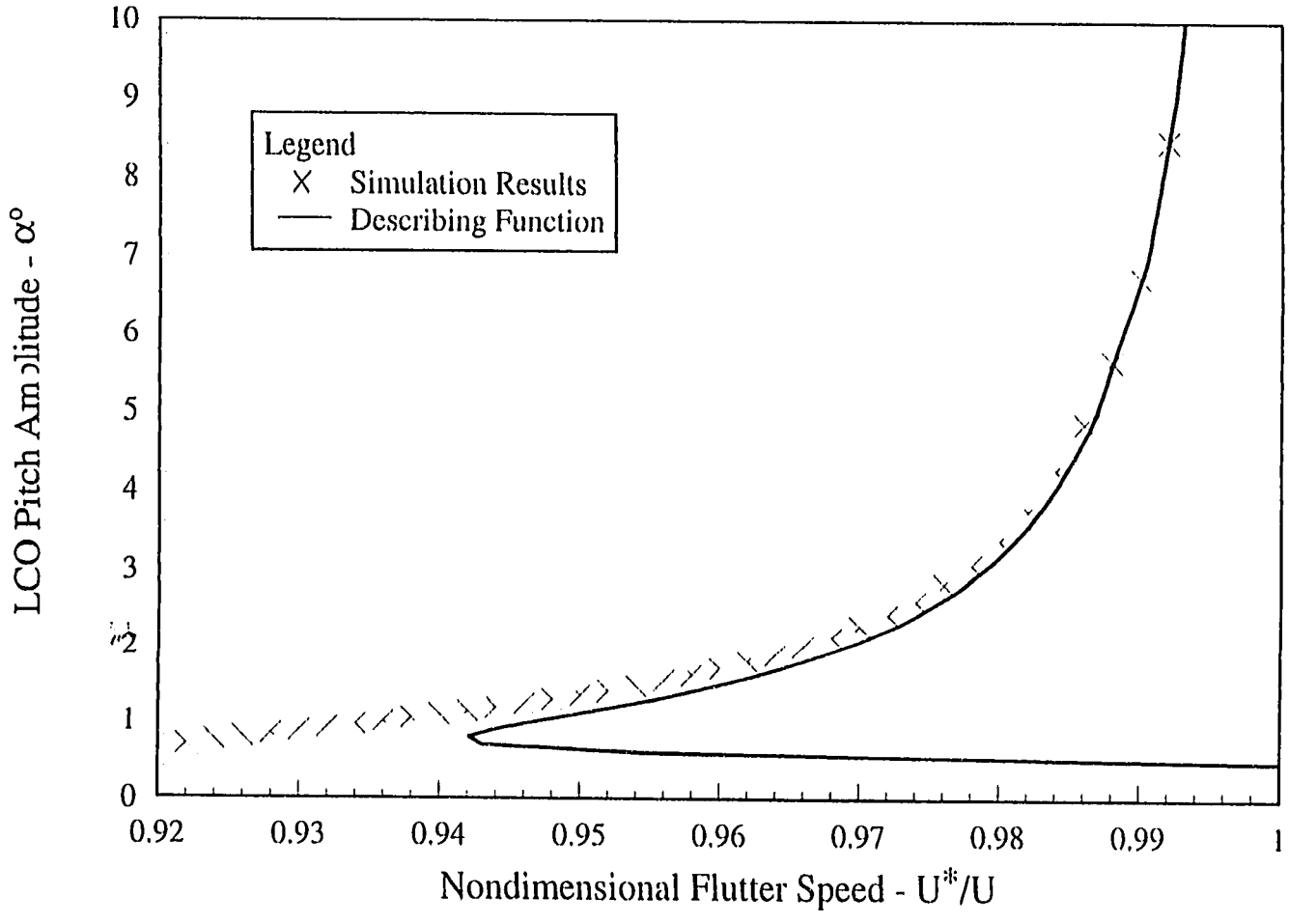

Figure 5.7c - Variation of LCO Amplitude with Speed:
μ=100, $\bar{\omega}$=0.8, ΔV=1.0°, ΔH=0.2°, symmetric

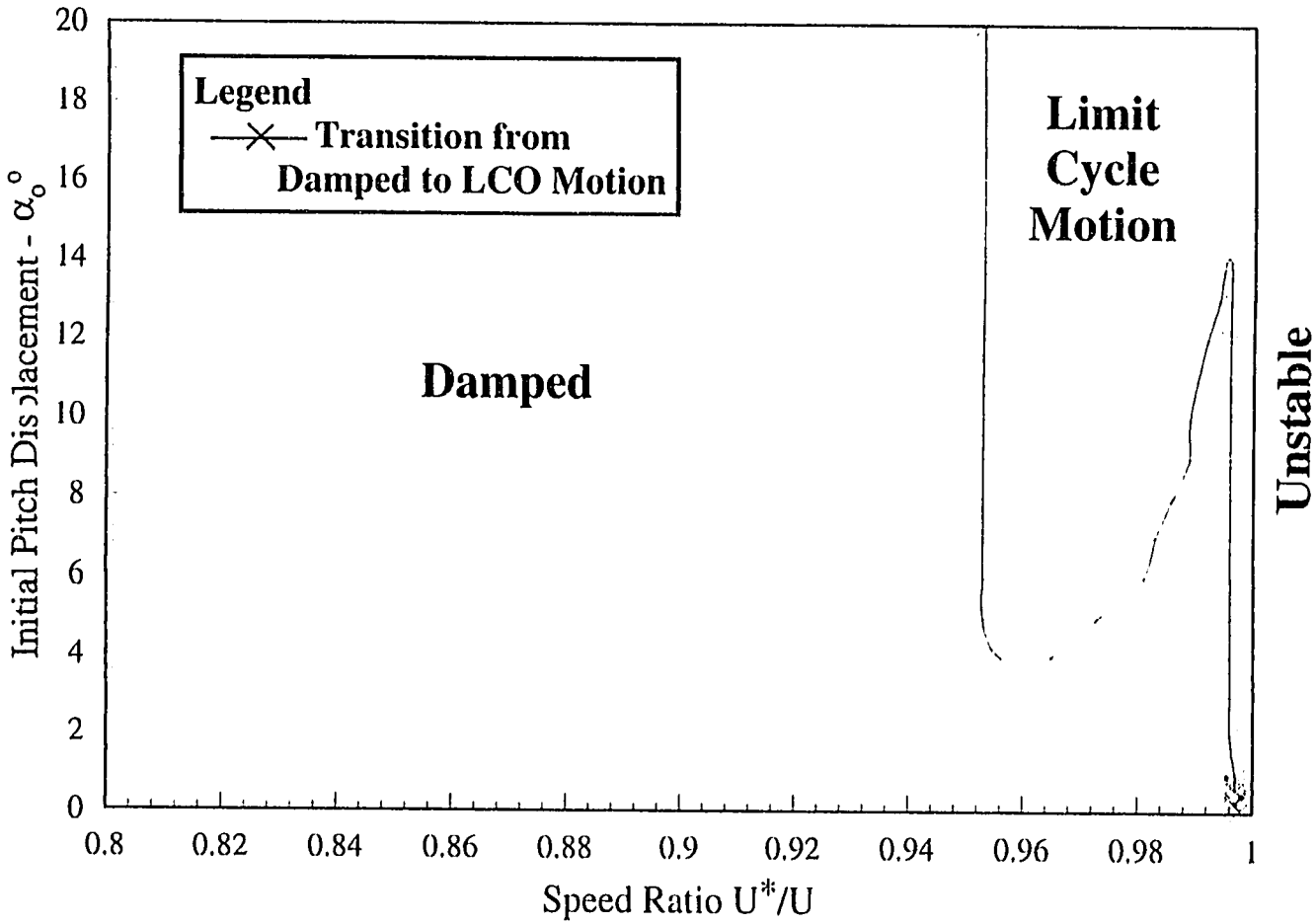

Figure 5.8a - Flutter Boundary for Hysteresis Nonlinearity:
μ=100, $\overline{\omega}$=0.8, ΔV=1.0^o, ΔH=0.1^o, Symmetric

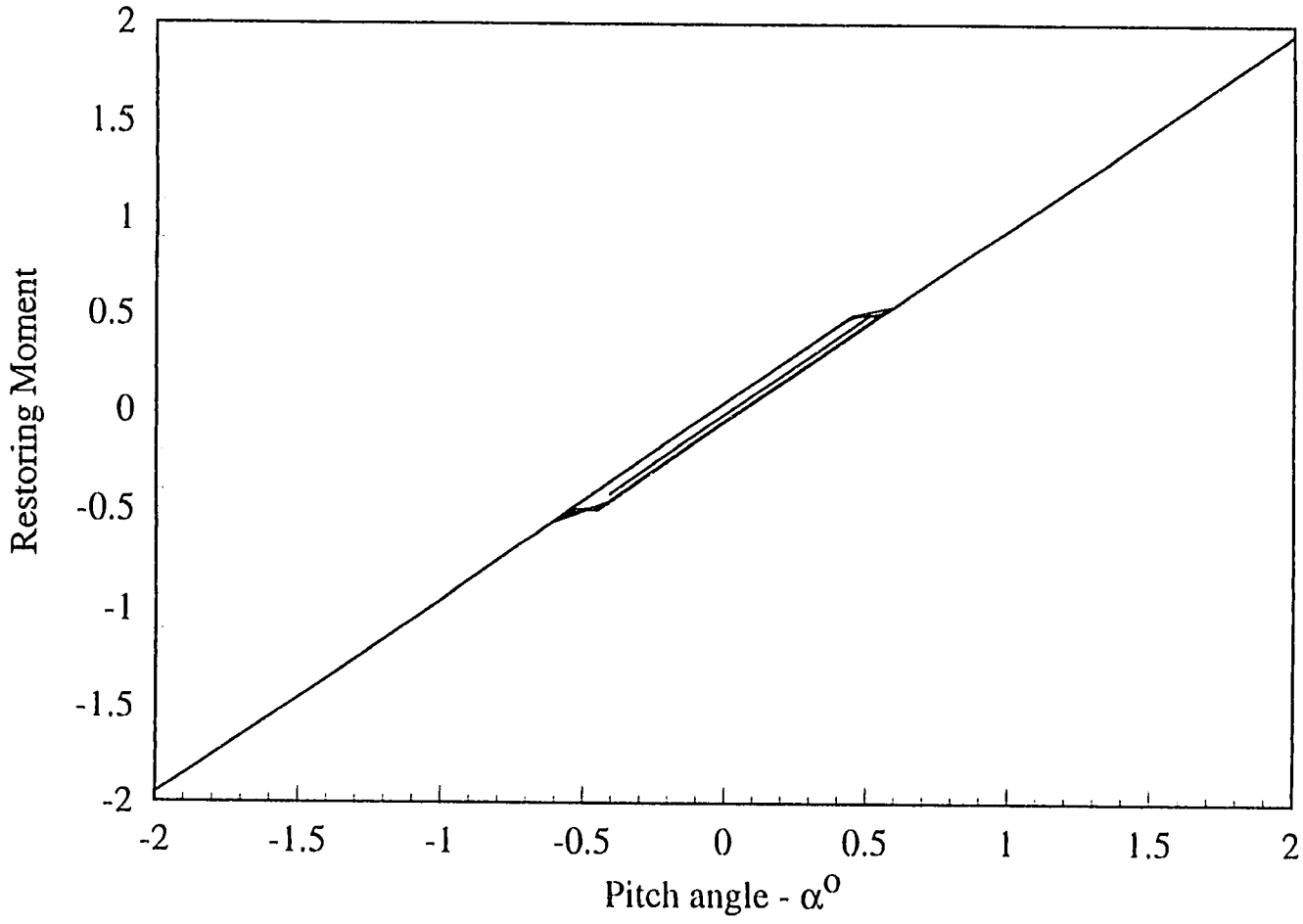

Figure 5.8b - Hysteretic Spring Response
α_0=10.0^o, U^*/U=0.985, ΔV=1.0, ΔH=0.1, $\overline{\omega}$=0.8, μ=100.0

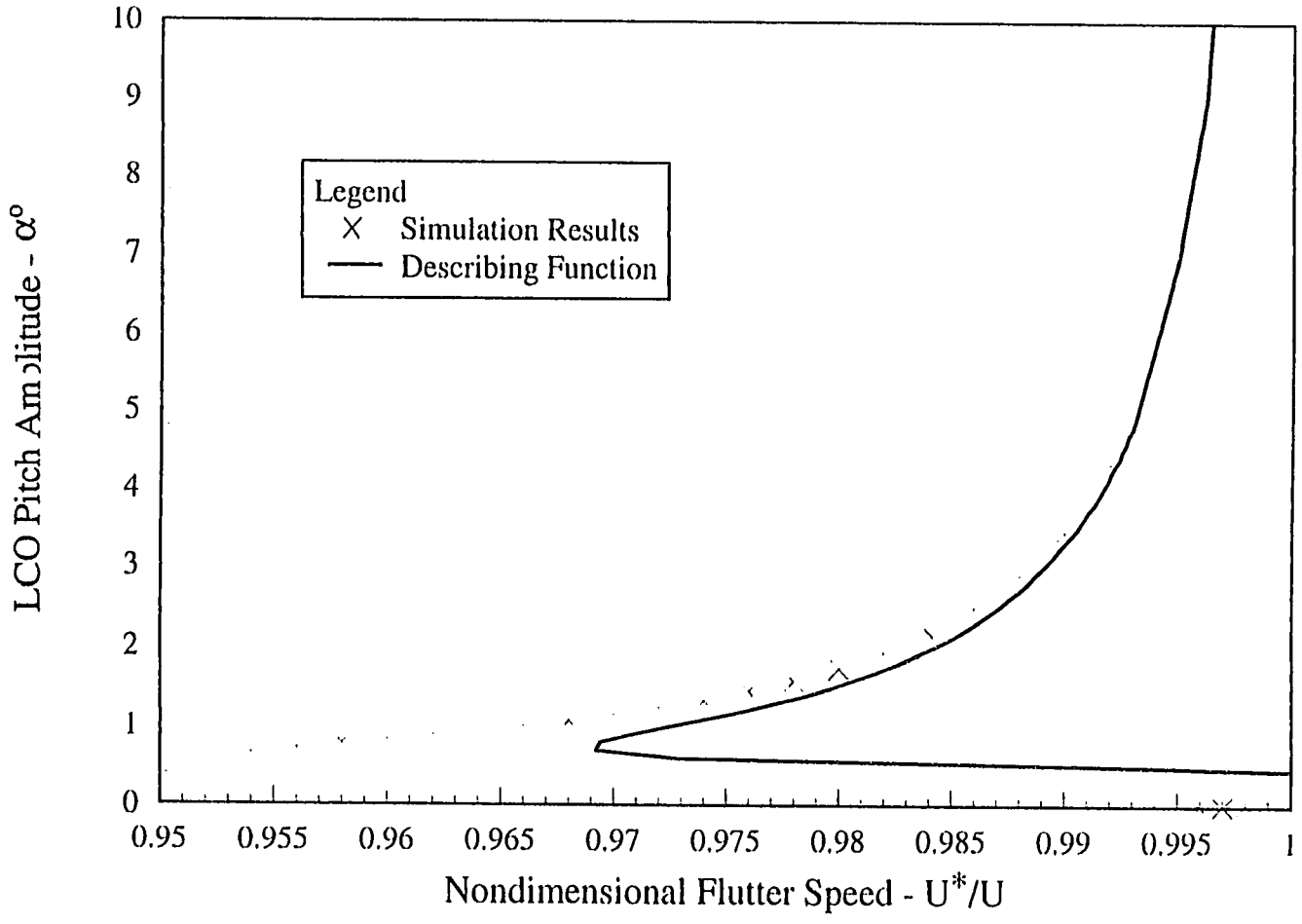

Figure 5.8c - Variation of LCO Amplitude with Speed:
μ=100, $\overline{\omega}$=0.8, ΔV=1.0°, ΔH=0.1°, symmetric

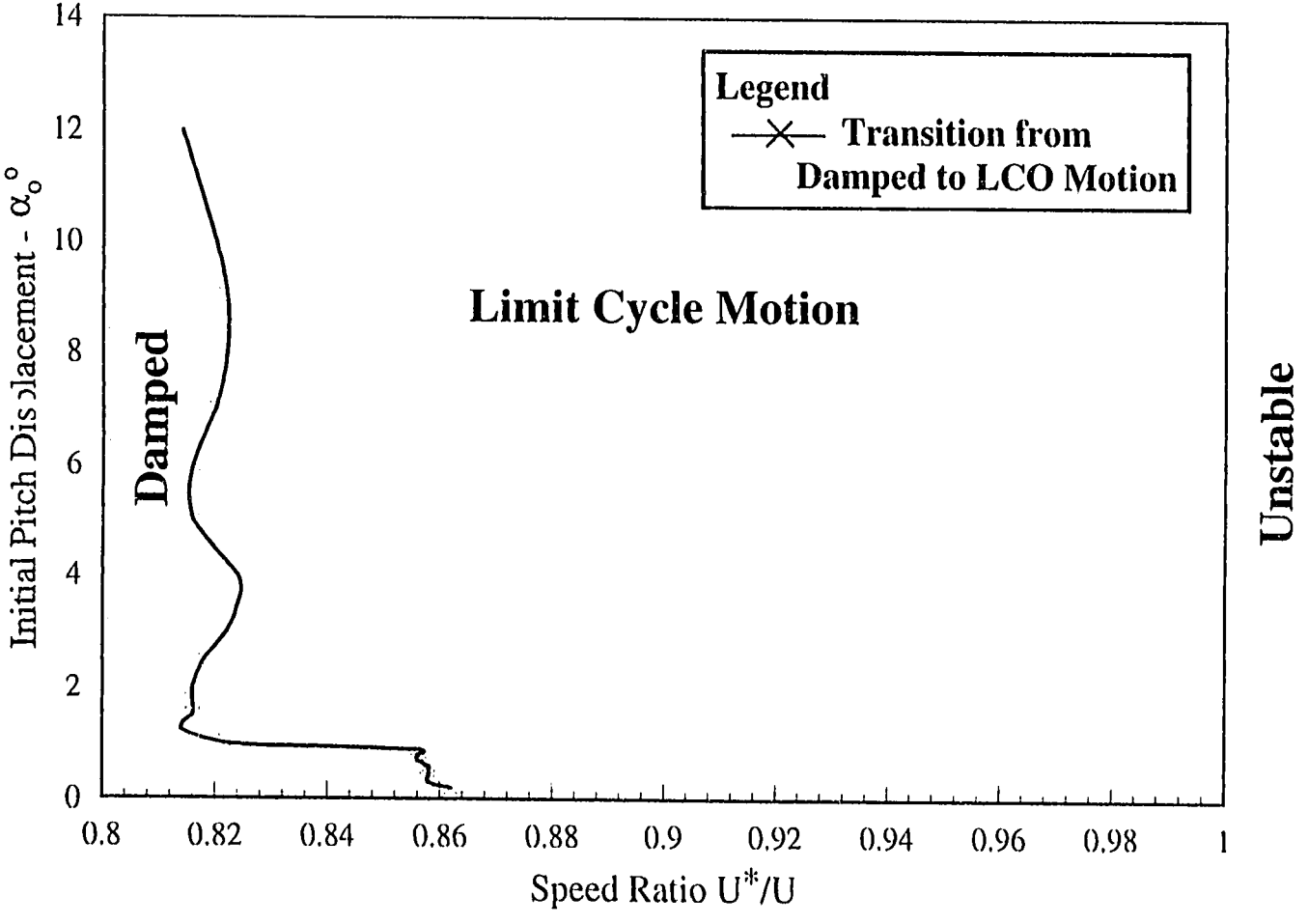

Figure 5.9a - Flutter Boundary for Hysteresis Nonlinearity:
μ=100, $\overline{\omega}$=0.8, ΔV=0.1^o, ΔH=1.0^o, Symmetric

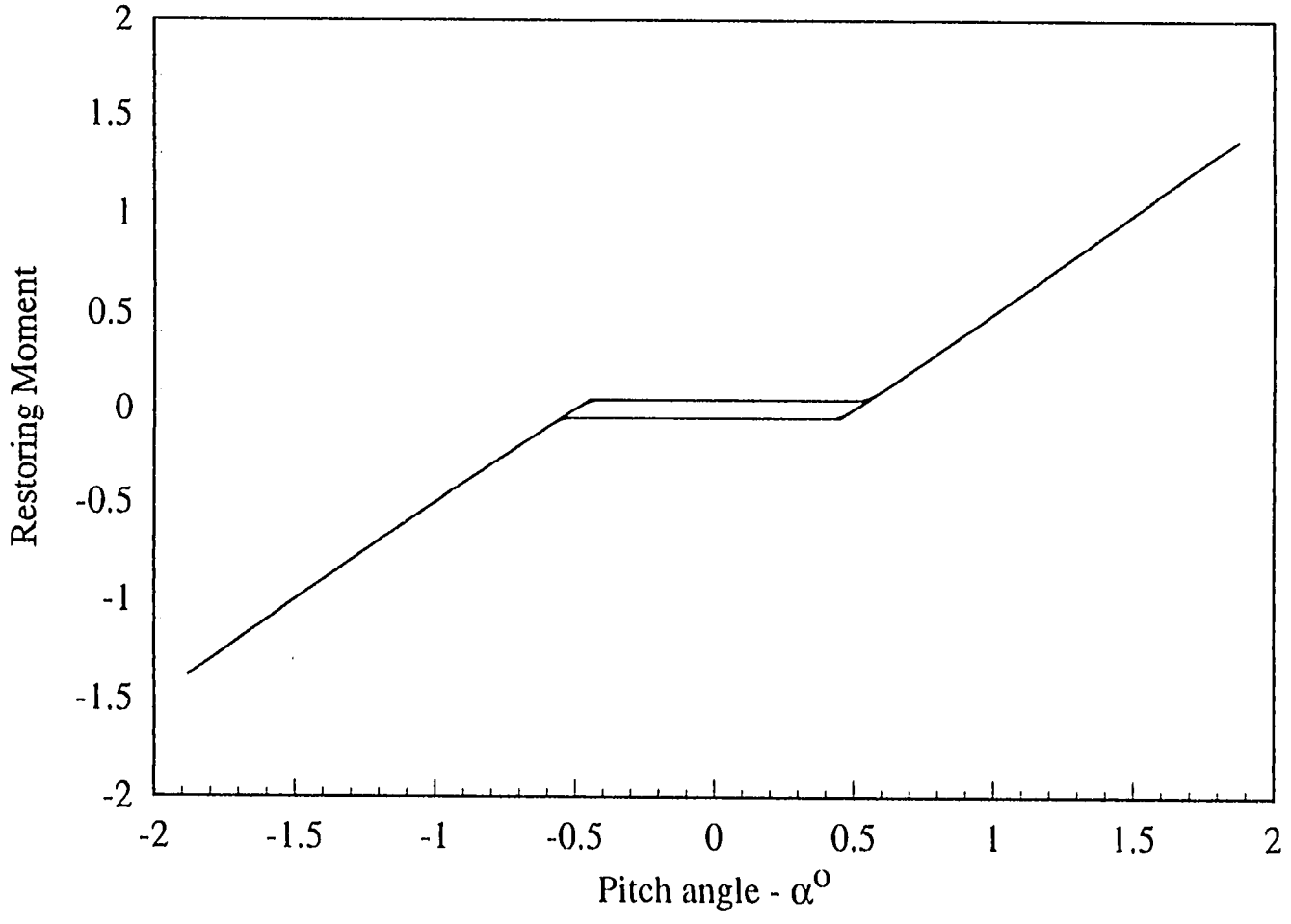

Figure 5.9b - Hysteretic Spring Response
α_o=1.5^o, ΔV=0.1, ΔH=1.0, $\overline{\omega}$=0.8, μ=100.0

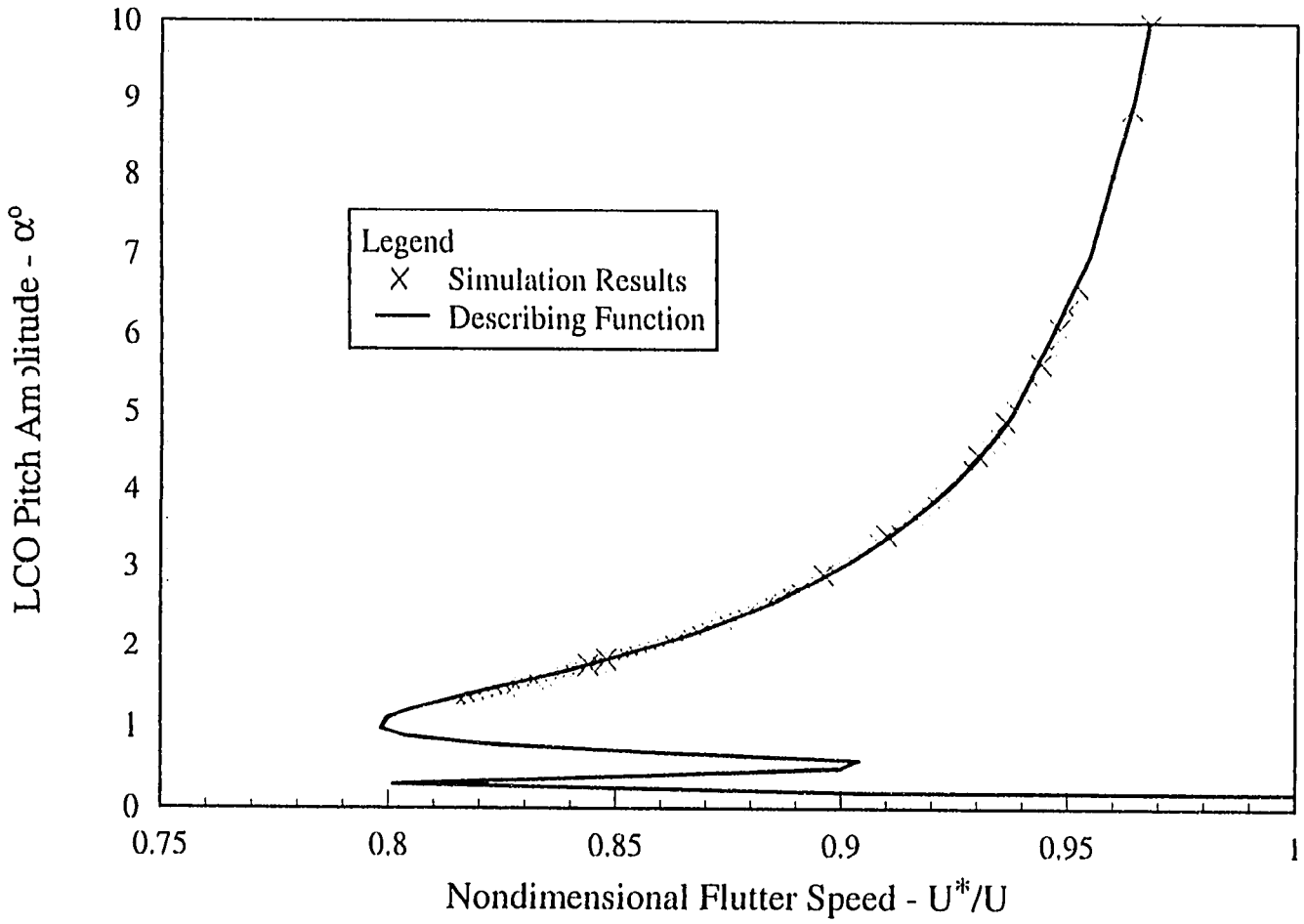

Figure 5.9c - Variation of LCO Amplitude with Speed:
μ=100, $\overline{\omega}$=0.8, ΔV=0.1°, ΔH=1.0°, symmetric

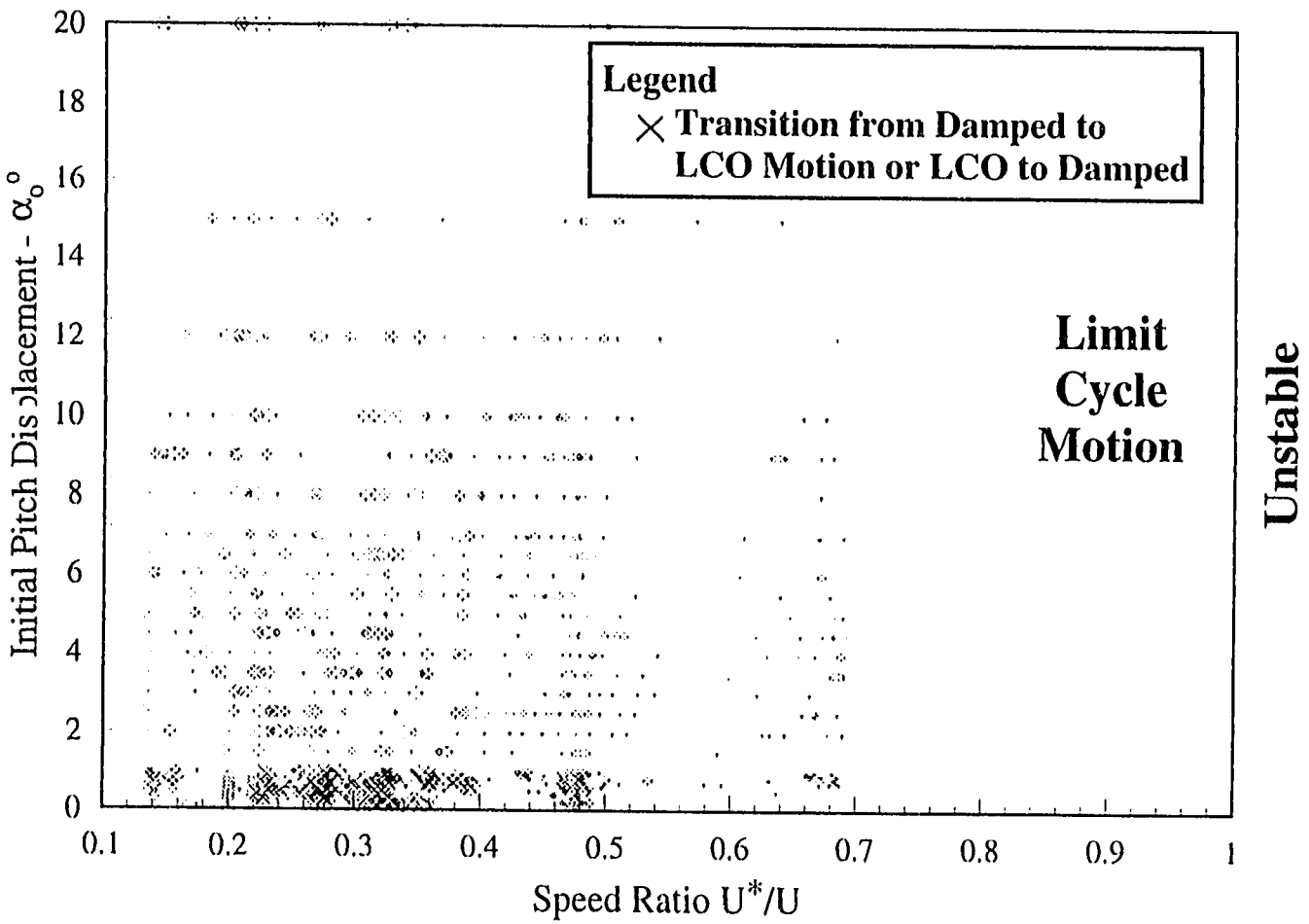

Figure 5.10a - Flutter Boundary for Hysteresis Nonlinearity:
μ=100, $\overline{\omega}$=0.2, ΔV=0.0^o, ΔH=0.5^o, Symmetric

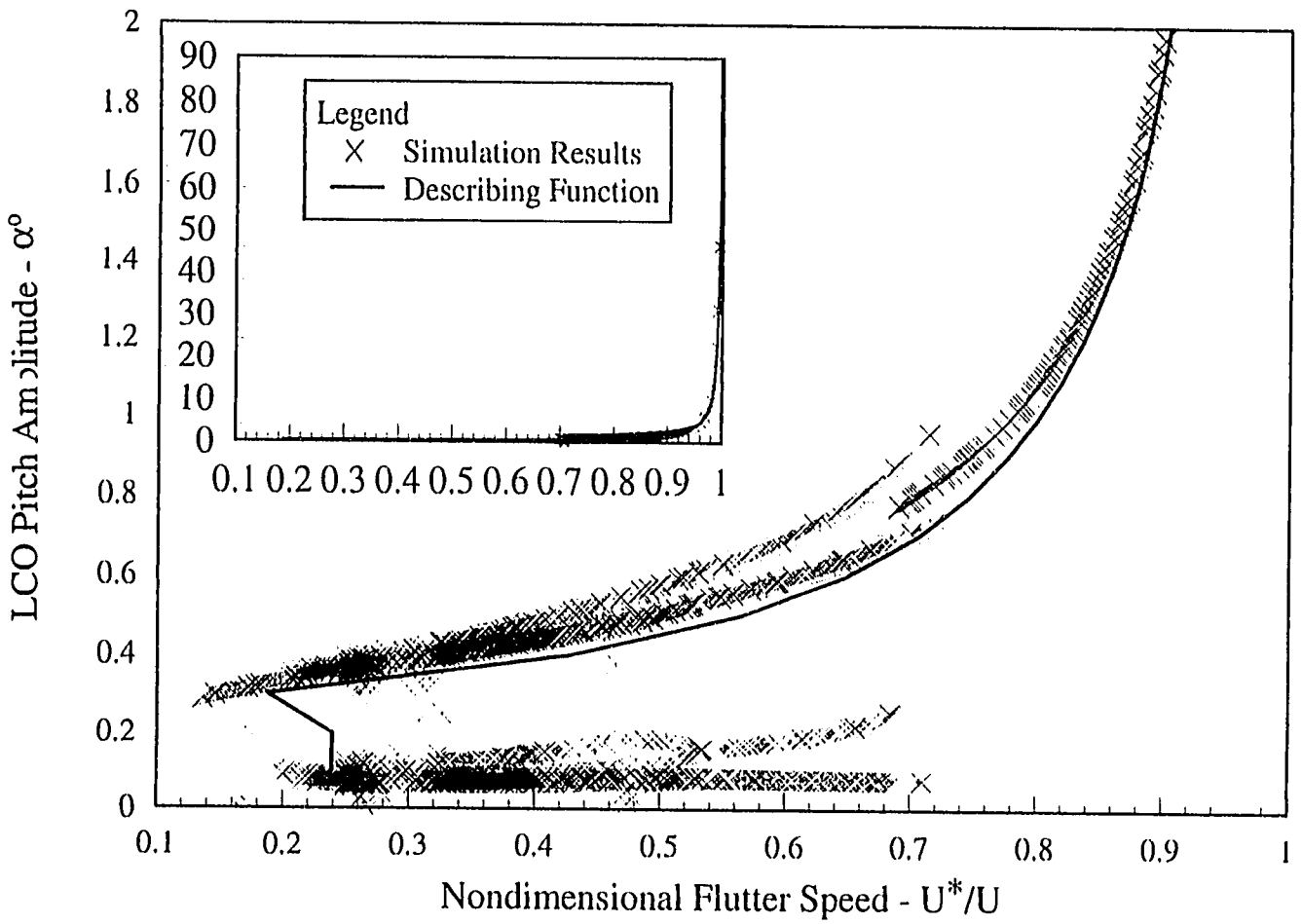

Figure 5.10c - Variation of LCO Amplitude with Speed:
μ=100, $\bar{\omega}$=0.2, ΔV=0.0°, ΔH=0.5°, symmetric

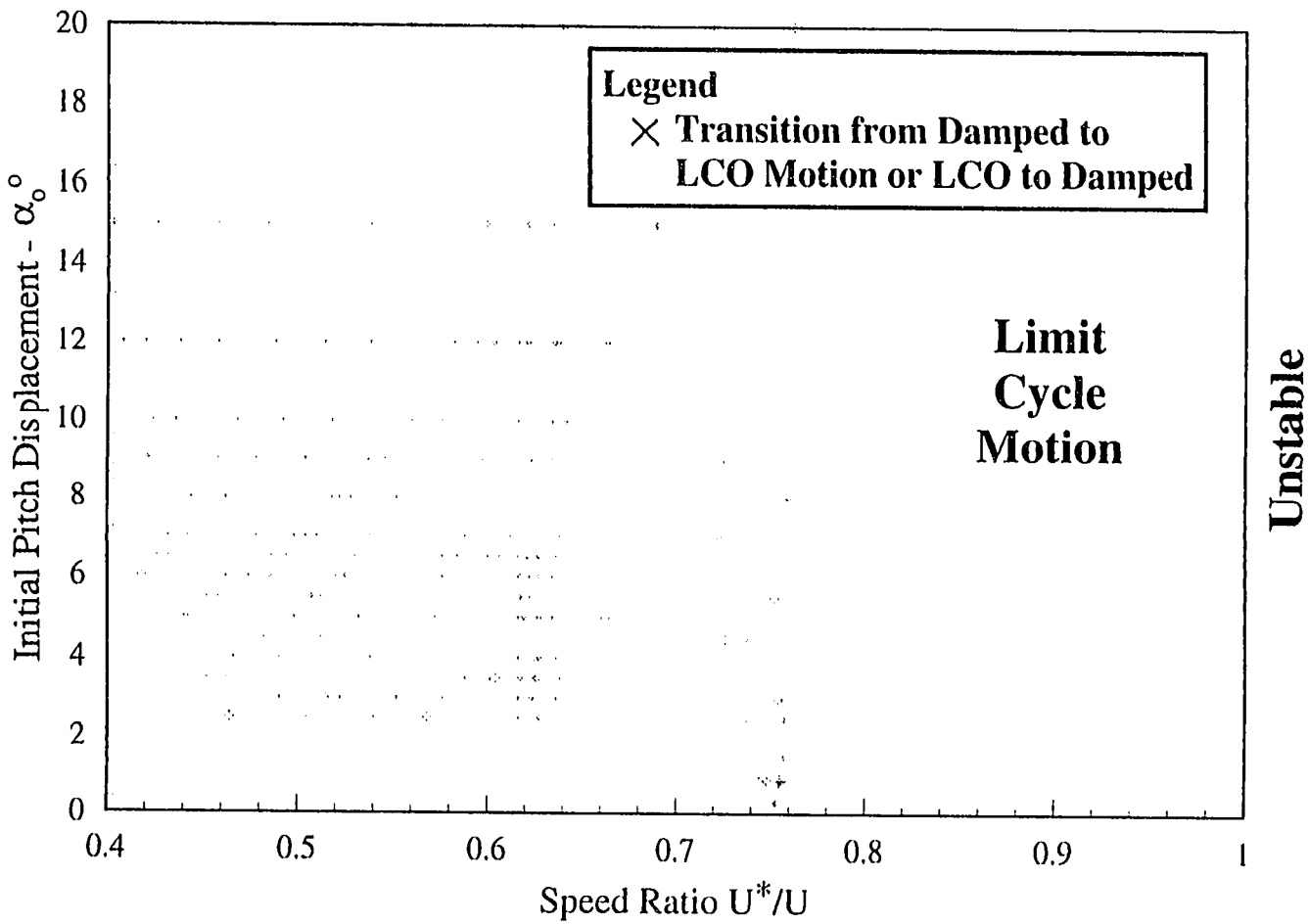

Figure 5.11a - Flutter Boundary for Hysteresis Nonlinearity:
μ=100, $\overline{\omega}$=0.2, ΔV=0.1°, ΔH=0.5°, Symmetric

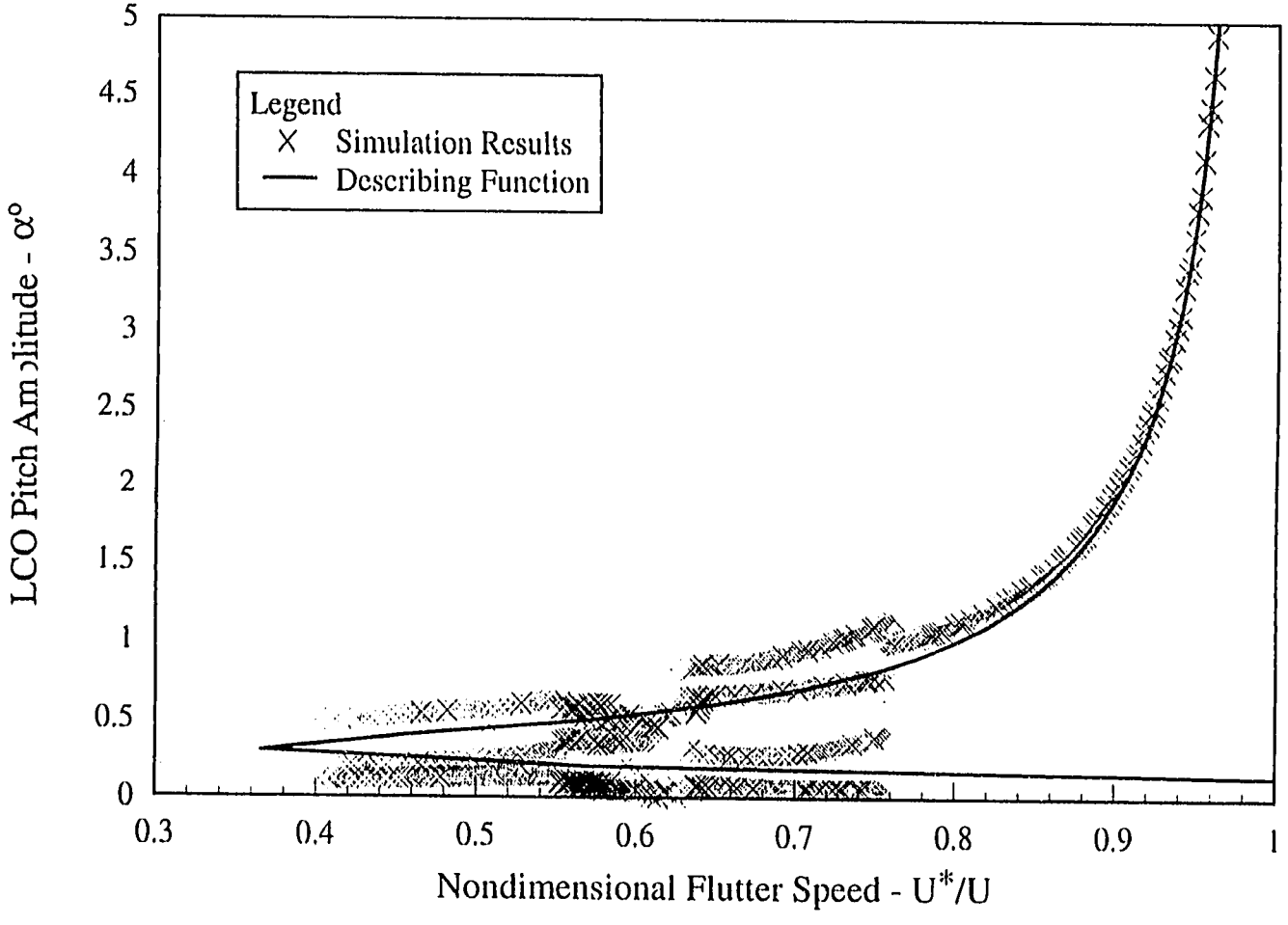

Figure 5.11c - Variation of LCO Amplitude with Speed:
μ=100, $\overline{\omega}$=0.2, ΔV=0.1°, ΔH=0.5°, symmetric

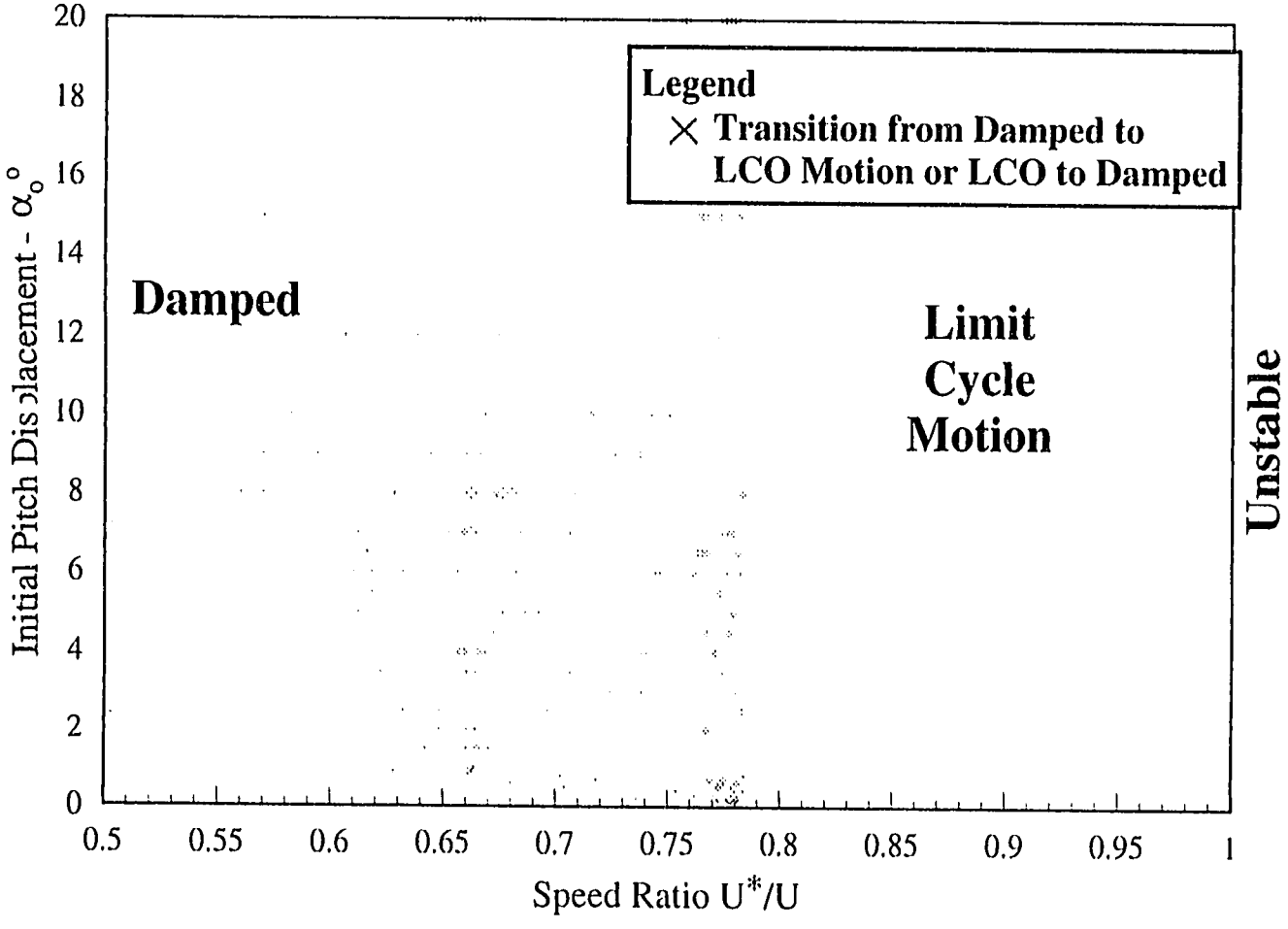

Figure 5.12a - Flutter Boundary for Hysteresis Nonlinearity:
μ=100, $\overline{\omega}$=0.2, $\Delta V=0.2^o$, $\Delta H=0.5^o$, Symmetric

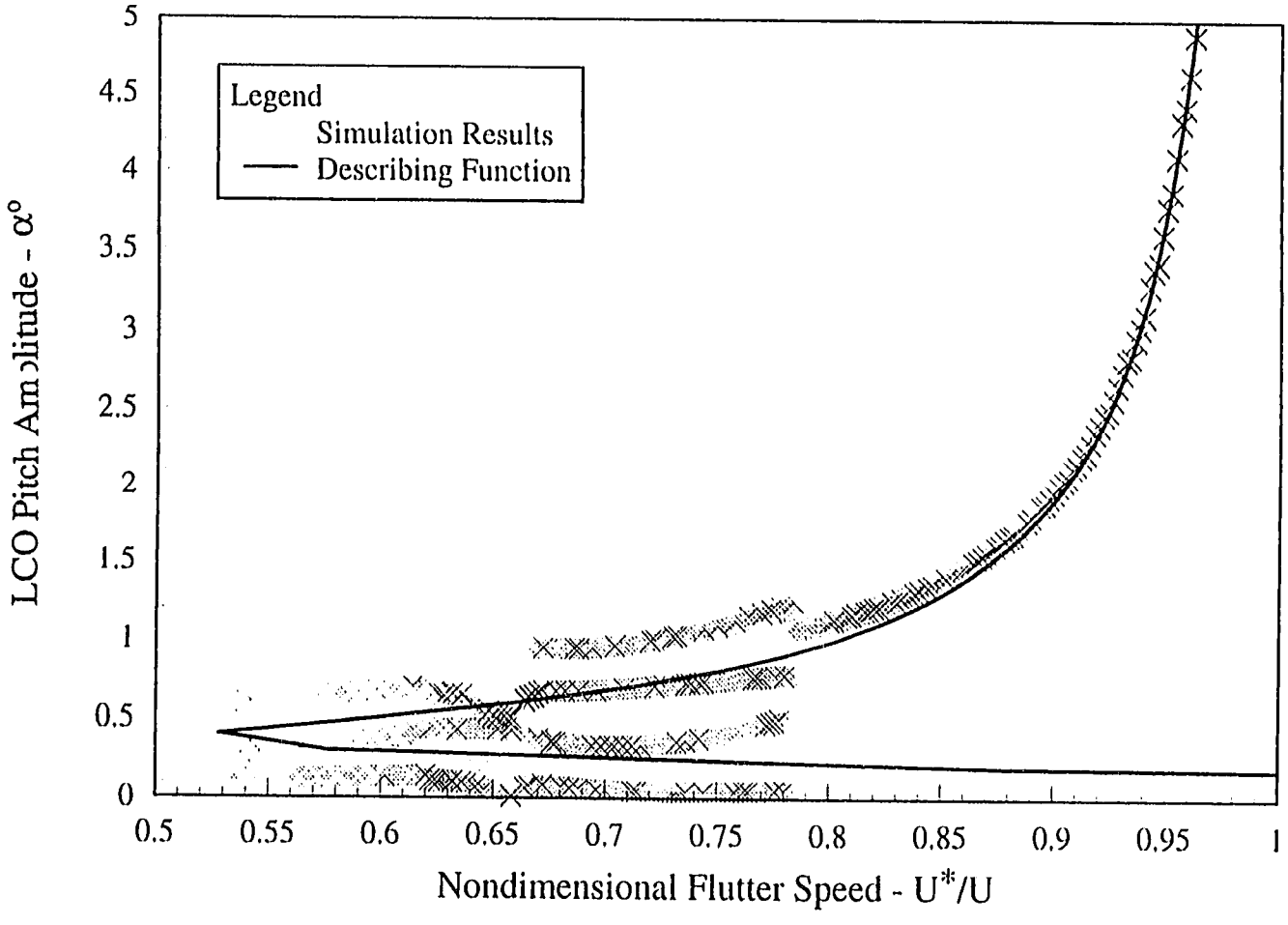

Figure 5.12c - Variation of LCO Amplitude with Speed:
μ=100, $\overline{\omega}$=0.2, ΔV=0.2°, ΔH=0.5°, symmetric

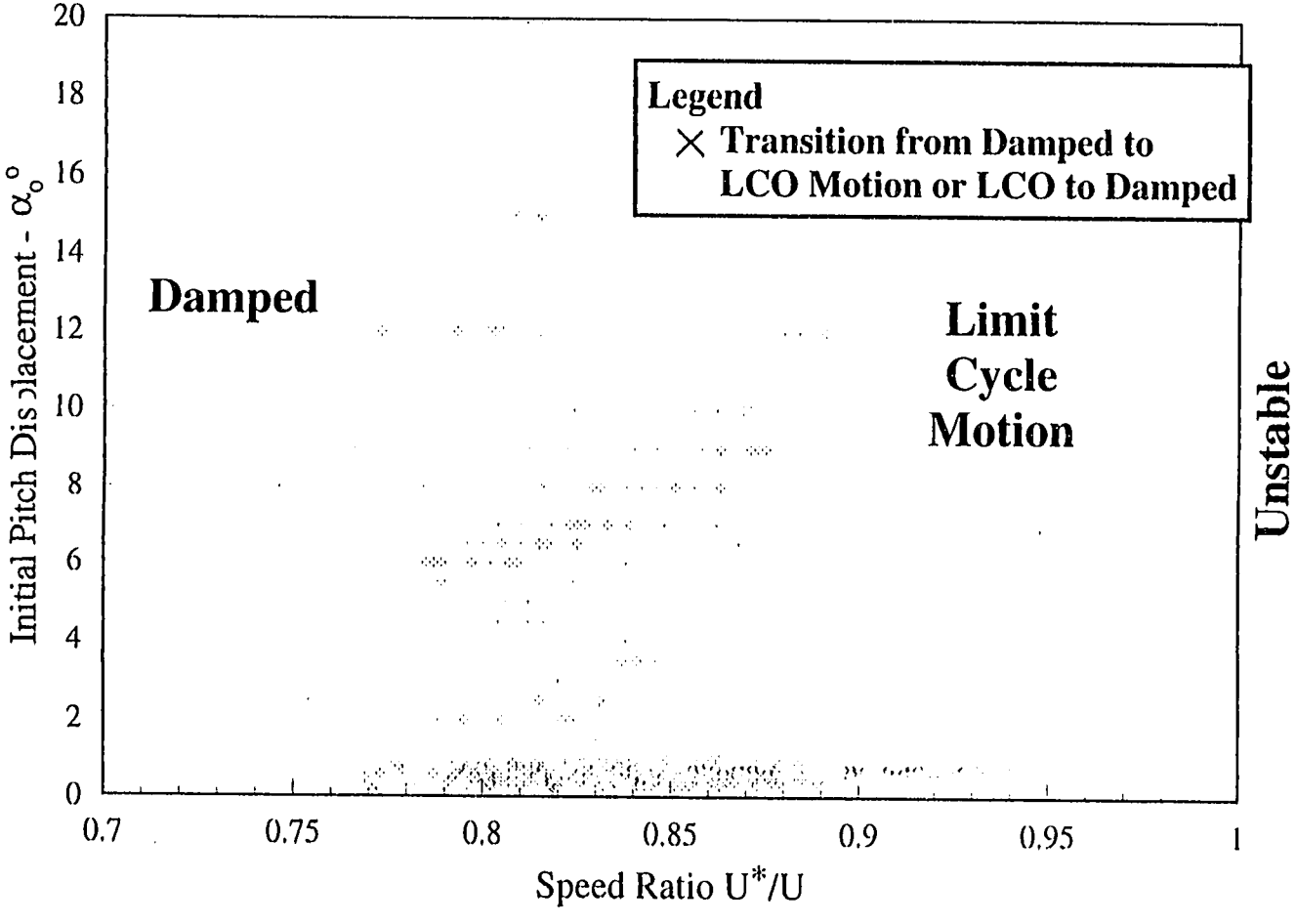

Figure 5.13a - Flutter Boundary for Hysteresis Nonlinearity:
μ=100, $\overline{\omega}$=0.2, ΔV=0.5°, ΔH=0.5°, Symmetric

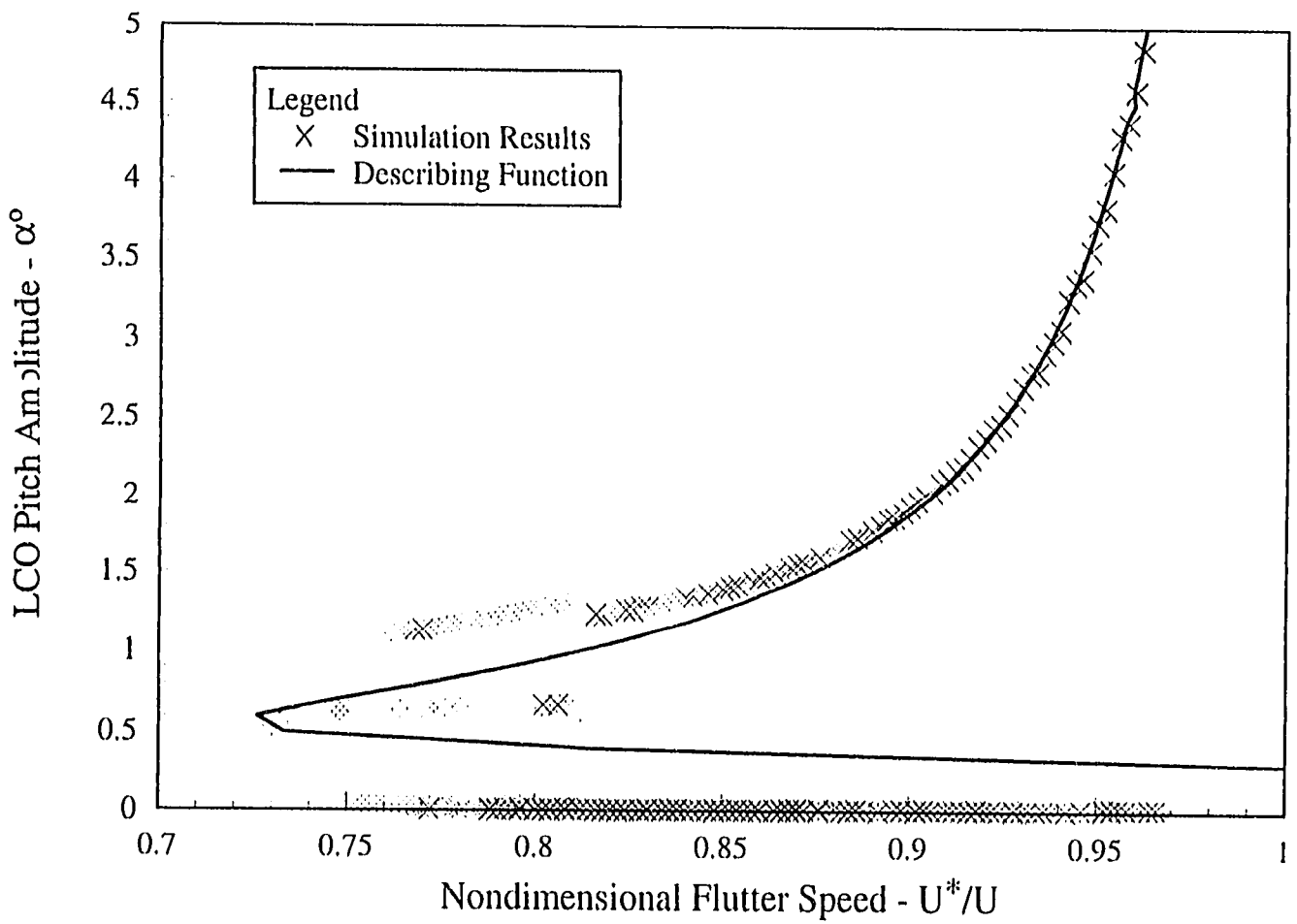

Figure 5.13c - Variation of LCO Amplitude with Speed:
μ=100, $\overline{\omega}$=0.2, ΔV=0.5°, ΔH=0.5°, symmetric

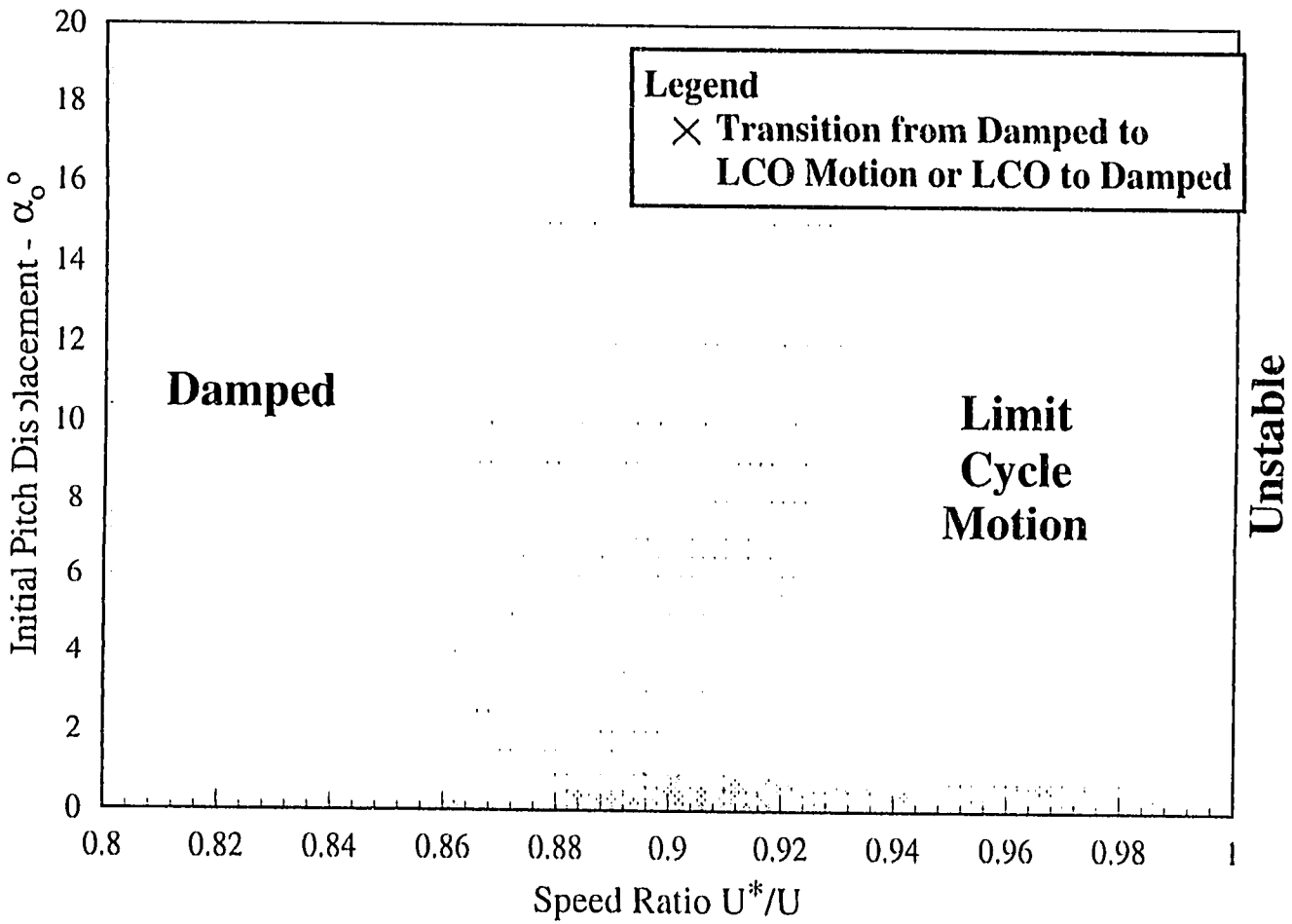

Figure 5.14a - Flutter Boundary for Hysteresis Nonlinearity:
μ=100, $\overline{\omega}$=0.2, ΔV=0.5°, ΔH=0.2°, Symmetric

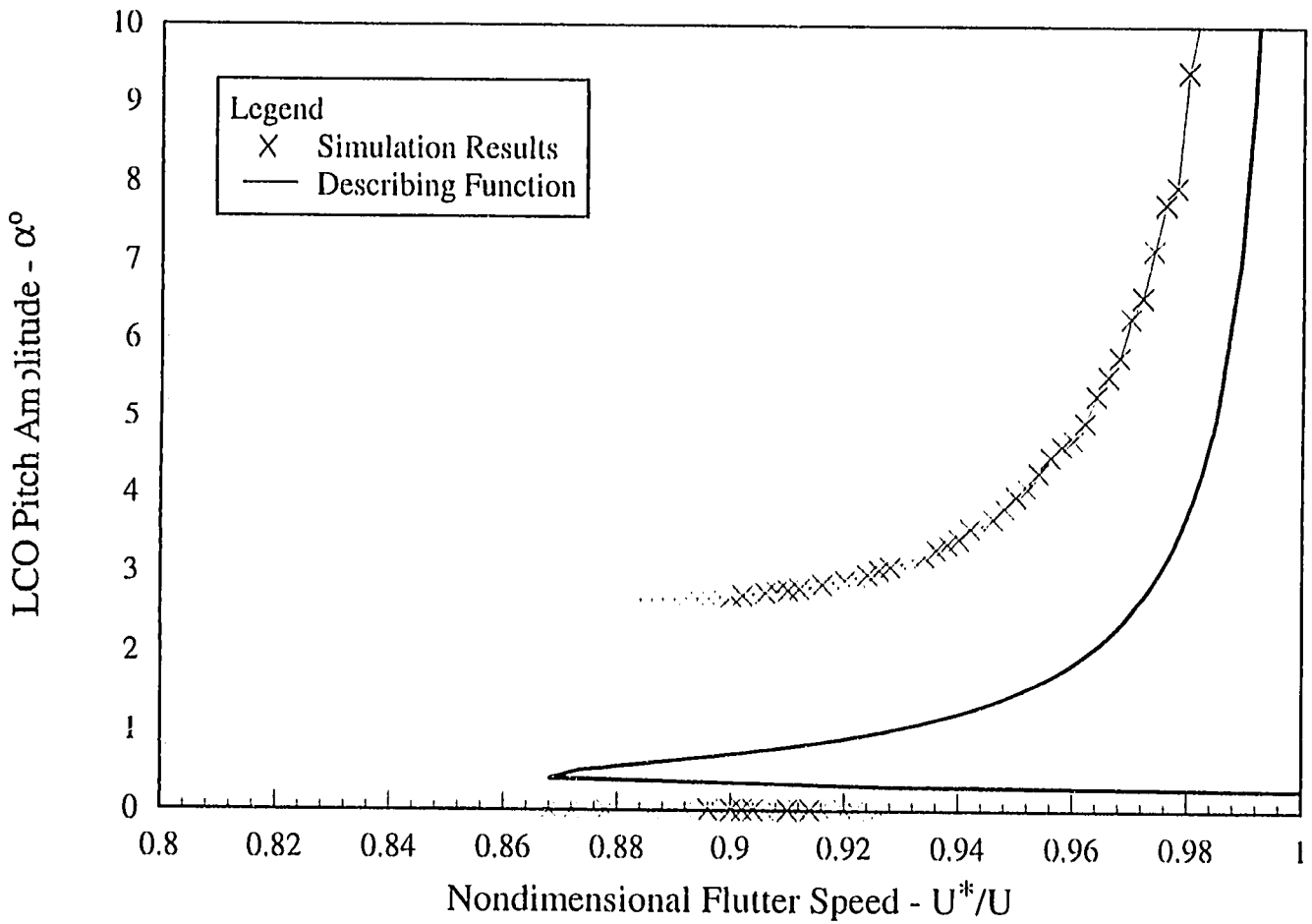

Figure 5.14c - Variation of LCO Amplitude with Speed:
μ=100, $\bar{\omega}$=0.2, ΔV=0.5°, ΔH=0.2°, symmetric

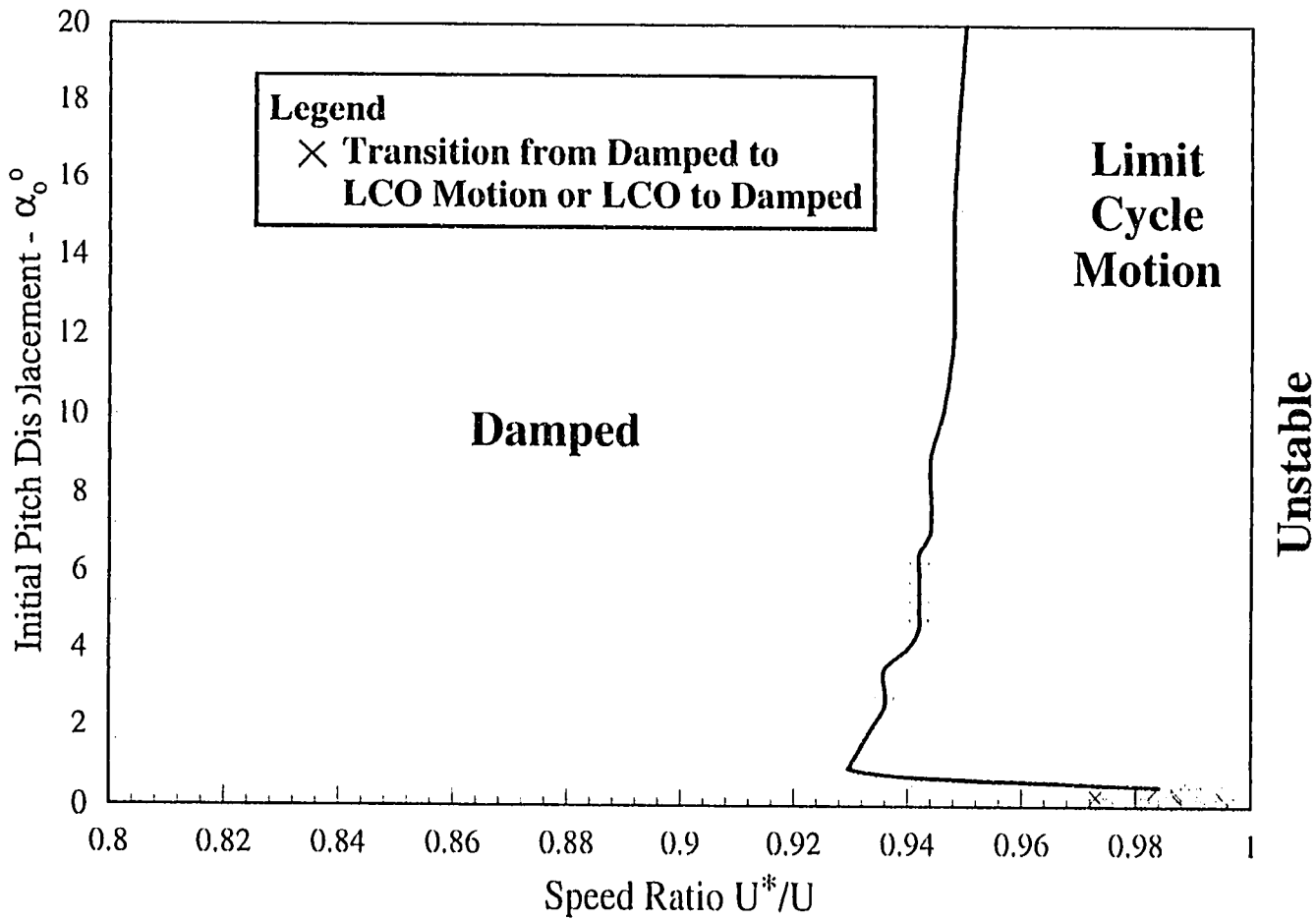

Figure 5.15a - Flutter Boundary for Hysteresis Nonlinearity:
μ=100, $\overline{\omega}$=0.2, $\Delta V=0.5^o$, $\Delta H=0.1^o$, Symmetric

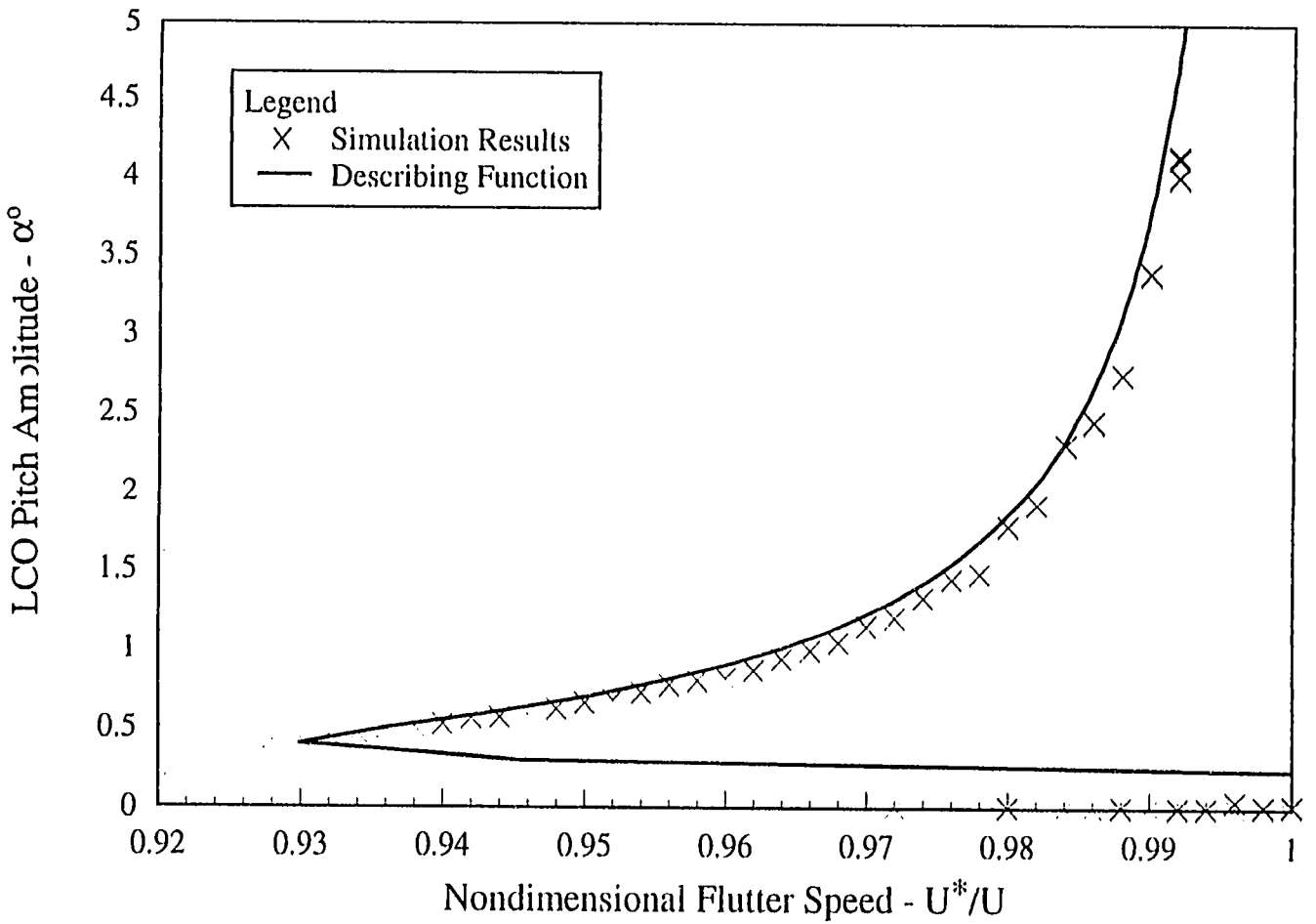

Figure 5.15c - Variation of LCO Amplitude with Speed:
μ=100, $\overline{\omega}$=0.2, ΔV=0.5°, ΔH=0.1°, symmetric

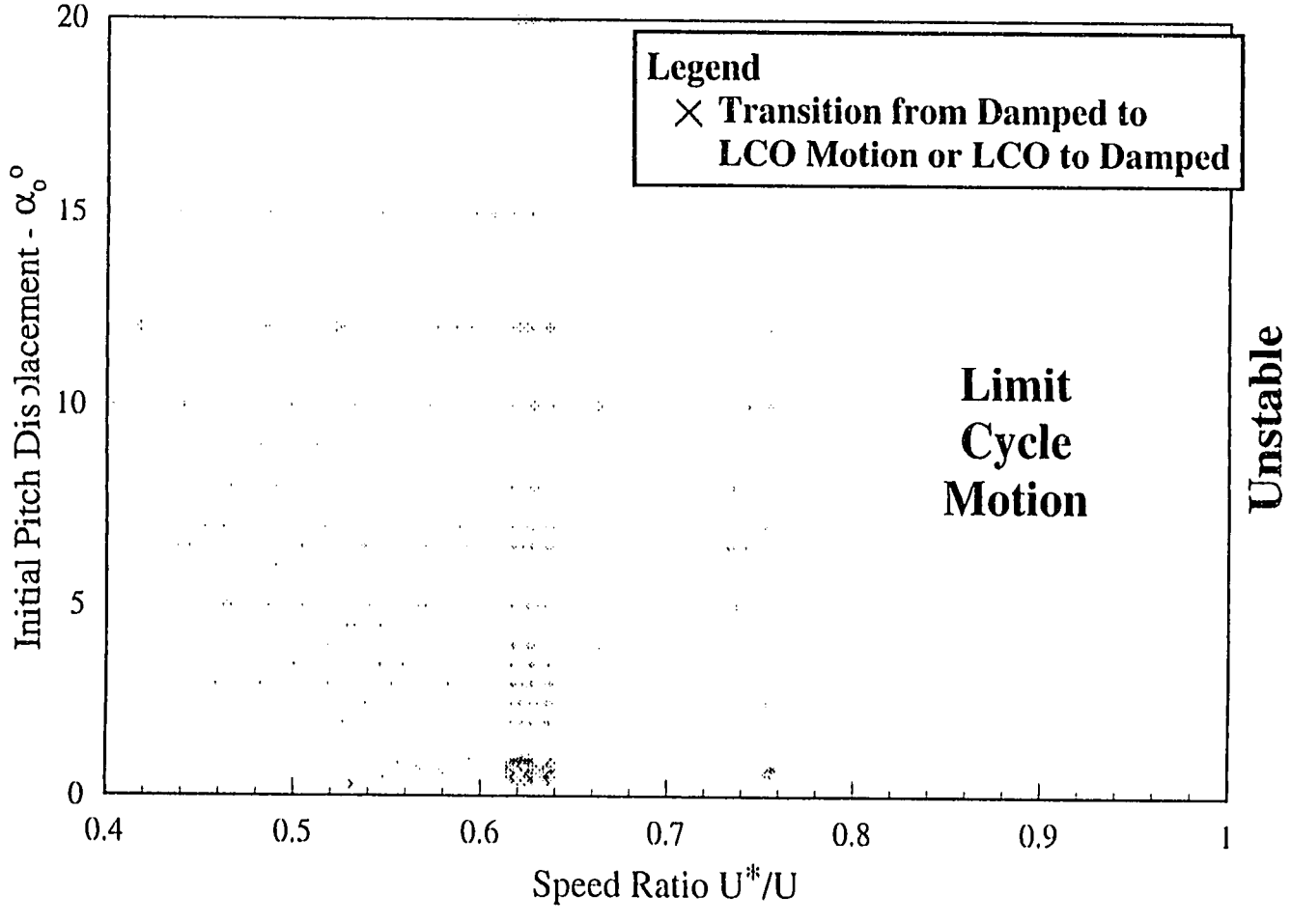

Figure 5.16a - Flutter Boundary for Hysteresis Nonlinearity:
μ=100, $\bar{\omega}$=0.8, $\Delta V=0.2^o$, $\Delta H=1.0^o$, Symmetric

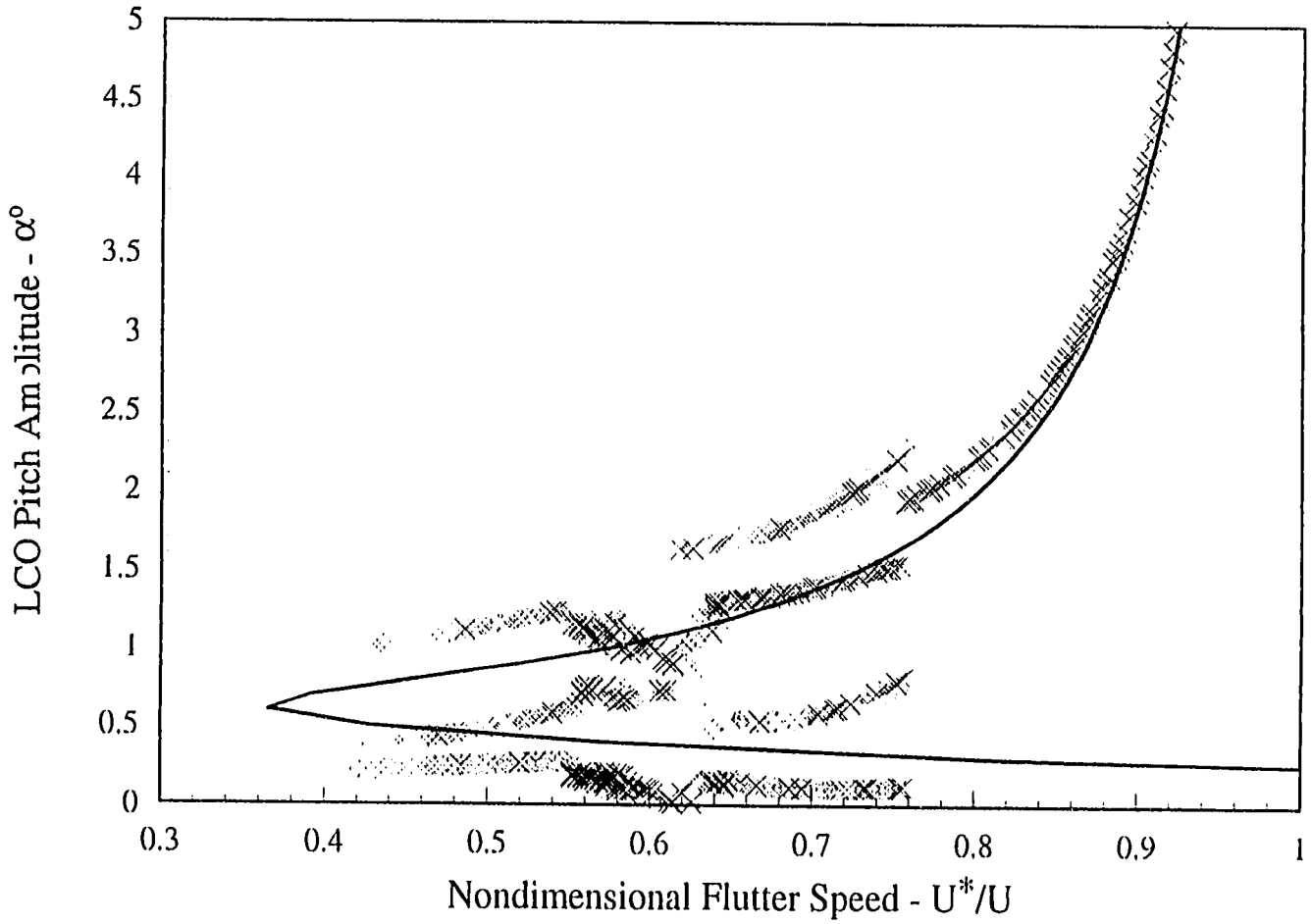

Figure 5.16c - Variation of LCO Amplitude with Speed:
μ=100, $\bar{\omega}$=0.2, ΔV=0.2°, ΔH=1.0°, symmetric

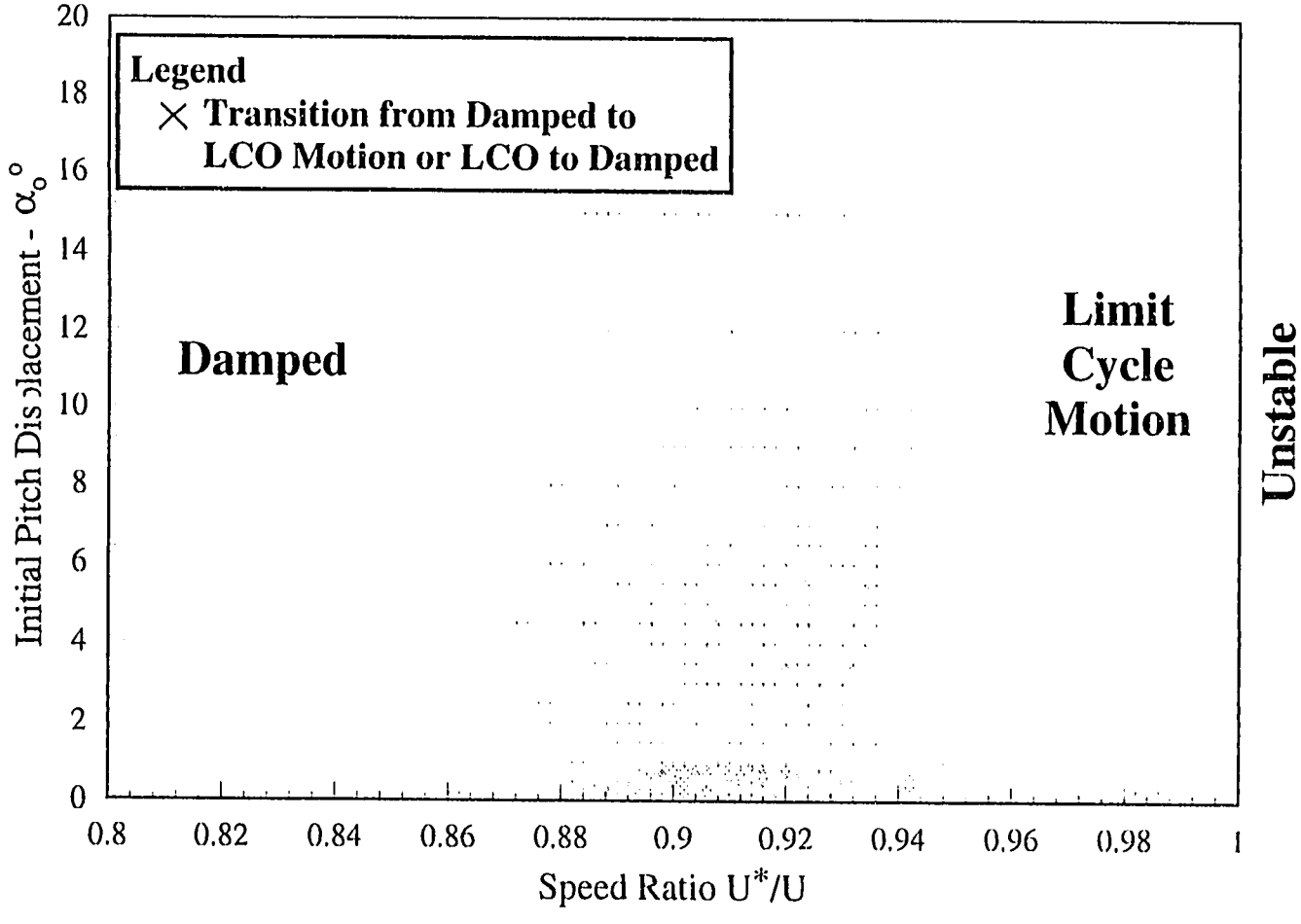

Figure 5.17a - Flutter Boundary for Hysteresis Nonlinearity:
μ=100, $\overline{\omega}$=0.2, ΔV=1.0^o, ΔH=0.2^o, Symmetric

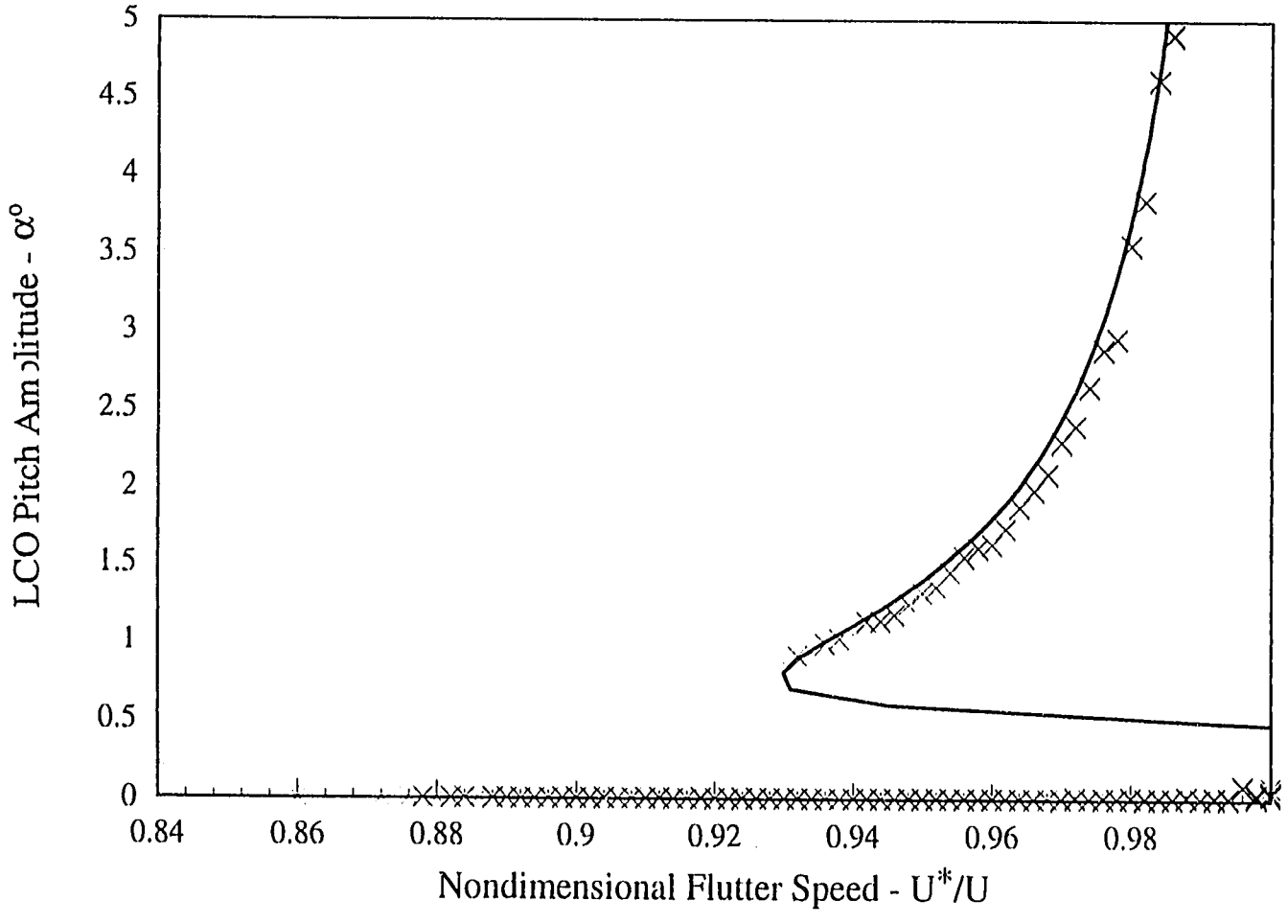

Figure 5.17c - Variation of LCO Amplitude with Speed:
μ=100, $\overline{\omega}$=0.2, ΔV=1.0°, ΔH=0.2°, symmetric

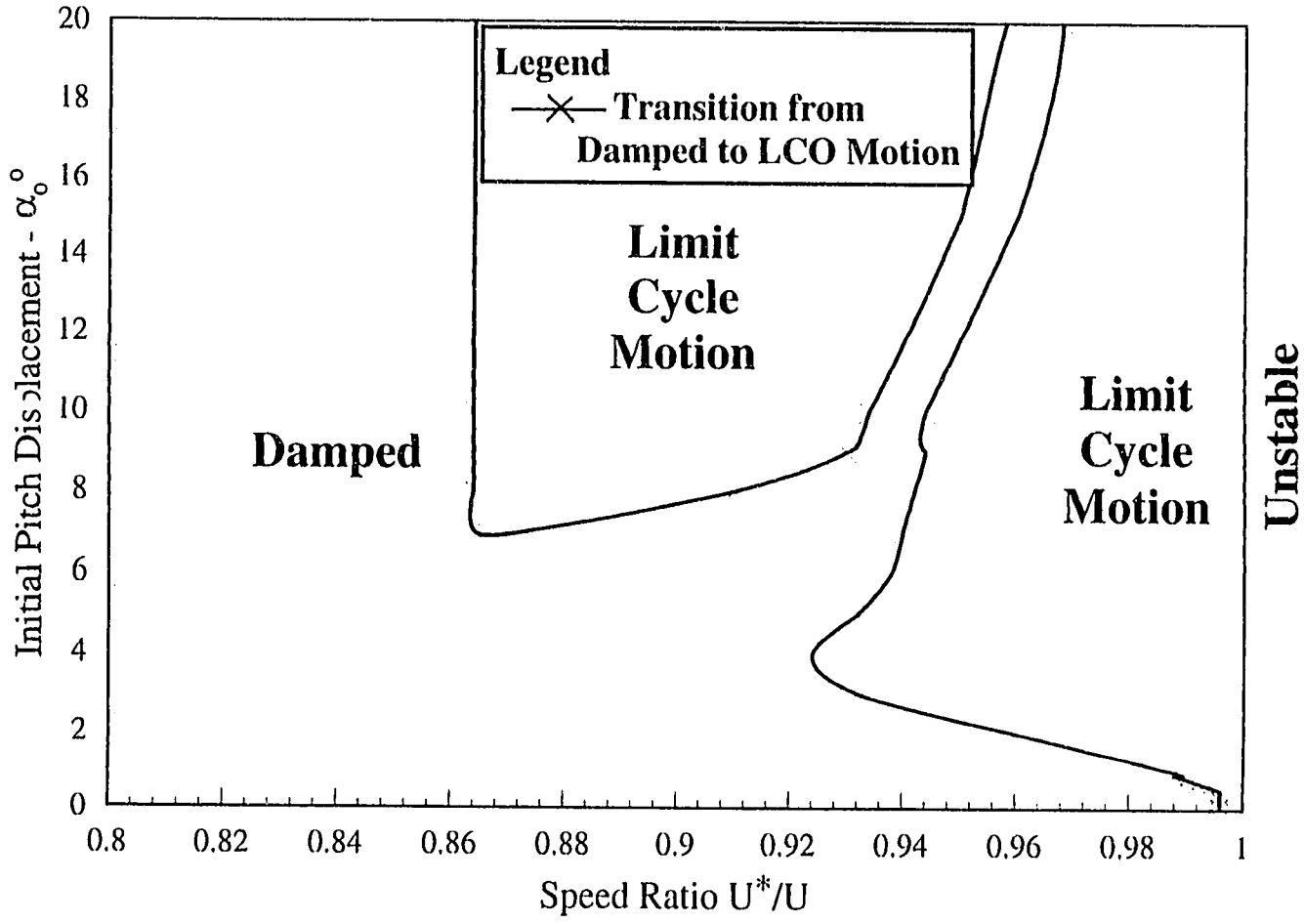

Figure 5.18a - Flutter Boundary for Hysteresis Nonlinearity:
μ=100, $\overline{\omega}$=0.8, ΔV=1.0^o, ΔH=1.0^o, V_{offset}=0.5, H_{offset}=0.0

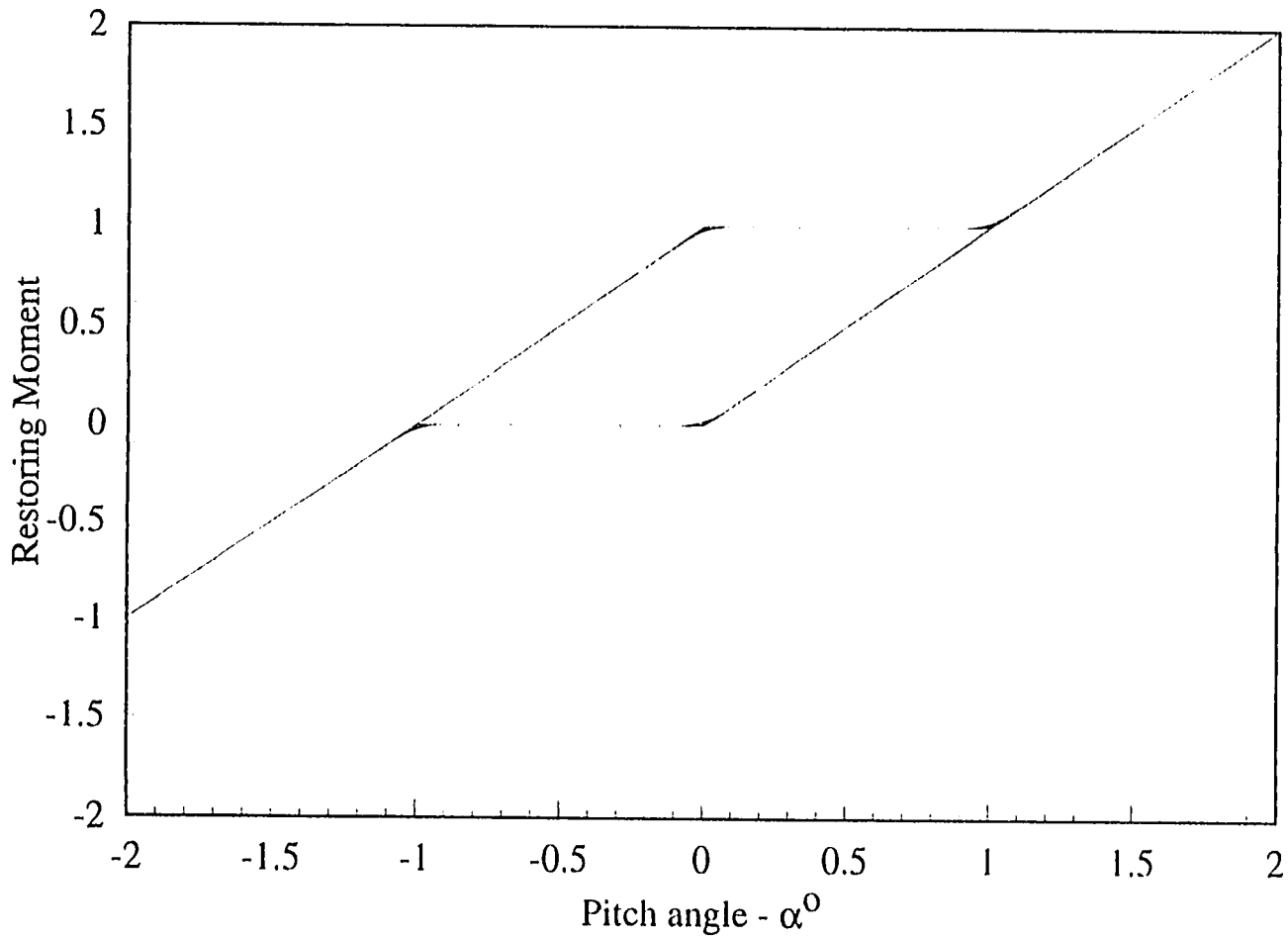

Figure 5.18b - Hysteretic Spring Response
α_o=10.0°, U*/U=0.932, ΔV=1.0°, ΔH=1.0°, $\overline{\omega}$=0.8, μ=100.0, V_{offset}=0.5, H_{offset}=0.0

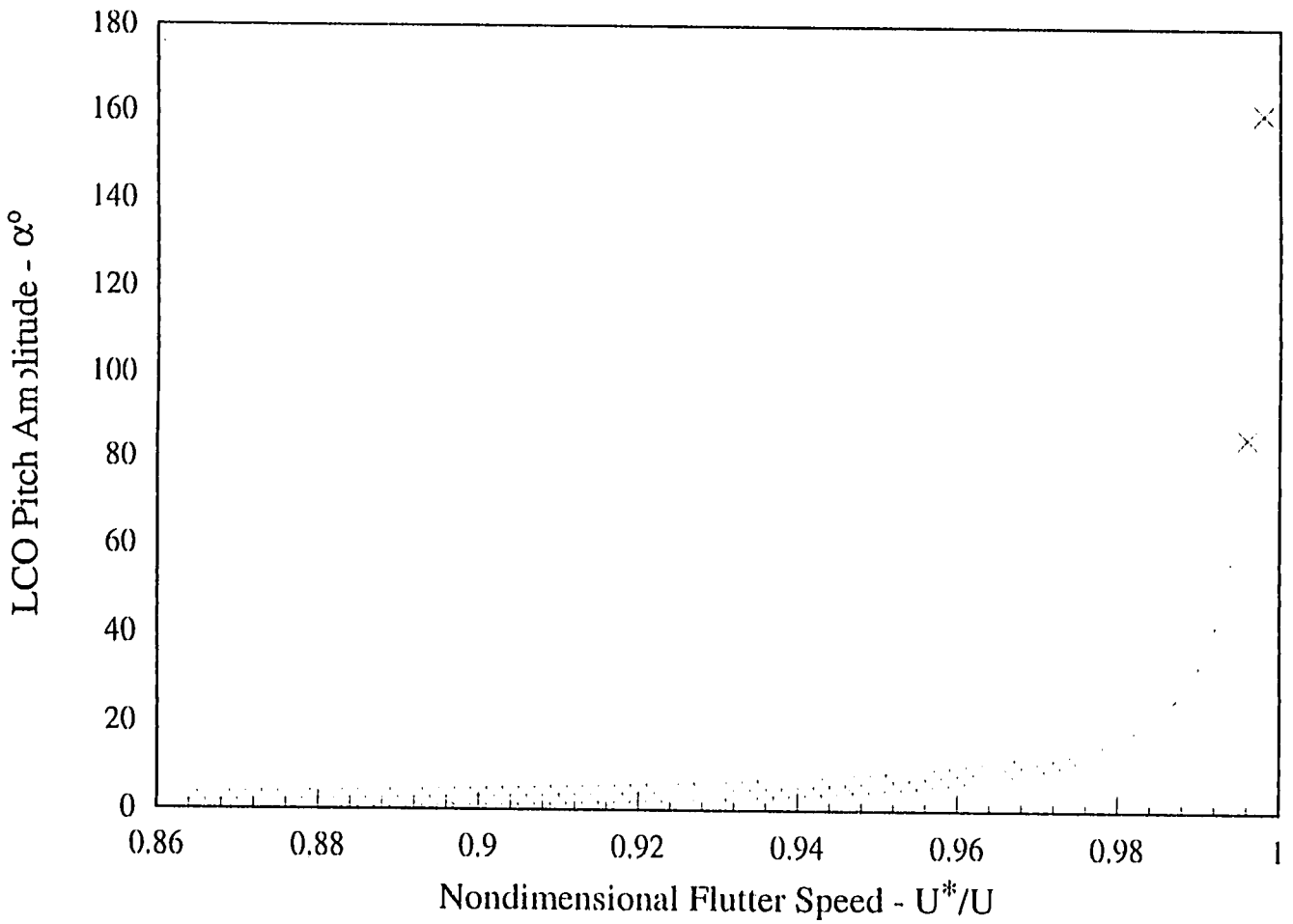

Figure 5.18c - Variation of LCO Amplitude with Speed:
μ=100, $\overline{\omega}$=0.8, ΔV=1.0°, ΔH=1.0°, V_{offset}=0.5, H_{offset}=0.0

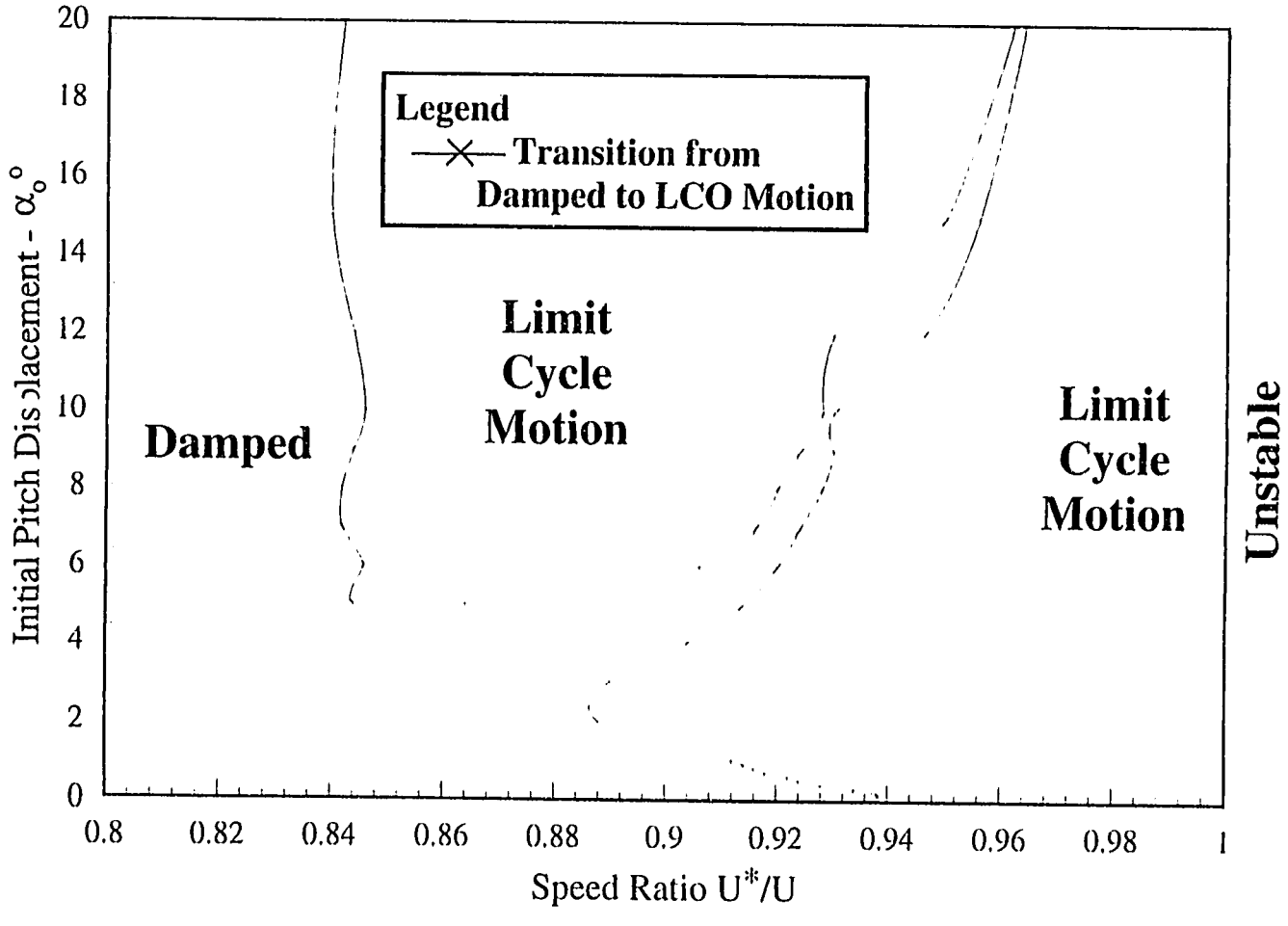

Figure 5.19a - Flutter Boundary for Hysteresis Nonlinearity:
μ=100, $\overline{\omega}$=0.8, $\Delta V=0.2^o$, $\Delta H=1.0^o$, V_{offset}=0.5, H_{offset}=0.0

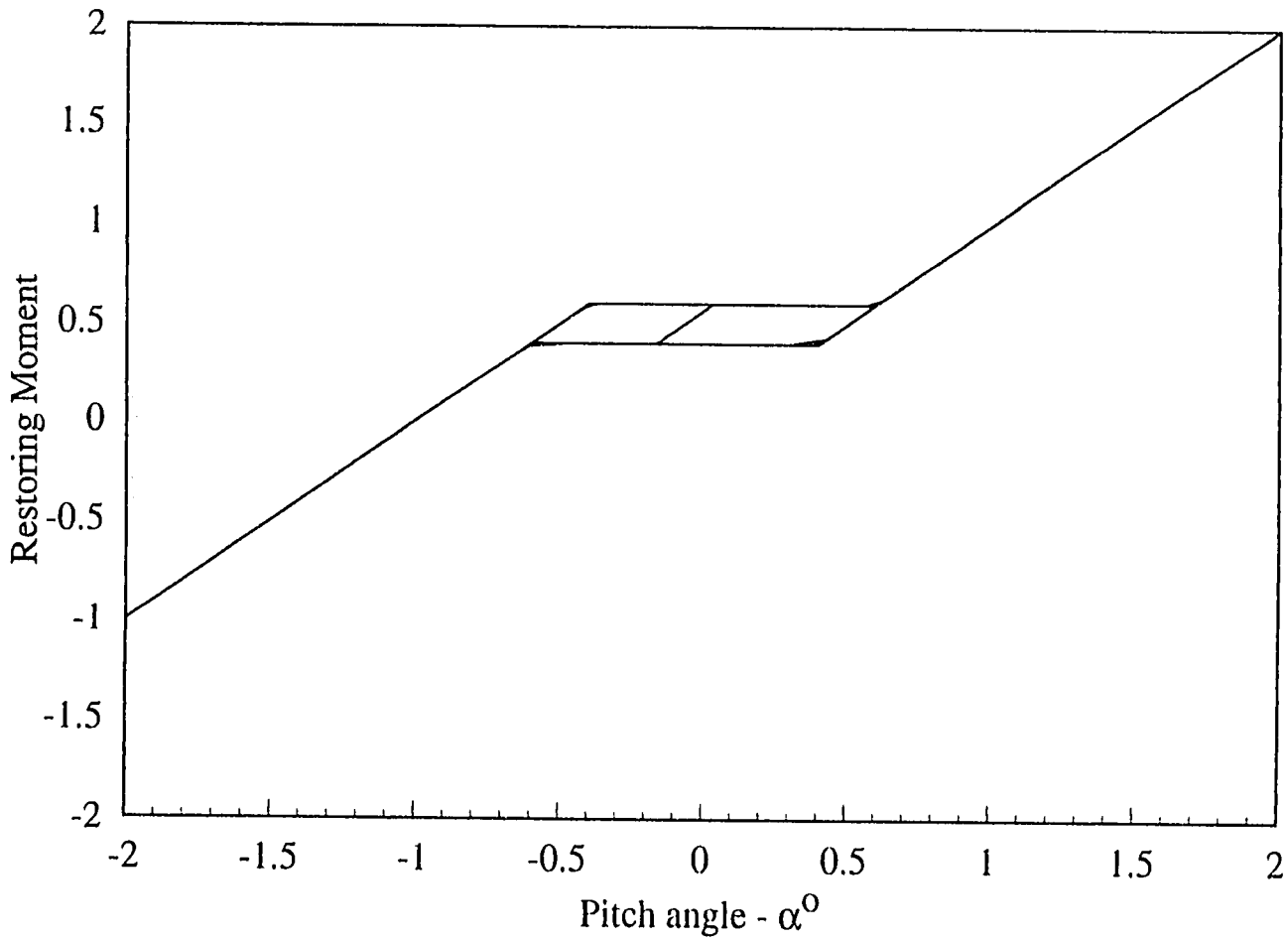

Figure 5.19b - Hysteretic Spring Response

α_o=5.0°, U*/U=0.845, ΔV=0.2°, ΔH=1.0°, $\overline{\omega}$=0.8, μ=100.0, V_{offset}=0.5, H_{offset}=0.0

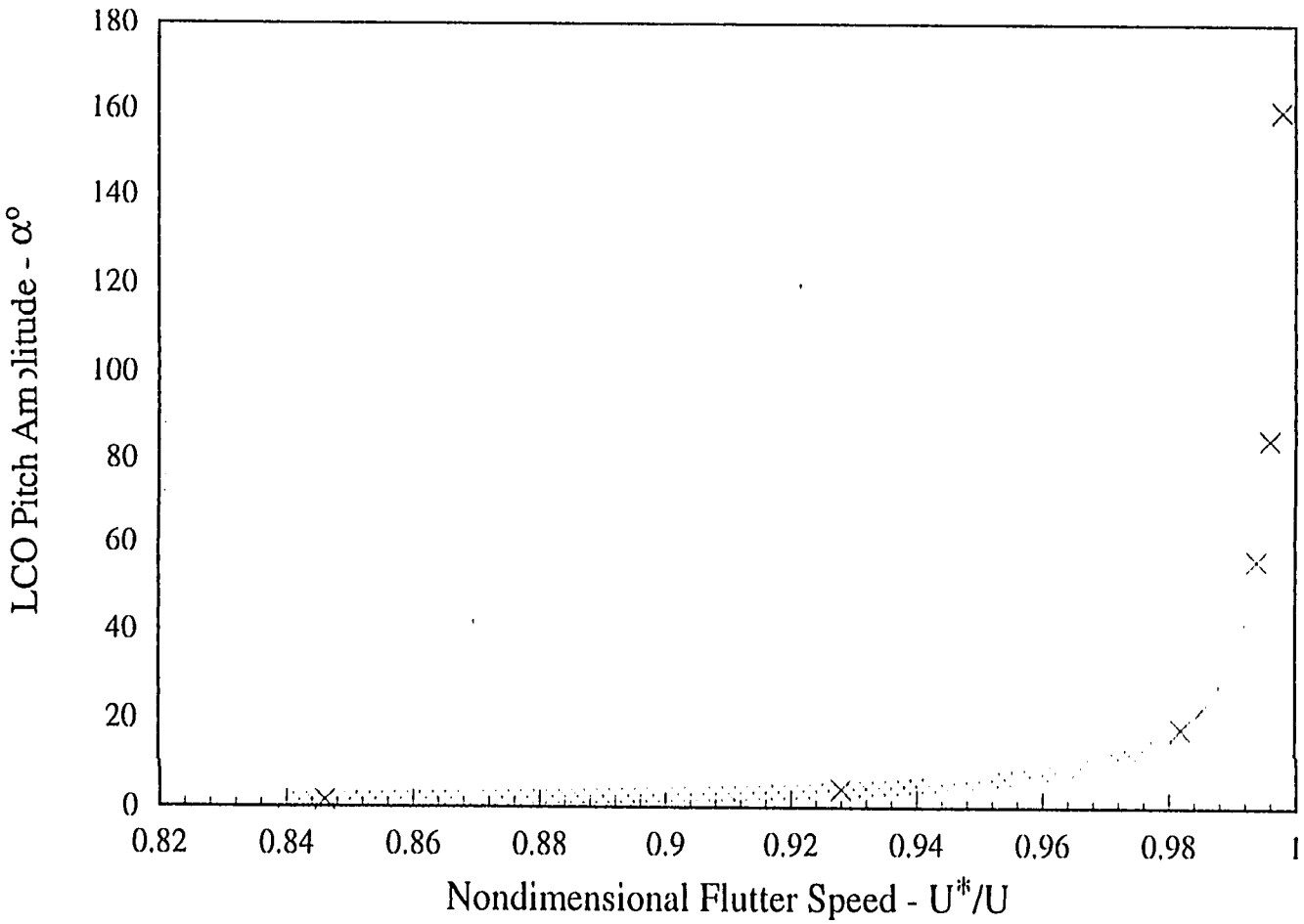

Figure 5.19c - Variation of LCO Amplitude with Speed:
μ=100, $\bar{\omega}$=0.8, ΔV=0.2°, ΔH=1.0°, V_{offset}=0.5, H_{offset}=0.0

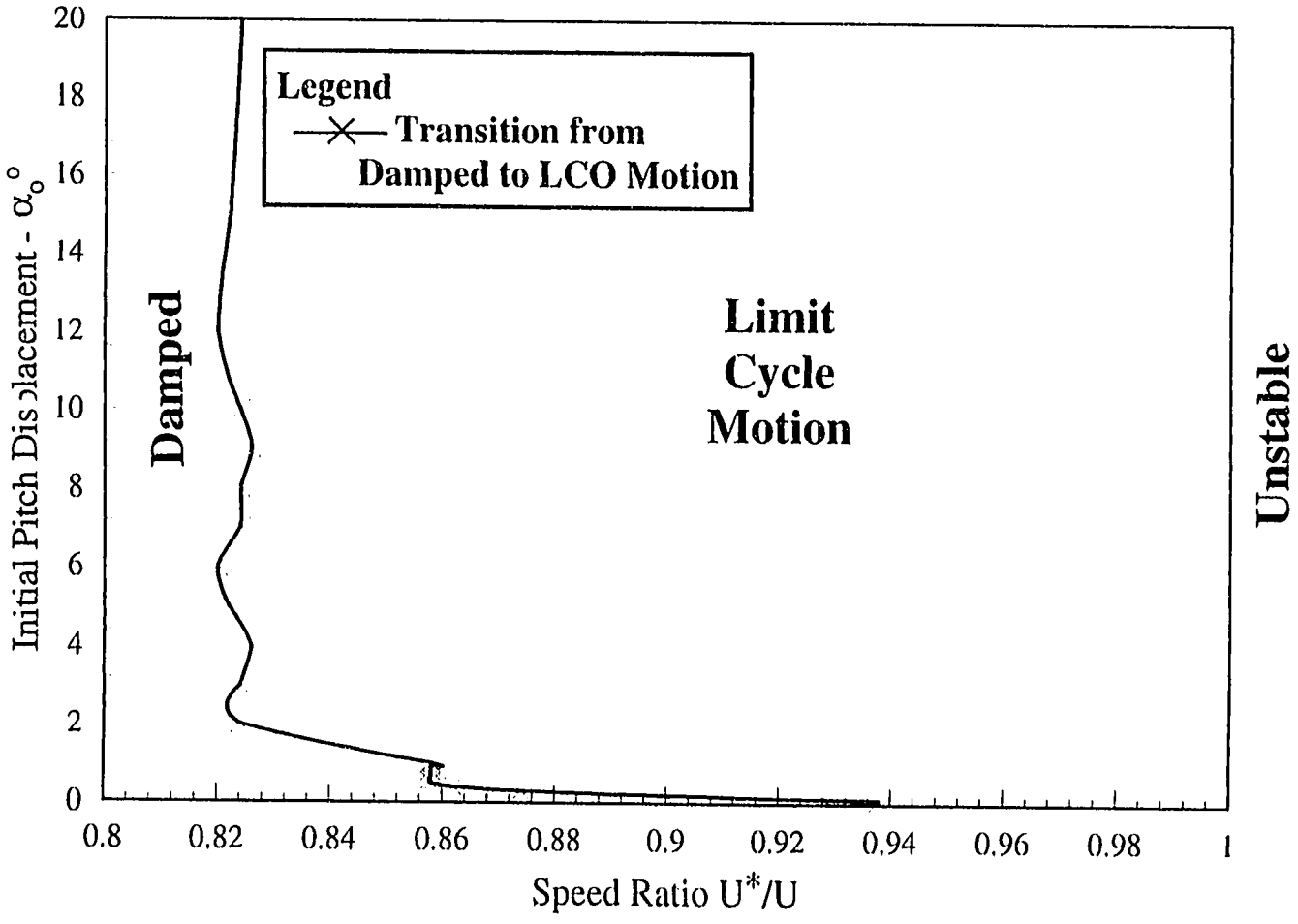

Figure 5.20a - Flutter Boundary for Hysteresis Nonlinearity:
μ=100, $\bar{\omega}$=0.8, ΔV=0.2°, ΔH=1.0°, V_{offset}=0.0, H_{offset}=0.5

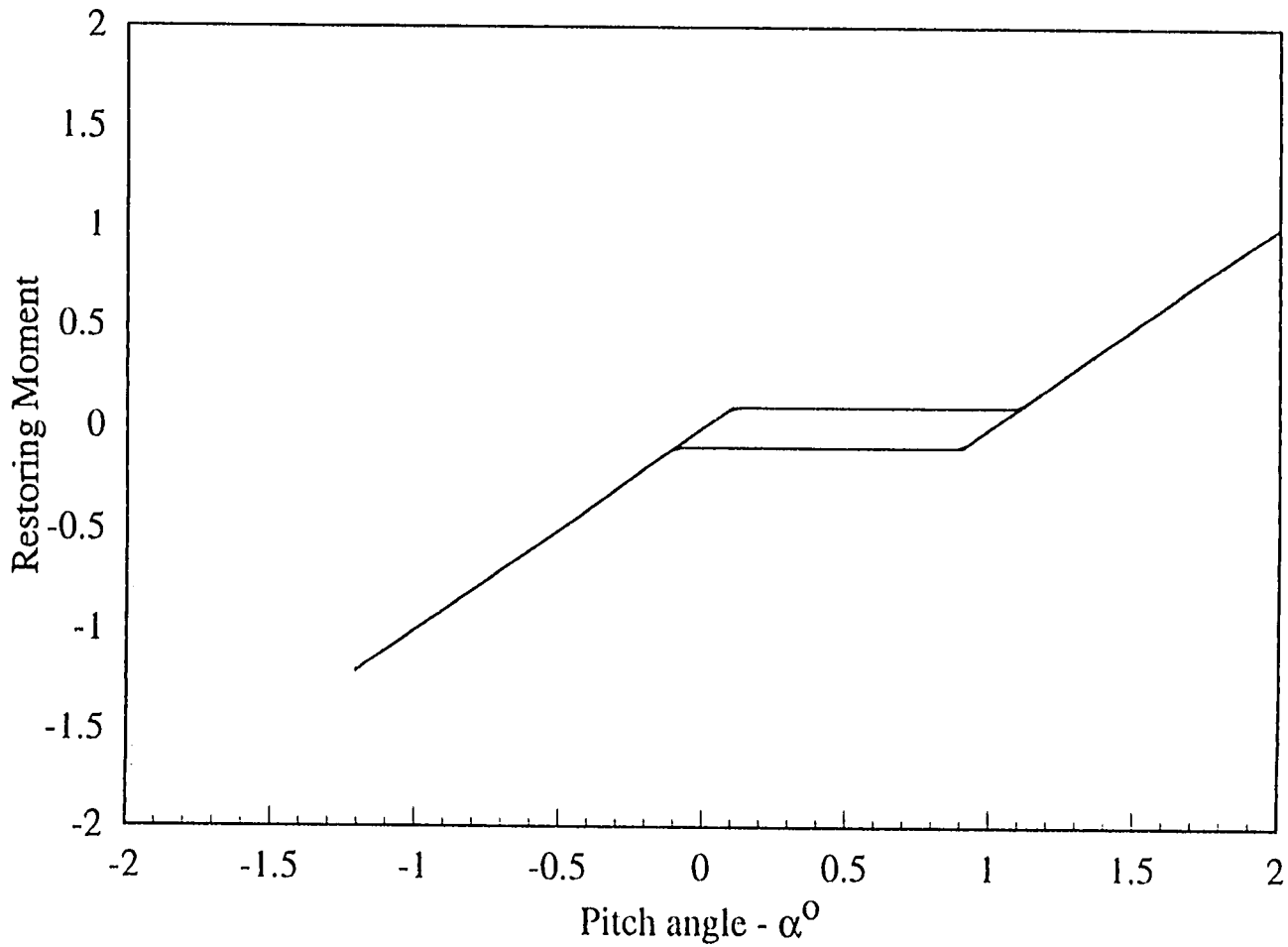

Figure 5.20b - Hysteretic Spring Response

α_o=2.0°, U*/U=0.824, ΔV=0.2°, ΔH=1.0°, $\overline{\omega}$=0.8, μ=100.0, V_{offset}=0.0, H_{offset}=0.5

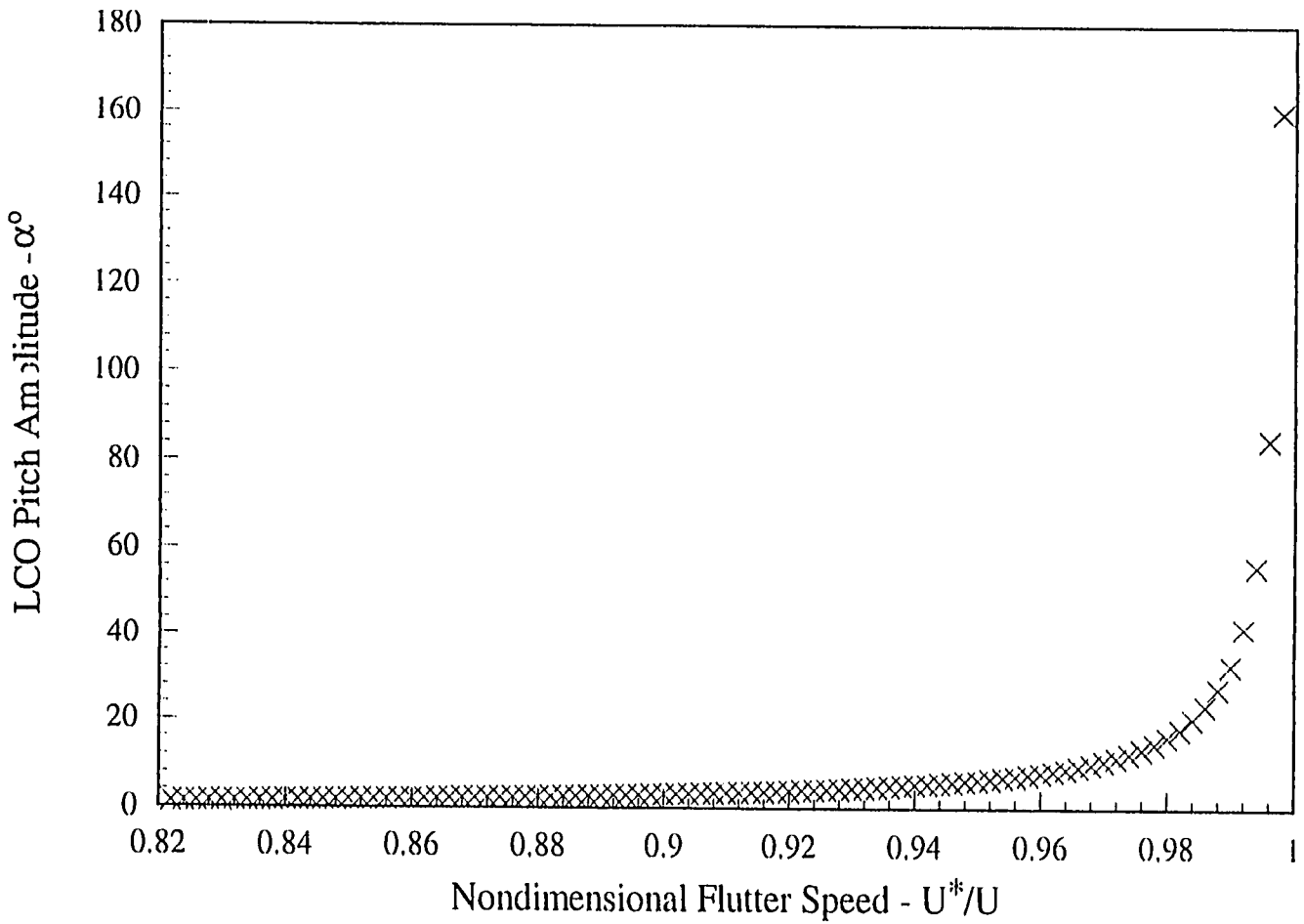

Figure 5.20c - Variation of LCO Amplitude with Speed:
μ=100, $\overline{\omega}$=0.8, ΔV=0.2°, ΔH=1.0°, V_{offset}=0.0, H_{offset}=0.5

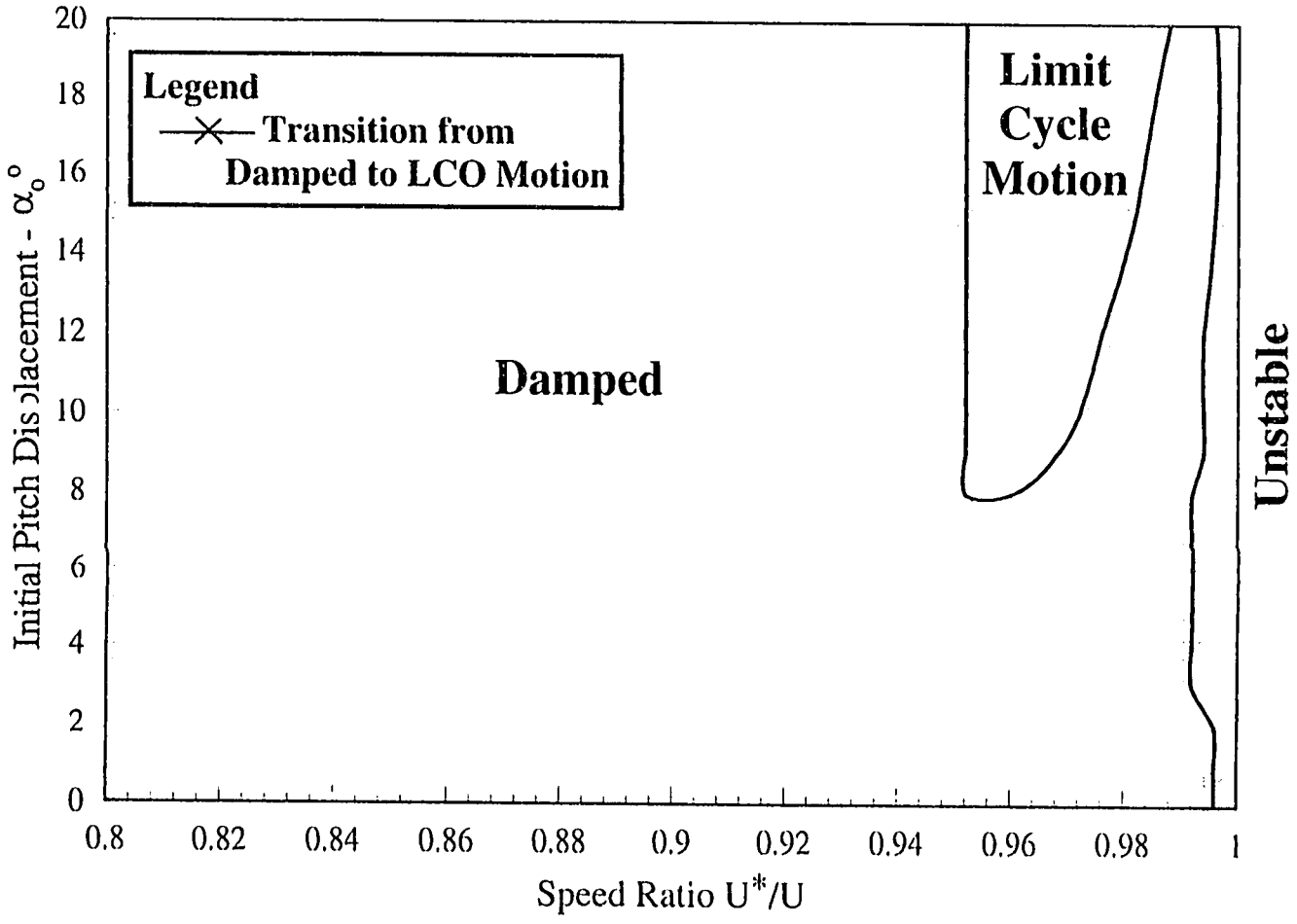

Figure 5.21a - Flutter Boundary for Hysteresis Nonlinearity:
μ=100, $\bar{\omega}$=0.8, ΔV=1.0^o, ΔH=0.2^o, V_{offset}=0.5, H_{offset}=0.0

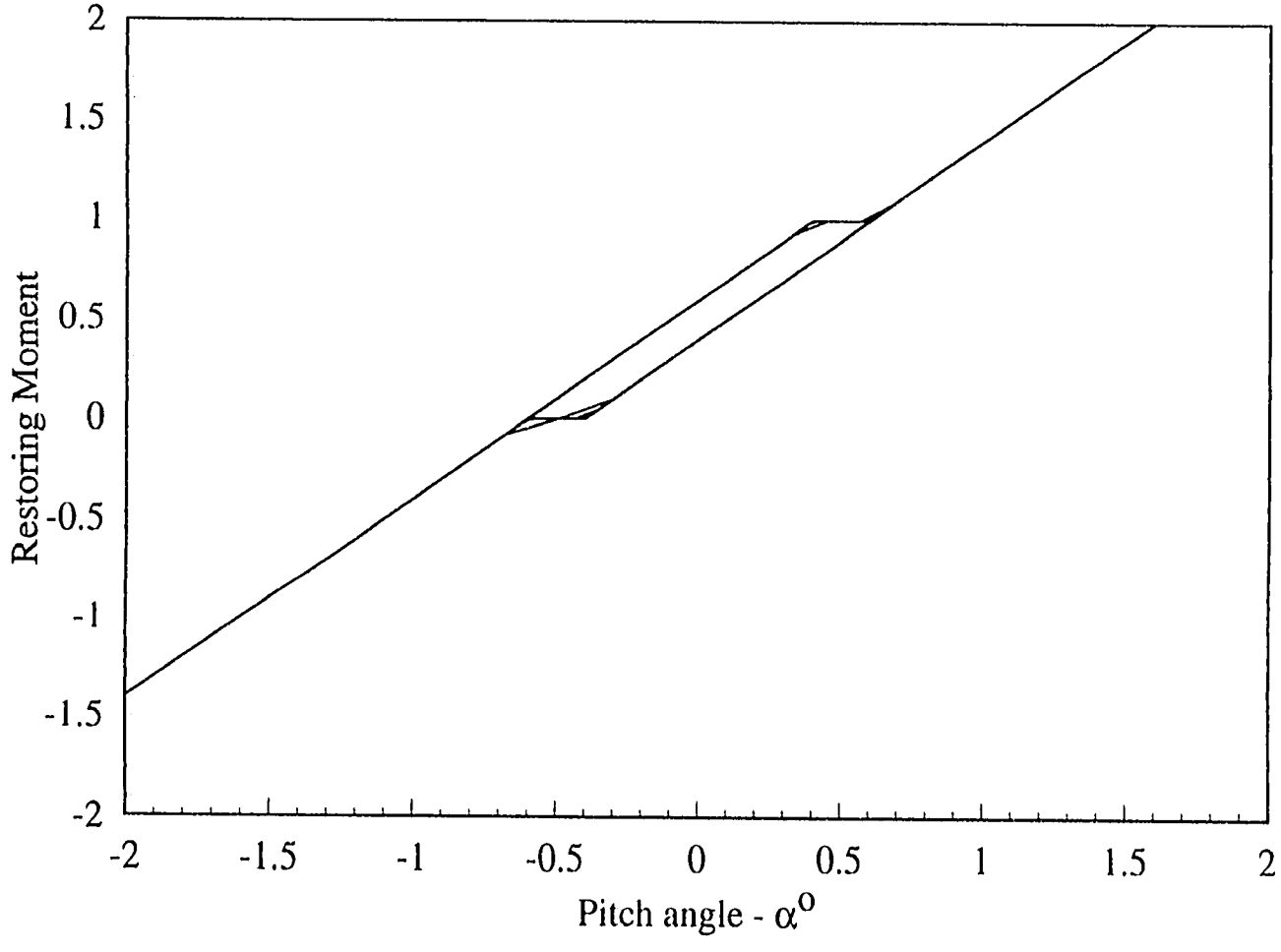

Figure 5.21b - Hysteretic Spring Response

α_o=8.0°, U*/U=0.952, ΔV=1.0°, ΔH=0.2°, $\overline{\omega}$=0.8, μ=100.0, V_{offset}=0.5, H_{offset}=0.0

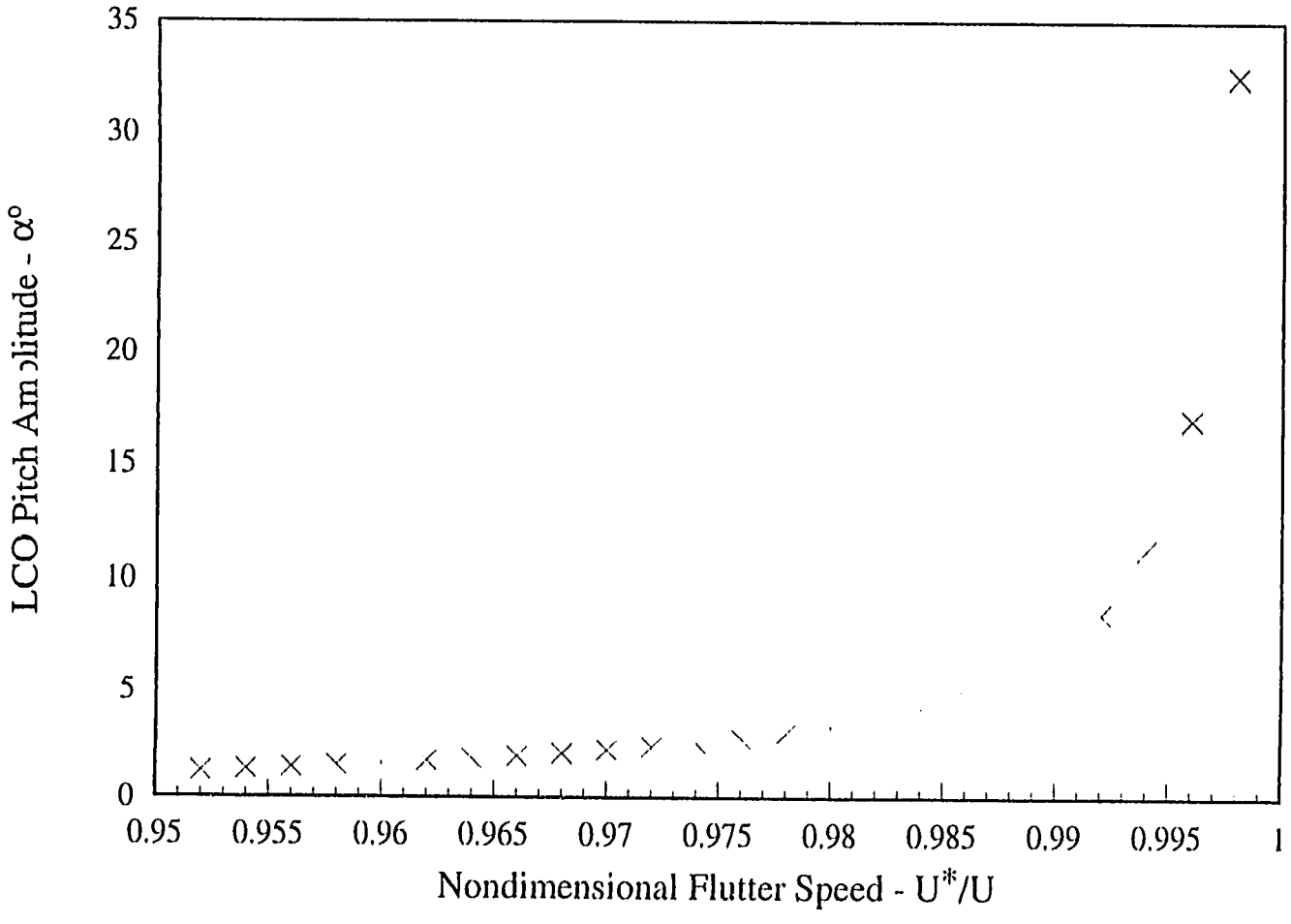

Figure 5.21c - Variation of LCO Amplitude with Speed:
μ=100, $\overline{\omega}$=0.8, ΔV=1.0°, ΔH=0.2°, V_{offset}=0.5, H_{offset}=0.0

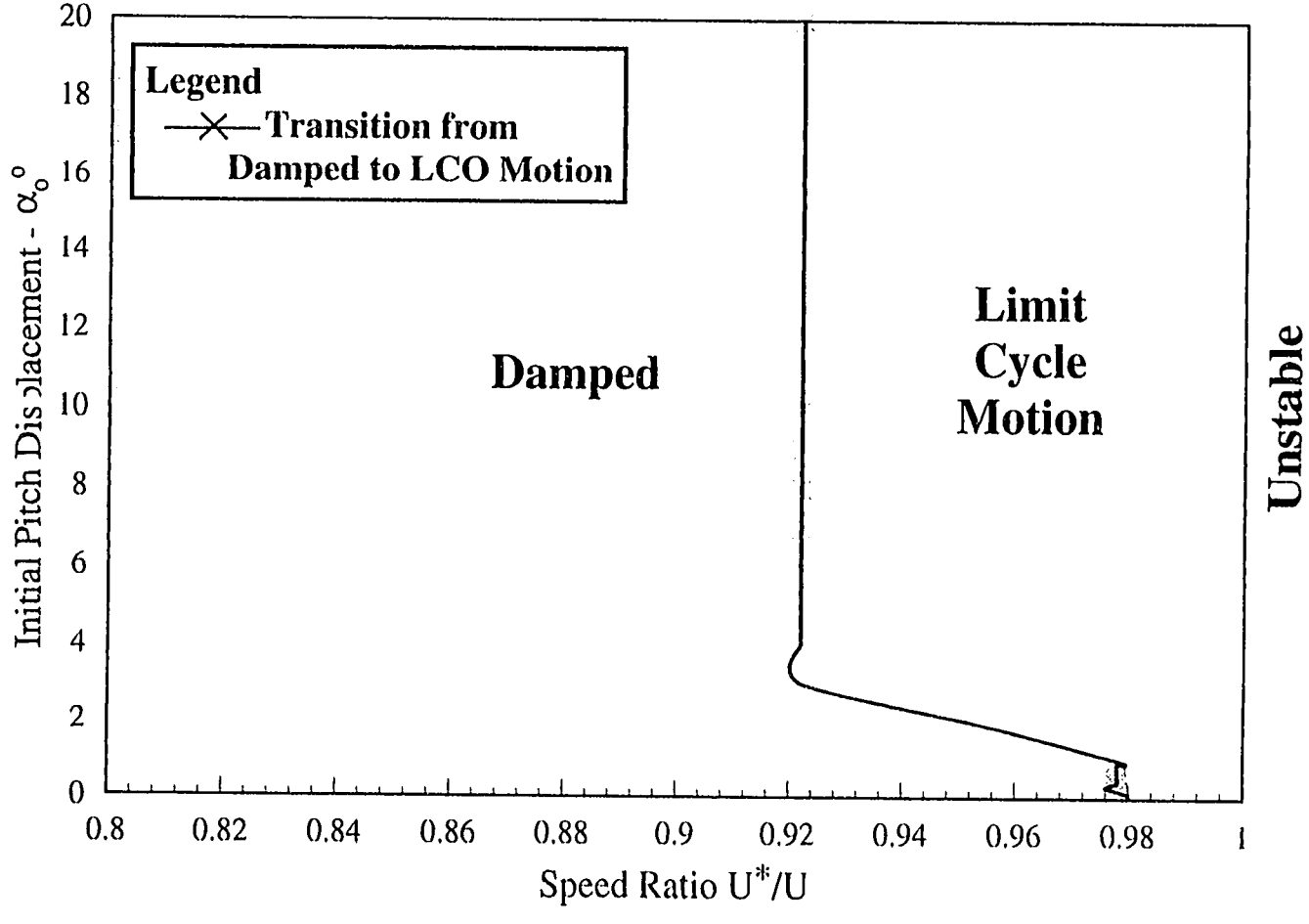

Figure 5.22a - Flutter Boundary for Hysteresis Nonlinearity:
μ=100, $\overline{\omega}$=0.8, ΔV=1.0^o, ΔH=0.2^o, V_{offset}=0.0, H_{offset}=0.5

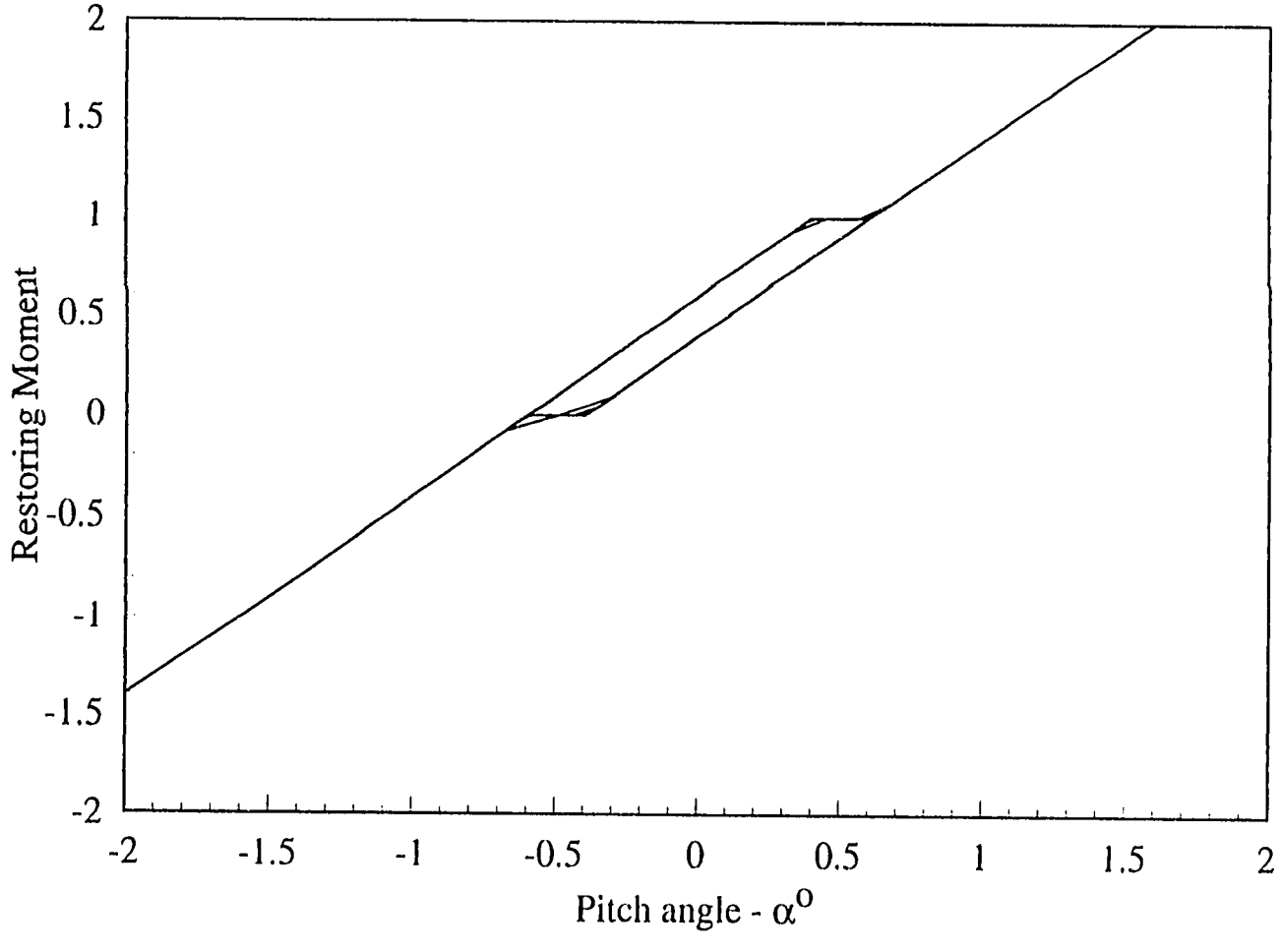

Figure 5.22b - Hysteretic Spring Response

α_o=4.0°, U*/U=0.922, ΔV=1.0°, ΔH=0.2°, $\overline{\omega}$=0.8, μ=100.0, V_{offset}=0.0, H_{offset}=0.5

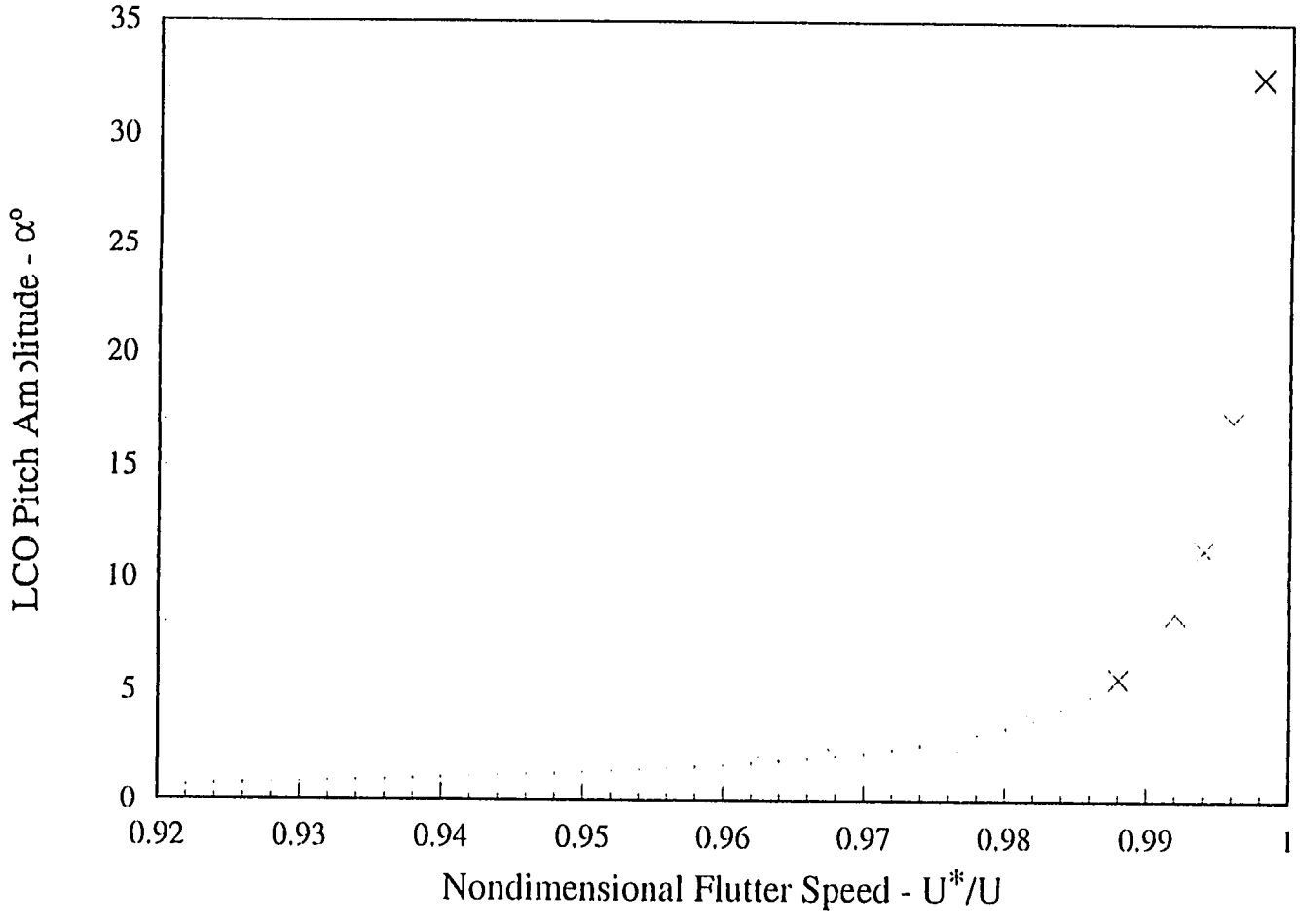

Figure 5.22c - Variation of LCO Amplitude with Speed:
μ=100, $\overline{\omega}$=0.8, ΔV=1.0°, ΔH=0.2°, V_{offset}=0.0, H_{offset}=0.5

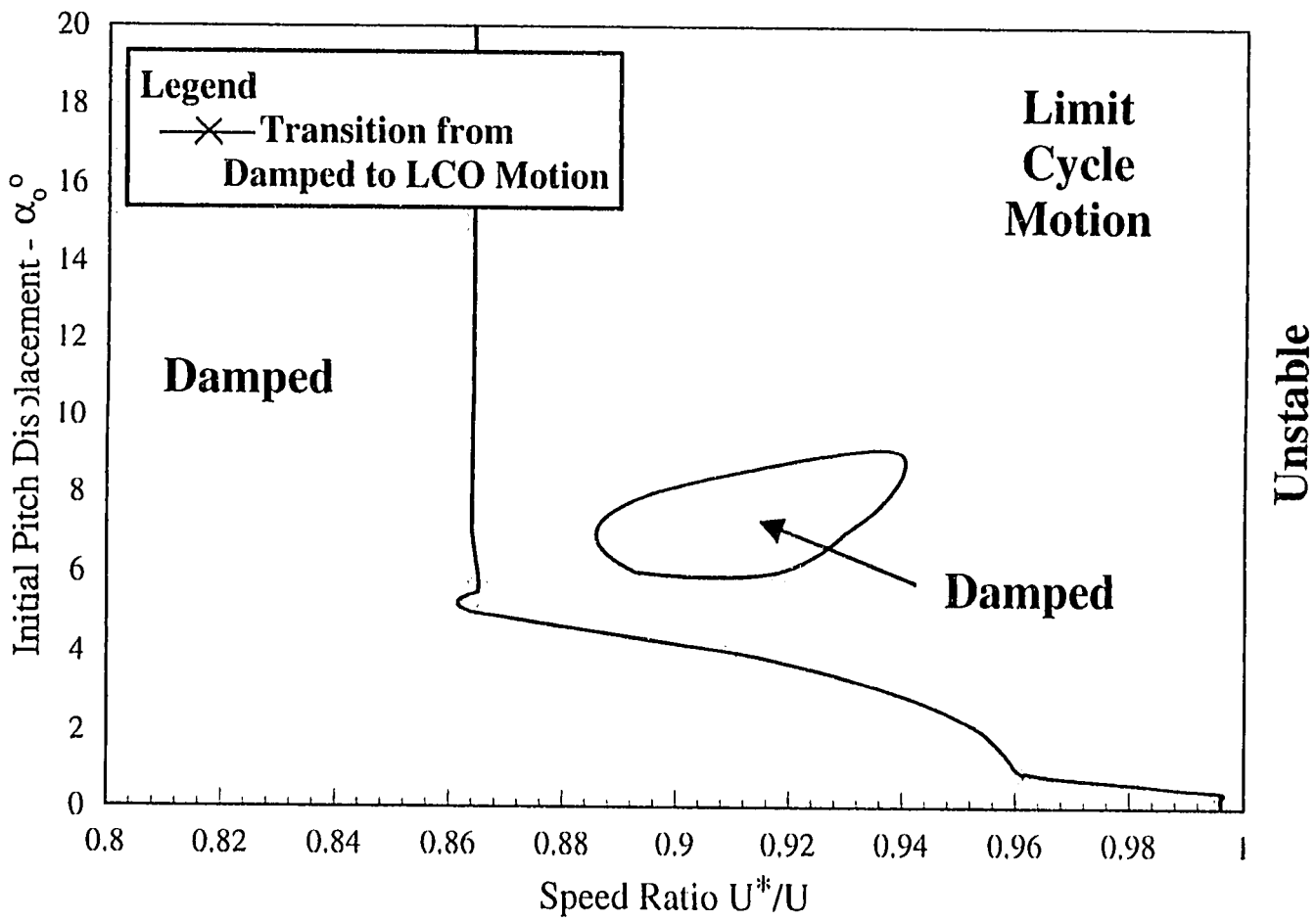

Figure 5.23a - Flutter Boundary for Hysteresis Nonlinearity:
μ=100, $\overline{\omega}$=0.8, $\Delta V=1.0^o$, $\Delta H=1.0^o$, V_{offset}=0.5, H_{offset}=0.5

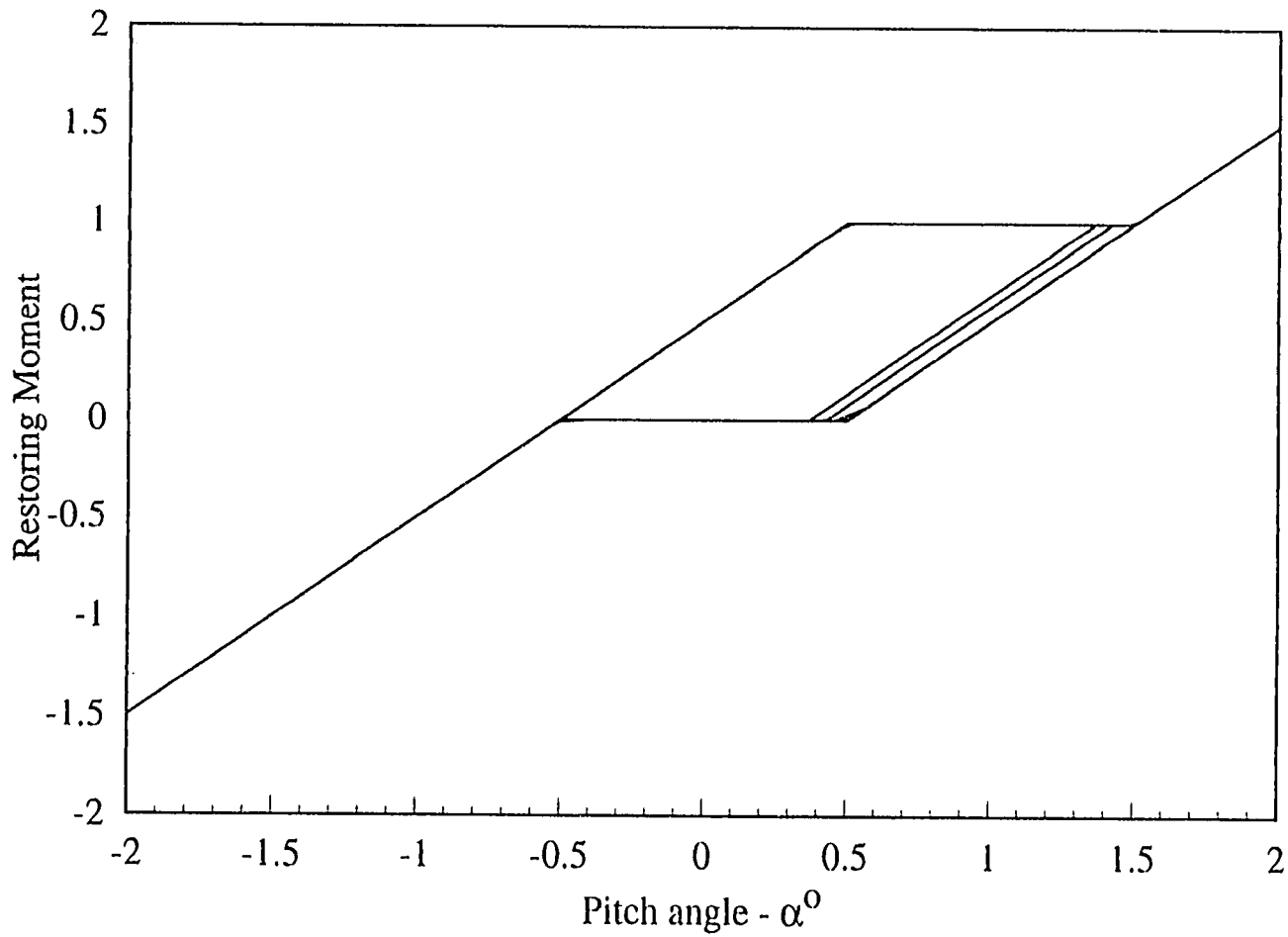

Figure 5.23b - Hysteretic Spring Response

α_o=5.0°, U*/U=0.864, ΔV=1.0°, ΔH=1.0°, $\overline{\omega}$=0.8, μ=100.0, V_{offset}=0.5, H_{offset}=0.5

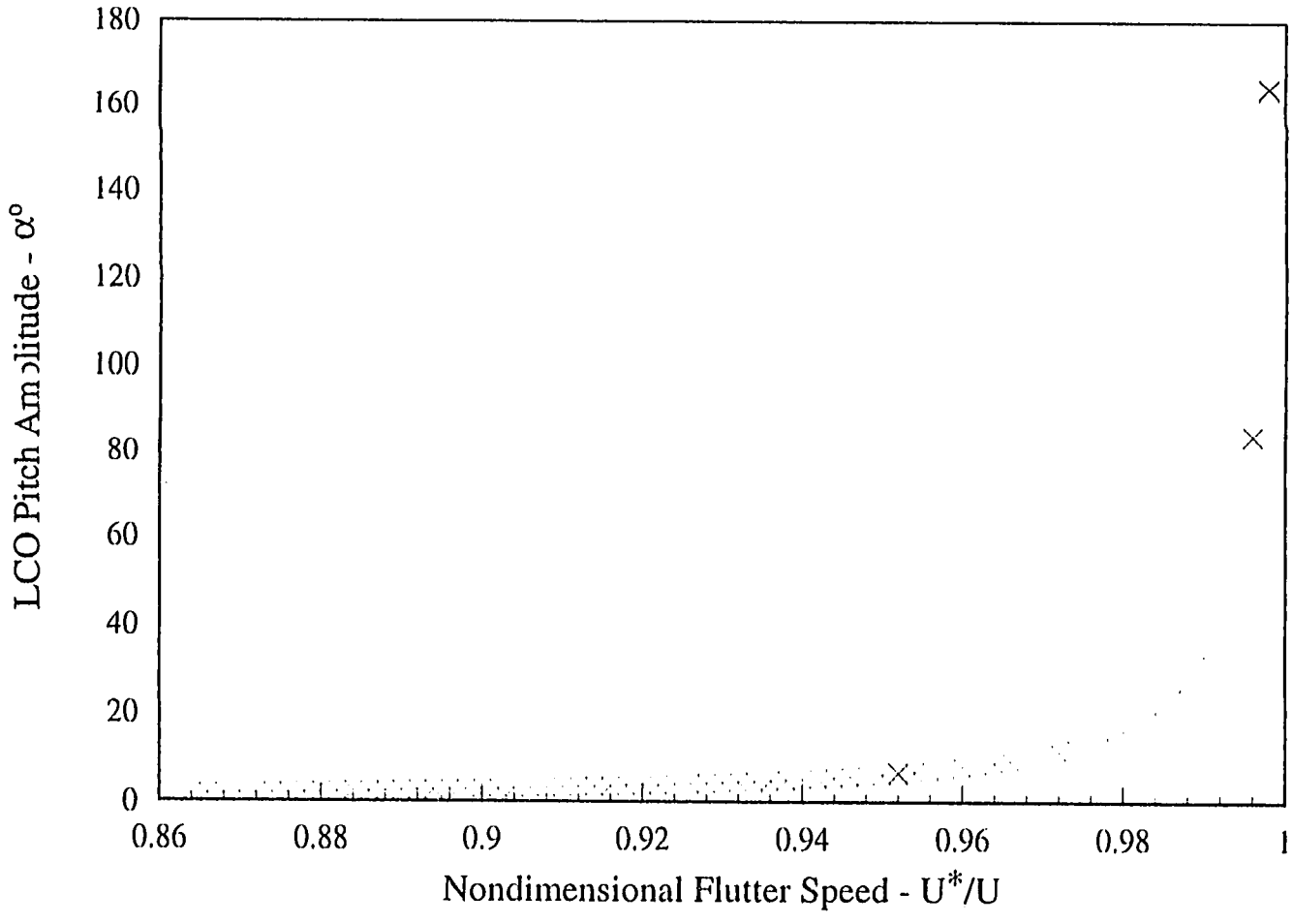

Figure 5.23c - Variation of LCO Amplitude with Speed:
μ=100, $\overline{\omega}$=0.8, ΔV=1.0°, ΔH=1.0°, V_{offset}=0.5, H_{offset}=0.5

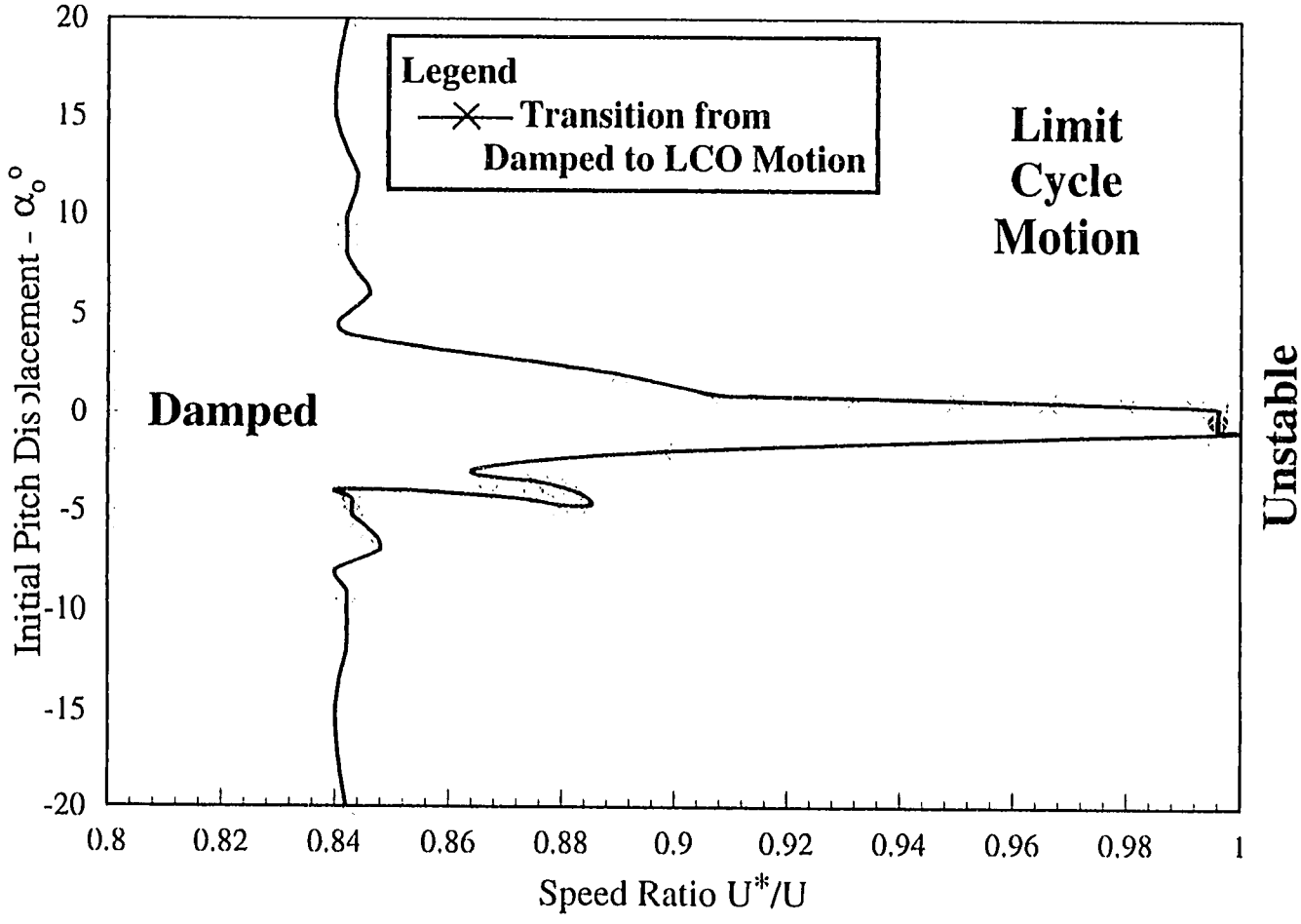

Figure 5.24a - Flutter Boundary for Hysteresis Nonlinearity:
μ=100, $\overline{\omega}$=0.8, ΔV=0.2^o, ΔH=1.0^o, V_{offset}=0.5, H_{offset}=0.5

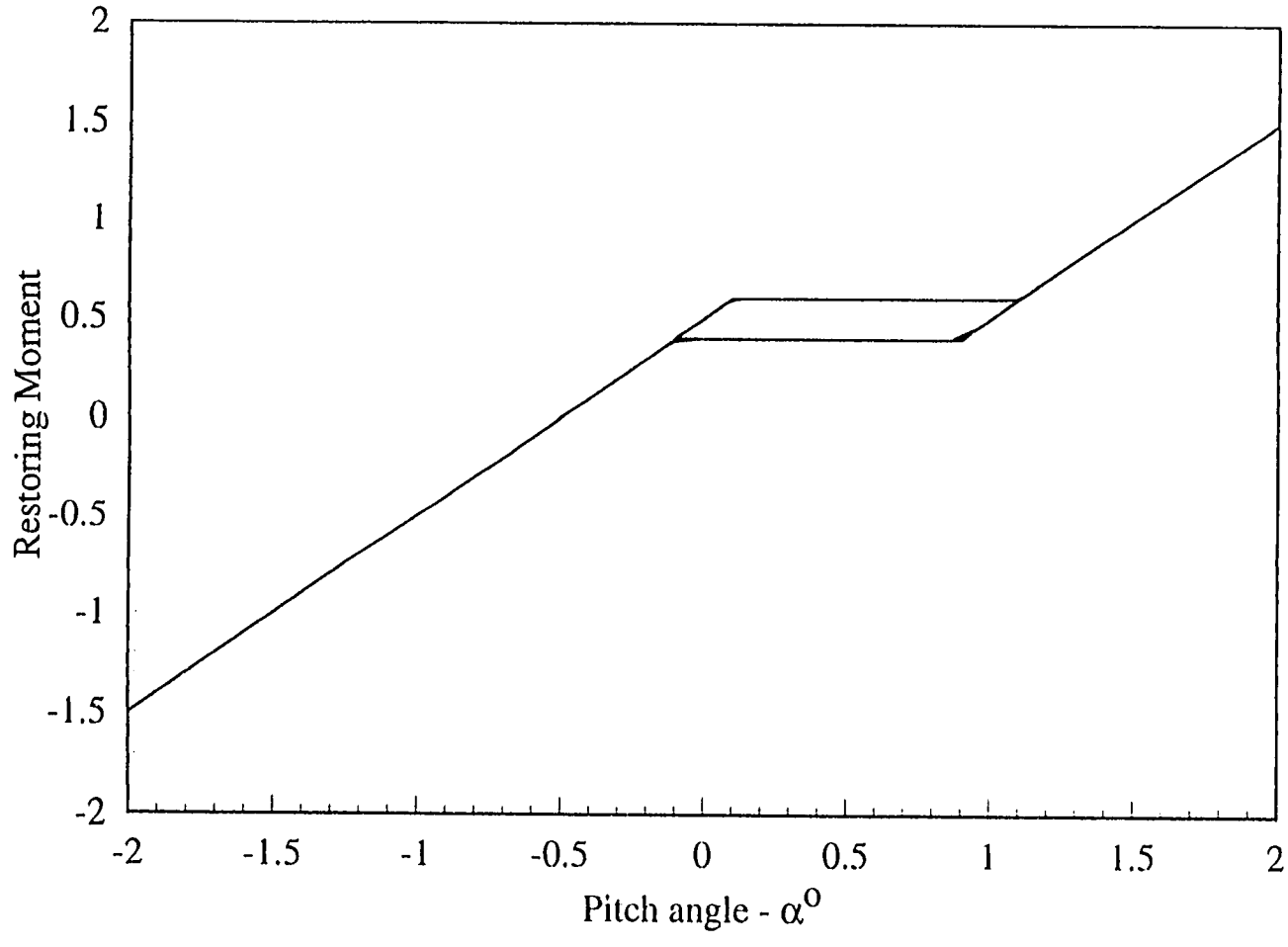

Figure 5.24a - Hysteretic Spring Response

α_o=4.0°, U*/U=0.844, ΔV=0.2°, ΔH=1.0°, $\overline{\omega}$=0.8, μ=100.0, V_{offset}=0.5, H_{offset}=0.5

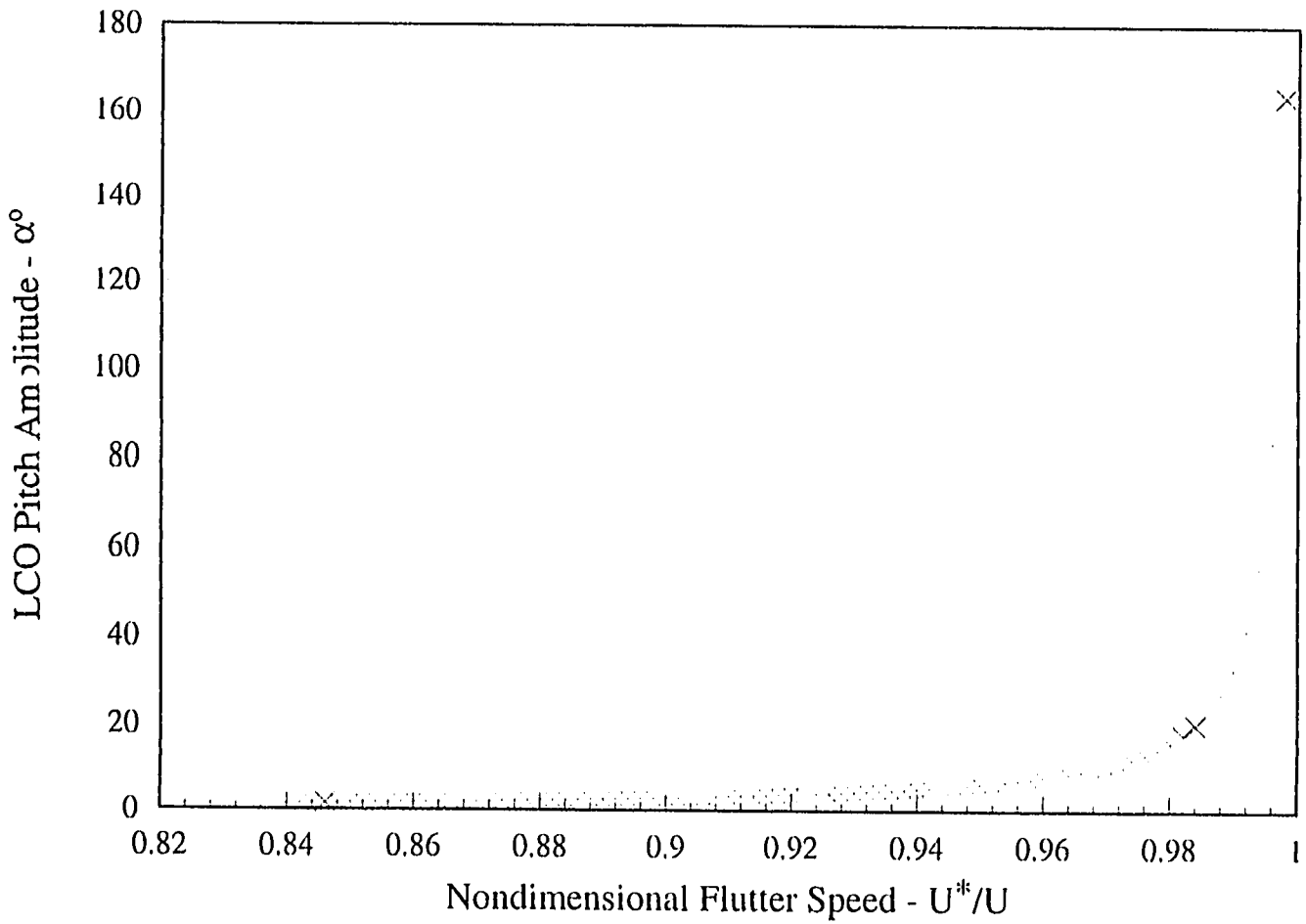

Figure 5.24c - Variation of LCO Amplitude with Speed:
μ=100, $\bar{\omega}$=0.8, ΔV=0.2°, ΔH=1.0°, V_{offset}=0.5, H_{offset}=0.5

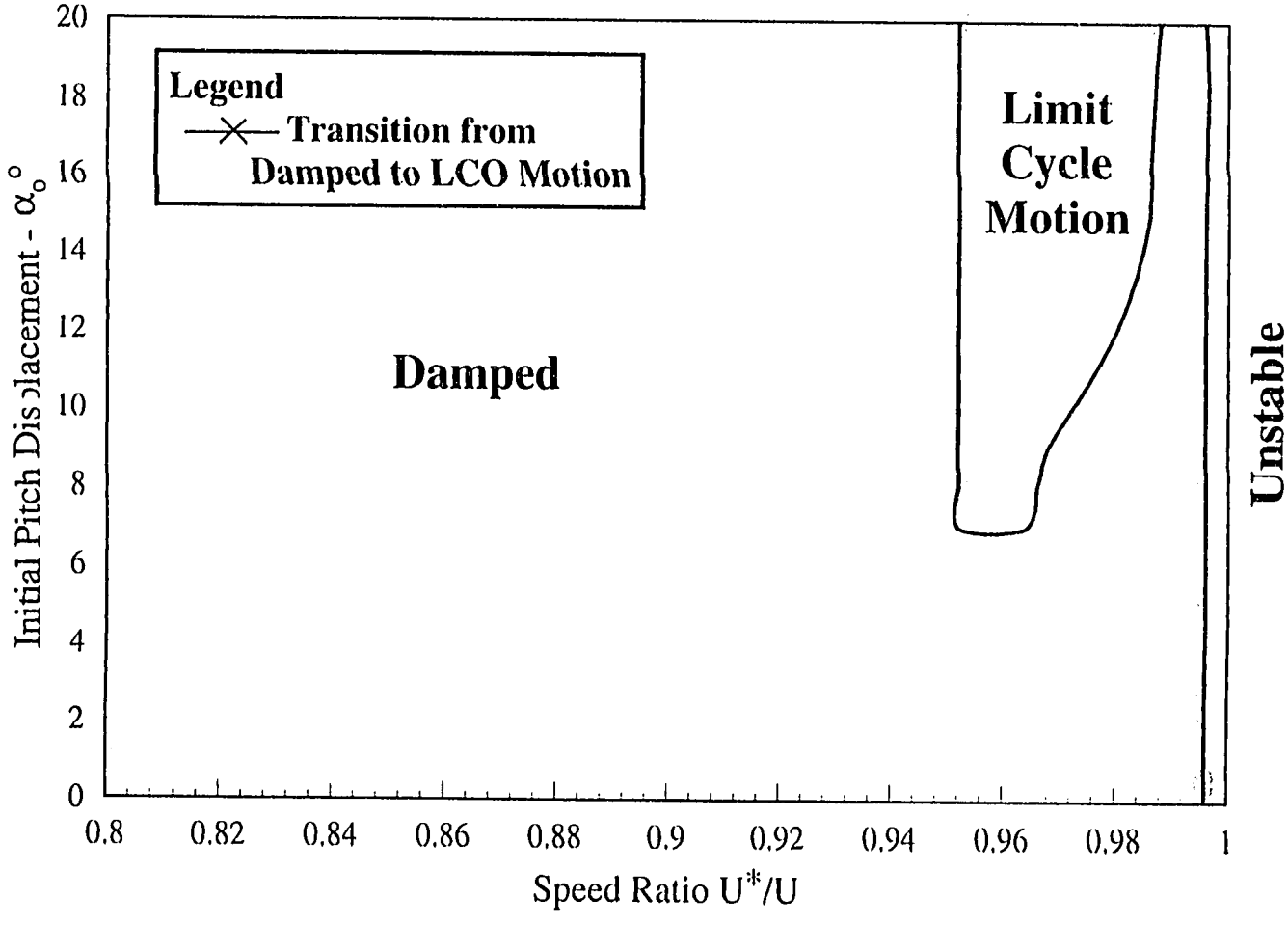

Figure 5.25a - Flutter Boundary for Hysteresis Nonlinearity:
μ=100, $\bar{\omega}$=0.8, ΔV=1.0^o, ΔH=0.2^o, V_{offset}=0.5, H_{offset}=0.5

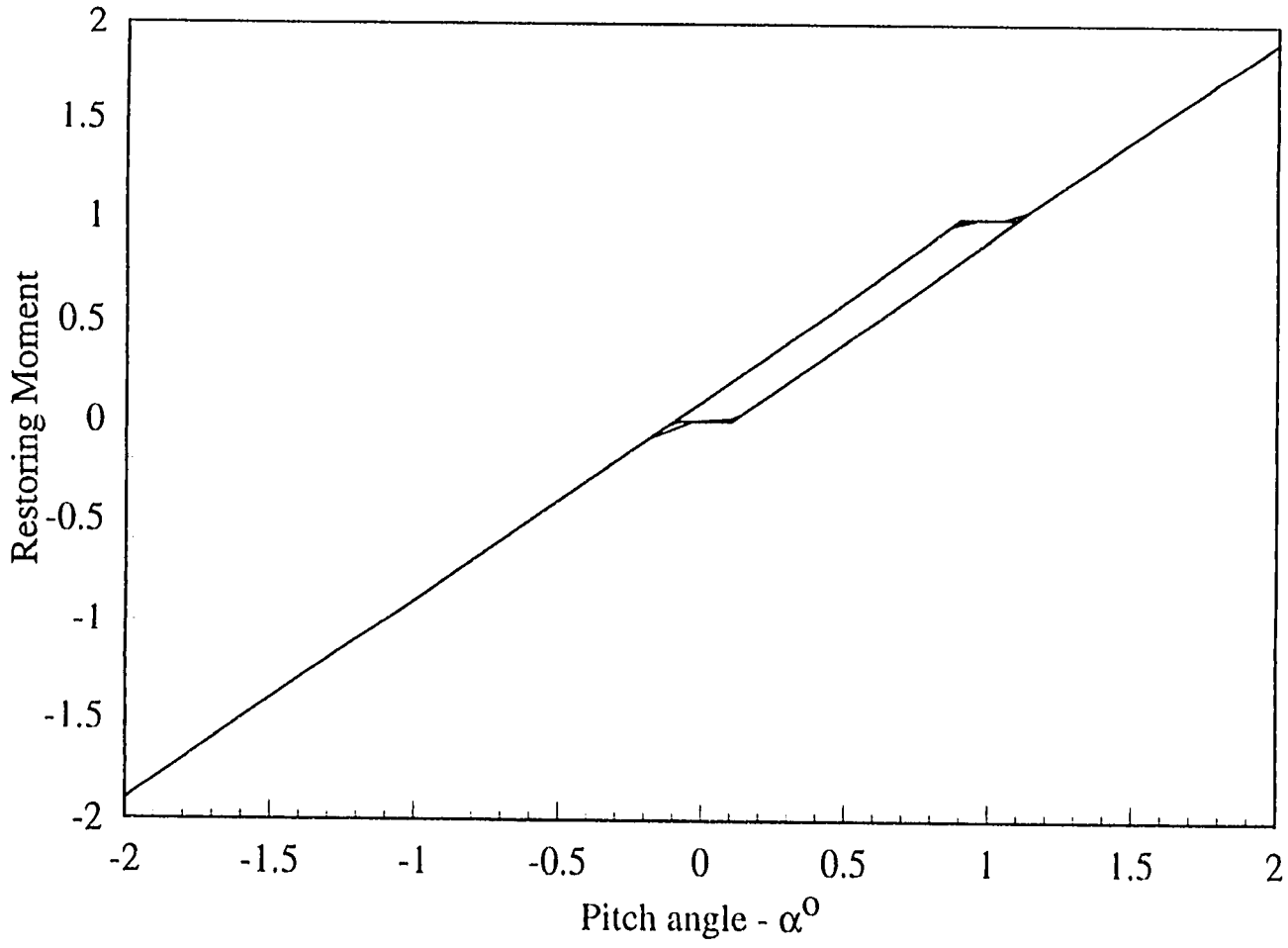

Figure 5.25a - Hysteretic Spring Response

α_o=7.0°, U*/U=0.952, ΔV=1.0°, ΔH=0.2°, $\overline{\omega}$=0.8, μ=100.0, V_{offset}=0.5, H_{offset}=0.5

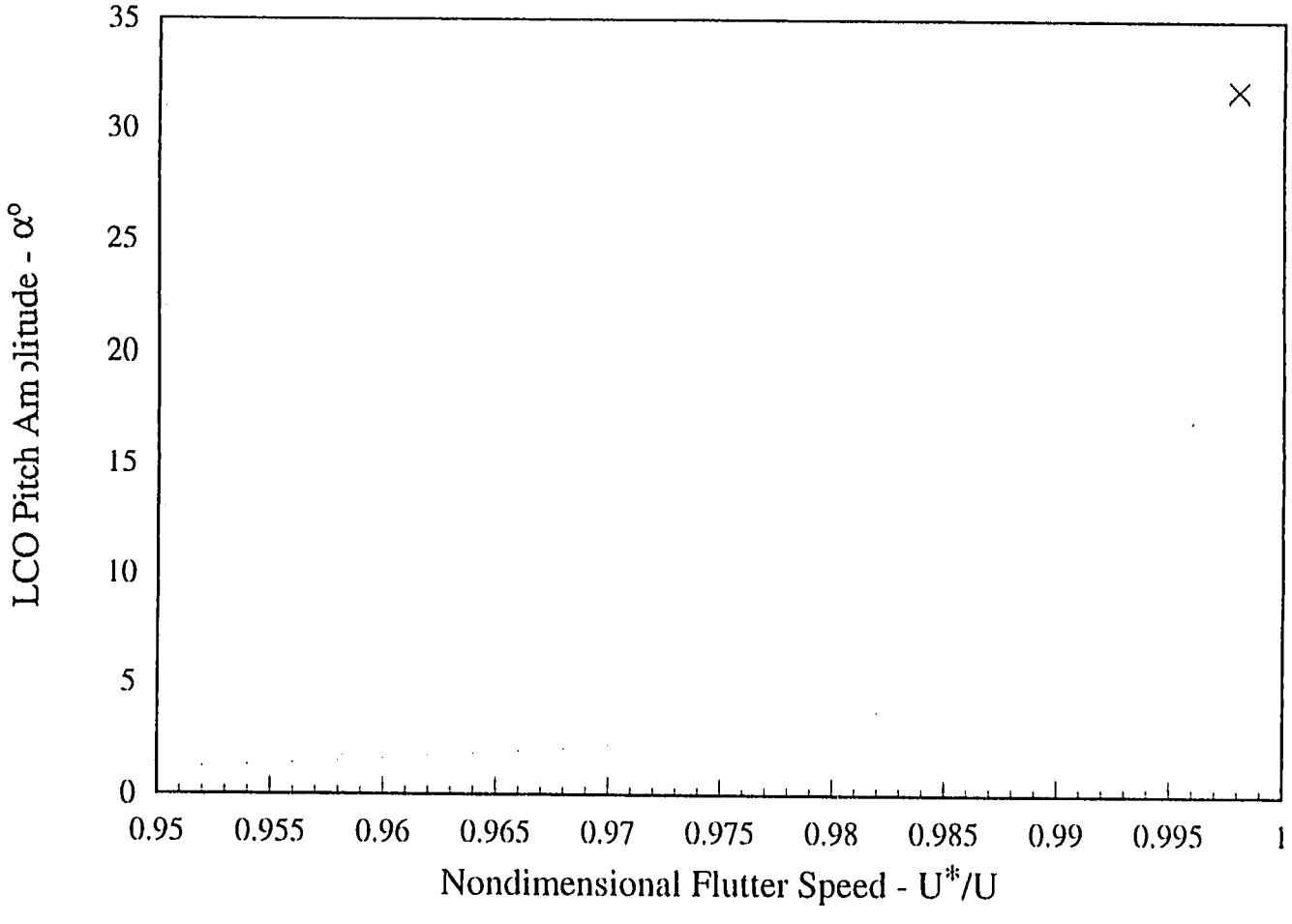

Figure 5.25c - Variation of LCO Amplitude with Speed:
μ=100, $\bar{\omega}$=0.8, ΔV=1.0°, ΔH=0.2°, V_{offset}=0.5, H_{offset}=0.5

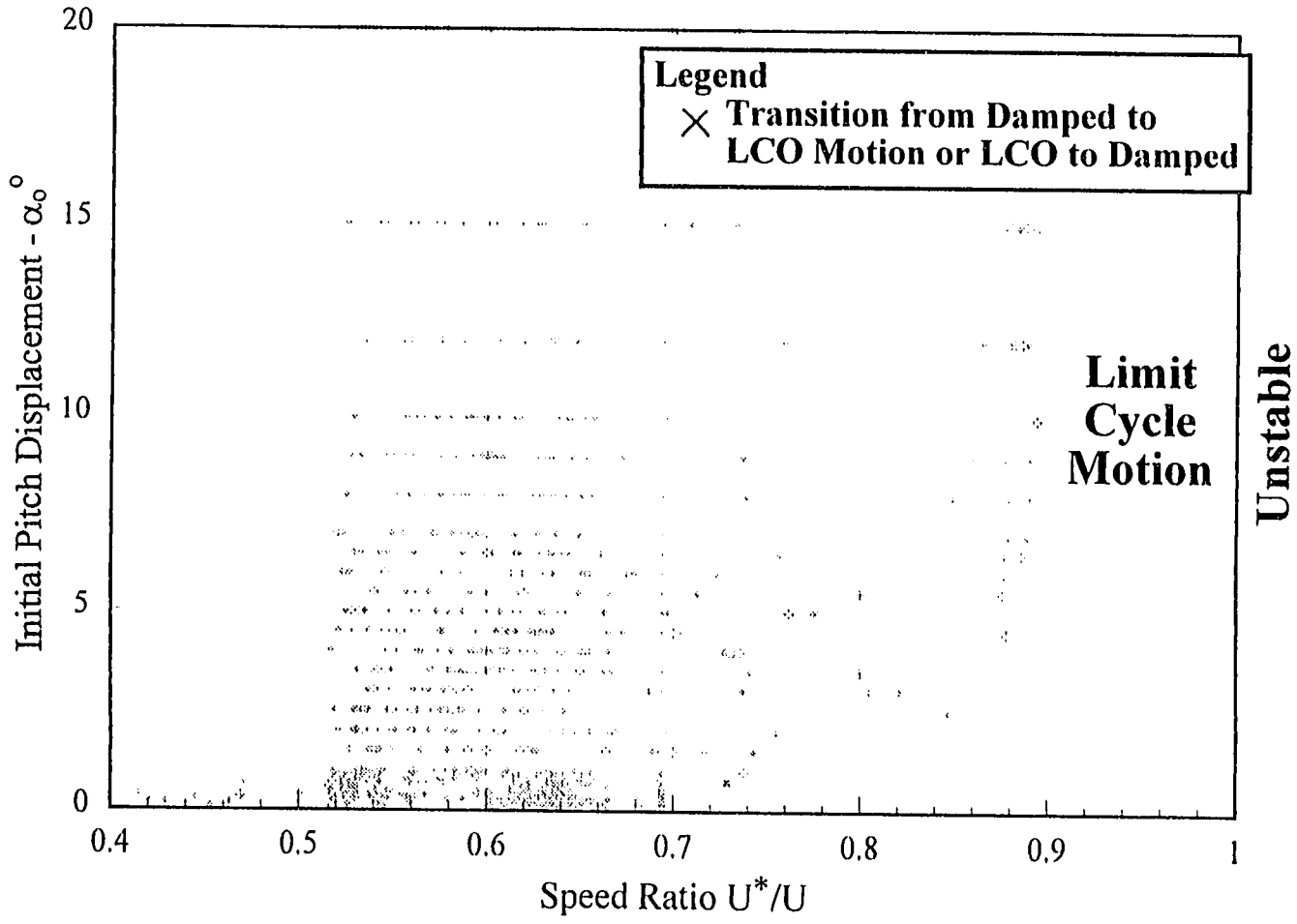

Figure 5.26a - Flutter Boundary for Hysteresis Nonlinearity:
μ=100, ω=0.2, ΔV=1.0°, ΔH=1.0°, V_{offset}=0.5, H_{offset}=0.0

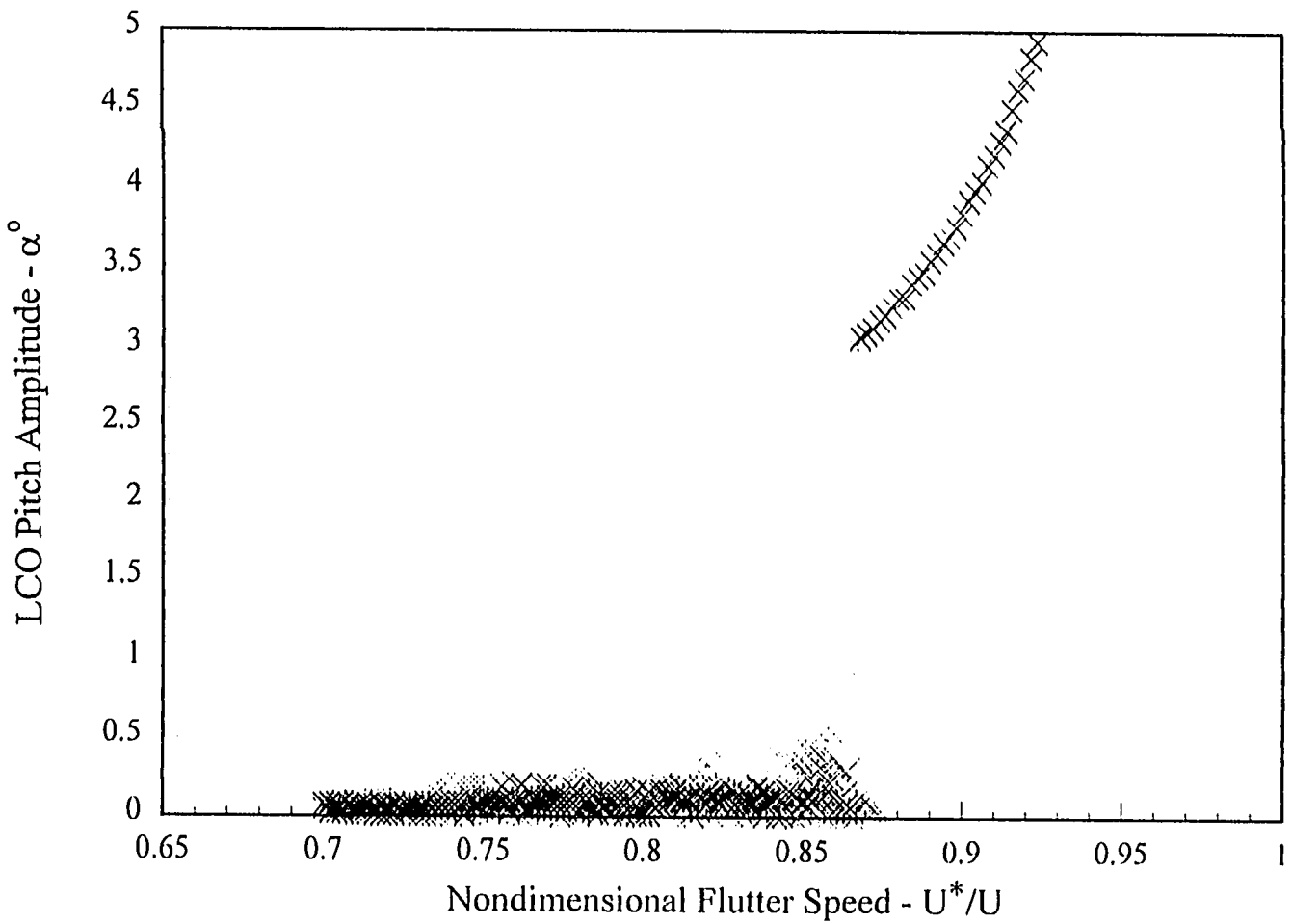

Figure 5.26c - Variation of LCO Amplitude with Speed:
μ=100, ω=0.2, ΔV=1.0°, ΔH=1.0°, V_{offset}=0.5, H_{offset}=0.0

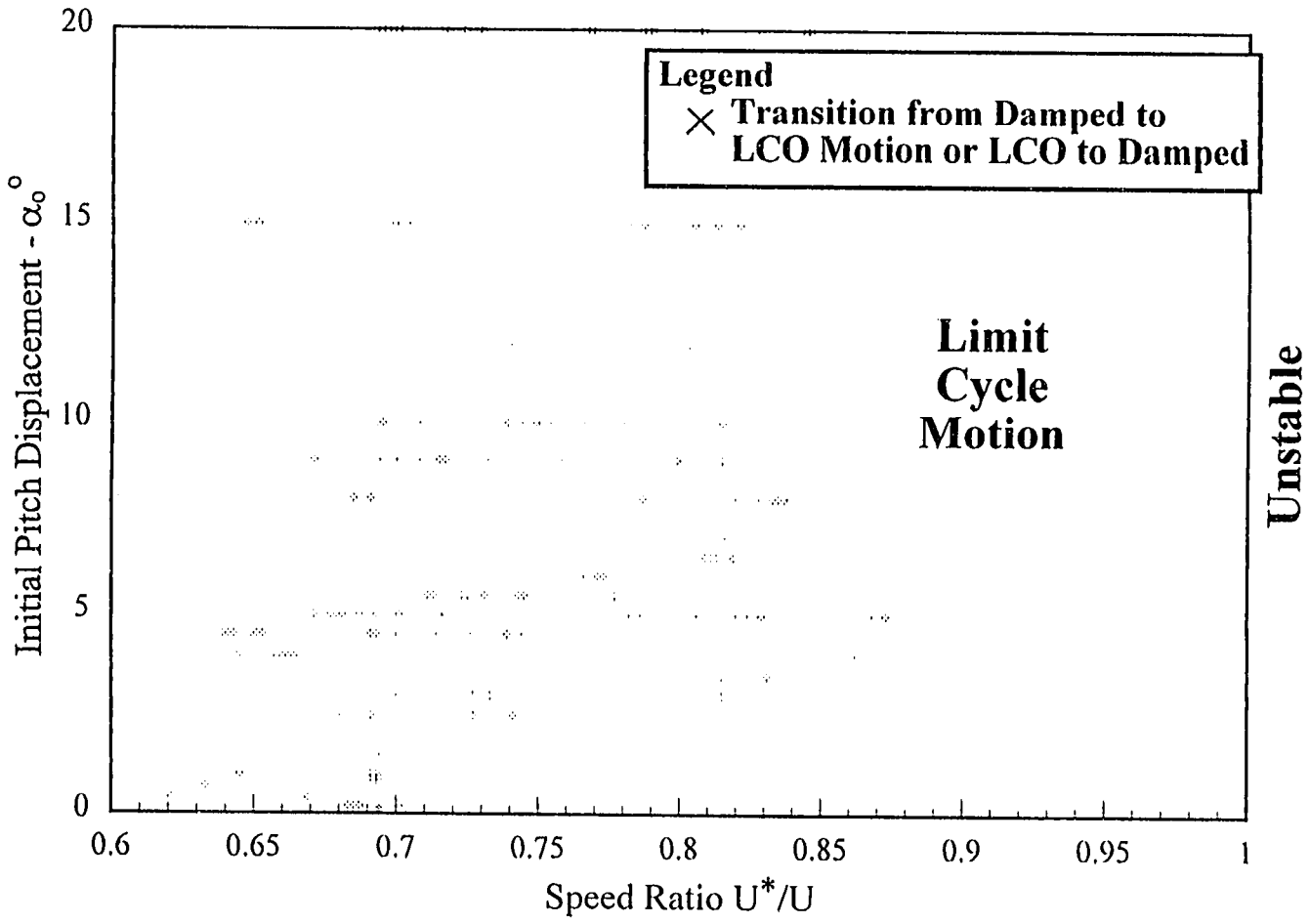

Figure 5.27a - Flutter Boundary for Hysteresis Nonlinearity:
μ=100, ω=0.2, ΔV=1.0°, ΔH=1.0°, V_{offset}=0.0, H_{offset}=0.5

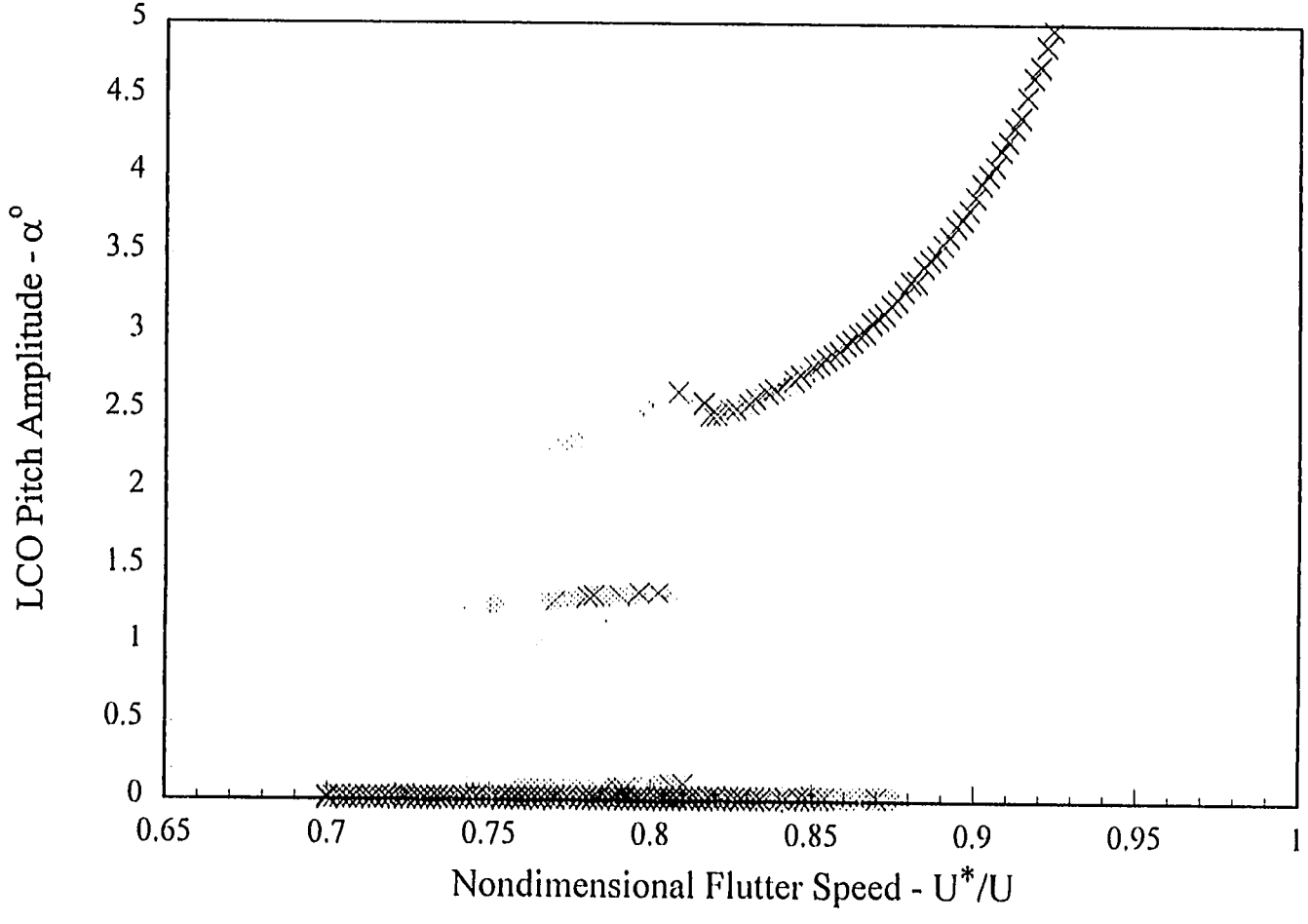

Figure 5.27c - Variation of LCO Amplitude with Speed:
μ=100, ω=0.2, ΔV=1.0°, ΔH=1.0°, V_{offset}=0.0, H_{offset}=0.5

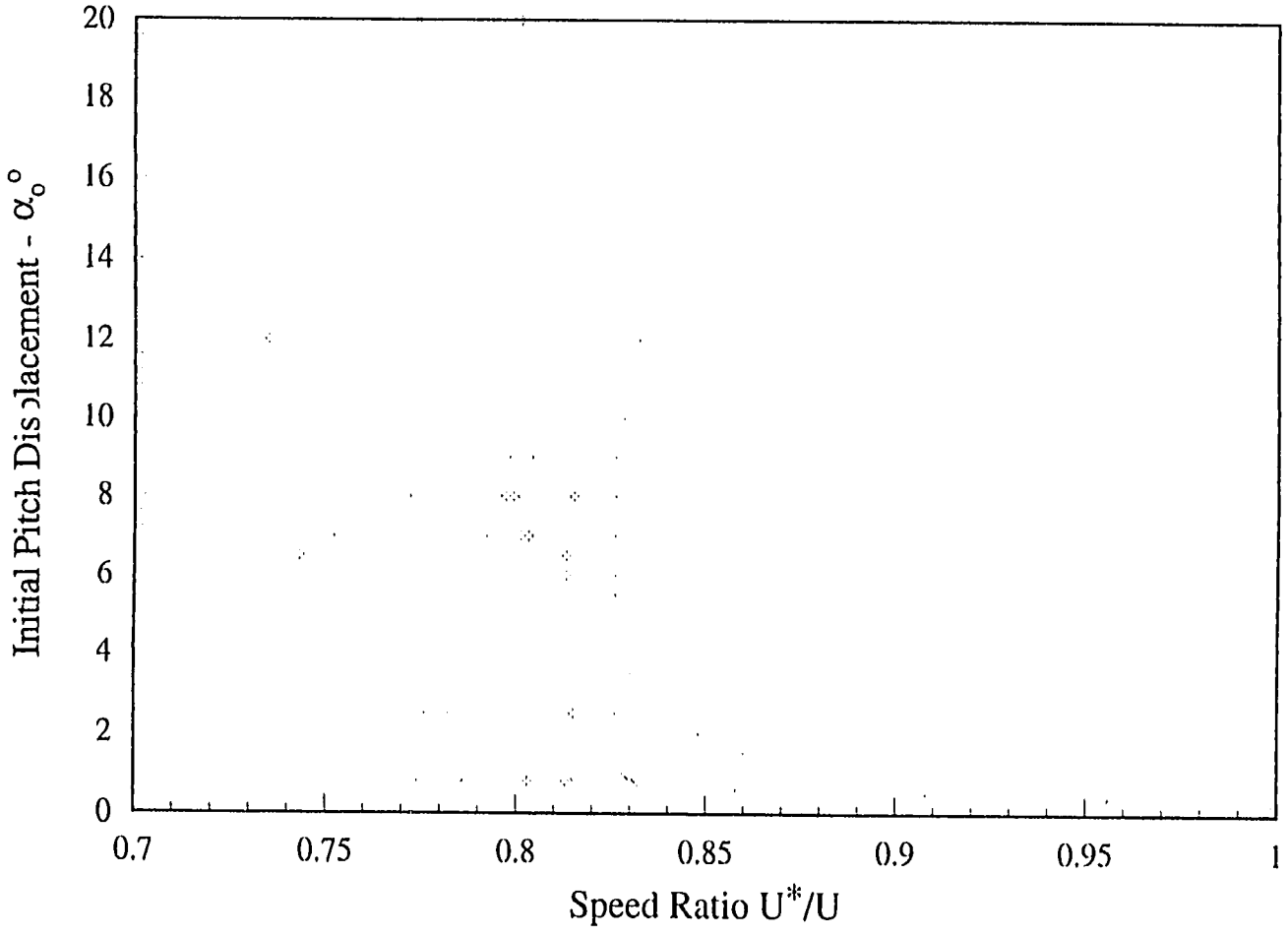

Figure 5.28a - Flutter Boundary for Hysteresis Nonlinearity:
μ=100, $\overline{\omega}$=0.2, ΔV=0.0°, ΔH=0.5°, V_{offset}=0.25, H_{offset}=0.5

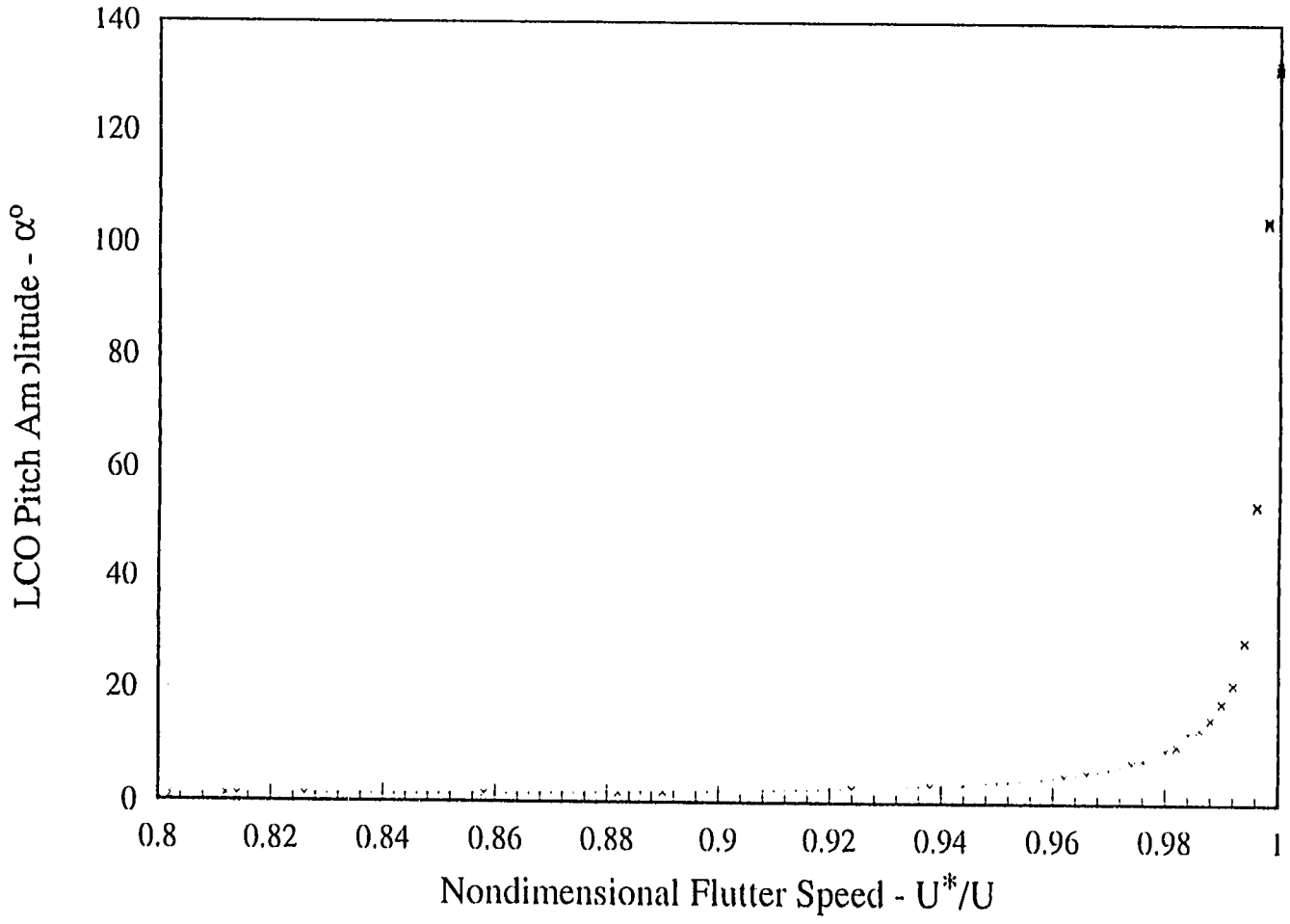

Figure 5.28c - Variation of LCO Amplitude with Speed:
μ=100, $\bar{\omega}$=0.2, ΔV=0.0°, ΔH=0.5°, V_{offset}=0.25, H_{offset}=0.5

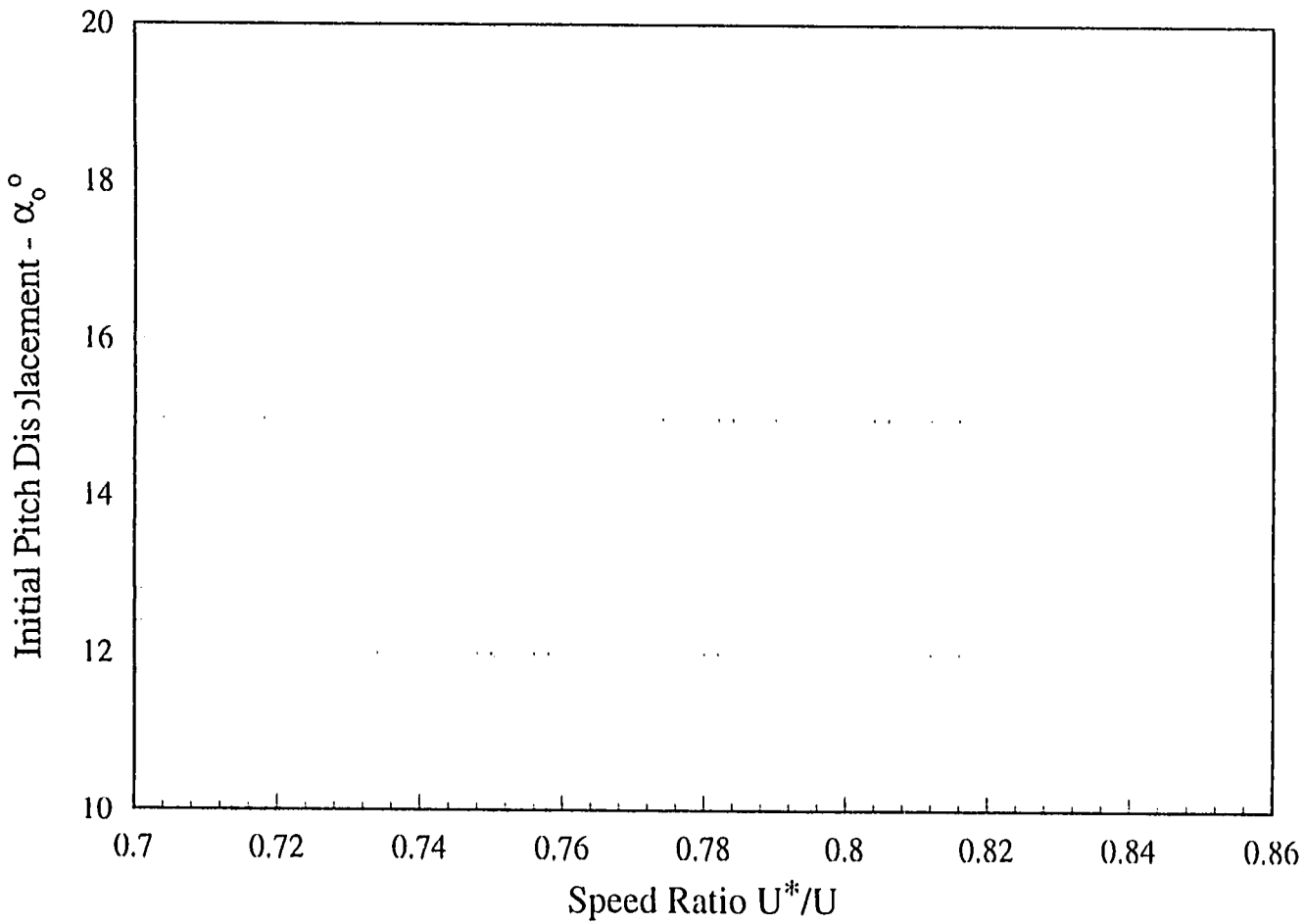

Figure 5.29a - Flutter Boundary for Hysteresis Nonlinearity:
μ=100, $\overline{\omega}$=0.2, $\Delta V=0.5^o$, $\Delta H=0.5^o$, V_{offset}=0.0, H_{offset}=0.25

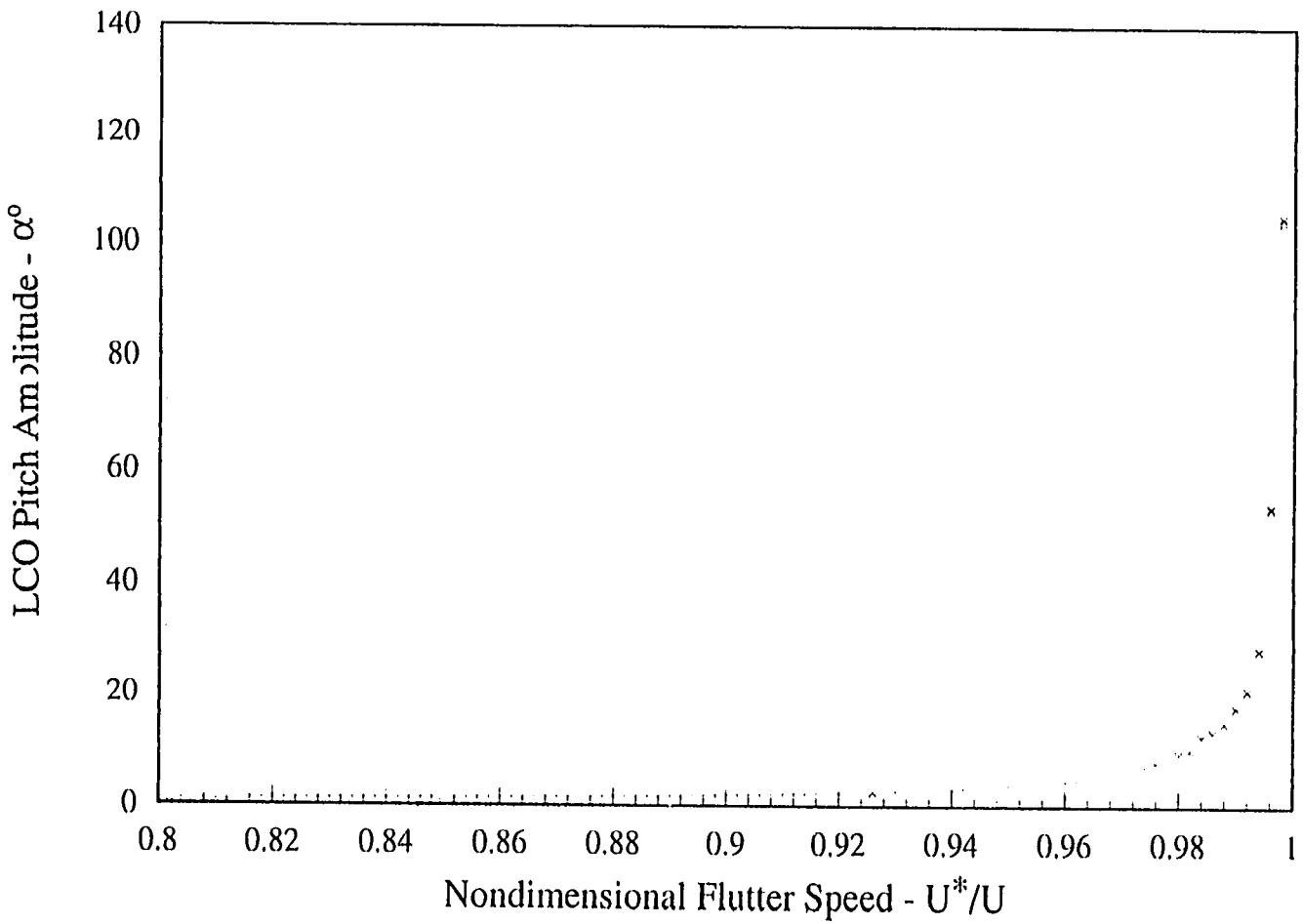

Figure 5.29c - Variation of LCO Amplitude with Speed:
μ=100, $\overline{\omega}$=0.2, ΔV=0.5°, ΔH=0.5°, V_{offset}=0.0, H_{offset}=0.25

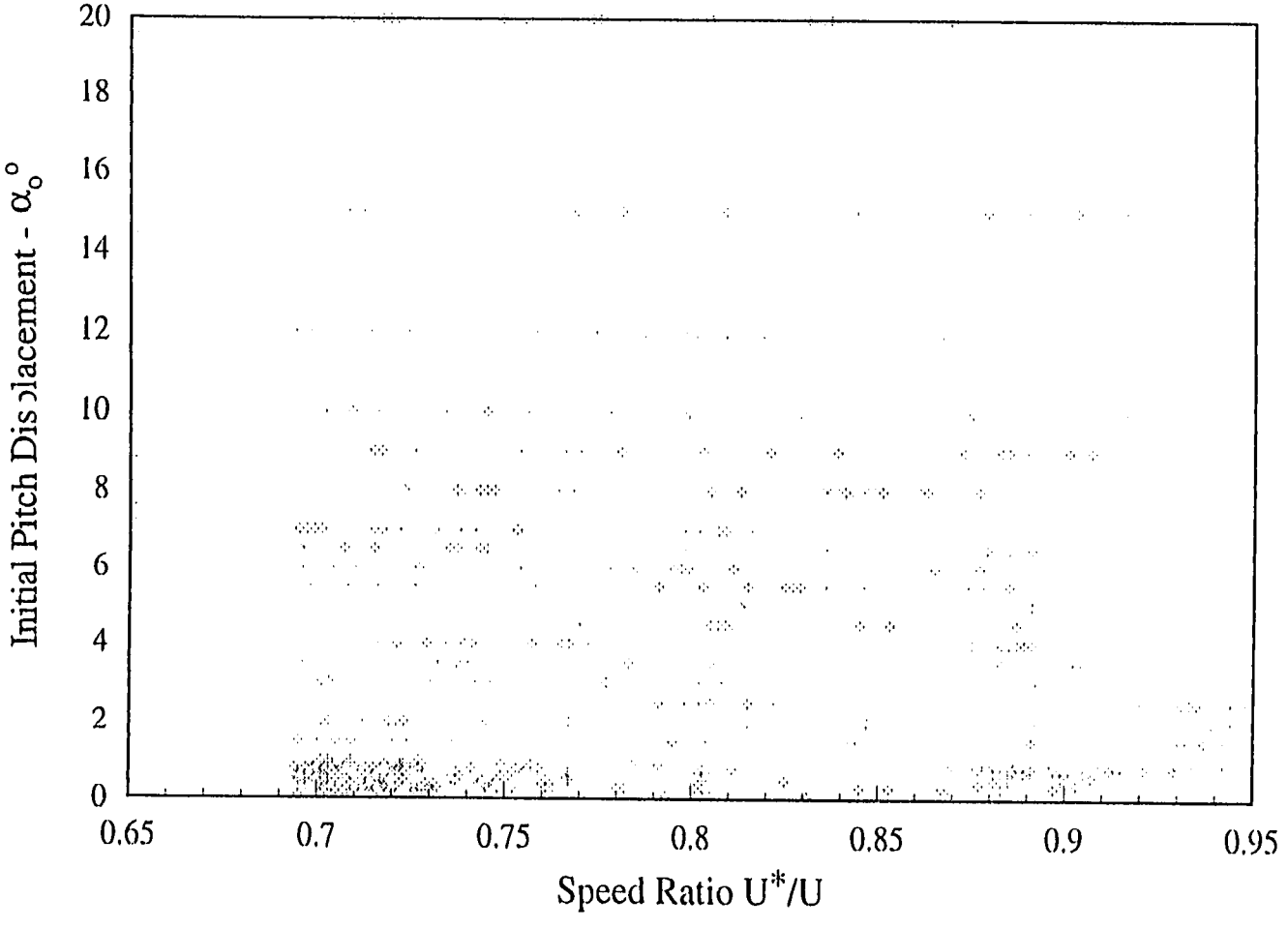

Figure 5.30a - Flutter Boundary for Hysteresis Nonlinearity:
μ=100, $\overline{\omega}$=0.2, ΔV=1.0^o, ΔH=0.5^o, V_{offset}=-0.25, H_{offset}=0.0

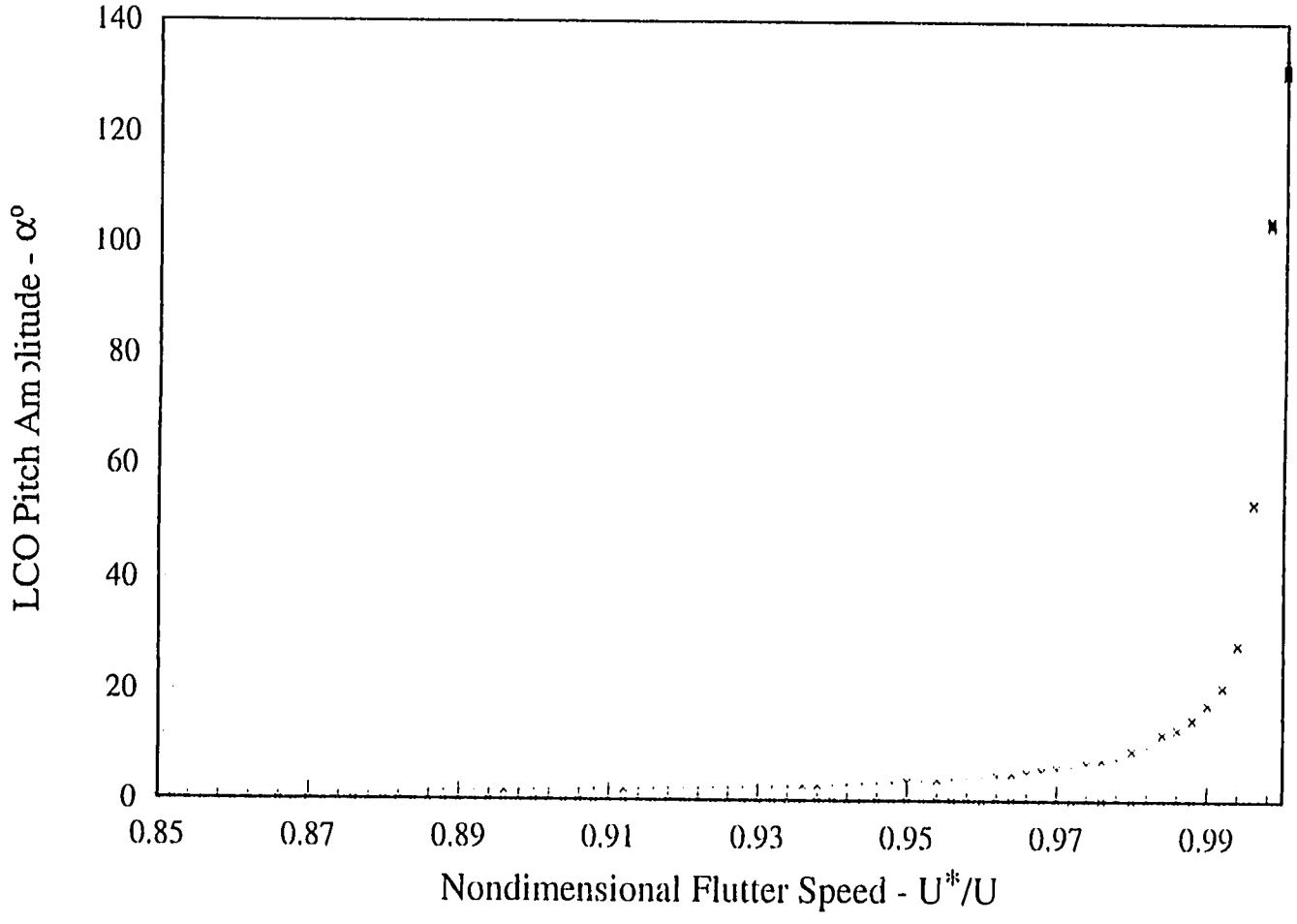

Figure 5.30c - Variation of LCO Amplitude with Speed:
μ=100, $\overline{\omega}$=0.2, ΔV=1.0°, ΔH=0.5°, V_{offset}=-0.25, H_{offset}=0.0

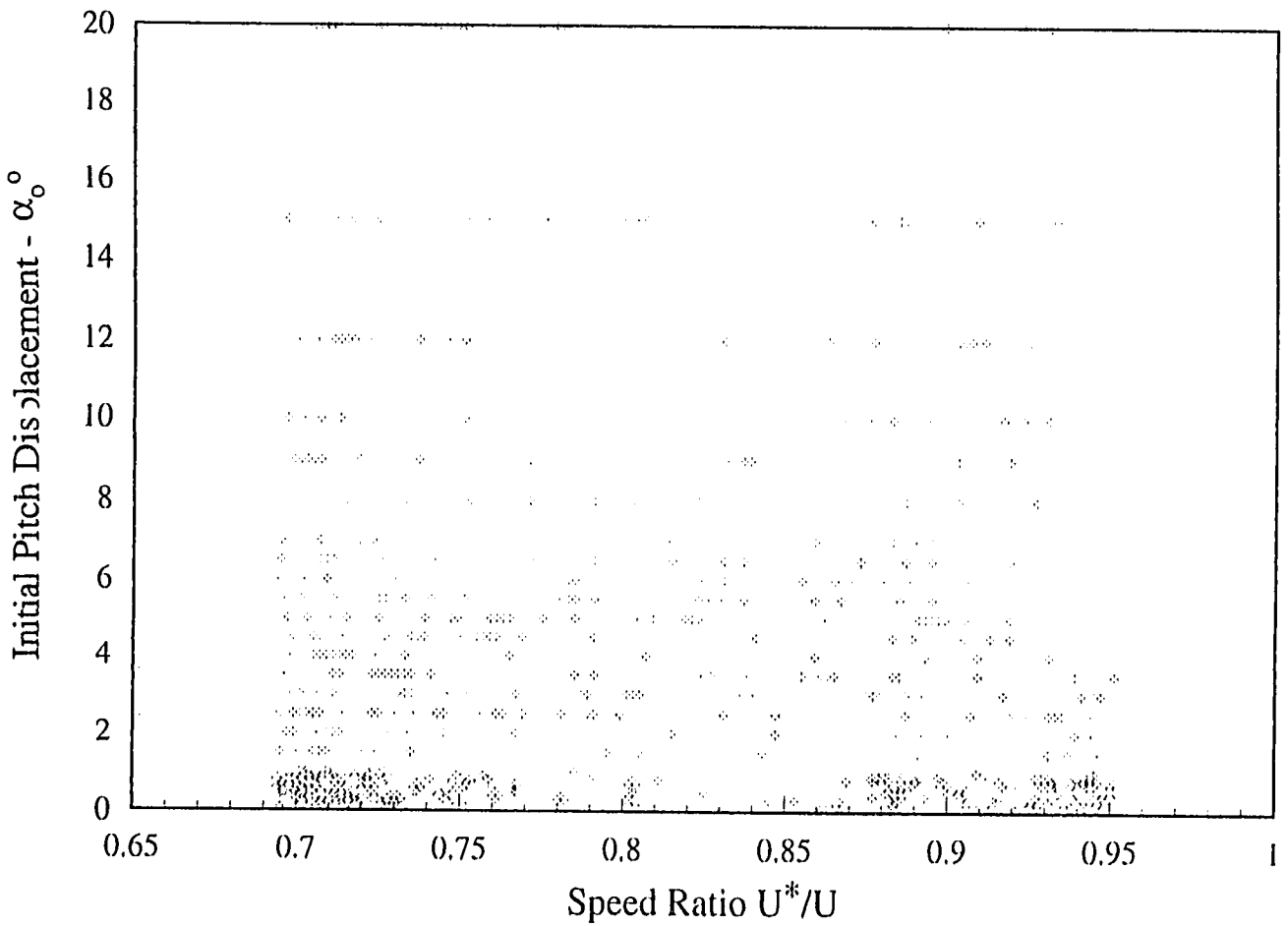

Figure 5.31a - Flutter Boundary for Hysteresis Nonlinearity:
μ=100, $\overline{\omega}$=0.2, $\Delta V=1.5^o$, $\Delta H=0.5^o$, V_{offset}=-0.5, H_{offset}=-0.25

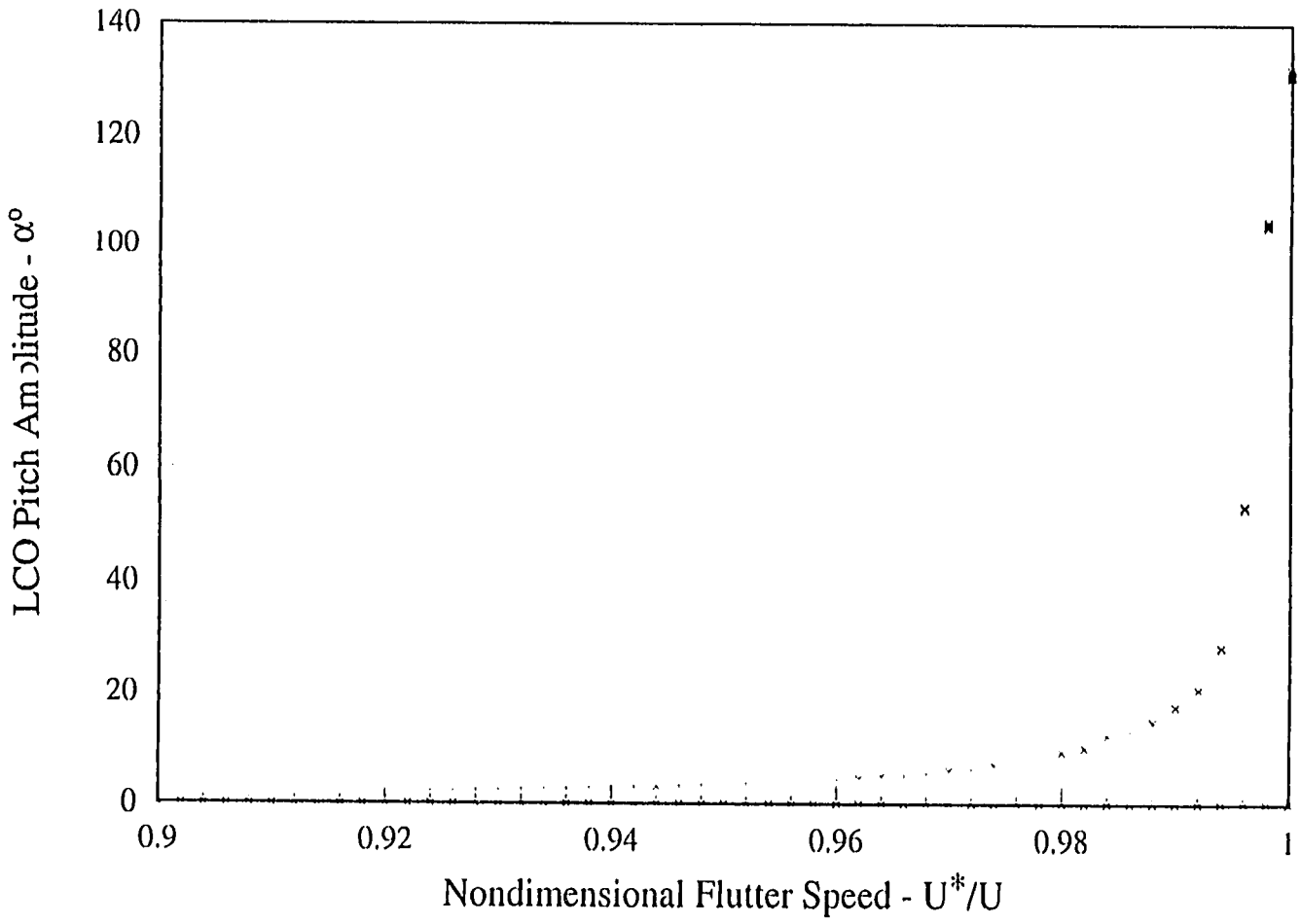

Figure 5.31c - Variation of LCO Amplitude with Speed:
μ=100, $\overline{\omega}$=0.2, ΔV=1.5°, ΔH=0.5°, V_{offset}=-0.5, H_{offset}=-0.25

APPENDIX A

APPENDIX A

PARAMETERS FOR EQUATION 3.29

$$\bar{P}[1,1] = \frac{2}{\mu\,\Delta\tau^2}\left(\mu X_\alpha - a_n\right) + \frac{1}{6\mu\,\Delta\tau}\left(11 + \left(\tfrac{1}{2} - a_n\right)\left(22\ell - 9(a+c)\right)\right)$$

$$+ \frac{1}{8\mu}\left(16\ell - 11(a+c)\right)$$

$$\bar{P}[1,2] = \frac{2}{\mu\,\Delta\tau^2}(1+\mu) + \frac{1}{6\mu\,\Delta\tau}\left(22\mu\zeta_\xi \frac{\bar{\omega}}{U^*} + 22\ell - 9(a+c)\right)$$

$$+ \frac{\bar{\omega}^2}{U^{*2}}$$

$$\bar{P}[2,1] = \frac{2}{\mu\,\Delta\tau^2}\left(\frac{1}{8}\left(\frac{1 + 8a_n^2}{r_\alpha^2}\right) + \mu\right) + \frac{1}{6\mu\,\Delta\tau}\left(\frac{22\mu\zeta_\alpha}{U^*} + \frac{\left(\tfrac{1}{2} - a_n\right)}{r_\alpha^2}\right.$$

$$\left.\left(11 - \left(\tfrac{1}{2} + a_n\right)\left(22\ell - 9(a+c)\right)\right)\right) - \frac{\left(\tfrac{1}{2} + a_n\right)}{8\mu\, r_\alpha^2}\left(16\ell - 11(a+c)\right)$$

$$\bar{P}[2,2] = \frac{2(\mu X_\alpha - a_n)}{\mu\,\Delta\tau^2\, r_\alpha^2} - \frac{\left(\tfrac{1}{2} + a_n\right)}{6\mu\,\Delta\tau\, r_\alpha^2}\left(22\ell - 9(a+c)\right)$$

$$\bar{X}[1] = \left[\frac{5(\mu X_2 - a_h)}{\mu \Delta\tau^2} + \frac{3}{4\mu\Delta\tau}\left(4 + \left(\tfrac{1}{2} - a_h\right)\left(8l - 5(a+c)\right)\right) - \frac{9(a+c)}{4\mu}\right]\alpha(\tau)$$

$$+ \left[\frac{5(1+\mu)}{\mu\Delta\tau^2} + \frac{3}{4\mu\Delta\tau}\left(\frac{8\mu\zeta_\xi\bar{\omega}}{U^*} + 8l - 5(a+c)\right)\right]\xi(\tau)$$

$$- \left[\frac{4(\mu X_\alpha - a_h)}{\mu\Delta\tau^2} + \frac{3}{2\mu\Delta\tau}\left(1 + \left(\tfrac{1}{2} - a_h\right)\left(2l - 2(a+c)\right) + \frac{9(a+c)}{8\mu}\right)\right]\alpha(\tau-\Delta\tau)$$

$$- \left[\frac{4(1+\mu)}{\mu+\Delta\tau^2} + \frac{3}{2\mu\Delta\tau}\left(\frac{2\zeta_\xi\mu\bar{\omega}}{U^*} + 2l - 2(a+c)\right)\right]\xi(\tau-\Delta\tau)$$

$$+ \left[\frac{(\mu X_\alpha - a_h)}{\mu+\Delta\tau^2} + \frac{1}{12\mu+\Delta\tau}\left(\frac{8\mu\zeta\bar{\omega}}{U^*} + 8l - 9(a+c)\right) - \frac{(a+c)}{4\mu}\right]\alpha(\tau-2\Delta\tau)$$

$$+ \left[\frac{1+\mu}{\mu(\Delta\tau)^2} + \frac{1}{12\mu\Delta\tau}\left(\frac{8\mu\zeta_\xi\bar{\omega}}{U^*} + 8l - 9(a+c)\right)\right]\xi(\tau-2\Delta\tau)$$

$$+ \left[\frac{19\Delta\tau}{12\mu}\left(ae^{-b\Delta\tau} + ce^{-d\Delta\tau}\right)\left(\ddot{\xi}(\tau) + \left(\tfrac{1}{2} - a_h\right)\ddot{\alpha}(\tau) + \dot{\alpha}(\tau)\right)\right]$$

$$- \left[\frac{5\Delta\tau}{12\mu}\left(ae^{-2b\Delta\tau} + ce^{-2d\Delta\tau}\right)\left(\ddot{\xi}(\tau-\Delta\tau) + \left(\tfrac{1}{2} - a_h\right)\ddot{\alpha}(\tau-\Delta\tau) + \dot{\alpha}(\tau-\Delta\tau)\right)\right]$$

$$+ \left[\frac{\Delta\tau}{12\mu}\left(ae^{-3b\Delta\tau} + ce^{-3d\Delta\tau}\right)\left(\ddot{\xi}(\tau-2\Delta\tau) + \left(\tfrac{1}{2} - a_h\right)\ddot{\alpha}(\tau-2\Delta\tau) + \dot{\alpha}(\tau-2\Delta\tau)\right)\right]$$

$$+ \left[\frac{2}{\mu}\left(ae^{-b(\tau+\Delta\tau)} + c^{-d(\tau+\Delta\tau)}\right)\dot{\xi}(0) + \left(\tfrac{1}{2} - a_h\right)\ddot{\alpha}(0) + \alpha(0)\right]$$

$$+ \left[\frac{2}{\mu}ae^{-b\Delta\tau}I_1(\tau) + \frac{2}{\mu}ce^{-d\Delta\tau}I_2(\tau)\right]$$

$$-\left[\frac{\Delta\tau\left(\frac{1}{2}+a_n\right)}{12\mu\, r_2^2}\left(ae^{-3b\Delta\tau}+ce^{-3d\Delta\tau}\right)\left(\ddot{\xi}(\tau-2\Delta\tau)+\left(\frac{1}{2}-a_n\right)\ddot{\alpha}(\tau-2\Delta\tau)+\dot{\alpha}(\tau-2\Delta\tau)\right)\right]$$

$$-\left[\frac{2\left(\frac{1}{2}+a_n\right)}{\mu r_2^2}\left(ae^{-b(\tau+\Delta\tau)}+ce^{-d(\tau+\Delta\tau)}\right)\left(\dot{\xi}(0)+\left(\frac{1}{2}-a_n\right)\dot{\alpha}(0)+\alpha(0)\right)\right]$$

$$-\left[\frac{2\left(\frac{1}{2}+a_n\right)}{\mu r_2^2}\left(ae^{-b\Delta\tau}\right)I_1(\tau)-\frac{2\left(\frac{1}{2}+a_n\right)}{\mu r_2^2}\left(ce^{-d\Delta\tau}\right)I_2(\tau)\right]$$

$$I_1(\tau)=\int_0^{\tau}\lambda(\sigma)e^{-b(\tau-\sigma)}\,d\sigma$$

$$I_2(\tau)=\int_0^{\tau}\lambda\sigma\, e^{-d(\tau-\sigma)}\,d\sigma$$

WHERE $\lambda(\sigma)=\ddot{\xi}(\sigma)+\left(\frac{1}{2}-a_n\right)\ddot{\alpha}(\sigma)+\dot{\alpha}(\sigma)$

$$
\begin{aligned}
\bar{X}[2] = {} & \left[\frac{5}{\mu\Delta\tau^2}\left(\frac{(1+8a_n^2)}{8r_\alpha^2}+\mu\right)+\frac{3}{4\mu\Delta\tau}\left(\frac{8\mu\zeta_\alpha}{U^*}+\frac{(\frac{1}{2}-a_n)}{r_\alpha^2}\cdot\right.\right. \\
& \left.\left.\left(4-(\tfrac{1}{2}+a_n)(8l-5(a+c))\right)\right)+\frac{9(\frac{1}{2}+a_n)}{4\mu r_\alpha^2}(a+c)\right]\alpha(\tau) \\
& +\left[\frac{5(\mu X_\alpha-a_n)}{\mu\Delta\tau^2 r_\alpha^2}-\frac{3(\frac{1}{2}+a_n)}{4\mu\Delta\tau r_\alpha^2}(8l-5(a+c))\right]\xi(\tau) \\
& -\left[\frac{4}{\mu\Delta\tau^2}\left(\frac{1}{8}\frac{(1+8a_n^2)}{r_\alpha^2}+\mu\right)+\frac{3}{2\mu\Delta\tau}\left(\frac{2\mu\zeta_\alpha}{U^*}+\frac{(\frac{1}{2}-a_n)}{r_\alpha^2}\left(1-(\tfrac{1}{2}+a_n)(2l-2(a+c))\right)\right)\right. \\
& \left.+\frac{9(\frac{1}{2}+a_n)}{8\mu r_\alpha^2}(a+c)\right]\alpha(\tau-\Delta\tau) \\
& -\left[\frac{4(\mu X_\alpha-a_n)}{\mu(\Delta\tau)^2 r_\alpha^2}-\frac{3(\frac{1}{2}+a_n)}{2\mu\Delta\tau r_\alpha^2}(2l-2(a+c))\right]\xi(\tau-\Delta\tau) \\
& +\left[\frac{1}{\mu\Delta\tau^2}\left(\frac{1}{8r_\alpha^2}(1+8a_n)^2+\mu\right)+\frac{1}{12\mu\Delta\tau}\left(\frac{8\mu\zeta_\alpha}{U^*}+\frac{(\frac{1}{2}-a_n)}{r_\alpha^2}\left(4-(\tfrac{1}{2}+a_n)(8l-9(a+c))\right)\right)\right. \\
& \left.+\frac{(\frac{1}{2}+a_n)}{4\mu r_\alpha^2}(a+c)\right]\alpha(\tau-2\Delta\tau) \\
& +\left[\frac{(\mu X_\alpha-a_n)}{\mu\Delta\tau^2 r_\alpha^2}-\frac{(\frac{1}{2}+a_n)}{12\mu\Delta\tau r_\alpha^2}(8l-9(a+c))\right]\xi(\tau-2\Delta\tau) \\
& -\left[\frac{19\Delta\tau}{12\mu r_\alpha^2}(\tfrac{1}{2}+a_n)\left(ae^{-b\Delta\tau}+ce^{-d\Delta\tau}\right)\ddot{\xi}(\tau)+(\tfrac{1}{2}-a_n)\ddot{\alpha}(\tau)+\dot{\alpha}(\tau)\right] \\
& +\left[\frac{5\Delta\tau(\frac{1}{2}+a_n)}{12\mu r_\alpha^2}\left(ae^{-2b\Delta\tau}+ce^{-2d\Delta\tau}\right)\ddot{\xi}(\tau-\Delta\tau)+(\tfrac{1}{2}-a_n)\ddot{\alpha}(\tau-\Delta\tau)+\dot{\alpha}(\tau-\Delta\tau)\right]
\end{aligned}
$$

$$-\left[\frac{\Delta\tau\left(\frac{1}{2}+a_n\right)}{12\mu r_\alpha^2}\left(ae^{-3b\Delta\tau}+ce^{-3d\Delta\tau}\right)\left(\ddot{\xi}(\tau-2\Delta\tau)+\left(\frac{1}{2}-a_n\right)\ddot{\alpha}(\tau-2\Delta\tau)+\dot{\alpha}(\tau-2\Delta\tau)\right)\right]$$

$$-\left[\frac{2\left(\frac{1}{2}+a_n\right)}{\mu r_\alpha^2}\left(ae^{-b(\tau+\Delta\tau)}+ce^{-d(\tau+\Delta\tau)}\right)\left(\dot{\xi}(0)+\left(\frac{1}{2}-a_n\right)\dot{\alpha}(0)+\alpha(0)\right)\right]$$

$$-\left[\frac{2\left(\frac{1}{2}+a_n\right)}{\mu r_\alpha^2}\left(ae^{-b\Delta\tau}\right)I_1(\tau)-\frac{2\left(\frac{1}{2}+a_n\right)}{\mu r_\alpha^2}\left(ce^{-d\Delta\tau}\right)I_2(\tau)\right]$$

HOUBOLT METHOD STARTING PROCEDURE

TAYLOR SERIES USED TO OBTAIN:

FOR $\tau = 0$

$$\alpha(-\Delta\tau) = \alpha(0) - \Delta\tau\dot{\alpha}(0) + \frac{\Delta\tau^2}{2}\ddot{\alpha}(0) + O(\Delta\tau^3)$$

$$\alpha(\Delta\tau) = \alpha(0) + \Delta\tau\dot{\alpha}(0) + \frac{\Delta\tau^2}{2}\ddot{\alpha}(0) + O(\Delta\tau^3)$$

SIMILAR FOR ξ

$$\dot{\alpha}(-\Delta\tau) = \dot{\alpha}(0) - \Delta\tau\ddot{\alpha}(0) + \frac{\Delta\tau^2}{2}\dddot{\alpha}(0) + O(\Delta\tau^3)$$

$$\dot{\alpha}(\Delta\tau) = \dot{\alpha}(0) + \Delta\tau\ddot{\alpha}(0) + \frac{\Delta\tau^2}{2}\dddot{\alpha}(0) + O(\Delta\tau^3)$$

SIMILAR FOR ξ

$$\ddot{\alpha}(-\Delta\tau) = \ddot{\alpha}(0) - \Delta\tau\dddot{\alpha}(0) + \frac{\Delta\tau^2}{2}\ddddot{\alpha}(0) + O(\Delta\tau^3)$$

$$\ddot{\alpha}(\Delta\tau) = \ddot{\alpha}(0) + \Delta\tau\dddot{\alpha}(0) + \frac{\Delta\tau^2}{2}\ddddot{\alpha}(0) + O(\Delta\tau^3)$$

SIMILAR FOR ξ

HIGHER DERIVATIVES FROM:

$$\begin{Bmatrix} \alpha^{(n)}(0) \\ \xi^{(n)}(0) \end{Bmatrix} = \left[Q\right]^{-1} \begin{Bmatrix} Y_1^{(n)} \\ Y_2^{(n)} \end{Bmatrix}$$

FOR $n = 2, 3, 4$

WHERE:

$$[Q] = \begin{bmatrix} \dfrac{(\mu x_2 - a_n)}{\mu} & \dfrac{(1+\mu)}{\mu} \\ \dfrac{1}{\mu}\left[\dfrac{\left(\frac{1}{8}+a_n^2\right)}{r_\alpha^2} + \mu\right] & \dfrac{\mu x_2 - a_n}{\mu r_2^2} \end{bmatrix}$$

$$Y_1^{(2)} = -\frac{1}{\mu}\left[1 + \left(\tfrac{1}{2} - a_n\right)\left[2l - 2(a+c)\right]\right]\dot{\alpha}(0)$$

$$-\frac{1}{\mu}\left[\frac{2\mu\zeta_\xi\bar{\omega}}{U^*} + 2l - 2(a+c)\right]\dot{\xi}(0)$$

$$-\frac{1}{\mu}\left[2l - 2(a+c)\right]\alpha(0) - \frac{1}{U^{*2}}\xi(0)$$

$$Y_2^{(2)} = -\frac{1}{\mu}\left[\frac{2\mu\zeta_\alpha}{U^*} + \frac{\left(\frac{1}{2}-a_n\right)}{r_\alpha^2}\left[1 - \left(\tfrac{1}{2}+a_n\right)\left(2l - 2(a+c)\right)\right]\right]\dot{\alpha}(0)$$

$$+\frac{1}{\mu}\left[\frac{\left(\frac{1}{2}+a_n\right)}{r_\alpha^2}\left(2l - 2(a+c)\right)\right]\dot{\xi}(0) + \frac{\left(\frac{1}{2}+a_n\right)}{\mu r_\alpha^2}\left(2l - 2(a+c)\right)\alpha(0)$$

$$-\frac{F(\alpha(0))}{U^{*2}}$$

$$Y_1^{(3)} = -\frac{1}{\mu}\left[1 + \left(\tfrac{1}{2}-a_n\right)\left(2l - 2(a+c)\right)\right]\ddot{\alpha}(0) - \frac{1}{\mu}\left(\frac{2\mu\zeta_\xi\bar{\omega}}{U^*} + 2l - 2(a+c)\right)\ddot{\xi}(0)$$

$$-\frac{1}{\mu}\left[2l - 2(a+c) + \left(\tfrac{1}{2}-a_n\right)\left(2ab + 2cd\right)\right]\dot{\alpha}(0)$$

$$-\left[\frac{1}{\mu}\left(2ab + 2cd\right) - \frac{\bar{\omega}^2}{U^{*2}}\right]\dot{\xi}(0) - \frac{1}{\mu}\left(2ab + 2cd\right)\alpha(0)$$

$$Y_2^{(3)} = -\frac{1}{\mu}\left[\frac{2\mu\xi_\alpha}{U^*} + \frac{\frac{1}{2}-a_n}{r_\alpha^2}\left(1-\left(\tfrac{1}{2}+a_n\right)\left(2l-2(a+c)\right)\right)\right]\ddot{\alpha}(0)$$

$$+\frac{1}{\mu}\left[\frac{\frac{1}{2}+a_n}{r_\alpha^2}\left(2l-2(a+c)\right)\right]\ddot{\xi}(0)$$

$$+\frac{1}{\mu}\frac{\left(\frac{1}{2}+a_n\right)}{r_\alpha^2}\left[2l-2(a+c)+\left(\tfrac{1}{2}-a_n\right)(2ab+2cd)\right]\dot{\alpha}(0)$$

$$+\frac{1}{\mu}\frac{\left(\frac{1}{2}+a_n\right)}{r_\alpha^2}\left[(2ab+2cd)\left(\dot{\xi}(0)+\alpha(0)\right)\right]-\frac{1}{U^{*2}}\frac{d}{d\tau}F(\alpha(0))$$

$$Y_1^{(4)} = -\frac{1}{\mu}\left[1+\left(\tfrac{1}{2}-a_n\right)\left(2l-2(a+c)\right)\right]\dddot{\alpha}(0) - \frac{1}{\mu}\left[\frac{2\mu\xi_\xi\bar{\omega}}{U^*}+2l-2(a+c)\right]\dddot{\xi}(0)$$

$$-\frac{1}{\mu}\left[2l-2(a+c)+\left(\tfrac{1}{2}-a_n\right)(2ab+2cd)\right]\ddot{\alpha}(0) - \left[\frac{1}{\mu}(2ab+2cd)+\frac{\bar{\omega}^2}{U^{*2}}\right]\ddot{\xi}(0)$$

$$-\frac{1}{\mu}\left[2ab+2cd-\left(\tfrac{1}{2}-a_n\right)(2ab^2+2cd^2)\right]\dot{\alpha}(0)$$

$$+\frac{1}{\mu}\left[2ab^2+2cd^2\right]\left[\dot{\xi}(0)+\alpha(0)\right]$$

$$Y_2^{(4)} = -\frac{1}{\mu}\left[\frac{2\mu\xi_\alpha}{U^*}+\frac{\left(\frac{1}{2}-a_n\right)}{r_\alpha^2}\left(1-\left(\tfrac{1}{2}+a_n\right)\left(2l-2(a+c)\right)\right)\right]\ddot{\alpha}(0)$$

$$+\frac{1}{\mu}\frac{\left(\frac{1}{2}-a_n\right)}{r_\alpha^2}\left(2l-2(a+c)\right)\dddot{\xi}(0)+\frac{1}{\mu}\left[\frac{\left(\frac{1}{2}+a_n\right)}{r_\alpha^2}\left(2l-2(a+c)+\left(\tfrac{1}{2}-a_n\right)(2ab-2cd)\right)\right]\ddot{\alpha}(0)$$

$$+\frac{1}{\mu}\frac{\left(\frac{1}{2}+a_n\right)}{r_\alpha^2}(2ab+2cd)\ddot{\xi}(0)+\frac{1}{\mu}\frac{\left(\frac{1}{2}+a_n\right)}{r_\alpha^2}\left(2ab+2cd-\left(\tfrac{1}{2}-a_n\right)(2ab^2+2cd^2)\right)\dot{\alpha}(0)$$

$$-\frac{1}{\mu}\frac{\left(\frac{1}{2}+a_n\right)}{r_\alpha^2}(2ab^2+2cd^2)\left(\dot{\xi}(0)+\alpha(0)\right)-\frac{1}{U^{*2}}\frac{d^2}{d\tau^2}F(\alpha(0))$$

APPENDIX B

```
c      Source code file Aeroelastic Flutter Analysis
c
c             Using Houbolt Finite Difference Simulation Method
c
c   Created by:      Brett Brooking, Carleton University
c
c                    MAY, 1998
c
cccccccccccccccccccccccccccccccccccccccccccccccccccccccccccccccccccccc
      PROGRAM HYST
      IMPLICIT LOGICAL (A-Z)
C Constant IBIGTIM:  Number of time steps to declare steady state
C          IPFREQ:  Frequency to output results
C          TIMECHEK: Inital time to allow transient effects to damp out
      INTEGER IBIGTIM, IPFREQ, TIMECHEK
C Constant THRESH: Threshold to determine damped system
      REAL THRESH
      PARAMETER (IBIGTIM=50000)
      PARAMETER (THRESH=0.001)
      PARAMETER (IPFREQ=5)
      PARAMETER (TIMECHEK=300)
      REAL F_I1,F_I2,LAMBDA(4),RECALP(IBIGTIM),RECXI(IBIGTIM)
      REAL HMU,DT,T,XA,AH,EL,A,B,C,D,ZETAAL,ZETAXI,OMEGA,USTAR,RA
      REAL ALPH0,DALPH0,DDALP0,TDALP0,QDALP0,XI0,DXI0,DDXI0,TDXI0
      REAL DALPH(4),DDALPH(4),DXI(4),DDXI(4)
      REAL*8 ALPH(4),XI(4)
      REAL V1,V2,H1MIN,H1MAX,H2MIN,H2MAX,ULIN,HIPEAK,LOPEAK,CONVRT
      REAL INCR,DV,DH,VOFF,HOFF,HIXI,LOXI,UMIN,UMAX,QDXI0
      REAL F_HOFF,F_H1MAX,F_H2MAX,ALIST(100)
      INTEGER I,LOOP,NUM,INDEX,STATE,NUMANG,COUNT,TYPE,INCREASE
      INTEGER SMPEAKS
      CHARACTER*30 INFILE,OUTFILE,TEMPFILE,AMPFILE,XIFILE
      CHARACTER*80 XLABEL,YLABEL
      CHARACTER*100 GTITLE,GSUBT
      CHARACTER*8 CHAR_TIME
      CHARACTER*9 TODAY
      COMMON /CONST/
      XA,AH,EL,A,B,C,D,ZETAAL,ZETAXI,OMEGA,USTAR,RA,V1,
     1
     V2,H1MIN,H1MAX,H2MIN,H2MAX,HMU,DT,DV,DH,VOFF,F_HOFF,CONVRT,
     2      HOFF,F_H1MAX,F_H2MAX
C
      CONVRT=0.1745329252
      TEMPFILE="temp"
C Find out if interactive, or data file
C      PRINT *,'Enter the name of the output file.'
C      READ (*,10)OUTFILE
      PRINT *
      PRINT *,'Enter: Flutter Map=1 (def) or Single run=2'
      READ (*,5)TYPE
5     FORMAT(I3)
      IF(TYPE.NE.2) THEN
          TYPE=1
      ENDIF
      IF(TYPE.EQ.2) THEN
          OUTFILE="pitchresp.dat"
          OPEN(UNIT=2,FILE=OUTFILE)
          OPEN(UNIT=10,FILE='spring.dat')
          PRINT *,'Enter the initial Alpha.'
          READ (*,20)ALIST(1)
          PRINT *,'Enter the Linear Flutter Speed - Ulin'
          READ (*,20)ULIN
```

```
            NUM=1
            NUMANG=1
            PRINT *,'Enter the flutter speed ratio: U*'
            READ (*,20)UMIN
            INCR=0.
            PRINT *,'Enter Delta V'
            READ (*,20)DV
            PRINT *,'Enter Delta H'
            READ (*,20)DH
            PRINT *,'Enter Vertical Offset: VOFF'
            READ (*,20)VOFF
            PRINT *,'Enter Horizontal Offset: HOFF'
            READ (*,20)HOFF
            PRINT *,'Enter the airfoil-air mass ratio: mu'
            READ (*,20)HMU
            PRINT *,'Enter the frequency ratio: omega'
            READ (*,20)OMEGA
C            GTITLE='Pitch Response'
            OPEN(UNIT=3,FILE=TEMPFILE)
            WRITE(3,15)'\\8m\\4 =',HMU,'  \\8v\\4 =',OMEGA,'
            \\8D\\NH',
      1     ' =',DH,' \\8D\\NV =',DV,'"\n#'
15          FORMAT (A8,F6.1,A10,F5.2,A9,A3,F4.2,A10,F4.2,A4)
            CLOSE(3)
            OPEN(UNIT=3,FILE=TEMPFILE)
            READ (3,10)GTITLE
            CLOSE(3)
            OPEN(UNIT=3,FILE=TEMPFILE)
            WRITE(3,25)'\\8a\\4\\s0\\N =',ALIST(1),'\\So\\N  ',
      1     'U\\S*\\N\\slinear\\N =',ULIN,'  U\\S*\\N\\snorm\\N
      =',UMIN,
      2     '"\n#'
25          FORMAT (A13,F6.2,A7,A18,F7.4,A19,F6.4,A4)
            CLOSE(3)
            OPEN(UNIT=3,FILE=TEMPFILE)
            READ (3,10)GSUBT
            CLOSE(3)
c            GSUBT=
C            GSUBT='hf+=',HFMAX,' hf-=',HFMIN,' vf=',VF
            YLABEL='Pitch Angle - \\8a\\4 \\So\\N"\n#'
            XLABEL='Non-Dimensional Time - \\8t\\4"\n#'
        ELSE
            OUTFILE="flutter.map"
            OPEN(UNIT=2,FILE=OUTFILE)
            PRINT *,'Enter the name of the input file.'
            READ (*,10)INFILE
C Get the input parameters and input data
            CALL
            GETDATA(INFILE,GTITLE,GSUBT,ULIN,NUMANG,NUM,INCR,UMIN,
      1UMAX,ALIST)
C            GTITLE='Flutter Map"\n#'
C            GSUBT=' '
C            GSUBT='hf+=',HFMAX,' hf-=',HFMIN,' vf=',VF
            YLABEL='Initial Displacement - \\8a\\4\\s0\\N
            \So\\N"\n#'
            XLABEL='Flutter Speed Ratio- U/U\\S*\\N\\slinear\\N"\n#'
        ENDIF
10      FORMAT (A)
20      FORMAT (F10.0)
        CALL GR_SETUP(OUTFILE,GTITLE,GSUBT,XLABEL,YLABEL,TYPE)
        call TIME(char_time)
        CALL DATE(TODAY)
        PRINT *, 'Starting: ',CHAR_TIME,'  ',TODAY
C       Assign const variables for this case
```

```
C       VOFF=0.25
C       HOFF=0.5
        V1=(DV/2+VOFF)*CONVRT
        V2=(-DV/2+VOFF)*CONVRT
        DV=DV*CONVRT
        DH=DH*CONVRT
        VOFF=VOFF*CONVRT
        HOFF=HOFF*CONVRT
        F_HOFF=HOFF
C Only ALPH0 is varied, DALPH0, XI0, DXI0 are const = 0
        AMPFILE="pitch.dat"
        OPEN(UNIT=11,FILE=AMPFILE)
        XIFILE="heave.dat"
        OPEN(UNIT=12,FILE=XIFILE)
C Master Loop: Loop once for each initial angle
        DO 90 COUNT=1,NUMANG
        ALPH0=ALIST(COUNT)*CONVRT
        WRITE(*,21)'Initial Pitch Angle: ',ALPH0/CONVRT
21      FORMAT(A22,F8.2)
        STATE=1
C Loop for each Speed Ratio
        DO 90 INDEX=1,NUM
C Variable Initialization
        SMPEAKS=0
        HOFF=F_HOFF
        H1MIN=((DV+DH)/2+HOFF)
        F_H1MAX=((DV-DH)/2+HOFF)
        H1MAX=F_H1MAX
        H2MIN=(-(DV+DH)/2+HOFF)
        F_H2MAX=(-(DV-DH)/2+HOFF)
        H2MAX=F_H2MAX
        USTAR=(UMIN+INCR*(INDEX-1))*ULIN
        HIPEAK=-1.
        LOPEAK=1.
        DALPH0=0.
        XI0=0.
        DXI0=0.
C
        AH=-0.5
        RA=0.5
        XA=0.25
        DT=0.1
        EL=1.
        A=0.165
        B=0.0455
        C=0.335
        D=0.3
        T=DT*2
        ZETAAL=0.0
        ZETAXI=0.0
C        WRITE(*,*)'V1=',V1/CONVRT
C        WRITE(*,*)'V2=',V2/CONVRT
C        WRITE(*,*)'H1-=',H1MIN/CONVRT
C        WRITE(*,*)'H1+=',H1MAX/CONVRT
C        WRITE(*,*)'H2-=',H1MIN/CONVRT
C        WRITE(*,*)'H2+=',H1MAX/CONVRT
C        WRITE(*,*)'DELTA V=',DV/CONVRT
C        WRITE(*,*)'DELTA H=',DH/CONVRT
C        WRITE(*,*)'VOFF=',VOFF/CONVRT
C        WRITE(*,*)'HOFF=',F_HOFF/CONVRT
C
C
C Starting Procedure
       CALL
```

```
      START1(ALPH0,DALPH0,XI0,DXI0,DDALP0,TDALP0,QDALP0,DDXI0,
     1TDXI0,QDXI0)
      ALPH(1)=ALPH0-DT*DALPH0+(DT**2)/2.*DDALP0
      ALPH(2)=ALPH0
      ALPH(3)=ALPH0+DT*DALPH0+(DT**2)/2.*DDALP0
      DALPH(1)=DALPH0-DT*DDALP0+(DT**2)/2.*TDALP0
      DALPH(2)=DALPH0
      DALPH(3)=DALPH0+DT*DDALP0+(DT**2)/2.*TDALP0
      DDALPH(1)=DDALP0-DT*TDALP0+(DT**2)/2.*QDALP0
      DDALPH(2)=DDALP0
      DDALPH(3)=DDALP0+DT*TDALP0+(DT**2)/2.*QDALP0
C
      XI(1)=XI0-DT*DXI0+(DT**2)/2.*DDXI0
      XI(2)=XI0
      XI(3)=XI0+DT*DXI0+(DT**2)/2.*DDXI0
      DXI(1)=DXI0-DT*DDXI0+(DT**2)/2.*TDXI0
      DXI(2)=DXI0
      DXI(3)=DXI0+DT*DDXI0+(DT**2)/2.*TDXI0
      DDXI(1)=DDXI0-DT*TDXI0+(DT**2)/2.*QDXI0
      DDXI(2)=DDXI0
      DDXI(3)=DDXI0+DT*TDXI0+(DT**2)/2.*QDXI0
C
      LAMBDA(1)=DDXI(1)+(0.5-AH)*DDALPH(1)+DALPH(1)
      LAMBDA(2)=DDXI(2)+(0.5-AH)*DDALPH(2)+DALPH(2)
      LAMBDA(3)=DDXI(3)+(0.5-AH)*DDALPH(3)+DALPH(3)
      F_I1=DT/6.*(2.*LAMBDA(3)+5.*LAMBDA(2)*EXP(-B*DT)-LAMBDA(1)*
     1    EXP(-2.*B*DT))
      F_I2=DT/6.*(2.*LAMBDA(3)+5.*LAMBDA(2)*EXP(-D*DT)-LAMBDA(1)*
     1    EXP(-2.*D*DT))
C
C End of starting procedure
      IF(ALPH0.GT.0) THEN
          INCREASE=0
c            WRITE(*,*)INCREASE,T
      ELSE
          INCREASE=1
c            WRITE(*,*)INCREASE,T
      ENDIF
C Begin looping
      DO 30 LOOP=3,IBIGTIM
      T=(LOOP-2)*DT
C      IF((MOD(LOOP,2000)).EQ.0) WRITE(*,*)T
      CALL
      STEP(ALPH,XI,DALPH,DDALPH,DDXI,DALPH0,DXI0,ALPH0,F_I1,F_I2,T
      ,
     1TYPE,INCREASE)
C
C Calculate F_I1 and F_I2
      F_I1=EXP(-B*DT)*F_I1+DT/24.*(9.*(DDXI(4)+(0.5-AH)*DDALPH(4)+
     1
     DALPH(4))+19.*(DDXI(3)+(0.5-AH)*DDALPH(3)+DALPH(3))*EXP(-B*DT
     )
     2   -5.*(DDXI(2)+(0.5-AH)*DDALPH(2)+DALPH(2))*EXP(-2.*B*DT)
     3   +(DDXI(1)+(0.5-AH)*DDALPH(1)+DALPH(1))*EXP(-3.*B*DT))
      F_I2=EXP(-D*DT)*F_I2+DT/24.*(9.*(DDXI(4)+(0.5-AH)*DDALPH(4)+
     1
     DALPH(4))+19.*(DDXI(3)+(0.5-AH)*DDALPH(3)+DALPH(3))*EXP(-D*DT
     )
     2   -5.*(DDXI(2)+(0.5-AH)*DDALPH(2)+DALPH(2))*EXP(-2.*D*DT)
     3   +(DDXI(1)+(0.5-AH)*DDALPH(1)+DALPH(1))*EXP(-3.*D*DT))
C
C     Keep track of the max and min pitch angles for each cycle.
      IF(T.GT.1.0) THEN
          IF(((ALPH(4).GT.ALPH(2)).AND.(ALPH(4).LT.ALPH(3))).OR.
```

```
     1 ((ALPH(4).LT.ALPH(2)).AND.(ALPH(3).GT.ALPH(2)))) THEN
                HIPEAK=ALPH(3)
C                WRITE(9,*)T,HIPEAK

            ELSEIF(((ALPH(4).GT.ALPH(2)).AND.(ALPH(3).LT.ALPH(2))).O
            R.
     1 ((ALPH(4).LT.ALPH(2)).AND.(ALPH(4).GT.ALPH(3)))) THEN
                LOPEAK=ALPH(3)
C                WRITE(9,*)T,LOPEAK
            ENDIF
            IF(((XI(4).GT.XI(2)).AND.(XI(4).LT.XI(3))).OR.
     1 ((XI(4).LT.XI(2)).AND.(XI(3).GT.XI(2)))) THEN
                HIXI=XI(3)
            ELSEIF(((XI(4).GT.XI(2)).AND.(XI(3).LT.XI(2))).OR.
     1 ((XI(4).LT.XI(2)).AND.(XI(4).GT.XI(3)))) THEN
                LOXI=XI(3)
            ENDIF

C
    IF((T.GT.TIMECHEK).AND.((ABS(HIPEAK-LOPEAK).LT.THRESH).OR.
C      1             (ALPH(4).EQ.ALPH(3)))) THEN
c     1             (ALPH(4).EQ.ALPH(3))) THEN
c          IF((ABS(HIPEAK-LOPEAK).LT.THRESH)) THEN
C      Check for decayed signal or unstable or alpha4=alpha3
            IF((T.GT.TIMECHEK).AND.(ABS(HIPEAK-LOPEAK).LT.THRESH))
            THEN
                    SMPEAKS=SMPEAKS+1
                    IF((SMPEAKS.GE.5).OR.(ALPH(4).EQ.ALPH(3))) THEN
                          GOTO 50
                    ENDIF
              ELSEIF(ABS(HIPEAK-LOPEAK).GT.(100.)) THEN
                          GOTO 70
              ENDIF
        ENDIF
C
C Rotation of arrays
        DO 30 I=1,3
            ALPH(I)=ALPH(I+1)
            RECALP(LOOP)=ALPH(I+1)
            DALPH(I)=DALPH(I+1)
            DDALPH(I)=DDALPH(I+1)
            XI(I)=XI(I+1)
            RECXI(LOOP)=XI(I+1)
            DXI(I)=DXI(I+1)
            DDXI(I)=DDXI(I+1)
            LAMBDA(I)=LAMBDA(I+1)
30      CONTINUE
C To reach here is to achieve LCO
        IF(TYPE.NE.1) THEN
            DO 40 I=3,LOOP-1,IPFREQ
C                WRITE(1,*)(I-2)*DT,RECALP(I)/CONVRT
                CALL
                GR_WRITE((I-2)*DT,RECALP(I)/CONVRT,RECXI(I)/CONVRT)
40          CONTINUE
        PRINT *,'LCO achieved at: U*=',USTAR/ULIN,' Pitch amp=',
       1(ABS(HIPEAK-LOPEAK)/2)/CONVRT
        ELSE
            IF(STATE.NE.2) THEN
                CALL GR_WRITE(USTAR/ULIN,ALPH0/CONVRT)
            ENDIF
C Output the amplitude
            WRITE(11,*)ALPH0/CONVRT,USTAR/ULIN,
     1              (ABS(HIPEAK-LOPEAK)/2)/CONVRT

```

```
            WRITE(12,*)ALPH0/CONVRT,USTAR/ULIN,(ABS(HIXI-LOXI)/2)/CO
            NVRT
        ENDIF
        STATE=2
        GOTO 90
C
50      CONTINUE
C Damped oscillation.
        IF(TYPE.NE.1) THEN
            DO 60 I=3,LOOP-1,IPFREQ
                CALL
                GR_WRITE((I-2)*DT,RECALP(I)/CONVRT,RECXI(I)/CONVRT)
60          CONTINUE
        PRINT *,'Damped Oscillation at: U*=',USTAR/ULIN,'Hi Peak=',
        1         HIPEAK,'Lo Peak=',LOPEAK,ALPH(4)-ALPH(3)
        ELSE
            IF(STATE.NE.1) THEN
                CALL GR_WRITE(USTAR/ULIN,ALPH0/CONVRT)
            ENDIF
        ENDIF
        STATE=1
        GOTO 90
70      CONTINUE
C Unstable oscillation.
        IF(TYPE.NE.1) THEN
            DO 80 I=3,LOOP-1,IPFREQ
                CALL
                GR_WRITE((I-2)*DT,RECALP(I)/CONVRT,RECXI(I)/CONVRT)
80          CONTINUE
        PRINT *,'Unstable Oscillation at: U*=',USTAR/ULIN
        ELSE
            IF(STATE.NE.3) THEN
                CALL GR_WRITE(USTAR/ULIN,ALPH0/CONVRT)
            ENDIF
        ENDIF
        STATE=3
90      CONTINUE
        CLOSE(2)
        CLOSE(11)
        CLOSE(12)
        IF(TYPE.NE.1) THEN
            CLOSE(10)
        ENDIF
        call TIME(char_time)
        CALL DATE(TODAY)
        PRINT *, 'Finished: ',CHAR_TIME,'  ',TODAY
c        CALL BEEPQQ(1000,1000)
        STOP
        END

C Calculate and return the value for alpha(t+dt) and xi(t+dt)
        SUBROUTINE
        STEP(ALPH,XI,DALPH,DDALPH,DDXI,DALPH0,DXI0,ALPH0,F_I1,
       1F_I2,T,TYPE,INCREASE)
C
        REAL P(2,2),INVP(2,2),X(2),F_I1,F_I2,SOL(2),T
        REAL
        R,T1,T2,T3,T4A,T4B,T5A,T5B,T5C,T6A,T6B,T7A,T7B,T7C,T8A,T8B
        REAL T9,T10,T11,T12,T13,T14,T15,DENOM,FA,FP,QDXI0
        REAL ALPH0,DALPH0,DDALP0,TDALP0,QDALP0,XI0,DXI0,DDXI0,TDXI0
        REAL DALPH(4),DDALPH(4),DXI(4),DDXI(4)
        REAL*8 ALPH(4),XI(4),ALPHAB
        REAL HY_FP,HY_FA
        INTEGER N,IP,TYPE,INCREASE
```

```
      COMMON /CONST/
      XA,AH,EL,A,B,C,D,ZETAAL,ZETAXI,OMEGA,USTAR,RA,V1,
     1
     V2,H1MIN,H1MAX,H2MIN,H2MAX,HMU,DT,DV,DH,VOFF,F_HOFF,CONVRT,
     2     HOFF,F_H1MAX,F_H2MAX
C Calculate P
      ALPHAB=2*ALPH(3)-ALPH(2)
400
P(1,1)=2./(HMU*DT**2)*(HMU*XA-AH)+1./(6.*HMU*DT)*(11.+(0.5-AH)*
     1     (22.*EL-9.*(A+C)))+1./(8.*HMU)*(16.*EL-11*(A+C))

      P(1,2)=2./(HMU*DT**2)*(1.+HMU)+1./(6.*HMU*DT)*(22.*HMU*ZETAX
      I*
     1     OMEGA/USTAR+22.*EL-9*(A+C))+OMEGA**2/(USTAR**2)

      P(2,1)=2./(HMU*DT**2)*(1./8.*(RA**(-2)*(1.+8.*AH**2))+HMU)+1
      ./(6.*
     1
     HMU*DT)*(22.*HMU*ZETAAL/USTAR+RA**(-2)*(0.5-AH)*(11.-(0.5+AH)
     *
     2
     (22.*EL-9*(A+C))))-1./(8.*HMU)*RA**(-2)*(0.5+AH)*(16.*EL-11.*
     3     (A+C))
      P(2,2)=2./(HMU*DT**2)*(RA**(-2)*(HMU*XA-AH))-1./(6.*HMU*DT)*
     1     RA**(-2)*(0.5+AH)*(22.*EL-9.*(A+C))
C
C Now factor in the restoring force
      P(2,1)=P(2,1)+USTAR**(-2)*HY_FP(ALPHAB,ALPH(3))
C Calculate the inverse of P
      DENOM=P(1,1)*P(2,2)-P(1,2)*P(2,1)
      INVP(1,1)=P(2,2)/DENOM
      INVP(1,2)=-P(1,2)/DENOM
      INVP(2,1)=-P(2,1)/DENOM
      INVP(2,2)=P(1,1)/DENOM
C Calculate X1 and X2
C
C First X1 :
       X(1)=ALPH(3)*(5.*(XA*HMU-AH)/(HMU*DT**2)
     *
     +3.*(4.+(.5-AH)*(8.*EL-5.*A-5.*C))/(4.*HMU*DT)
     *                  -9.*(A+C)/(4.*HMU))
     *       +XI(3)*(5.*(1.+HMU)/(HMU*DT**2)
     *
     +3.*(8.*HMU*ZETAXI*OMEGA/USTAR+8.*EL-5.*A-5.*C)
     *                   /(4.*HMU*DT))
     *       -ALPH(2)*(4.*(XA*HMU-AH)/(HMU*DT**2)
     *                   +3.*(1.+(.5-AH)*2.*(EL-A-C))/(2.*HMU*DT)
     *                   -9.*(A+C)/(8.*HMU))
     *       -XI(2)*(4.*(1.+HMU)/(HMU*DT**2)
     *                   +3.*(2.*ZETAXI*HMU*OMEGA/USTAR+2.*(EL-A-C))
     *                   /(2.*HMU*DT))
     *       +ALPH(1)*((XA*HMU-AH)/(HMU*DT**2)
     *                   +(4.+(.5-AH)*(8.*EL-9.*(A+C)))/(12.*HMU*DT)
     *                   -(A+C)/(4.*HMU))
     *       +XI(1)*((1.+HMU)/(HMU*DT**2)
     *                   +(8.*ZETAXI*HMU*OMEGA/USTAR+8.*EL-9.*(A+C))
     *                   /(12.*HMU*DT))
     *       +(DALPH(3)+DDXI(3)+(.5-AH)*DDALPH(3))
     *            *(A*exp(-B*DT)+C*exp(-D*DT))*19.*DT/(12.*HMU)
     *       -(DALPH(2)+DDXI(2)+(.5-AH)*DDALPH(2))
     *
     *(A*exp(-2.*B*DT)+C*exp(-2.*D*DT))*5.*DT/(12.*HMU)
     *       +(DALPH(1)+DDXI(1)+(.5-AH)*DDALPH(1))
     *            *(A*exp(-3.*B*DT)+C*exp(-3.*D*DT))*DT/(12.*HMU)
```

```
     *       +(ALPH0+DXI0+(.5-AH)*DALPH0)
     *            *(A*exp(-B*(T+DT))+C*exp(-D*(T+DT)))*2./HMU
     *       +(A*exp(-B*DT)*F_I1+C*exp(-D*DT)*F_I2)*2./HMU


C Now X2 :
C
      R=RA**(-2)
      T1=5.*((1.+8.*(AH**2))*R/8.+HMU)/(HMU*(DT**2))

      T2=3./(4.*HMU*DT)*(8.*HMU*ZETAAL/USTAR+R*(0.5-AH)*(4.-(0.5+A
      H)*
     1   (8.*EL-5.*(A+C))))
      T3=9./(4.*HMU)*R*(0.5+AH)*(A+C)
      T4A=5./(HMU*(DT**2))*R*(HMU*XA-AH)
      T4B=3./(4.*HMU*DT)*R*(0.5+AH)*(8.*EL-5.*(A+C))
      T5A=4.*((1.+8.*(AH**2))*R/8+HMU)/(HMU*(DT**2))

      T5B=3./(2.*HMU*DT)*(2.*HMU*ZETAAL/USTAR+R*(0.5-AH)*(1.-(0.5+
      AH)*
     1    (2.*EL-2.*(A+C))))
      T5C=9./(8.*HMU)*R*(0.5+AH)*(A+C)
      T6A=4.*(HMU*XA-AH)*R/(HMU*(DT**2))
      T6B=3.*(0.5+AH)*(2.*EL-2.*(A+C))/(2.*HMU*DT)*R
      T7A=1.*((1.+8.*(AH**2))*R/8+HMU)/(HMU*(DT**2))

      T7B=1./(12.*HMU*DT)*(8.*HMU*ZETAAL/USTAR+R*(0.5-AH)*(4.-(0.5
      +AH)*
     1    (8.*EL-9.*(A+C))))
      T7C=1./(4.*HMU)*R*(0.5+AH)*(A+C)
      T8A=1./(HMU*(DT**2))*R*(HMU*XA-AH)
      T8B=1./(12.*HMU*DT)*R*(0.5+AH)*(8.*EL-9.*(A+C))
      T9=19.*DT/(12.*HMU)*R*(0.5+AH)*(A*EXP(-B*DT)+C*EXP(-D*DT))

      T10=5.*DT/(12.*HMU)*R*(0.5+AH)*(A*EXP(-2.*B*DT)+C*EXP(-2.*D*
      DT))

      T11=DT/(12.*HMU)*R*(0.5+AH)*(A*EXP(-3.*B*DT)+C*EXP(-3.*D*DT)
      )
      T12=2./HMU*R*(0.5+AH)*(A*EXP(-B*(T+DT))+C*EXP(-D*(T+DT)))
      T13=2./HMU*R*(0.5+AH)*(A*EXP(-B*DT))
      T14=2./HMU*R*(0.5+AH)*(C*EXP(-D*DT))
      T15=0.5-AH
C

      X(2)=(T1+T2+T3)*ALPH(3)+(T4A-T4B)*XI(3)-(T5A+T5B+T5C)*ALPH(2
      )-
     1   (T6A-T6B)*XI(2)+(T7A+T7B+T7C)*ALPH(1)+(T8A-T8B)*XI(1)-T9*
     2
     (DDXI(3)+T15*DDALPH(3)+DALPH(3))+T10*(DDXI(2)+T15*DDALPH(2)+
     3
     DALPH(2))-T11*(DDXI(1)+T15*DDALPH(1)+DALPH(1))-T12*(DXI0+T15*
     4   DALPH0+ALPH0)-T13*F_I1-T14*F_I2
C Now add in the restoring force
      X(2)=X(2)-(USTAR**(-2))*HY_FA(ALPHAB,ALPH(3))
C
      ALPH(4)=INVP(1,1)*X(1)+INVP(1,2)*X(2)
      XI(4)=INVP(2,1)*X(1)+INVP(2,2)*X(2)
C
      IF((ALPH(4).GT.ALPH(3)).AND.(INCREASE.EQ.0)) THEN
C Change to increasing
          IF((ALPH(3).GE.H2MAX).AND.(ALPH(3).LT.H1MIN)) THEN
              HOFF=HOFF+(DH)
              H1MAX=HOFF+F_H1MAX-F_HOFF
```

```
                H2MAX=F_H2MAX
                INCREASE=1
c                WRITE(*,*)INCREASE,T
                ALPHAB=ALPH(4)
                GOTO 400
            ELSEIF((ALPH(3).GT.H2MIN).AND.(ALPH(3).LT.H2MAX)) THEN
                HOFF=F_HOFF+(ALPH(3)-H2MIN)
                H1MAX=HOFF+F_H1MAX-F_HOFF
                H2MAX=F_H2MAX
                INCREASE=1
c                WRITE(*,*)INCREASE,T
                ALPHAB=ALPH(4)
                GOTO 400
            ELSE
                INCREASE=1
c                WRITE(*,*)INCREASE,T
                HOFF=F_HOFF
                H1MAX=F_H1MAX
                H2MAX=F_H2MAX
            ENDIF
        ELSEIF((ALPH(4).LT.ALPH(3)).AND.(INCREASE.EQ.1)) THEN
C Change to decreasing
            IF((ALPH(3).LE.H1MAX).AND.(ALPH(3).GT.H2MIN)) THEN
                HOFF=HOFF-(DH)
                H2MAX=HOFF+F_H2MAX-F_HOFF
                H1MAX=F_H1MAX
                INCREASE=0
c                WRITE(*,*)INCREASE,T
                ALPHAB=ALPH(4)
                GOTO 400
            ELSEIF((ALPH(3).LT.H1MIN).AND.(ALPH(3).GT.H1MAX)) THEN
                HOFF=F_HOFF+(ALPH(3)-H1MIN)
                H2MAX=HOFF+F_H2MAX-F_HOFF
                H1MAX=F_H1MAX
                INCREASE=0
c                WRITE(*,*)INCREASE,T
                ALPHAB=ALPH(4)
                GOTO 400
            ELSE
                INCREASE=0
c                WRITE(*,*)INCREASE,T
                HOFF=F_HOFF
                H2MAX=F_H2MAX
                H1MAX=F_H1MAX
            ENDIF
        ENDIF
C        IF((ALPH(4).GT.ALPH(3)).AND.(INCREASE.EQ.0)) THEN
C            INCREASE=1
C        ELSEIF((ALPH(4).LT.ALPH(3)).AND.(INCREASE.EQ.1)) THEN
C            INCREASE=0
C        ENDIF

        N=2
        IP=1

        DALPH(4)=(11.*ALPH(4)-18.*ALPH(3)+9.*ALPH(2)-2.*ALPH(1))/(6.
        *DT)
        DXI(4)=(11.*XI(4)-18.*XI(3)+9.*XI(2)-2.*XI(1))/(6.*DT)
        DDALPH(4)=(2.*ALPH(4)-5.*ALPH(3)+4.*ALPH(2)-ALPH(1))/(DT**2)
        DDXI(4)=(2.*XI(4)-5.*XI(3)+4.*XI(2)-XI(1))/(DT**2)
        IF(TYPE.NE.1) THEN
            WRITE(10,410)ALPHAB/CONVRT,(HY_FA(ALPHAB,ALPH(3))+
        1
        HY_FP(ALPHAB,ALPH(3))*ALPHAB)/CONVRT,T,HOFF/CONVRT,
```

```
     2
     H1MIN/CONVRT,H1MAX/CONVRT,H2MIN/CONVRT,H2MAX/CONVRT,
    3       ALPH(3)/CONVRT,ALPH(4)/CONVRT,INCREASE
410
FORMAT(F8.3,F8.3,F8.1,F8.3,F8.3,F8.3,F8.3,F8.3,F12.8,F12.8,I2)
      ENDIF
C
      RETURN
      END
C
C Calculate and return the initial values of the 2nd, 3rd, & 4th derivs
C     of alpha & xi
      SUBROUTINE
      START1(ALPH0,DALPH0,XI0,DXI0,DDALP0,TDALP0,QDALP0,DDXI0
     1,TDXI0,QDXI0)
C Starting Procedure
      REAL Q(2,2),INVQ(2,2),Y1,Y2
      REAL
      T1,T2,T3,T4,T5,T6,T7,T8,DENOM,T11,T12,T13,T14,T15,T16,T17
      REAL ALPH0,DALPH0,DDALP0,TDALP0,QDALP0,XI0,DXI0,DDXI0,TDXI0
      REAL HY_DF,HY_F,DDF,T,QDXI0
      COMMON /CONST/
      XA,AH,EL,A,B,C,D,ZETAAL,ZETAXI,OMEGA,USTAR,RA,V1,
     1
     V2,H1MIN,H1MAX,H2MIN,H2MAX,HMU,DT,DV,DH,VOFF,F_HOFF,CONVRT,
     2    HOFF,F_H1MAX,F_H2MAX
C Calculate Q
      Q(1,1)=1./HMU*(HMU*XA-AH)
      Q(1,2)=1./HMU*(1.+HMU)
      Q(2,1)=1./HMU*(RA**(-2)*(1./8.+AH**2)+HMU)
      Q(2,2)=1./HMU*RA**(-2)*(HMU*XA-AH)
C Calculate the inverse of Q = INVQ
C Calculate the inverse of P
      DENOM=Q(1,1)*Q(2,2)-Q(1,2)*Q(2,1)
      INVQ(1,1)=Q(2,2)/DENOM
      INVQ(1,2)=-Q(1,2)/DENOM
      INVQ(2,1)=-Q(2,1)/DENOM
      INVQ(2,2)=Q(1,1)/DENOM
C Calculate the Y matrices
      T3=2.*EL-2.*(A+C)
      T1=1.+(0.5-AH)*T3
      T2=2.*HMU*ZETAXI*OMEGA/USTAR+T3
      T4=2.*A*B+2.*C*D
      T5=T3+(0.5-AH)*T4
      T6=1./HMU*T4+OMEGA**2/(USTAR**2)
      T8=2.*A*(B**2)+2.*C*(D**2)
      T7=T4-(0.5-AH)*T8
C
      T11=RA**(-2)*(0.5+AH)
      T12=T3

      T13=2.*HMU*ZETAAL/USTAR+(RA**(-2)*(0.5-AH))*(1.-(0.5+AH)*T12
      )
      T15=T4
      T14=T11*T12
      T16=T11*(T12+(0.5-AH)*T15)
      T17=T11*T7
C

      Y1=-1./HMU*T1*DALPH0-1./HMU*T2*DXI0-1./HMU*T3*ALPH0-1./USTAR
      **2*
     1    XI0
      Y2=-1./HMU*T13*DALPH0+1./HMU*T14*(DXI0+ALPH0)-1./USTAR**2*
```

```
     1HY_F(ALPH0,ALPH0*2)
C
      DDALP0=INVQ(1,1)*Y1+INVQ(1,2)*Y2
      DDXI0=INVQ(2,1)*Y1+INVQ(2,2)*Y2
C

      Y1=-1./HMU*T1*DDALP0-1./HMU*T2*DDXI0-1./HMU*T5*DALPH0-T6*DXI
      0-1./
     1    HMU*T4*ALPH0

      Y2=-1./HMU*T13*DDALP0+1./HMU*T14*DDXI0+1./HMU*T16*DALPH0+1./
      HMU*
     1    T14*(DXI0+ALPH0)-1./USTAR**2*HY_DF(ALPH0,ALPH0*2)
C
      TDALP0=INVQ(1,1)*Y1+INVQ(1,2)*Y2
      TDXI0=INVQ(2,1)*Y1+INVQ(2,2)*Y2
C

      Y1=-1./HMU*T1*TDALP0-1./HMU*T2*TDXI0-1./HMU*T5*DDALP0-T6*DDX
      I0-1./
     1    HMU*T7*DALPH0+1./HMU*T8*(DXI0+ALPH0)

      Y2=-1./HMU*T13*TDALP0+1./HMU*T14*TDXI0+1./HMU*T16*DDALP0+1./
      HMU*
     1
     T14*DDXI0+1./HMU*T17*DALPH0-1./HMU*T11*T8*(DXI0+DALPH0)-1./
     2    USTAR**2*DDF(ALPH0)
C
      QDALP0=INVQ(1,1)*Y1+INVQ(1,2)*Y2
      QDXI0=INVQ(2,1)*Y1+INVQ(2,2)*Y2
      RETURN
      END
C
C Function to calculate the response force F() for a given pitch
  angle
C     alpha.
c bookmark
      REAL FUNCTION HY_F(ALPHA2,ALPHA1)
      REAL ALPHA1,ALPHA2
      COMMON /CONST/
      XA,AH,EL,A,B,C,D,ZETAAL,ZETAXI,OMEGA,USTAR,RA,V1,
     1
     V2,H1MIN,H1MAX,H2MIN,H2MAX,HMU,DT,DV,DH,VOFF,F_HOFF,CONVRT,
     2    HOFF,F_H1MAX,F_H2MAX
      IF(ALPHA2.GT.ALPHA1) THEN
C Pitch is increasing
          IF(ALPHA2.GE.H1MIN) THEN
C Pitch is above nonlinearity
              HY_F=ALPHA2-DH/2-F_HOFF+VOFF
          ELSEIF(ALPHA2.LE.H1MAX) THEN
C Pitch is in left branch or below nonlinearity
              HY_F=ALPHA2+DH/2-HOFF+VOFF
          ELSE
C Pitch is in flat band
              HY_F=V1
          ENDIF
      ELSE
C Pitch is decreasing
          IF(ALPHA2.GE.H2MAX) THEN
C Pitch is in right branch or above nonlinearity
              HY_F=ALPHA2-DH/2-HOFF+VOFF
          ELSEIF(ALPHA2.LE.H2MIN) THEN
C Pitch is below nonlinearity
              HY_F=ALPHA2+DH/2-F_HOFF+VOFF
```

```
            ELSE
C Pitch is in flat band
                HY_F=V2
            ENDIF
        ENDIF
        RETURN
        END
        REAL FUNCTION HY_FP(ALPHA2,ALPHA1)
        REAL*8 ALPHA1,ALPHA2
          REAL H1MIN,H1MAX,M2MIN,H2MAX
        COMMON /CONST/
        XA,AH,EL,A,B,C,D,ZETAAL,ZETAXI,OMEGA,USTAR,RA,V1,
       1
       V2,H1MIN,H1MAX,H2MIN,H2MAX,HMU,DT,DV,DH,VOFF,F_HOFF,CONVRT,
       2     HOFF,F_H1MAX,F_H2MAX
C
C
IF((((ALPHA2.LT.H1MAX).OR.(ALPHA2.GT.H1MIN)).AND.(ALPHA2.GT.
C     1ALPHA1)).OR.((ALPHA2.LT.H2MIN).OR.(ALPHA2.GT.H2MAX))) THEN
        IF(ALPHA2.GT.ALPHA1) THEN
            IF((ALPHA2.LT.H1MAX).OR.(ALPHA2.GT.H1MIN)) THEN
                HY_FP=1.0
            ELSE
                HY_FP=0.0
            ENDIF
        ELSEIF((ALPHA2.LT.H2MIN).OR.(ALPHA2.GT.H2MAX)) THEN
            HY_FP=1.0
        ELSE
            HY_FP=0.0
        ENDIF
        RETURN
        END
        REAL FUNCTION HY_FA(ALPHA2,ALPHA1)
C Pass in alpha(i)=ALPHA2, alpha(i-1)=ALPHA1, and alpha(1+1) is
returned
        REAL*8 ALPHA1,ALPHA2
        COMMON /CONST/
        XA,AH,EL,A,B,C,D,ZETAAL,ZETAXI,OMEGA,USTAR,RA,V1,
       1
       V2,H1MIN,H1MAX,H2MIN,H2MAX,HMU,DT,DV,DH,VOFF,F_HOFF,CONVRT,
       2     HOFF,F_H1MAX,F_H2MAX
C
        IF(ALPHA2.GT.ALPHA1) THEN
            IF(ALPHA2.GE.H1MIN) THEN
                HY_FA=-DH/2-F_HOFF+VOFF
            ELSEIF(ALPHA2.LE.H1MAX) THEN
                HY_FA=DH/2-HOFF+VOFF
            ELSE
                HY_FA=V1
            ENDIF
        ELSE
            IF(ALPHA2.GE.H2MAX) THEN
                HY_FA=-DH/2-HOFF+VOFF
            ELSEIF(ALPHA2.LE.H2MIN) THEN
                HY_FA=DH/2-F_HOFF+VOFF
            ELSE
                HY_FA=V2
            ENDIF
        ENDIF
        RETURN
        END
C
C Function to calculate the response force slope F'()=DF() for a
given
```

```
C     pitch angle alpha.
      REAL FUNCTION HY_DF(ALPHA2,ALPHA1)
      REAL ALPHA1,ALPHA2
        REAL H1MIN,H1MAX,M2MIN,H2MAX
      COMMON /CONST/
      XA,AH,EL,A,B,C,D,ZETAAL,ZETAXI,OMEGA,USTAR,RA,V1,
     1
     V2,H1MIN,H1MAX,H2MIN,H2MAX,HMU,DT,DV,DH,VOFF,F_HOFF,CONVRT,
     2    HOFF,F_H1MAX,F_H2MAX
C
      IF(ALPHA2.GT.ALPHA1) THEN
          IF((ALPHA2.LT.H1MAX).OR.(ALPHA2.GT.H1MIN)) THEN
              HY_DF=1.0
          ELSE
              HY_DF=0.0
          ENDIF
      ELSEIF((ALPHA2.LT.H2MIN).OR.(ALPHA2.GT.H2MAX)) THEN
          HY_DF=1.0
      ELSE
          HY_DF=0.0
      ENDIF
      RETURN
      END
C
C Function to calculate the response force curvature F"()=DDF()
  for a
C     given pitch angle alpha. Note that here there is no
  curvature.
      REAL FUNCTION DDF(ALPHA)
      REAL ALPHA
C
      DDF=0.
      RETURN
      END
C
C Subrouthing to extract data from input file
      SUBROUTINE
      GETDATA(INFILE,TITLE,SUBTITLE,ULIN,NUMANG,NUM,INCR,
     1UMIN,UMAX,ALIST)
      DIMENSION ALIST(100)
      INTEGER NUMANG,NUM,I
      REAL ULIN,INCR,UMIN,UMAX,ALIST
      CHARACTER*30 INFILE
      CHARACTER*70 DUMMY
      CHARACTER*100 TITLE,SUBTITLE
      COMMON /CONST/
      XA,AH,EL,A,B,C,D,ZETAAL,ZETAXI,OMEGA,USTAR,RA,V1,
     1
     V2,H1MIN,H1MAX,H2MIN,H2MAX,HMU,DT,DV,DH,VOFF,F_HOFF,CONVRT,
     2    HOFF,F_H1MAX,F_H2MAX
C
      OPEN(UNIT=1,FILE=INFILE)
      READ(1,310)TITLE
      READ(1,310)SUBTITLE
      READ(1,320)DV,DH,VOFF,HOFF,ULIN
      READ(1,330)NUMANG,UMIN,UMAX,INCR
      READ(1,340)HMU,OMEGA
      NUM=(UMAX-UMIN)/INCR+1
      DO 300 I=1,NUMANG
          READ(1,350)ALIST(I)
300   CONTINUE
310   FORMAT(A)
320   FORMAT(4F5.2,F8.4)
330   FORMAT(I5,F7.4,F7.4,F7.4)
```

```
340   FORMAT(F7.2,F5.3)
350   FORMAT(F7.0)
      CLOSE(1)
      RETURN
      END
C
      SUBROUTINE GR_WRITE(X,Y,Z)
      REAL X,Y,Z
      WRITE(2,600)X,Y,Z
600   FORMAT(3F20.10)
      RETURN
      END
C
      SUBROUTINE GR_SETUP(OUTFILE,GTITLE,GSUBT,XLABEL,YLABEL,TYPE)
      CHARACTER*30 OUTFILE
      CHARACTER*80 XLABEL,YLABEL
      CHARACTER*100 GTITLE,GSUBT
      INTEGER TYPE
C
      WRITE(2,510)'# ACE/gr parameter file'
      WRITE(2,510)'#'
      WRITE(2,510)'#'
      WRITE(2,510)'@page 5'
      WRITE(2,510)'@page inout 5'
      WRITE(2,510)'@link page off'
      WRITE(2,510)'@default linestyle 1'
      WRITE(2,510)'@default linewidth 1'
      WRITE(2,510)'@default color 1'
      WRITE(2,510)'@default char size 1.000000'
      WRITE(2,510)'@default font 4'
      WRITE(2,510)'@default font source 0'
      WRITE(2,510)'@default symbol size 1.000000'
      WRITE(2,510)'@with g0'
      WRITE(2,510)'@g0 on'
      WRITE(2,510)'@g0 label off'
      WRITE(2,510)'@g0 hidden false'
      WRITE(2,510)'@g0 type xy'
      WRITE(2,510)'@g0 autoscale type AUTO'
      WRITE(2,510)'@g0 fixedpoint off     '
      WRITE(2,510)'@g0 fixedpoint type 0  '
      WRITE(2,510)'@g0 fixedpoint xy 0.000000, 0.000000 '
      WRITE(2,510)'@g0 fixedpoint format general general'
      WRITE(2,510)'@g0 fixedpoint prec 6, 6'
      WRITE(2,510)'@g0 autoscale type AUTO'
      IF(TYPE.EQ.1) THEN
          WRITE(2,510)'@    world xmin 0.7     '
          WRITE(2,510)'@    world xmax 1       '
          WRITE(2,510)'@    world ymin -10     '
          WRITE(2,510)'@    world ymax 20      '
      ENDIF
      WRITE(2,510)'@    view xmin 0.150000 '
      WRITE(2,510)'@    view xmax 0.850000 '
      WRITE(2,510)'@    view ymin 0.150000 '
      WRITE(2,510)'@    view ymax 0.850000 '
      WRITE(2,500)'@    title "',GTITLE,'"'
      WRITE(2,510)'@    title font 4       '
      WRITE(2,510)'@    title size 1.000000'
      WRITE(2,510)'@    title color 1      '
      WRITE(2,510)'@    title linewidth 1  '
      WRITE(2,500)'@    subtitle "',GSUBT,'"'
      WRITE(2,510)'@    subtitle font 4        '
      WRITE(2,510)'@    subtitle size 1.000000 '
      WRITE(2,510)'@    subtitle color 1       '
      WRITE(2,510)'@    subtitle linewidth 1   '
```

```
      WRITE(2,510)'@    s0 type xy              '
      IF(TYPE.EQ.1) THEN
          WRITE(2,510)'@    s0 symbol 9'
          WRITE(2,510)'@    s0 symbol size 0.5'
      ELSE
          WRITE(2,510)'@    s0 symbol 0'
          WRITE(2,510)'@    s0 symbol size 1.0'
      ENDIF
      WRITE(2,510)'@    s0 symbol fill 0       '
      WRITE(2,510)'@    s0 symbol color 1      '
      WRITE(2,510)'@    s0 symbol linewidth 1  '
      WRITE(2,510)'@    s0 symbol linestyle 1  '
      WRITE(2,510)'@    s0 symbol center false '
      WRITE(2,510)'@    s0 symbol char 0       '
      WRITE(2,510)'@    s0 SKIP 0              '
      IF(TYPE.EQ.1) THEN
          WRITE(2,510)'@    s0 linestyle 0'
      ELSE
          WRITE(2,510)'@    s0 linestyle 1'
      ENDIF
      WRITE(2,510)'@    s0 linewidth 1'
      WRITE(2,510)'@    s0 color 1'
      WRITE(2,510)'@    s0 fill 0'
      WRITE(2,510)'@    s0 fill with color          '
      WRITE(2,510)'@    s0 fill color 1             '
      WRITE(2,510)'@    s0 fill pattern 0           '
      WRITE(2,510)'@    s0 errorbar type BOTH       '
      WRITE(2,510)'@    s0 errorbar length 1.000000 '
      WRITE(2,510)'@    s0 errorbar linewidth 1     '
      WRITE(2,510)'@    s0 errorbar linestyle 1     '
      WRITE(2,510)'@    s0 errorbar riser on        '
      WRITE(2,510)'@    s0 errorbar riser linewidth 1'
      WRITE(2,510)'@    s0 errorbar riser linestyle 1'
      WRITE(2,510)'@    s0 xyz 0.000000, 0.000000   '
      WRITE(2,500)'@    s0 comment "',OUTFILE,'"'
      WRITE(2,510)'@    xaxis  tick on              '
      WRITE(2,510)'@    xaxis  tick major 0.1       '
      WRITE(2,510)'@    xaxis  tick minor 0.05      '
      WRITE(2,510)'@    xaxis  tick offsetx 0.000000'
      WRITE(2,510)'@    xaxis  tick offsety 0.000000'
      WRITE(2,500)'@    xaxis  label "',XLABEL,'"'
      WRITE(2,510)'@    xaxis  label layout para    '
      WRITE(2,510)'@    xaxis  label place auto     '
      WRITE(2,510)'@    xaxis  label char size 1.000000'
      WRITE(2,510)'@    xaxis  label font 4         '
      WRITE(2,510)'@    xaxis  label color 1        '
      WRITE(2,510)'@    xaxis  label linewidth 1    '
      WRITE(2,510)'@    xaxis  ticklabel on         '
      WRITE(2,510)'@    xaxis  ticklabel type auto  '
      WRITE(2,510)'@    xaxis  ticklabel prec 2     '
      WRITE(2,510)'@    xaxis  ticklabel format decimal'
      WRITE(2,510)'@    xaxis  ticklabel append ""  '
      WRITE(2,510)'@    xaxis  ticklabel prepend "" '
      WRITE(2,510)'@    xaxis  ticklabel layout horizontal'
      WRITE(2,510)'@    xaxis  ticklabel SKIP 0     '
      WRITE(2,510)'@    xaxis  ticklabel stagger 0  '
      WRITE(2,510)'@    xaxis  ticklabel op bottom  '
      WRITE(2,510)'@    xaxis  ticklabel sign normal'
      WRITE(2,510)'@    xaxis  ticklabel start type auto '
      WRITE(2,510)'@    xaxis  ticklabel start 0.000000 '
      WRITE(2,510)'@    xaxis  ticklabel stop type auto '
      WRITE(2,510)'@    xaxis  ticklabel stop 0.000000  '
      WRITE(2,510)'@    xaxis  ticklabel char size 1.000000'
      WRITE(2,510)'@    xaxis  ticklabel font 4     '
```

```
      WRITE(2,510)'@    xaxis  ticklabel color 1      '
      WRITE(2,510)'@    xaxis  ticklabel linewidth 1 '
      WRITE(2,510)'@    xaxis  tick major on          '
      WRITE(2,510)'@    xaxis  tick minor on          '
      WRITE(2,510)'@    xaxis  tick default 6         '
      WRITE(2,510)'@    xaxis  tick in                '
      WRITE(2,510)'@    xaxis  tick major color 1     '
      WRITE(2,510)'@    xaxis  tick major linewidth 1'
      WRITE(2,510)'@    xaxis  tick major linestyle 1'
      WRITE(2,510)'@    xaxis  tick minor color 1     '
      WRITE(2,510)'@    xaxis  tick minor linewidth 1'
      WRITE(2,510)'@    xaxis  tick minor linestyle 1'
      WRITE(2,510)'@    xaxis  tick log off           '
      WRITE(2,510)'@    xaxis  tick size 1.000000     '
      WRITE(2,510)'@    xaxis  tick minor size 0.500000'
      WRITE(2,510)'@    xaxis  bar off            '
      WRITE(2,510)'@    xaxis  bar color 1        '
      WRITE(2,510)'@    xaxis  bar linestyle 1    '
      WRITE(2,510)'@    xaxis  bar linewidth 1    '
      IF(TYPE.EQ.1) THEN
          WRITE(2,510)'@    xaxis  tick major grid on'
          WRITE(2,510)'@    xaxis  tick minor grid on'
      ELSE
          WRITE(2,510)'@    xaxis  tick major grid off'
          WRITE(2,510)'@    xaxis  tick minor grid off'
      ENDIF
      WRITE(2,510)'@    xaxis  tick op both       '
      WRITE(2,510)'@    xaxis  tick type auto     '
      WRITE(2,510)'@    xaxis  tick spec 0        '
      WRITE(2,510)'@    yaxis  tick on            '
      WRITE(2,510)'@    yaxis  tick major 10      '
      WRITE(2,510)'@    yaxis  tick minor 5       '
      WRITE(2,510)'@    yaxis  tick offsetx 0.000000'
      WRITE(2,510)'@    yaxis  tick offsety 0.000000'
      WRITE(2,500)'@    yaxis  label "',YLABEL,'"'
      WRITE(2,510)'@    yaxis  label layout para '
      WRITE(2,510)'@    yaxis  label place auto  '
      WRITE(2,510)'@    yaxis  label char size 1.000000'
      WRITE(2,510)'@    yaxis  label font 4            '
      WRITE(2,510)'@    yaxis  label color 1           '
      WRITE(2,510)'@    yaxis  label linewidth 1       '
      WRITE(2,510)'@    yaxis  ticklabel on            '
      WRITE(2,510)'@    yaxis  ticklabel type auto     '
      WRITE(2,510)'@    yaxis  ticklabel prec 1        '
      WRITE(2,510)'@    yaxis  ticklabel format decimal'
      WRITE(2,510)'@    yaxis  ticklabel append ""'
      WRITE(2,510)'@    yaxis  ticklabel prepend ""'
      WRITE(2,510)'@    yaxis  ticklabel layout horizontal'
      WRITE(2,510)'@    yaxis  ticklabel SKIP 0            '
      WRITE(2,510)'@    yaxis  ticklabel stagger 0         '
      WRITE(2,510)'@    yaxis  ticklabel op left           '
      WRITE(2,510)'@    yaxis  ticklabel sign normal       '
      WRITE(2,510)'@    yaxis  ticklabel start type auto   '
      WRITE(2,510)'@    yaxis  ticklabel start 0.000000    '
      WRITE(2,510)'@    yaxis  ticklabel stop type auto    '
      WRITE(2,510)'@    yaxis  ticklabel stop 0.000000     '
      WRITE(2,510)'@    yaxis  ticklabel char size 1.000000'
      WRITE(2,510)'@    yaxis  ticklabel font 4       '
      WRITE(2,510)'@    yaxis  ticklabel color 1      '
      WRITE(2,510)'@    yaxis  ticklabel linewidth 1 '
      WRITE(2,510)'@    yaxis  tick major on          '
      WRITE(2,510)'@    yaxis  tick minor on          '
      WRITE(2,510)'@    yaxis  tick default 6         '
      WRITE(2,510)'@    yaxis  tick in                '
```

```
      WRITE(2,510)'@    yaxis  tick major color 1    '
      WRITE(2,510)'@    yaxis  tick major linewidth 1'
      WRITE(2,510)'@    yaxis  tick major linestyle 1'
      WRITE(2,510)'@    yaxis  tick minor color 1    '
      WRITE(2,510)'@    yaxis  tick minor linewidth 1'
      WRITE(2,510)'@    yaxis  tick minor linestyle 1'
      WRITE(2,510)'@    yaxis  tick log off          '
      WRITE(2,510)'@    yaxis  tick size 1.000000    '
      WRITE(2,510)'@    yaxis  tick minor size 0.500000'
      WRITE(2,510)'@    yaxis  bar off               '
      WRITE(2,510)'@    yaxis  bar color 1           '
      WRITE(2,510)'@    yaxis  bar linestyle 1       '
      WRITE(2,510)'@    yaxis  bar linewidth 1       '
      IF(TYPE.EQ.1) THEN
          WRITE(2,510)'@    yaxis  tick major grid on'
          WRITE(2,510)'@    yaxis  tick minor grid on'
      ELSE
          WRITE(2,510)'@    yaxis  tick major grid off'
          WRITE(2,510)'@    yaxis  tick minor grid off'
      ENDIF
      WRITE(2,510)'@    yaxis  tick op both          '
      WRITE(2,510)'@    yaxis  tick type auto        '
      WRITE(2,510)'@    yaxis  tick spec 0           '
      WRITE(2,510)'@    zeroxaxis  tick on           '
      WRITE(2,510)'@    zeroxaxis  tick major 0.05 '
      WRITE(2,510)'@    zeroxaxis  tick minor 0.025'
      WRITE(2,510)'@    zeroxaxis  tick offsetx 0.000000'
      WRITE(2,510)'@    zeroxaxis  tick offsety 0.000000'
      WRITE(2,510)'@    zeroxaxis  label ""              '
      WRITE(2,510)'@    zeroxaxis  label layout para     '
      WRITE(2,510)'@    zeroxaxis  label place auto      '
      WRITE(2,510)'@    zeroxaxis  label char size 1.000000'
      WRITE(2,510)'@    zeroxaxis  label font 4          '
      WRITE(2,510)'@    zeroxaxis  label color 1         '
      WRITE(2,510)'@    zeroxaxis  label linewidth 1     '
      WRITE(2,510)'@    zeroxaxis  ticklabel off         '
      WRITE(2,510)'@    zeroxaxis  ticklabel type auto'
      WRITE(2,510)'@    zeroxaxis  ticklabel prec 2      '
      WRITE(2,510)'@    zeroxaxis  ticklabel format decimal'
      WRITE(2,510)'@    zeroxaxis  ticklabel append ""'
      WRITE(2,510)'@    zeroxaxis  ticklabel prepend ""'
      WRITE(2,510)'@    zeroxaxis  ticklabel layout horizontal'
      WRITE(2,510)'@    zeroxaxis  ticklabel SKIP 0      '
      WRITE(2,510)'@    zeroxaxis  ticklabel stagger 0   '
      WRITE(2,510)'@    zeroxaxis  ticklabel op bottom   '
      WRITE(2,510)'@    zeroxaxis  ticklabel sign normal '
      WRITE(2,510)'@    zeroxaxis  ticklabel start type auto'
      WRITE(2,510)'@    zeroxaxis  ticklabel start 0.000000 '
      WRITE(2,510)'@    zeroxaxis  ticklabel stop type auto '
      WRITE(2,510)'@    zeroxaxis  ticklabel stop 0.000000  '
      WRITE(2,510)'@    zeroxaxis  ticklabel char size 1.000000'
      WRITE(2,510)'@    zeroxaxis  ticklabel font 4      '
      WRITE(2,510)'@    zeroxaxis  ticklabel color 1     '
      WRITE(2,510)'@    zeroxaxis  ticklabel linewidth 1 '
      WRITE(2,510)'@    zeroxaxis  tick major off        '
      WRITE(2,510)'@    zeroxaxis  tick minor on         '
      WRITE(2,510)'@    zeroxaxis  tick default 6        '
      WRITE(2,510)'@    zeroxaxis  tick in               '
      WRITE(2,510)'@    zeroxaxis  tick major color 1    '
      WRITE(2,510)'@    zeroxaxis  tick major linewidth 1'
      WRITE(2,510)'@    zeroxaxis  tick major linestyle 1'
      WRITE(2,510)'@    zeroxaxis  tick minor color 1    '
      WRITE(2,510)'@    zeroxaxis  tick minor linewidth 1'
      WRITE(2,510)'@    zeroxaxis  tick minor linestyle 1'
```

```
992     WRITE(2,510)'@    zeroxaxis  tick log off          '
993     WRITE(2,510)'@    zeroxaxis  tick size 1.000000    '
994     WRITE(2,510)'@    zeroxaxis  tick minor size 0.500000'
995     WRITE(2,510)'@    zeroxaxis  bar off              '
996     WRITE(2,510)'@    zeroxaxis  bar color 1          '
997     WRITE(2,510)'@    zeroxaxis  bar linestyle 1      '
998     WRITE(2,510)'@    zeroxaxis  bar linewidth 1      '
999     WRITE(2,510)'@    zeroxaxis  tick major grid on   '
1000    WRITE(2,510)'@    zeroxaxis  tick minor grid on   '
1001    WRITE(2,510)'@    zeroxaxis  tick op both         '
1002    WRITE(2,510)'@    zeroxaxis  tick type auto       '
1003    WRITE(2,510)'@    zeroxaxis  tick spec 0          '
1004    WRITE(2,510)'@    zeroyaxis  tick on              '
1005    WRITE(2,510)'@    zeroyaxis  tick major 10        '
1006    WRITE(2,510)'@    zeroyaxis  tick minor 5         '
1007    WRITE(2,510)'@    zeroyaxis  tick offsetx 0.000000'
1008    WRITE(2,510)'@    zeroyaxis  tick offsety 0.000000'
1009    WRITE(2,510)'@    zeroyaxis  label ""'
1010    WRITE(2,510)'@    zeroyaxis  label layout para    '
1011    WRITE(2,510)'@    zeroyaxis  label place auto     '
1012    WRITE(2,510)'@    zeroyaxis  label char size 1.000000'
1013    WRITE(2,510)'@    zeroyaxis  label font 4         '
1014    WRITE(2,510)'@    zeroyaxis  label color 1        '
1015    WRITE(2,510)'@    zeroyaxis  label linewidth 1    '
1016    WRITE(2,510)'@    zeroyaxis  ticklabel off        '
1017    WRITE(2,510)'@    zeroyaxis  ticklabel type auto  '
1018    WRITE(2,510)'@    zeroyaxis  ticklabel prec 1     '
1019    WRITE(2,510)'@    zeroyaxis  ticklabel format decimal'
1020    WRITE(2,510)'@    zeroyaxis  ticklabel append "" '
1021    WRITE(2,510)'@    zeroyaxis  ticklabel prepend ""'
1022    WRITE(2,510)'@    zeroyaxis  ticklabel layout horizontal'
1023    WRITE(2,510)'@    zeroyaxis  ticklabel SKIP 0     '
1024    WRITE(2,510)'@    zeroyaxis  ticklabel stagger 0  '
1025    WRITE(2,510)'@    zeroyaxis  ticklabel op left    '
1026    WRITE(2,510)'@    zeroyaxis  ticklabel sign normal '
1027    WRITE(2,510)'@    zeroyaxis  ticklabel start type auto '
1028    WRITE(2,510)'@    zeroyaxis  ticklabel start 0.000000 '
1029    WRITE(2,510)'@    zeroyaxis  ticklabel stop type auto '
1030    WRITE(2,510)'@    zeroyaxis  ticklabel stop 0.000000 '
1031    WRITE(2,510)'@    zeroyaxis  ticklabel char size 1.000000'
1032    WRITE(2,510)'@    zeroyaxis  ticklabel font 4     '
1033    WRITE(2,510)'@    zeroyaxis  ticklabel color 1    '
1034    WRITE(2,510)'@    zeroyaxis  ticklabel linewidth 1 '
1035    WRITE(2,510)'@    zeroyaxis  tick major off       '
1036    WRITE(2,510)'@    zeroyaxis  tick minor on        '
1037    WRITE(2,510)'@    zeroyaxis  tick default 6       '
1038    WRITE(2,510)'@    zeroyaxis  tick in              '
1039    WRITE(2,510)'@    zeroyaxis  tick major color 1   '
1040    WRITE(2,510)'@    zeroyaxis  tick major linewidth 1'
1041    WRITE(2,510)'@    zeroyaxis  tick major linestyle 1'
1042    WRITE(2,510)'@    zeroyaxis  tick minor color 1   '
1043    WRITE(2,510)'@    zeroyaxis  tick minor linewidth 1'
1044    WRITE(2,510)'@    zeroyaxis  tick minor linestyle 1'
1045    WRITE(2,510)'@    zeroyaxis  tick log off         '
1046    WRITE(2,510)'@    zeroyaxis  tick size 1.000000   '
1047    WRITE(2,510)'@    zeroyaxis  tick minor size 0.500000'
1048    WRITE(2,510)'@    zeroyaxis  bar off              '
1049    WRITE(2,510)'@    zeroyaxis  bar color 1          '
1050    WRITE(2,510)'@    zeroyaxis  bar linestyle 1      '
1051    WRITE(2,510)'@    zeroyaxis  bar linewidth 1      '
1052    WRITE(2,510)'@    zeroyaxis  tick major grid on'
1053    WRITE(2,510)'@    zeroyaxis  tick minor grid on'
1054    WRITE(2,510)'@    zeroyaxis  tick op both         '
1055    WRITE(2,510)'@    zeroyaxis  tick type auto       '
```

```
      WRITE(2,510)'@    zeroyaxis  tick spec 0       '
      WRITE(2,510)'@    legend off                   '
      WRITE(2,510)'@    legend loctype view          '
      WRITE(2,510)'@    legend layout 0              '
      WRITE(2,510)'@    legend vgap 2                '
      WRITE(2,510)'@    legend hgap 1                '
      WRITE(2,510)'@    legend length 4              '
      WRITE(2,510)'@    legend box off               '
      WRITE(2,510)'@    legend box fill off          '
      WRITE(2,510)'@    legend box fill with color   '
      WRITE(2,510)'@    legend box fill color 0  '
      WRITE(2,510)'@    legend box fill pattern 1'
      WRITE(2,510)'@    legend box color 1       '
      WRITE(2,510)'@    legend box linewidth 1   '
      WRITE(2,510)'@    legend box linestyle 1   '
      WRITE(2,510)'@    legend x1 0.8            '
      WRITE(2,510)'@    legend y1 0.8            '
      WRITE(2,510)'@    legend font 4            '
      WRITE(2,510)'@    legend char size 1.000000'
      WRITE(2,510)'@    legend linestyle 1       '
      WRITE(2,510)'@    legend linewidth 1       '
      WRITE(2,510)'@    legend color 1           '
      WRITE(2,510)'@    frame on                 '
      WRITE(2,510)'@    frame type 0             '
      WRITE(2,510)'@    frame linestyle 1        '
      WRITE(2,510)'@    frame linewidth 1        '
      WRITE(2,510)'@    frame color 1            '
      WRITE(2,510)'@    frame fill off           '
      WRITE(2,510)'@    frame background color 0 '
      WRITE(2,510)'@WITH G0'
      WRITE(2,510)'@G0 ON  '
      WRITE(2,510)'@TYPE xy'
C
500   FORMAT(3A)
510   FORMAT(A)
      RETURN
      END
```

IMAGE EVALUATION
TEST TARGET (QA-3)

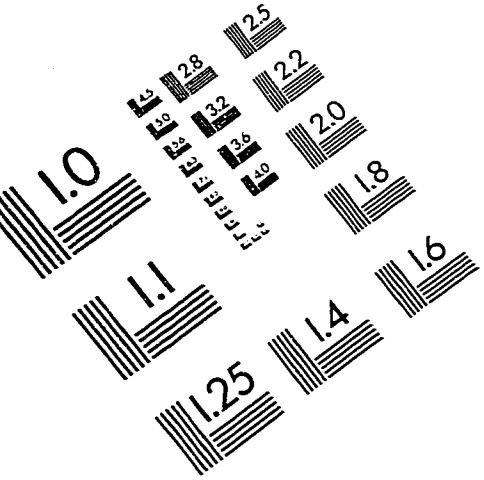

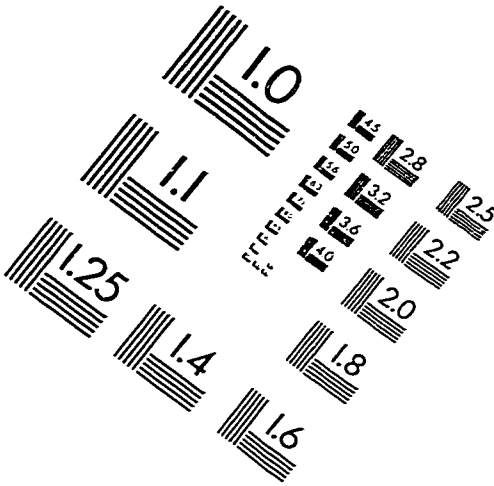

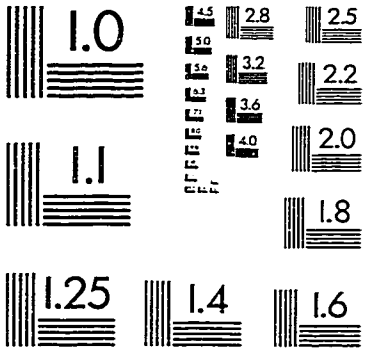

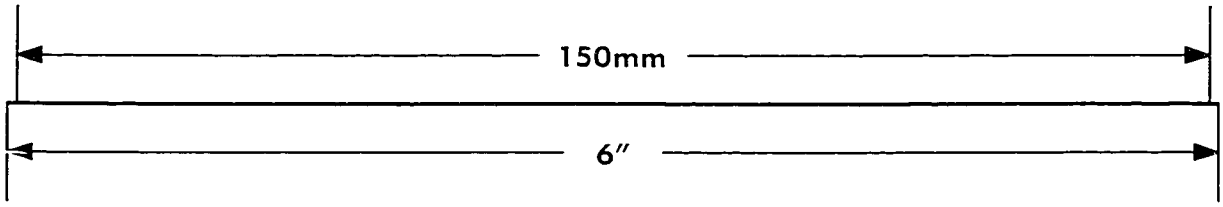

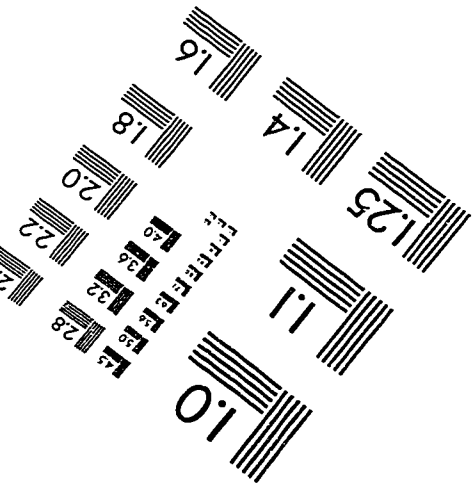

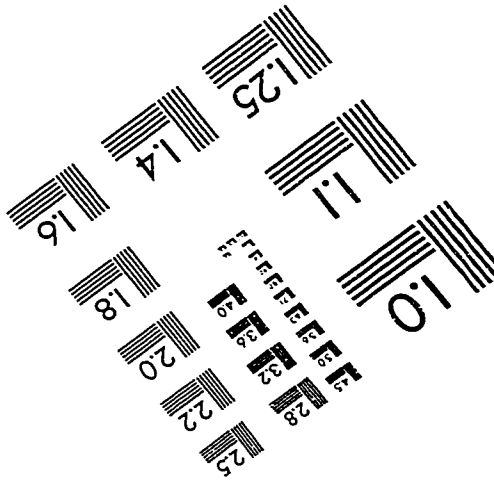

APPLIED IMAGE, Inc
1653 East Main Street
Rochester, NY 14609 USA
Phone: 716/482-0300
Fax: 716/288-5989